MONASH University

On the Development of Immunomodulators for Attenuation of Airway Inflammation

Amlan Chakraborty

Master of Technology (Biotechnology)
Bachelor of Technology (Biotechnology)

A thesis submitted for the degree of

Doctor of Philosophy

at Monash University

2019

Department of Chemical Engineering, Faculty of Engineering

Department of Immunology, Faculty of Medicine, Nursing and Health Sciences

Monash University

To my beloved wife and best friend, Moumita.

Sharing our life and love along this journey together is a blessing beyond words.
My lovely parents, the reason of what I become today

karmanye vadhika raste,
ma phaleshu kadachana;
ma karma phala he tur bhuh,
ma te sangvasta karmani.

Holy Bhagavad Gita (Ch.2, verse 47)

*To action alone hast thou a right and never at all to its fruits; let not the fruits of
action be thy motive; neither let there be in thee any attachment to inaction*

Copyright Notice

Declaration of Authorship

I, AMLAN CHAKRABORTY, declare that this thesis titled, "On the Development of Immunomodulators for Attenuation of Airway Inflammation" and the work presented in it are my own. I confirm that:

- This work was done wholly or mainly while in candidature for a Doctor of Phillosophy degree at Monash University.

- This thesis contains no material which has been accepted for the award of any other degree or diploma at any university or equivalent institution.

- Where I have consulted the published work of others, this is always clearly attributed.

- Where I have quoted from the work of others, the source is always given. With the exception of such quotations, this thesis is entirely my own work.

- I have acknowledged all main sources of help.

- Where the thesis is based on work done by myself jointly with others, I have made clear exactly what was done by others and what I have contributed myself.

- To the best of my knowledge and belief, this thesis contains no material previously published or written by another person, except where due reference is made in the text of the thesis.

Signature:
_____

Print Name: Mr Amlan Chakraborty
_____

Date: April 09, 2019
_____

Acknowledgements

If you want to leave your footprints on the sands of time, do not drag your feet

-Dr A.P.J. Abdul Kalam

I still cannot believe that I'm now writing this final section of my thesis and most important it will not be peer reviewed. There are a lot of emotions associated with this thesis. Firstly, it is a stepping stone for me towards my dream to be a scientist. Secondly, my dad was diagnosed with asthma and COPD when I was in secondary school. I have seen him suffer and therefore wanted to make a contribution in this field to help him and hundreds of patients who are suffering. That is my motivation for working in this project and keep me going for the past three and a half years.

Firstly, I would like to thank all of my supervisors for their consistent help, support, guidance, mentoring throughout this journey. Cordelia, you are the best supervisor a student can have. Thank you so much for giving me the opportunity to work in this project and supporting me throughout the process of learning. Whenever I needed guidance and mentoring you were always there to support me. I learnt a lot from you including being patient, management and focusing on the research problem from newer perspectives. I do not have enough words to thank you for supporting me with all the experiments needed to support this project. I would miss our fortnightly meetings with tons of bullet points to cover up and ask for your feedback and advice in moving forward with the project. Thanks would be too small to say for your contribution. Magdalena, I owe you my immunology skills, learning and understanding of the field. You believed in me that I will surpass the difficult times and I would be a good researcher. You always inspire me and will always be an idol for me to look up to and be one in future. Our lab meetings and after-hours meetings even when you moved to RMIT were really helpful. Thank you for your support and guidance that you have given me to learn immunology and apply them to be a confident researcher with critical thinking ability. Simon, you have been a friend, mentor and an excellent teacher. You helped me develop an interest in pharmacology and pulmonary diseases. I'm very thankful for the endless hours you spent helping me learn small animal surgery and our meetings to discuss data. I have met very few people as good as you who is humorous, sensitive, soft-spoken and a teacher. Thank you for supporting me in this project and helping me develop the skills required for working in this field. I will still look up to you in times of stress,

to have an informal chat and bursting out into laughter. Thank you so much for all the guidance and support and helping me improve my writing after my pre-submission seminar. Mark, a big thank you for all the discussions we had regarding dendritic cells and the experiments. Also, I'm very thankful to you for your dedication to help me during my pre-submission seminar even in your busiest days. Jennifer, thank you so much for teaching me critical thinking and motivating me that I will get to the end one day and will smile back to remember the tough days. Thank you for believing in me and spending quality time in discussions, scientific writing and data analysis amongst all the stress. I would also like to mention, a big thank you for making me a coffee lover and teaching me brewing and filtering ground coffee.

Secondly, I would like to thank all the past and present lab members of both MAPEL and VID lab, I have been a part of. These 3.5 years I would especially like to thank Dr Kirsty Wilson (VID lab) for teaching me flow cytometry and data analysis, animal handling and spending hours with me to give my project a good shape. I would especially like to thank Peter and Liam to be there with me in both the labs for helping me out with scientific discussion and morally supporting me whenever I was frustrated. A big thank you to Ruohui for her help in explaining me glycine microcarriers and Martin for teaching me spray-drying and helping me optimize the drying conditions. I would also like to mention my other lab members who have supported me throughout this journey notably Daisy (a great friend), Grace, Krystel, Yitian, George and Hassan from MAPEL and Nirmala, Gao, Sue, Michelle, Jack, Brad, Julie from VID lab. I'm also thankful to Meipeng from Xiwang's group, Tigabwa from Akshat's group to be my office colleague and best friends. I'm also thankful to Prof. Margaret Hibbs for providing the SHIP KO mice and Evelyn for her help in SHIP KO mice DC and macrophage characteristics. I would also like to thank Lakshanie, Pei, Kat in Immunology for the help with cells and providing me with good lab environment. I would like to acknowledge Vivian in pharmacology for her immense help in lung function tests and Cem for help with histoindex. Seriously, without your help, it would not have been possible to keep up with the sensitization time-lines. Also, thank you so much to be a supportive labmate. I would also like to thank A/Prof. Chrishan Samuel for supporting me to work in his lab for Simon in doing my experiments and Jane with the discussion of ALI models. Finally, I would like to acknowledge my admin and academic programs manager Jill and Lilyanne for putting up everything on time so that I do not have to worry about the schedule. You two are great.

I would like to thank the research platforms for supporting me with instrumentations and helping me learn new techniques. I thank Jade, Ali and Jonathan from Monash Histology Platform for their help and discussion in histology and immunohistochemistry. I thank Flame, Xi Ya, Tim and Emily for the course-work in SEM imaging and teaching

in science. I would like to mention about my university friends Abhijeet, Pranav, Abhinay, Kavita, Nida and my school friends for your motivational calls and texts. I would also like to thank three of my school teachers, Dr Moonmoon Majumdar, Dr Gautam Dutta and Mr Sanjeev Sen for teaching me biology, chemistry, mathematics but above all teaching me moral values.

Coming to my family, I would like to bow and say more than thanks to my lovely wife Moumita (Titli) for bearing with me since the start of my PhD. We got engaged and then, married for 2 years. We both shared this journey together and at every step, you were there by me to support me. I cried on your shoulder out of frustration and grief on a bad day. I smiled with you when things were moving on well. You always supported me for whatever I am and the tantrums I've given you. I know I've been quite annoying and nagging at times to make some dessert in the middle of the night. But you took it with a smile. Of course, writing this thesis itself was a challenge. And I vow it would not have been possible without your scolding and shouting at me. Thank you so much for showering me with love, affection, the lovely dishes that you made and listening to my presentations before any talk.

Finally to my parents, Jayanti (mom), Gautam (dad) and Rupali (mother-in-law) for their never-ending love and support. Your phone calls every day listening to my research, and enjoying every bit of it motivated me. Thank you for coming to my pre-submission seminar. You two always wanted me to grow up and be a good human being and do something for mankind. Hope this project is a good contribution to science and I have made you two proud. I wish my grandparents were alive to see this day and I also thank them for showering love to me and instilling me an interest in science.

Abstract

Aggravating levels of pollution containing ultra-fine particles have contributed to increase the frequency of inflammatory lung diseases such as asthma and chronic obstructive pulmonary diseases (COPD). The lung is a non-sterile environment due to direct contact with air containing factors such as bacteria, irritants and agricultural dusts, which can enter the lung and lead to airways inflammation. The bacterial cell wall component lipopolysaccharide (LPS) is one of the major triggers for airways inflammation. LPS leads to airway hyperresponsiveness (AHR), which is an exaggerated response of the airways involving bronchospasm, airway mucus production and allergen-specific T cells. These cells, resident in the lung or its draining lymph nodes, can produce cytokines which further exacerbate inflammation as well as help perpetuate an allergic response. In addition, hypoxemia, pulmonary oedema and alveolar damage leads to secretion of pro-inflammatory mediators and neutrophil infiltration. This results in acute pulmonary inflammation, equivalent to a clinical condition called acute respiratory distress syndrome (ARDS). Current treatments for ARDS utilise bronchodilators and anti-inflammatory drugs such as corticosteroids (e.g. prednisone, beclomethasone and cromolyn in paediatrics), augmented with short-acting β-2-agonists. These therapies can prevent neutrophilic damage, but prolonged use can cause adverse effects, resistance and increased risk of immunosuppression, potentially leading to increased risk of infection.

Natural compounds in foods like salmon, berries and tomatoes are claimed to be anti-inflammatory. Glycine is the smallest amino acid present in these foods and has been previously used in an ingestible form for the treatment of inflammatory bowel disease. Therefore, we investigated the direct anti-inflammatory potential of glycine in attenuating airway inflammation including ARDS. We established the anti-inflammatory potential of glycine in curbing ARDS and developed biodegradable nanoparticles for pulmonary delivery of glycine. We hypothesized glycine could be mediating its effects via Src homology 2 domain containing inositol polyphosphate 5-phosphatase 1 (SHIP-1) and therefore we investigated the responses of bone marrow derived dendritic cells lacking SHIP-1. As predicted, in the absence of SHIP-1 we found glycine was incapable of attenuating LPS mediated up-regulation of activation markers, indicating the observed effects were SHIP-1 dependent. Glycine attenuated airway inflammation by preventing neutrophil influx and increase of alveolar macrophages. It also reduced the production

of pro-inflammatory mediators and improved pulmonary function, promoting lung heal-ing. Furthermore, glycine conjugated on biodegradable super-paramagnetic iron oxide nanoparticles (GSPIONs) was taken up preferentially by alveolar macrophages and neu-trophils in the lung, without induction of pro-inflammatory cytokines or increases in airway resistance. The GSPIONs being non-inflammatory, may be useful for further de-velopment as theranostic agents. For example, in addition to their immunomodulatory role, we demonstrated for the first time the use of GSPIONs as novel contrast agents for lung magnetic resonance imaging, which is not a usual clinical practice, due to lack of contrast agents, techniques and water molecules in the lung.

Pulmonary inflammation requires both immediate and sustained therapy for better man-agement of the disease. In addition, pulmonary delivery of drugs is disease-specific such as the upper airways in asthma, or the alveoli in COPD. We encapsulated our glycine conjugated biodegradable nanoparticles in uniform, mono-disperse, porous, cenospheric spray-dried glycine microparticles based excipients for pulmonary administration. The nanoparticles were designed to be used as immunomodulators and magnetic resonance contrast agents for pulmonary delivery. The glycine microparticles may be used both as an excipient to bypass the oropharyngeal region, avoiding mucociliary clearance of the nanoparticles, and to provide an anti-inflammatory effect in the lung. Overall, the glycine based immunomodulators developed in these studies demonstrate potential for future development as clinical theranostics in pulmonary inflammation.

Publications

- Amlan Chakraborty, Jennifer C. Boer, Cordelia Selomulya, Magdalena Plebanski (2018), *Amino Acid Functionalised Nanoparticles as Cutting-Edge Therapeutic and Diagnostic Agents.* **ACS Bioconjugate Chemistry**; 29(3), pp 657-671.

- Amlan Chakraborty, Jennifer C. Boer, Cordelia Selomulya, Magdalena Plebanski, Simon G. Royce (2018), *Insights into endotoxin mediated lung inflammation and future treatment strategies.* **Expert Review of Respiratory Medicine**;12(11), pp 941-955.

Conference Publication

- Amlan Chakraborty, Liam Powles, Kirsty Wilson, Simon Royce, Cordelia Selomulya and Magdalena Plebanski (2019), *Superparamagnetic iron oxide nanoparticles with natural non-inflammatory surface coatings for diverse biological applications.* **International Nanomedicine Conference**.

- Amlan Chakraborty, Jennifer Boer, Simon Royce, Kirsty Wilson, Cordelia Selomulya and Magdalena Plebanski (2018), *Effect of a small natural dietary compound on lung pathology in airway inflammation.* **European Respiratory Journal**; 52, pp PA1045.

Thesis including published works Declaration

I, AMLAN CHAKRABORTY hereby declare that this thesis contains no material which has been accepted for the award of any other degree or diploma at any university or equivalent institution and that, to the best of my knowledge and belief, this thesis contains no material previously published or written by another person, except where due reference is made in the text of the thesis.

This thesis includes 2 original papers published in peer reviewed journals and 3 submitted publications. The core theme of the thesis is the development of an immunomodulator for attenuation of airway inflammation with possiible theranostic approaches across a diverse respiratory and inflammatory diseases. The ideas, development and writing up of all the papers in the thesis were the principal responsibility of myself, the student, working collaboratively across multiple academic units within the Department of Chemical Engineering, Department of Immunology and Department of Pharmacology under the supervision of Professor Cordelia Selomulya, Professor Magdalena Plebanski, Dr Simon Guy Royce, Dr Jennifer Carla Boer and Associate Professor Mark Wright.

The inclusion of co-authors reflects the fact that the work came from active collaboration between researchers and acknowledges input into team-based research. Parts of Chapter 1 and most of Chapter 2 recites the review articles in their original wording. Chapter 3 is a methods chapter with certain protocols present in their original wording as submitted for publication. Chapter 4 has not been published any where and is presented here solely for the thesis. Chapter 5, 6 and 7 each recite one research article of which I am first author with most of the parts in their original wording and distributed across the different chapters in order to have a better understanding. These chapters are introduced with additional information in between texts to embed the individual studies into the wider context of the thesis.

I have renumbered the chapters, tables and figures of the published and submitted articles to harmonize the nomenclature in order to generate a consistent presentation within the thesis. The aerodynamic performance section is presented in Chapter 7 which originally belongs to the article submitted for for chapter 6. This bifarcation in presentation was used in order to have a better cohessivity of the thesis and a better understanding of the main theme of the work. For all the Chapters, one consolidated bibliography and one consolidated list of acknowledgements are presented in this thesis with an index at the end to guide the reader to different keywords and their presence in the thesis.

Signature: **Date:** April 09, 2019

Print Name: Mr Amlan Chakraborty

Thesis Chapter	Publication Title	Status	Nature and % of contribution	Co-author names, nature and % of co-author's contribution	Co-author Monash student?
1 and 2	Insights into endotoxin-mediated lung inflammation and future treatment strategies	Published	90% (concept, manuscript preparation)	1. Selomulya: 2% Discussion of manuscript	No
				2. Plebanski: 3% Discussion and guidance in manuscript development	No
				3. Royce: 3% Manuscript preparation, guidance, critical arguement	No
				4. Boer: 2% Discussion	No
1 and 2	Amino Acid Functionalized Inorganic Nanoparticles as Cutting-Edge Therapeutic and Diagnostic Agents	Published	85% (concept, manuscript preparation)	1. Selomulya: 5% Discussion and ideas	No
				2. Plebanski: 5% Discussion and guidance in manuscript development	No
				3. Boer: 5% Discussion and development of figures	No

The undersigned hereby certify that the above declaration correctly reflects the nature and extent of the student?s and co-authors? contributions to this work. In instances where I am not the responsible author I have consulted with the responsible author to agree on the respective contributions of the authors.

Main Supervisor Signature: **Date:** April 09, 2019

Print Name: Prof. Cordelia Selomulya

Contents

List of Figures

List of Tables

Abbreviations

2ME	2-Mercapto Ethanol
3D−UTE	3 Dimensional Utrashort Echo time
AB−PAS	Alcian Blue- Periodic Acid Schiff
AMREP	Alfred Medical Research Precinct
ANOVA	Analysis of Variance
APC	Antigen Presenting Cells
AHR	Airway Hyper Responsiveness
APC	Antigen Presenting Cells
ARDS	Acute Respiratory Distress Syndrome
ALI	Acute Lung Injury
BALF	Broncho Alveolar Lavage
BMDC	Bone Marrow Derived Dendritic Cells
CD	Cluster of Differentiation
cDyn	Dynamic compliance
DC	Dendritic Cells
DLS	Dynamic Light Scattering
DMEM	Dulbecco's Modified Eagle's Medium
dPmax	Maximum Dynamic Pressure
dPpl	Dynamic Pleural Pressure
EDX	Energy Dispersive Xray
FBS	Foetal Bovine Serum
FTIR	Fourior Transform Infrared Radiation
Gly	Glycine
GlyR	Glycine Receptor
GSPION	Glycine Conjugated Super- Paramagnetic Iron Oxide Nanoparticle

GM−CSF	**G**ranular **M**onocyte **C**ell **S**timulating **F**actor
H&E	**H**ematoxylin and **E**osin
Ig	**I**mmunoglobulin
IL	**I**nterleukin
in	**i**ntra **n**asal
ip	**i**ntra **p**eritoneal
IUPAC	**I**nternational **U**nion of **P**ure **A**pplied **C**hemistry
KO	**K**nock **O**ut
LPS	**L**ipo**p**oly**s**accharide
MDSC	**M**yeloid **D**ervied **S**uppressor **C**ell
MCh	Acetyl-β-**M**etha**c**holine
MFI	**M**ean **F**luorescent **I**ntensity
MHC	**M**ajor **H**istocompatibility **C**omplex
MRI	**M**agnetic **R**esonance **I**maging
NBF	**N**eutral **B**uffered **F**ormalin
NGI	**N**ext **G**eneration lung **I**mpactor
PAMP	**P**attern **A**ssociated **M**olecular **P**atterns
PBMC	**P**eripheral **Blood** **M**ono-nuclear **C**ells
PBS	**P**hosphate **B**uffered **S**aline
PI3	**P**hospho **I**nositide 3
PRR	**P**attern **R**ecognition **R**eceptor
RH	**R**elative **H**umidity
RPMI	**R**oswell **P**ark **M**emorial **I**nstitute
ROI	**R**egion **O**f **I**nterest
Rs	**R**esistance
SABA	**S**hort **A**cting β2 **A**gonist
SD	**S**tandard **D**eviation
SEM	**S**canning **E**lectron **M**icroscope
SHIP-1	**SH2**-containing **i**nositol 5? **p**hosphatase
TEM	**T**ransmission **E**lectron **M**icroscope
TGA	**T**hermo **G**ravimetric **A**nalysis
Th1	**T**ype 1 **T** **H**elper cell
Th2	**T**ype 2 **T** **H**elper cell

Th17	**T**ype 17 **T** **H**elper cell
TLR	**T**oll **L**ike **R**eceptor
TNF-α	**T**umor **N**ecrosis **F**actor α
VSM	**V**ibrating **S**ample **M**agnetometer
WT	**W**ild **T**ype
XRD	**X** **R**ay **D**iffraction
XRay-CT	**X** **R**ay- **C**omputerised **T**omography

Symbols

α	alpha
β	beta
δ	delta
Δ	Delta
°C	degree celcius
emu	**e**lectromagnetic **u**nit
ϵ	Epsilon
$\geqslant$	greater or equal to
g	**g**ram
G	**G**auge
γ	gamma
Hz	**H**ertz- unit of frequency
^{hi}	high expression of a marker
κ	kappa
kOe	**k**ilo **O**ersted- unit for auxillary magnetic field H
λ	lambda
^{low}	lower expression of a marker
ml	**m**illi **l**itre
mg/ml	**m**illi **g**ram per **m**illi **l**itre
mM	**m**illi Molar
mmol/l	**m**illi **m**ole per **l**itre; same as **mM**
mm^3	**m**illi-**m**etre cubed
μ**g**	**m**icro **g**ram
μ**g/ml**	**m**icro **g**ram per **m**illi **l**itre
μ**m**	**m**icro **m**etre

μ**l**	**mi**cro litre
nm	**n**ano **m**etre
$neg-lo$	Negative to low expression of a marker
®	**R**egistered
U/ml	**U**nit per **m**illi litre
ζ	**z**eta-potential
$+$	presence/expression of marker
$-$	absence of marker
$-/-$	functionally null alleles (representing knock out)
$+/+$	functionally wild type alleles

Chapter 1

Introduction

1.1   Background

I nflammatory lung diseases such as asthma and chronic obstructive pulmonary disease (COPD) are very common with over four million deaths per year(Ferkol and Schraufnagel, 2014). Apart from rising levels of pollution, other factors such as bacteria, irritants, avian-derived proteins and agricultural dust can lead to inflammation of the airway. The lung is a non-sterile organ as it is in direct contact with the outside environment including bacteria. Their cell walls are composed of lipopolysaccharide (LPS)/endotoxin, hence this is a major contributor to the development of airway inflammation(Allen, 2013; Knapp, 2009). However, immune recognition and response to LPS also play a role in the defense against invading Gram-negative bacteria. LPS is known to increase airway hyper-responsiveness(AHR)(Starkhammar et al., 2014). Airway hyperresponsiveness is defined by an exaggerated response of the airways to non-specific stimuli, which results in airway obstruction and contraction of airways triggered by bronchospasm. In addition, AHR results in airway mucus production and cytokines are released from allergen specific T cells which can further exacerbate symptoms of inflammation as well as perpetuate an allergic response.

In airway inflammatory disease such as asthma, impaired breathing due to bronchoconstriction leads to repeated/routine exacerbations which impact human health. Therefore, not only availability of anti-inflammatory drugs but proper management is essential. Current treatments include the use of bronchodilators with corticosteroids such as prednisone, beclomethasone, fluticasone in adults and cromolyn in children (Chakraborty et al., 2018). In adults, this is augmented by a short-acting beta-2-agonists and is considered as gold standard therapy. These drugs aim in reducing infiltration of neutrophils and eosinophils along with a reduction of proinflammatory cytokines. However, prolonged use of this treatment leads to impaired growth of children, decreased bone mineral density, skin thinning, bruising, and cataracts(Dahl, 2006). Albeit the treatment is successful in reducing exacerbations, yet there has been the issue of development of resistance(Barnes, 2013) and fails in a clinical setting due to increased risk of immunosuppresion potentially leading to increased risk of infection(Fardet et al., 2016; Desai et al., 2017; Coutinho and Chapman, 2011). Hence there is a requirement to develop newer anti-inflammatories associated with systemic or oral administration. Novel anti-inflammatories would cater to the pharmacotherapeutic considerations and give both an immediate and sustaining

effect without having adverse side effects.

The recent era of surface functionalized nanoparticles generated, and specifically amino acid coated particles are found to be biocompatible owing to their surface functionalization. Particle internalization is chemistry dependent where the charge and size matters in particle uptake by the APCs. The importance of particle size has been demonstrated by Plebanski and colleagues on polystyrene(Hardy et al., 2013) and Akagi and colleagues with 200 nm glutamic acid nanoparticles(Akagi et al., 2007). But the response with same smaller size glutamic acid particles by Hyungji and colleagues showed higher activation of the DCs hence finding potential use as antigen carriers and vaccine adjuvants(Kim et al., 2010a). There have been considerable developments in understanding the uptake by antigen presenting cells of biodegradable amino acid coated nanoparticles. With respect to charge, it has been shown $in-vitro$ that positively charged particles are taken up efficiently by DCs(Vela Ramirez et al., 2014). Macrophages demonstrate that their monocytic precursors show a preference for positively charged particles(Lunov et al., 2011). Altogether it is still unknown whether amino acid conjugated nanoparticles are able to provide simultaneously anti-inflammatory effects and long-term immuneimprinting to the tissue exposed. The mechanism underlying this phenomenon also needs to be investigated.

In light of the development of newer anti-inflammatories, Plebanski and colleagues have found 50 nm polystyrene nanoparticles coated with glycine are also easily taken up by pulmonary DC and in atopic animals this exposure renders the lung resistant to a subsequent challenge with allergen effectively preventing lung inflammation(Hardy et al., 2013). Furthermore, these 50 nm polystyrene nanoparticles were used as vaccine carriers which stimulate a type I immune response (characterized by $IFN-\gamma$ production) whereas larger (>100 nm) or smaller (<20nm) are far less effective(Hardy et al., 2013). Therefore, we investigated the role of glycine as an immunomodulatory agent and developed anti-inflammatories by conjugating glycine on biodegradable iron-oxide nanoparticles for pulmonary delivery.

1.2 Aims

This PhD thesis focuses on understanding the immunomodulatory role of glycine and subsequently on the development of immunomodulators for both immediate and sustained anti-inflammatory effect along with bypassing the mucociliary clearance (by disrupting mucus). The primary aim of this research is to investigate the immunomodulatory role of glycine *in-vitro* (specifically on Antigen Presenting Cells) and hence in a model of Acute Respiratory Distress Syndrome (ARDS) induced by LPS. Secondly, the aim was to develop immunomodulators capable of providing an immediate and sustainable anti-inflammatory effect as well as bypassing the mucociliary clearance for pulmonary nanoparticle delivery. Finally, we conclude this thesis by providing a proof of concept of these immunomodulators, harnessing them for effective pulmonary delivery to help treat and prevent airways inflammation. In addition to their pulmonary delivery, we also developed an approach for naturally targetting critical lung immune cells, without provoking respiratory changes or inflammation, and supported non-invasive magnetic resonance imaging of the lung. More specifically, the following aims are considered:

1. To investigate the immunomodulatory role of glycine *in vitro* achieved by investigation of:

   - The effect of glycine is investigated on APCs such as BMDCs and Macrophages.

   - The effect of glycine and LPS on costimulatory cell surface markers on APCs.

   - Glycine-mediated immunomodulation through a SHIP$^{-/-}$ mice, as it is well known that SHIP regulates the $NF - \kappa\beta$ transcription factor.

   - GlyR mediated immunomodulation, an insight on the possible mechanism.

2. To investigate the role of glycine in reducing airway inflammation, achieved by investigation of:

   - The effect of glycine in reducing LPS mediated ARDS is evaluated by invasive plethysmography to evaluate the lung function.

   - The expression of pro-inflammatory cytokines in the airways, lung parenchyma and scored for signs of damage.

   - Inflammatory cells in the BALF, to develop an insight on airway inflammation.

- Glycine treatment on airways and lung parenchyma.

3. To develop glycine immunomodulators to exert an immediate as well as sustaining effect on lung, achieved by developing:

    - Biodegradable super-paramagnetic iron oxide nanoparticles conjugated with glycine (GSPIONs) was synthesized and characterized for size, structure, crystallinity, magnetic property, dispersion and stability.

    - GSPIONs for pulmonary delivery and escaping the mucociliary clearance, glycine microparticles were designed by spray drying.

    - GSPIONs encapsulated in glycine microparticles as excipients to bypass the mucociliary clearance and delivery of GSPIONs to the periphery.

4. A proof of concept of the theranostic role of the developed immunomodulators along with a non-invasive lung imaging, achieved by:

    - A Next Generation Impactor (NGI) was used to determine the capability of the spray dried glycine microparticle based excipient to pass the oropharnygeal region and compared against the dense, solid commercial excipient Lactohale 200^{TM}.

    - Investigating the aerodynamic performance of the immunomodulators to support the NGI data in terms of aerodynamic performance.

    - Investigating the interaction of GSPIONs with lung immune cells.

    - Evaluating the use of GSPIONs for lung 3D UTE MR imaging and their biodistribution in order to consolidate our findings and define the future theranostic application of these immunomodulators.

1.3   Thesis Outline

Chapter 2: Literature Review

The literature review of this thesis focuses on Acute Respiratory Distress Syndrome, airway inflammation, specifically LPS mediated inflammation and its mechanisms. It also talks about the currently available therapeutics and their disadvantages citing the need to develop new immunomodulators. As LPS induced lung pathology is initiated by APCs, an insight to the different immune cells playing a role in responding to LPS

is reviewed. Furthermore, we introduce amino acid conjugated nanoparticles and their different applications such as in MR imaging and as immunomodulators. Finally, it summarises the literature in which LPS mediated ARDS is reviewed and the gaps in therapies are identified with a new strategy having a potential for the treatment of inflammatory lung diseases.

Chapter 3: Materials and Methods

This chapter outlines all the reagents, materials, types of equipment, biological models, methodologies, data analysis and statistics applied throughout this thesis.

Chapter 4: Immunomodulatory effect of glycine on Antigen Presenting Cells

To study the immunomodulatory effect of glycine on antigen presenting cells. Bone marrow derived cells have shown in the past to be activated in presence of lipopolysaccharide (LPS). We found that glycine can abrogate this effect. The scope of this chapter is limited to bone marrow derived cells to understand the immunomodulatory effect of glycine in general. This is extended to an understanding of glycine's immunomodulatory role involving SH2-containing inositol 5'- phosphatase (SHIP). This phosphatase regulates the $NF - \kappa\beta$ transcription factor which is involved in the production of activation markers and pro-inflammatory cytokines. We intend to determine if SHIP regulates TLR induced bone marrow derived DCs activation and glycine mediated immunomodulation. It will provide insights into the possible mechanism. Furthermore, glycine signals in the brain and spinal cord through a hetero-pentameric channel protein called as glycine receptor. We think that this receptor is actively involved in immune cells for the immunomodulatory effect, as we have some evidence of its presence on alveolar macrophages. Detailed mechanisms and receptor functionality are beyond the scope of this project as it is too broad.

Chapter 5: Role of glycine in attenuating airway inflammation

Based on our initial results in the previous chapter suggesting the immunomodulatory role of glycine in antigen presenting cells, we thought of investigating its role in attenuating airway inflammation. The airway is exposed to antigens (bacteria and its cell wall component, LPS) which are processed by the submucosal dendritic cells leading to activation and migration to lymph nodes. Therefore, we utilized a model of Acute Respiratory Distress Syndrome(ARDS) induced by LPS. ARDS is an acute lung disease characterized by rapid onset respiratory failure, severe hypoxemia and decrease in static respiratory system compliance which accounts for morbidity of around 40%. Pulmonary inflammation in the acute phase (1-6 days) is characterized by damaged endothelium and

surface epithelium along with oedema, with neutrophil and macrophage accumulation. Glycine was administered intra-nasally with or without LPS and the effect was quantified and observed by the improvement of resistance and dynamic compliance. Furthermore, histology and immunohistochemistry of paraffin embedded lung sections were studied to identify signs of inflammation and the secretion of pro-inflammatory cytokines such as $IL-1\beta$, $IL-6$, $TNF-\alpha$. To have an idea of the infiltration of immune cells post infection, we performed a differential cell count on the Broncho-Alveolar Lavage Fluid (BALF). Overall, this chapter provides information on the attenuation of the airway inflammation and the possible role of glycine preventing neutrophil infiltration.

Chapter 6: To develop glycine immunomodulators for pulmonary delivery

This chapter is on the development of glycine immunomodulators for pulmonary delivery of glycine to induce an immediate and sustained immunomodulatory effect in the lung. The sustained effect is achieved by glycine conjugated nanoparticles and the immediate effect is imparted by the microparticles formed by spray drying glycine. The nanoparticles synthesized are biodegradable made of iron oxide with a hydrodynamic size less than 100 nm. These nanoparticles are further encapsulated in spray dried glycine microparticles which are monodisperse, uniform and serve as excipients preventing mucociliary clearance of the nanoparticles by mucus disruption. This chapter summarises the development of the immunomodulators for pulmonary delivery and the use of spray dried glycine microparticles as excipient.

Chapter 7: Delivery of immunomodulators-Proof of Principle

This chapter provides a proof of concept that these immunomodulators are capable of pulmonary delivery. To understand the efficacy and aerodynamic performance of these immunomodulators to bypass the oropharyngeal region, we compared the GSPIONs encapsulated in spray dried glycine microparticles based excipient to that of commercial excipient lactohale $200TM$ by X-Ray CT and NGI. Both the methods are used to find the aerodynamic nature, porosity and deposition of the particles with respect to human pulmonary delivery. Furthermore, we explored the use of the developed immunomodulators for non-invasive lung MR imaging. Lung MR imaging is difficult as there is lack of hydrogen protons and water molecules, given it is full of air and the fast breathing rate of mice. We, therefore, developed a 3D ultra-short echo time MR imaging using the GSPIONs as MR contrast agents capable of showing their biodistribution. We also investigated the different cells which take up the immunomodulators and correlated with our results outlined in chapter 5. The results of this chapter are significant in translating

these immunomodulators to the clinic for theranostic applications and opens up new questions for further research.

Chapter 8: Conclusion and Future Recommendation

The closing chapter summarises the highlights of the results of each experimental chapter and the implications of the chapter to the thesis. This chapter also provides background and questions to pursue further work and provides insights on to studies needed to be done in order to translate these immunomodulators to the clinic.

Chapter 2

Literature Review

2.1   Inflammation of the airway

Inflammation is a phenomenon of the body in the form of an immediate response to triggers like tissue injury, infection by pathogens or by noxious chemicals(Ashley et al., 2012). Based on the duration of response, inflammation is characterised by acute and chronic inflammation. Acute inflammation is generally short term with an early (IgE mediated hypersensitivity type I reaction) and late phase reaction associated with T_H2 cells(Galli et al., 2008). Acute inflammation lasts for around two days, and symptoms are dependent on the region of inflammation such as bronchial smooth muscle contraction(Kay, 2001) due to various types of airway allergens. On the other hand, chronic inflammation lasts for over six months. Chronic inflammation is a feature of both asthma and COPD. In patients with COPD, it has been found that $IL-33$ is responsible for chronic inflammation and leads to enhanced secretion of proinflammatory cytokines(Shang et al., 2015). Similarly, IL-33 is responsible for increased AHR, inflammation and remodelling in asthma(Sjöberg et al., 2017). However, persistent exposure to a certain allergen result in the recruitment of cells of the innate and adaptive immune response to the site of exposure(Galli et al., 2008). The nature of inflammation is different in asthma and COPD. In asthma, the nature of inflammation is driven by the infiltration of eosinophils and $CD4^+$ T cells. Whereas, in COPD, it is mostly driven by neutrophils and $CD8^+$ T cells(Buist, 2003). The chronic inflammation in asthma is alluded to frequent wheezing episodes with increased AHR and coughing, whereas in COPD it is more of limited airflow to the lung.

The most obvious effect observed with airway inflammation is the recruitment of eosinophils. T_H2 lymphocytes release interleukin 5 (IL-5) which attracts, activates and stimulates eosinophils, therefore, perpetuating the inflammatory response(Greenfeder et al., 2001). In the inflammatory response, the airway walls become thickened due to hypertrophic and hyperplastic mucous glands as well as infiltration of macrophages, neutrophils and cytotoxic T lymphocytes as well as proliferation of resident structural cells in the chronic setting(Aoshiba and Nagai, 2004; Moldoveanu et al., 2009). Cytokines such as interleukin 8 (IL-8), tumour necrosis factor α ($TNF-\alpha$ are released by the inflammatory cells leading to tissue damage and oxidative stress. The entry of an allergen is associated with a complex response in the host as different immune cells play their role in dealing with the allergen. The understanding of the cells and the cytokines they produce can serve

as therapeutic targets. Therefore, we need to gain insight on how airway inflammation takes place after allergen entry.

2.1.1 Mechanistic insights in airway inflammation

The airway lumen contains mucus for the entrapment of dust particles. But is still exposed to antigens (bacteria and its cell wall component, LPS) which are processed by the submucosal dendritic cells leading to activation and migration to lymph nodes. The immune response to acute inflammation sensitizes the mast cells in the individual due to the production of IgE specific to the antigen (Figure 2.1). Although the response is seen in the mast cell, the T_H2 cytokines actively play a role in activating the B cells for the production of the antigen-specific IgE(Galli et al., 2008). The sensitization releases mediators including amines like histamines and serotonin. This series of steps induce bronchoconstriction of the airway and vasodilation (Figure 2.2). As a result, there is increased mucus formation and stimulation of the nociceptors on the airway. The production of several cytokines by T_H2 cells results in the activation of B cells (Figure 2.1) which is responsible for the synthesis of allergen-specific antibodies. The antibodies in the systemic circulation move from the lymph node and bind the $Fc\mathcal{E}RI$ receptor (Figure 2.1) on the mast cell. When a second invasion of the allergen is encountered, the host is already sensitized, and the response is very rapid.
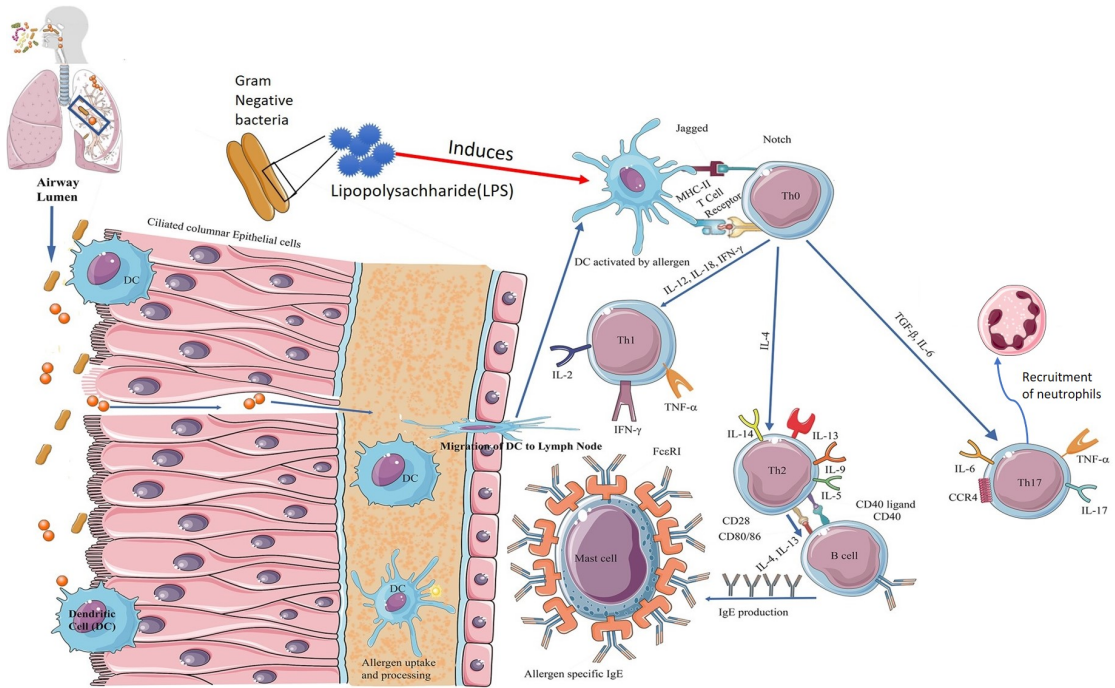
FIGURE 2.1: **Sensitization of dendritic cells by allergens in the airway lumen**. Different bacteria enter through the nasal cavity into the lung. In the airway lumen, these bacteria are captured by the patrolling DCs. The DCs become activated by the cell wall component LPS of gram-negative bacteria. The mature DCs then migrate to the regional lymph node such as the mediastinal lymph node for lungs. At the LN they present the processed allergen by MHCII to naïve T cells. The naïve T cells acquire the characteristics of T_H2 cells by the interaction of MHCII and jagged receptor on activated DC to TCR and Notch receptor respectively on naïve T cells. Two important T_H2 pro-inflammatory cytokines $IL-4$ and $IL-13$ lead to ligation of costimulatory molecules CD40 and CD80/86 on T_H2 cells with CD40 L and CD28 on B cells. The activation leads the B cells to produce allergen-specific IgE which binds to the high-affinity receptor $FC\epsilon RI$ on tissue-resident mast cells. The process sensitizes them to respond when the host is later exposed to the same bacteria and/or LPS. Modified and reproduced with permission from (Chakraborty et al., 2018), copyright 2018 Taylor and Francis.

In addition, mast cells rapidly release TNF, IL-8, $TGF - \beta$, $IL - 10$ for the activation of other immune cells like T cells, B cells and DCs(Bradding et al., 2006). The hypersensitivity reaction develops in two to six hours after exposure and reaches the climax after six to nine hours(Kay, 2001). Although there is a clear distinction between acute and chronic inflammation phases, it is yet unclear how local inflammation in the airway converts to chronic inflammation. Cytokines such as $IL - 33$ have been found to induce chronic inflammation in the airway epithelium along with the enhanced production of $IL-6$ and $IL-8$ in COPD pathogenesis(Shang et al., 2015). Several layers of the airway mucosa are affected by chronic asthma with increased numbers of goblet and mast cells along with the presence of common respiratory viruses (Figure 2.2)(Folkerts et al., 1998).

Another aspect of airway inflammation is the recruitment of neutrophils. Cells secreting $IL - 17$ (i.e. T_H17 cells) recruit neutrophils at the mucosal surface(Pelletier et al., 2010)(Figure 2.2). Because of neutrophil recruitment, there is constriction of the smooth muscle in the airway wall causing shortening of breath, in patients with COPD(Baraldo et al., 2004). Along with lumen constriction, airway remodelling is also observed in both COPD and asthma. Airway remodelling is driven by the epithelial-mesenchymal trophic unit (EMTU), the interaction between structural and immune cells. Due to the increased number of neutrophils in COPD patients, there is activation of the EMTU. A successful response to an allergen is associated with its elimination, resolution and repair phase. The inducer of inflammation can be categorised into exogenous and endogenous inducers(Medzhitov, 2008). Exogenous inducers include microbial and non-microbial inducers like irritants, foreign bodies and toxins. Endogenous inducers are released from stressed or damaged cells such as heat shock proteins, uric acid and endogenous molecules like alarmins(Chan et al., 2012) etc. reviewed in detail by Creagh and colleagues(Creagh and O'Neill, 2006). In the coming section, we will focus on bacterial endotoxin-mediated inflammation in the airway.
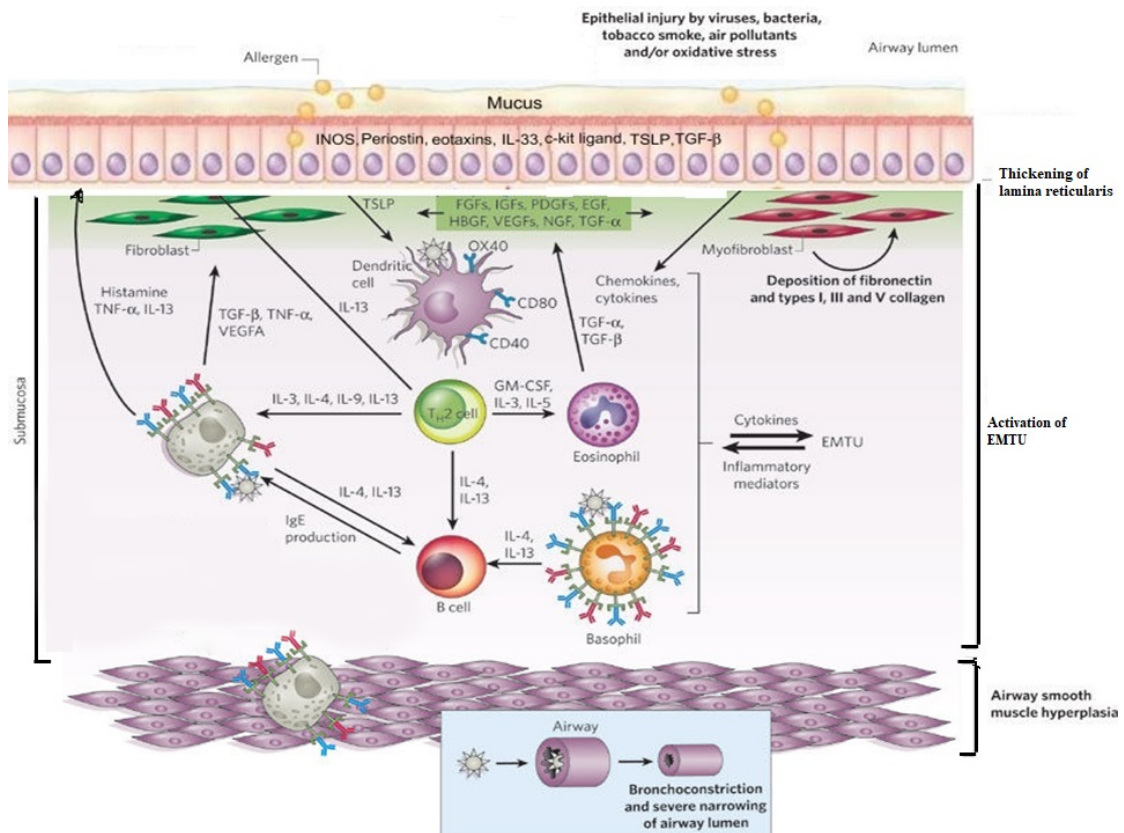
FIGURE 2.2: **The chronic aspect of allergen-induced airway inflammation.**
Repeated and persistent exposure of allergens such as bacteria leads to chronic inflammation which has several effects. In the tissues, cells of the innate immune system including eosinophils, basophils, neutrophils and monocyte–macrophage lineage cells are found. Other cells including T_H2 cells, other types of T cells, and B cells of an adaptive immune response are also present in the tissues. Mast cells develop in the tissue, and these cells display large amounts of IgE bound to $Fc\epsilon RI$. Last, complex interactions are initiated between recruited and tissue-resident innate and adaptive immune cells, epithelial cells and structural cells. These cells include fibroblasts, myofibroblasts and airway smooth muscle cells along with blood vessels and lymphatic vessels. Repetitive epithelial injury due to chronic allergic inflammation can be exacerbated by exposure to pathogens or environmental factors, and the consequent repair response results in the epithelial–mesenchymal trophic unit (EMTU) being activated. This unit is thought to sustain T_H2-cell-associated inflammation, to promote sensitization to additional allergens or allergen epitopes (for example, epithelial-cell-derived TSLP can upregulate the expression of co-stimulatory molecules such as CD40 and CD80 by dendritic cells). These processes result in many functionally important changes in the structure of the affected tissue such as hyperplasia of goblet cells, which is associated with increased mucus production. These changes include substantial thickening of the airway walls. In individuals who have such thickened airway walls, bronchoconstriction can result in more severe narrowing of the airway lumen than occurs in airways with normal wall thickness. In some individuals, especially those with severe asthma, T_H17 cells (which secrete IL-17) may also contribute to the recruitment of neutrophils to sites of inflammation (shown in Figure 2.1). Modified and reproduced with permission from (Chakraborty et al., 2018), copyright 2018 Taylor and Francis.

2.1.1.1 Bacterial endotoxin-mediated airway inflammation

A range of bacteria such as *Staphylococcus aureus*, *Pseudomonas aeruginosa*, *Streptococcus pneumoniae*, *Klebsiella pneumoniae*, *Mycobacterium tuberculosis* cause pathological lung infections. In response to infection and tissue injury, innate immune cells of the body such as DCs, macrophages and mast cells recognise pathogens and damaged cells by Pattern Recognition Receptors (PRRs) which are germline-encoded intra-cellular or surface expressed. These PRRs detect Pathogen Associated Molecular Patterns (PAMPS) such as bacterial and viral nucleic acids and cell wall components. The toll-like receptor (TLR) family is one of the major PRRs that can detect pathogens as well as tissue damage. It induces both innate (immediate) and adaptive immune responses. Whilst the adaptive immune response results in B cells and cytotoxic T cells, it is the innate cells which offer the first line of recognition of pathogens by the TLRs. The TLRs have leucine-rich repeats and can recognise bacterial and viral PAMPs extracellularly or through endo-lysosomes. TLR1, TLR2, TLR4, TLR5, TLR6, TLR11 are extracellular whereas TLR3, TLR7, TLR8, TLR9 and TLR10 are endo-lysosomal.

Lipopolysaccharide is the main agonist of Toll-Like Receptor 4. LPS binds to LPS binding protein (LBP), MD-2, CD14 and TLR4. Therefore, stimulation using LPS needs the participation of several molecules, not just TLR4. The signalling downstream upon LPS binding has been divided into MyD88 dependent and independent pathways. The MyD88 dependent pathway results in pro-inflammatory cytokines production whereas the MyD88 independent pathway mediates the induction of Type I interferons. MyD88 recruits and activates IRAK4 which after subsequent downstream activation induces the transcription factors $NF - \kappa\beta$ and AP1. This results in the production of pro-inflammatory cytokines such as $TNF - \alpha, IL - 1\beta, IL - 6, IL - 12, IL - 23$ and activation markers such as $CD40, CD80, CD86$ and $MHCII$. The LPS-TLR4 pathway has been reviewed elsewhere(Lu et al., 2008).

Toll-Like Receptor 2(TLR2) responds to the cell wall of Gram-positive bacteria which is composed of peptidoglycan(Yoshimura et al., 1999). The TLR2 response activates cytotoxic $CD8^+$ T cells and produces $IFN - \gamma$. In alveolar macrophages, the expression of TLR2 and TLR4 are reduced in patients with COPD and in smokers(Droemann et al., 2005) in comparison to autologous monocytes. Continuous exposure to LPS

present in cigarette smoke (cell wall from colonised bacteria, surviving combustion during smoking) may down-modulate the pulmonary immune response(Droemann et al., 2005). The reason could be due to the natural selection of a heterogeneous subpopulation of macrophages or a general alveolar macrophage phenotype under environmental stress. The reduced expression of these TLRs means that COPD patients are much more prone to lower respiratory tract infection. Bacterial infection is not only associated with the bacterial cell wall, other components such as flagella are also important (recognised by TLR5(Zhang et al., 2005)). Therefore, the Toll-like receptors have a significant role in recognition of a pathogen and responding via downstream signalling. Interaction of antigen presenting cells with LPS is essential in understanding the adaptive immune response.

When monocytes and DCs come in contact with a PRR, they express costimulatory molecules for T lymphocyte activation and are said to induce an adaptive immune response(Thompson et al., 2011). In an analogous way, macrophages undergo cell activation in response to LPS or $IFN - \gamma$(Dobrovolskaia et al., 2003). When immature macrophages circulating in the blood come across bacterial or viral infections or bacterial components such as LPS they undergo activation. Studies of these cells of the innate immune system by Thompson et al and others have revealed that the subsets have specialised in secreting cytokines that have different targets and function. For example, macrophages secrete pro-inflammatory cytokines which include $IL - 1, IL - 6, IL - 12, TNF - \alpha$ and $IFN - \gamma$(Thompson et al., 2011). Other than these cytokines, $IL - 8$ secretion leads to infiltration by neutrophils and $TNF - \alpha$ leads to increased production of cell adhesion molecules in the lung capillary endothelial cells for neutrophil attachment. Neutrophils are self-recruiting, secreting $IL - 8$ themselves to promote chemotactic invasion of more neutrophils(Takahashi et al., 1993).

2.1.2   Role of LPS in Acute Pulmonary Inflammation

Acute pulmonary inflammation has a high mortality rate with the absence of specific treatment. Acute lung injury(ALI) is defined as an acute lung disease characterised by rapid onset respiratory failure, severe hypoxemia and decrease in static respiratory system compliance which accounts for morbidity of around 40%(Matthay and Zemans, 2011). Pulmonary inflammation in the acute phase (1-6 days) is characterized by damaged endothelium and surface epithelium along with oedema, with neutrophil and macrophage

accumulation. The clinical condition of pulmonary inflammation is known as Acute Respiratory Distress syndrome (ARDS) which is characterized by sepsis, pneumonia and major trauma. The severity of ARDS can be attributed to its diverse demographic occurrence throughout the world with 34 per 100,000 persons per year in Australia and 78.9 per 100,000 persons per year in the USA(Walkey et al., 2012).The injury to the lung epithelium and endothelium is caused primarily by neutrophils and platelets respectively. However, there is a lack of successful pharmacologic therapy. The pathophysiology and resolution of ARDS have been reviewed previously(Matthay and Zemans, 2011). Therefore, the role of neutrophils in initiating the inflammation and the damage it causes needs to be understood.

Neutrophils are the first immune cells to reach the site of inflammation in the lung post an insult with LPS. Transmigrated neutrophils then secrete proteolytic enzymes and reactive oxygen species (ROS) which damages the lung endothelium and epithelium. The harm does not end in oedema. The ROS leads to promutagenic alterations in DNA and causes a carcinogenic response post chronic inflammation. Transcriptome analysis by Gungor and colleagues showed 218 genes which are differentially expressed with LPS induction in the presence of neutrophils(Güngör et al., 2010). Many pathways were found altered. Importantly complement pathways, CCR3 signalling, $IL - 10$ signalling and antigen presentation by MHCI were altered between LPS with and without neutrophils. CCR3 is responsible for eosinophil activation pointing towards a chronic inflammatory state. Whereas, $IL - 10$ a pleiotropic anti-inflammatory cytokine represses the pro-inflammatory cytokines such as $TNF - \alpha$, $IL - 6$ and $IL - 1\beta$secreted by macrophages. Pharmacotherapeutic studies using proteins such as B7H3 and bufexamac has shown potential in attenuating LPS-induced injury(Li et al., 2016; Xiao et al., 2016). This opens the possibility of utilising these molecules in ameliorating the clinical condition of pulmonary inflammation. Vascular compartments, pulmonary tissue and the underlying endothelial cells are also affected by LPS. Since LPS affects vascular compartments and pulmonary tissue therefore, the factors which alter them needs to be studied.

It has been observed that higher concentrations of endotoxin similar to that present in sepsis exhibits several pro-inflammatory responses. These responses include the increased expression of cell adhesion molecules, ROS production, loss of endothelial monolayer integrity and barrier function(Stoll et al., 2004). ROS generated in the vasculature

from endothelial cells are produced from a family of oxidases. These oxidases, specifically NADPH oxidases (Nox) are involved in lung inflammation, ischemia and sepsis. Two Nox enzymes, Nox2 and Nox4 are responsible for endothelial cell migration and production of ROS(Pendyala et al., 2009). Redox -active endosomes in endothelial and other pulmonary cells generate superoxides in the endosome lumen in response to pro-inflammatory cytokines $TNF - \alpha$ and $IL - 1\beta$. The loss of mono-layer integrity of endothelial cells leads to leaking of the lung capillaries and as a result, the fluid fills up the alveolar airspace causing pulmonary oedema. The protein thrombomodulin(TM) and activated protein C(APC) are involved in maintaining homeostasis and vascular integrity(Ikezoe, 2015). LPS induces the expression of tissue factor (TF) on vascular endothelial cells causing hypercoagulability. The TM/ APC axis is also affected with LPS. A lectin-like domain in thrombomodulin is essential for the survival of mice exposed to LPS. The absence of the domain leads to neutrophil infiltration. In the naïve lung, the polymorphonuclear leukocytes appear to be marginated to the vascular wall. During inflammation, immune cells and pre-marginated cells undergo transendothelial and transepithelial migration into alveolar space and the interstitium in the lung.

2.1.3 Acute Lung Injury (ALI) model to understand the clinical condition of ARDS

Acute lung injury is characterized by alveolar epithelial and endothelial damage. This leads to secretin of pro-inflammatory mediators in the host along with severe hypoxemia, pulmonary oedema. To study the pathophysiological mechanism of ALI, treatment of laboratory animals with bacterial LPS is the most accepted model. LPS can be administered directly or indirectly to give injury to the lung. Direct administration of LPS into the lung involves intratracheal or intranasal administration, otherwise, it is administered intraperitoneally. Direct injury to the lung affects the lung epithelium, whereas, an indirect injury leads to disruption of the vascular endothelium. Not limited to this, there are several differences between direct and indirect challenge such as less oedema is observed in indirect injury which has been reviewed by others(Shaver and Bastarache, 2014). Administration of LPS directly in the lung leads to neutrophil recruitment within four hours and induces the production of pro-inflammatory cytokines, chemokines, activation markers and adhesion molecules leading to damage to the lung tissue. The acute lung injury model is reviewed elsewhere(Johnson and Matthay, 2010; Matute-Bello et al., 2008).

The ALI model is useful for studying lung inflammation but needs the addition of specific endpoints to replicate the physical aspects of the disease. For example, introducing plethysmography as a readout for resistance and dynamic compliance is useful when demonstrating the severity of the disease. Other non-invasive techniques such as nebulization is effective in administering LPS. The method is of clinical relevance in studying and designing trials. With fluorescent molecules which can be conjugated to antibodies, it is possible visually study emphysema and airway constriction. Therefore, live imaging of the tissue coupled with plethysmography would be an ideal solution to understand lung injury in detail and for the development of minimally invasive ways to study drug responses.

2.2 The myeloid system

Myeloid lineage cells are usually the first to respond to the invasion of a pathogen and communicate the presence of an insult to cells of the lymphoid lineage. Their origin lies with the multipotent hematopoietic stem cells. Myeloid cells can recognize damage and PAMPs through the help of germline-encoded surface receptors. When the cells lose their ability to self-renewal they are committed to one single type of development. The myeloid lineage comprises of neutrophils, basophils, eosinophils, monocytes, mast cells and dendritic cells. The commitment associated with progenitor cells depends on the growth factors and cytokines. As discussed above, when induced they express costimulatory molecules for T lymphocyte activation. A network of cells is present in the bone marrow which is responsible for providing the microenvironment for haematopoiesis; these are known as stromal cells(Kindt et al., 2007). The primary and most significant function of the myeloid system is in providing innate immunity to the body(Janeway et al., 2001). The receptors of the cells participating in innate immunity recognize broad structural motifs that are highly conserved within microbial species but are generally absent from the host. These receptors are the pattern recognition receptors (described previously in section 2.1.1.1). The cells of the innate immune system have been found to secrete cytokines that have different targets and function. For example, the cytokines secreted by the macrophages in the next section include pro-inflammatory cytokines such as $IL-1$, $IL-6$, $IL-12$, $TNF-\alpha$, $IFN-\gamma$(Janeway et al., 2001).

The formation of all lymphoid cell types including monocytes, macrophages and dendritic cells (DC) have originated from human multi-lymphoid progenitors identified as a distinct population of $Thy-1^{neg-lo}$ CD45RA$^+$ cells in the CD34$^+$CD38$^-$ stem cell confinement(Doulatov et al., 2010). Therefore in humans, these myeloid lineages arise specifically in early lymphoid lineage. Lymph node-resident DCs (LN-DCs) is subdivided into conventional DC (cDC) subsets in mice. The subsets are CD11b and CD8a in mice whereas in humans they are BDCA1 and BDCA3. Robbins and colleagues hence showed through clustering analysis that a distinct branch is formed in the leukocyte family with a conserved transcriptional signature in all LN-DC subsets(Robbins et al., 2008). The myeloid progenitor cells giving rise to monocytes have macrophages and dendritic cells as their subtypes. Several surface markers like CD14, CD40, CD11b. CD64, CD68 and F4/80(murine) or EMR1(human), Lysozyme M, MAC-1/MAC-3 are found on macrophages which help researchers to distinguish them from monocytes(Khazen et al., 2005). Dendritic cells and macrophages share a common origin (the myeloid progenitor) but macrophages remain fixed in the tissue and DCs migrate towards the site of infection. Also, macrophages can be identified by the expression of CD64 in humans(Zaba et al., 2007). Studying the expression profile of human DCs, it has been determined that MHCII is highly expressed, whereas lineage markers like CD3 (for T cells), CD19/20 (for B cells) and CD56 (for NK cells) are absent and therefore DCs have been further classified according to these markers(Ziegler-Heitbrock et al., 2010).

2.2.1 Macrophage differentiation and subtypes

During the early stages of inflammation CCR2^{hi}Ly6C$^+$ inflammatory and CCR^{low}Ly6C$^-$ resident monocytes differentiate into M1 and M2 macrophages respectively(Auffray et al., 2007) (see Table 2.1). It is possible that monocytes, macrophages and DC are highly plastic and can cross-differentiate into different subsets in response to environmental changes by activating diverse pathways. For example, (i) Ly6C downregulation is associated with M2 macrophage function(Arnold et al., 2007), (ii) Ly6C$^+$ monocytes preferentially differentiate to CXC3CR1^{hi} macrophages(Rivollier et al., 2012), (ii) CCR7 and CCR8 Ly6C^{middle} macrophages differentiate into DCs(Qu et al., 2004), (iv) and anti-inflammatory M2 macrophage induction can be promoted from inflammatory monocytes by basophil-derived $IL-4$ at sites of inflammation(Egawa et al., 2013). When imma-

TABLE 2.1: **A summary of phenotypic and functional markers on murine macrophages and its subsets.** The development of each subset, its function, phenotypic and functional markers, cytokines and chemokines produced.

Subset	Cell development	Function	Surface Markers	Cytokines produced	Chemokines induced	References
			MACROPHAGE			
M1	They are formed from Monocytes when induced with LPS or $TNF-\alpha, IFN-\gamma$ in the presence of GM-CSF	These cells promote the development of T_h1 lymphocytes. They also promote metabolism of arginine into nitric oxide and citrulline. Therefore they play a key role in killing of pathogens and tumor cells.	They express prototypic M1 polarization markers, such as the indoleamine-pyrrole 2,3 dioxygenase; the lysosomal-associated membrane protein 3; IL-7R; CD86; MHCII; CD16/32; CD38; Gpr18; Fpr2; CD80; IL-1R I; TLR2; TLR4.	They produce proinflammatory cytokines: TNF-α, IL-1β, IL-6, IL-12, IL-23. Other secretions include ROS, RNS and iNOS	They secrete chemokines such as CCL2, CCL3, CCL4, CCL5, CCL8, CCL9, CCL10, CCL11	Gordon (2003); Gordon and Taylor (2005a); Martinez et al. (2008, 2006); Kigerl et al. (2009); Hissong et al. (1995); Jablonski et al. (2015); Duluc et al. (2007); Hao et al. (2012); Gundra et al. (2014)
M2	M2a- IL-4, IL-13	M2a secretes chemokines which leads to the buildup of T_h2 cells, eosinophils, basophils.	They express Arg1, CD206, Egr2, c-Myc; CD163; MHCII; SR; MR; TGM2; DecoyR; IL-1R II; Mice(only): Ym1, Fizz1, Arg1	They produce IL-10, $TGF-\beta$, IL-1Ra	They produce CCL17, CCL22, CCL24	Kigerl et al. (2009); Jablonski et al. (2015); Duluc et al. (2007); Hao et al. (2012); Gundra et al. (2014)
	M2b- LPS, ICs, ApC, IL-1Ra	M2b macrophages promote recruitment of Tregs and eosinophils that support a T_H2 response.	They express Arg1, CD206, Egr2, c-Myc; CD86; MHCII	They produce $TNF-\alpha$, IL-1b, IL-6, IL-10	They only produce CCL1	Kigerl et al. (2009); Duluc et al. (2007); Hao et al. (2012)
	M2c- IL-10, $TGF-\beta$, Gluc	They promote the development of T_H2 lymphocytes and Tregs. Promotes tissue regeneration and angiogenesis.	They express Arg1, CD206, Egr2, c-Myc; CD163; TLR1; TLR8	They produce IL-10, $TGF-\beta$	They only produce CCR2	Kigerl et al. (2009); Hao et al. (2012); Duluc et al. (2007)
	M2d induced by IL-6, LIF, MCF	Their function is similar to Ovarian TAMs but different from the other subsets	They express VEGF	They produce IL-10, IL-12, $TNF-\alpha, TGF-\beta$	They produce CCL5, CXCL10, CXCL16	Duluc et al. (2007); Hao et al. (2012)

Subset	Cell development	Function	Surface Markers	Cytokines produced	Chemokines induced	References
Alveolar Macrophages	Develop from fetal monocytes during embryogenesis. GM-CSF induces expression of $PPAR - \gamma$ which leads to differentiation into alveolar macrophages.	Primary phagocytes of the innate immune system clearing infectious, toxic and allergic particles. Recruits activated neutrophils into the alveolar spaces.	$CD11c^{hi}Mac - 1^{-/lo}$, and were $c-fms^+$ and $Ly6c^-$	IL-1; IL-6, $TNF - \alpha$	Arachidonic metabolites, IL-8	Gleissner et al. (2010)
M4	CXCL4	Suppressed phagocytosis. Expression of Proatherogenic and anti-atherogenic genes along with a higher expression of MMP7 and MMP12. Promote cholesterol efflux.	SR-A, CD86, MHCII, CCR7, TLR2, TLR4.	IL-6, IL-12, IL-10, $TNF - \alpha$, TN-FSF10(TRAIL), iNOS, Arg1	CCL1, CCL2, CCL5, CCL18, CCL22	Gleissner et al. (2010)
Regulatory	LPS, ICs	Parasite persistence; IL-10 produced leads the macrophage to an activating effect of $IFN - \gamma$ and hence prefers the release of IL-4 and IL1-10 by T cells. Modulate inflammatory immune responses, and thereby limit tissue damage.	CD206 but no other reliable, stable markers have been identified till date	IL-4, IL-10- high levels and low levels of IL-12, IL-23	CCL18, HB-EGF	Miles et al. (2005); Edwards et al. (2006, 2009); Fleming and Mosser (2011)
$CD4^+/CD8^+$	GM-CSF in a dose dependent manner	Able to kill tumor cells in a dose dependent manner without MHC restriction	FasL, perforin, Granzyme b, NKR-P2(rat homolog of human NKG2D).	IL-18, $IFN - \gamma$, RANTES	Non-significant Monocyte Derived chemokine (MDC)	Baba et al. (2006)

Subset	Cell development	Function	Surface Markers	Cytokines produced	Chemokines induced	References
Tumor-associated (TAM)	LPS; pro-inflammatory cytokines: IL-1, IL-6, $TNF-\alpha$, and chemokine CCL3	Found in stroma of tumors, these cells are able to regulate either positively or negatively the growth of various malignant cells.	Resting, TAM: phagocytosis mediated receptors- Msr2, C1q	Resting TAM: immuno-suppressive cytokines: IL-10, $TGF-\beta$	$IFN-\gamma$ induced chemokines: CCL5, CXCL9, CXCL10, CXCL16	Biswas et al. (2006); Mantovani et al. (2002); Ohno et al. (2003)
Tissue resident	CSF1R, M-CSF	Clearance of cells like erythrocyte(along with its nuclei during maturation), apoptotic cells; development of bone degradation and angiogenesis; regulation of metabolism like in insulin sensitivity and thermogenesis in adipose tissue; immune patrol; clearance of inflammatory debris; initiating inflammation and regulation of tissue homeostasis	Depends on location and function of the tissue. A wide range of markers included in this category are: $F4/80^+, CD45^+, CX3CR1^+, Ly-6c^{lo}, CD169^+, ER-HR3^+, CD11b^+, CD163^+, CD45^{hi}, CD11c^+, CD64^+, Galectin-3^+, CD80^{lo/-}, PPAR\delta, SiglecF^+, MARCO^+, CD206^+, Dectin1^+, Tim4^-, MHCII^{hi}, Langerin^+$ etc.	Pro-inflammatory cytokines: IL-8, MIP-2, $TNF-\alpha$	CCL5, CXCL9, MCP-1	Kurosaka et al. (2001); Iijima and Iwasaki (2014); Davies et al. (2013)
Small	LPS	Found in sputum of patients with CF and COPD. Also an increased level is seen in paediatric CF bronchoalveolar lavage	$CD14^+, CD45^+, HLA-DR^+, CD66b^-, CD68^+$	Pro-inflammatory cytokine $TNF-\alpha$	-	Garratt et al. (2012)
Alveolar	LPS, IL-4, $IFN-\gamma$	There function is to clear pathogens and particulates without inducing inflammatory response that may affect gaseous exchange. Associated with diseases like COPD, Asthma, Idiopathic pulmonary fibrosis. They have a dual role in lung cancer by promoting and/or inhibiting tumor growth. They play a key role in determining viral lung infections	$CD200^+$, scavenger receptors, $CD64^+$, MER (by monocyte-derived alveolar macrophages only)	Pro-inflammatory cytokine $TNF-\alpha$, IL-6,IL-13,NOs,Arg-1,$TGF-\beta$	-	Morales-Nebreda et al. (2015); Leema George et al. (2014); Almatroodi et al. (2014); Pribul et al. (2008)
Interstitial lung	LPS, $IFN-\gamma$	They are involved in daily homeostasis and protection against continuous pathogen exposure from the environment. Unavailability or depletion of these cells correlates with AIDS progression and pulmonary tissue damage	$HLA-DR^{hi}, CD11b^{hi}, CD163^+$	Pro-inflammatory cytokine $TNF-\alpha$	-	Cai et al. (2014)

ture macrophages encounter an infection or LPS they undergo activation. A classically-activated macrophage refers to an M1 macrophage that has been activated in response to LPS or $IFN - \gamma$ (Gordon, 2003). Cell activation of macrophages by T_h1 cytokines $IFN - \gamma$ and $TNF - \alpha$ is type I activation where the cytokines produced by M1 macrophages are $IL-1\beta, IL-12, IL-6, TNF-\alpha$. Alternatively, activated macrophages are also called M2 macrophage which refers to macrophages having undergone cell activation in response to IL-4 or glucocorticoids producing cytokines IL-10, IL-1ra and $TGF-\beta$(Ma et al., 2014)(Table 2.1). It has been found that M1 macrophages have more expression of IL-12 and IL-23 but low IL-10 with immunostimulatory properties for T_h1 cell activation. Similarly, M2 macrophages have a higher IL-10 and CD206 expression but lower levels of IL-12 and IL-23 but express scavenger receptors which M1 macrophages do not(Martinez et al., 2006). M2 macrophages are bestowed with a pro-antigen presenting capacity, promote angiogenesis, tissue remodelling and repair, suppressing immunity involving T_h1 cells. They support the T_h2 cell response which is deemed necessary for encapsulating and killing parasites where the M2 macrophages are activated by IL-4 and IL-13(Martinez et al., 2008). Receptor expression in M2 macrophages is specific and higher expression of mannose receptor 1, Dectin-1 and arginase has been found(Gordon and Taylor, 2005b).

Another category of macrophage known as M4 macrophage (Table 2.1) is induced by the chemokine CXCL4 from platelets(Gleissner et al., 2010). A separate subset of macrophages, CD4^{+} and CD8^{+} macrophage kill tumour cells by a mechanism involving NKG 2D receptors, granzymes and perforin(Baba et al., 2006). In the tumour microenvironment, different cells provide support to the tumour cells during the transition to malignancy. The macrophages present in the tumour microenvironment plays a pro-tumoral role and are called as Tumour Associated Macrophages. The TAMs originate from the circulating Ly6C^{+} CCR2^{+} monocytes, which are derived from bone marrow hematopoietic stem cells(Liu, Li and Xu, 2014). TAMs in the resting stage express immune-suppressive cytokines IL-10, phagocyte related receptor Msr2 and C1g, inflammatory cytokines CCL2 and CCL5 and chemokines CXCL9, CXCL10, CXCL16 where the expression is inducible by interferons. During the activation of TAMs by LPS, several pro-inflammatory cytokines such as $IL - 1\beta$, $IL - 6$, $TNF - \alpha$ and chemokine CCL3 was aberrantly expressed but upregulated the expression of immune-suppressive

cytokines $IL-10$, $TGF-\beta$ as well as IFN inducible chemokines CCL5, CXCL9, CXCL10, CXCL16(Biswas et al., 2006).

2.2.1.1 Alveolar macrophages

Alveolar macrophages defend the body against any pathogens or allergic particles, infectious agents and toxins by preventing their entry through the nasal route (see Table 2.1). They remain in the lung and do not migrate to the lymph nodes, unlike DCs. Alveolar macrophages secrete a range of cytokines eg: $IL-1\beta$, $IL-6$, $TNF-\alpha$ and chemokines including $IL-8$ along with arachidonic metabolites(Haslett, 1999). Alveolar macrophages take up inhaled antigens. Polymorphonuclear neutrophils undergo apoptosis during resolution of inflammation and hence several surface markers like phosphatidylserine, loss of sialic acid residues on antigens, and lowered expression of surface CD16 moieties takes place(Schagat et al., 2001). When these neutrophils undergo phagocytosis, production of anti-inflammatory cytokines such as $TGF-\beta$ and $IL-10$ takes place along with a reduction in the levels of production of pro-inflammatory cytokines by macrophages(Haslett, 1999).

In one study by Knapp and colleagues, it was observed that in macrophage depleted mice, there were higher levels of $TNF-\alpha$, $IL-1\beta$ and mouse chemokine KC along with activated neutrophils in the blood. Alveolar macrophages are the major phagocytic effector cells in the lung capable of clearing an infection. Depletion of these cells led to high numbers of apoptotic and necrotic cells which explains the necessity of the alveolar macrophages and the lack of efficient pathogen removal without their presence. An insult to the lung with LPS induces pulmonary inflammation by inducing necrosis in alveolar macrophages leading to pro-IL-1a and neutrophil recruitment in the lung(Dagvadorj et al., 2015). These CD11c$^+$ alveolar macrophages are the source of IL-23 during LPS induced ARDS which is T_H17 regulator. The alveolar macrophages express a high level of complement receptor (CR), mannose receptor (MR) and immunoglobulin receptor (fcR) along with a range of scavenger receptors(Mosser and Edelson, 1984) (see Table 2.1). These macrophages have an active plasma membrane capable of phagocytosis of both opsonised and non-opsonised particles and have the capacity of recycling the entire plasma membrane every 30 minutes, therefore, ensuring that they internalize particles,

pathogens, surfactants by a range of receptor-independent plasma membrane shuffling and folding(Gordon and Read, 2002).

2.2.2 Dendritic cell differentiation and subtypes

Dendritic cells have long membranous extensions resembling dendrites of nerve cells. These extend and retract dynamically. Lymph node resident DCs (LN-DCs) is subdivided into conventional DC (cDC) subsets in mice as CD11b and CD8a whereas in humans as BDCA1 and BDCA3 along with plasmacytoid DCs (Table 2.2). Robbins and colleagues showed through clustering analysis that a distinct branch is formed in the leukocyte family with a conserved transcriptional signature in all LN-DC subsets(Robbins et al., 2008). However, whether the same LN-DC subsets are present in lung needs to be validated. Different subsets of DCs migrate to the lungs during infection. DCs capture antigen at one place and present in another place. For example, DCs capture antigen in the lungs and then migrate to the lung draining lymph node and present the antigen(Desch et al., 2014). But, DCs from local draining lymph nodes after a systemic challenge is immature in mice absent of $TNF - \alpha$ versus in wild type mice. For the maturation of DCs several signals like $TNF - \alpha$ and LPS are necessary. Outside the lymph nodes, immature dendritic cells monitor for antigens and capture antigens. Then they migrate to lymph nodes where they present the antigen to naïve T cells. This process is known as an innate adaptive immune response. DCs require an increased level of CCR7, α6-cadherins, CD40, MMP-2 and/or MMP-9 and decreased level of E-cadherin for migration(Lutz and Schuler, 2002). However, it is unclear as to how α6-cadherins assist migration. Immature DCs patrol the interstitial space of peripheral tissue in search of foreign particles. This patrolling behaviour of immature DCs is slowed down during their movement for efficient detection and vigilance in antigen capture. This is a result of myosin IIA disrupting the motor protein gradient(Chabaud et al., 2015). However, this is beneficial as it enhances the antigen capture ability of the DCs.

In both mice and humans, dendritic cells express different subsets(Robbins et al., 2008) each having their own specific function (Table 2.2). Conventional DC (cDC) refers to mice CD8α(+) cells expressing high levels of CD11c that enters lymph nodes by migrating from peripheral tissue via a lymphatic route(Shortman and Liu, 2002) (Table 2.2). The human thymus is the niche of cDC and plasmacytoid DCs among which a cDCs subset called BDCA3^{hi} DCs, expressing CD13 and low-intermediate levels of CD11c, CLEC9A, and high levels XCR1, IRF8 and TLR3 and HLA-DR exhibiting to TLR3 a strong stimulatory response which releases high levels of $IFN - \lambda 1$ and CXCL10(Martinez et al., 2015). Another subset of DCs, called Double Negative T cells (DNT) with CD4$^-$ and CD8$^-$ express memory markers CD44, CD11a, CD103 and FasL with intermediate levels of TCR/CD3 and has subsets of $\gamma\delta$ T cells, CD1α inactive iNKT cells, NK1.1$^+$ NKT-like cells and NK1.1- DN T cells(Neyt et al., 2015).

As macrophages play a significant role in maintaining inflammation by extending the extravasion of immature monocytes and neutrophils, allergen-specific cytotoxic T lymphocytes also play a key role in airway inflammation. Allergen-specific cytotoxic T lymphocytes (CTLs) strongly reduce airway inflammation. These CTLS produce IL-4 and IL-13 by the lung T_h2 cells. These CTLSs are specific for increased caspase$^+$ DC production in mediastinal lymph node (MLN) along with fewer CD103$^+$ and CD11b$^+$ DCs in the lung(Daniels et al., 2016). T_h2 immunity is triggered by the phosphorylation of DNA dependent protein kinase which is important in adaptive immunity mediated by DCs in allergic asthma. Traditional treatments for asthma decrease the number of DCs in the airway. Since the airway lacks DCs, macrophages may be the key cells involved in regulation and clearance of allergens from the airway during the treatments. However, this aspect needs investigation. House dust mites induce phosphorylation, thereby triggering T_h2 immunity by a mechanism involving an impaired presentation of mite antigens and generation of intracellular reactive oxygen species(Mishra et al., 2015). Another example is syndecan-4 (SDC4) expressed in DCs (Table 2.2) activating T_h2 mediated asthma(Polte et al., 2015).

TABLE 2.2: **A summary of phenotypic and functional markers on murine dendritic cells and its subsets.** The development of each subset, its function, phenotypic and functional markers, cytokines and chemokines produced.

Subset	Sub-subset	Cell development	Function	Dendritic cell Surface Markers	Cytokines produced	Chemokines induced	References
Myeloid DCs (mDCs)	$CD1c^+$ myeloid	LPS, IC, flagellin, R848	These cells express a diverse range of TLRs and Lectins for Antigen uptake, transport and presentation. Good stimulators of naïve CD4 T cells	CD11b, CD11c, CD13, CD33, CD172 (SIRPa) and CD45RO; Dectin-1, Dectin-2	$TNF-\alpha$, IL-8, IL-10, IL-23; IL-12 is produced in response to activation by R848 when it ligates to the TLR 7/8 receptor.	$IFN-\gamma$ inducible protein-10 (IP-10), monokine induced by interferon γ (MIG) and, thymus activation-regulated chemokine (TARC)	Collin et al. (2013); van der Aar et al. (2007); Mittag et al. (2011); Morelli et al. (2005); Moret et al. (2013)
	$CD141^{hi}$ myeloid	ICs, R848	The cells take up dead cells via CLEC9A. They also cross-present antigen to $CD8^+$ T cell along with sensing viral nucleic acids using TLR3 and TLR8.	Wide expression of CD141 on $CD14^+$ migratory DCs, $CD1c^+$ DCs and monocytes cultered with Vit. D. Therefore differentiation is based on the lower expression of CD11b and CD11c	$TNF-\alpha$ and lower levels of IL-12 and p70	CXCL10, $IFN-\gamma$	Bachem et al. (2010); Lauterbach et al. (2010); Haniffa et al. (2012); Desch et al. (2014)
	$CD14^+$	Histamine	They do not stimulate naïve T cells efficiently. They have the ability to differentiate into Langerhans cells and mature DCs. Therefore they are quiescent tissue monocytes.	CD11c common with monocytes but lack CD1c and CD141, CCR7. Express: CD209, FXIIIA, CD163, CD141	IL-10	-	Collin et al. (2013)

Subset	Sub-subset	Cell development	Function	Surface Markers	Cytokines produced	Chemokines induced	References
Plasmacytoid DCs(pDCs)	They lack myeloid antigens CD11b, CD11c,CD13 and CD33. They are present in Lymph Node in almost 20% $MHCII^+$ cells	On coming in contact with active or inactivated pathogenic viruses, bacteria, and parasites.	Formation of Follicular T_H Cell. They can instigate T cell response and also respond to viral infections by secretion of large amounts of $IFN-\gamma$. Fresh pDCs do not prime naïve T cells and hence are immature. They induce T_{Reg} cells and are able to sense DNA released from apoptotic cells.	CD45RA, variable CD2 and CD7 and may have TCR; CD123; CD303; CD304; TLR7, TLR9. CCR5, CCR7, and CXCR3	type-I IFNs, $TNF-\alpha$, and IL-6	$IFN - \gamma$,pro-inflammatory chemokine CCL3/macrophage inflammatory protein (MIP)-1α	Collin et al. (2013); Gilliet et al. (2008); Colomna et al. (2004); Ogata et al. (2013); Penna et al. (2002); Liu (2005)
Langerhans Cells	They mature from $CD34^+$ myeloid cells that are $CD14^-$. They can be found in skin-draining lymph nodes (para cortex region)	$TNF - \alpha$ from $CD34^+CD14^-$ T cells	They mature and work in antigen presentation but lack TLRs hence induce T_{Reg} cells and produce IL-22	Langerin, CD1a, CD36, ATPase, FCεRI	IL-15, IL-22	macrophage-derived chemokine/stimulated T cell chemotactic protein(CCL22), Th1/Th2 profile	Collin et al. (2013); Banchereau et al. (2012); Ross et al. (1999); Ito et al. (1999); de Jong et al. (2010)
Inflammatory DCs	Derived from $CD14^+$ blood monocytes	GM-CSF and IL-4	Different inflammatory environment generates a diverse range of monocyte derived DCs. They stimulate naïve $CD4^+$ T cell and also are involved in antigen presentation to $CD8^+$ T cell.	CD1c, CD1a, $CD206, Fc\varepsilon R1$, SIRPα and CD209 and lack CD16	IL-1β, TNF-α IL-6 and IL-23 and stimulate T_H17 responses; IL-1, IL-6, TNF-α, IL-12 and IL-23	MCP-1, RANTES, T_H1/T_H17 profile	Collin et al. (2013); Romani et al. (1994); Ebner et al. (2001); Kejian et al. (2000)
SLAN DCs	A subset of $CD16^+$ monocyte	LPS in presence of Histamine	They are reactive to self-RNA-LL37	6-Sulpho LacNAc (SLAN), H4R	TNF-α, IL-1β, IL-6 and IL-12	T_H1/T_H17 profile	Collin et al. (2013); Hänsel et al. (2011); Gschwandtner et al. (2011)

2.3   Agents targetting inflammatory pathways

T_h2 inflammation involves the activation of effector responses evolved against multicellular parasites such as helminths. T_h2 cells provide help to B cells for antibody production, especially for IgE class switching. Two main cytokines ($IL-4$ and $IL-13$) characterize T_h2 inflammation. $IL-4$ differentiates naïve $CD4^+$ T cells to T_h2 phenotype and participates in the chemotaxis of eosinophils and class switching of IgE. $IL-13$ also influences eosinophil chemotaxis and class switching of IgE but also mediates goblet cell metaplasia and smooth muscle contractility(Gandhi et al., 2017). Therefore, these two cytokines are prime targets in inflammatory pathways. Several humanized monoclonal antibodies have been made to target these cytokines but are discontinued either because the primary goals are met or due to failure to inhibit the cytokines towards activation of the inflammatory pathways. Summary of the antibodies directed towards the blocking of $IL-4$ and $IL-13$ are reviewed elsewhere(Gandhi et al., 2017). Out of all the trialled antibodies, dupilumab and lebrikizumab were able to decrease the chemokine CCL17 thereby preventing the induction and chemotaxis of T cells(Wenzel et al., 2013; Corren et al., 2011). These biologics also lowered the total amount of IgE. A single cytokine blocker, tralokinumab inhibits $IL-13$. Tralokinumab proved to be successful at two high doses after twelve weeks of treatment(Popovic et al., 2017). However, blocking one cytokine was not beneficial in comparison to dupilumab which targeted both $L-4$ and $IL-13$. Other anti-$IL-13$ antibodies such as anrukinzumab and anti-$IL-4$ antibodies such as pascolizumab, pitakinra have been trialled yet dupilumab is efficient in reducing the symptoms of T_h2 inflammation in asthma(Bagnasco et al., 2016). Since inflammation is not only Th2 based therefore we focus on to another type of inflammation which involves neutrophils.

Another type of inflammation, T_H17-mediated, is responsible for the recruitment of neutrophils at the site of infection. T_h17-mediated inflammation aims at extracellular pathogens for an adaptive immune response. T_H17 cells are responsible for the production of $IL-17$ family of cytokines but do not express $IL-4$. Pro-inflammatory effects of IL-17 include accumulation of neutrophils and proteolytic enzymes such as neutrophil elastase and MMP9(Linden and Dahlen, 2014). Type 3 ILCs are important for airway neutrophilia as they express IL-17A during ALI induced by LPS(Roos and Stampfli, 2017). Earlier studies by Roos and colleagues showed that the *il17a* gene was observed

only in alveolar macrophages of smoke-exposed mice(Roos and Stampfli, 2017). Furthermore, increased expression of submucosal IL17A in lung tissue of COPD patients was observed. In asthma, $IL-17A$ not only recruits' neutrophils and releases their proteases but is also involved in negative feedback on the release of $IL-23$ from macrophages, therefore, constituting a $T_h 17$ regulator. This prevents excess signalling and maintains an efficient antibacterial host defence without tissue damage(Linden and Dahlen, 2014). These observations suggest that the cytokine has a key role in the pathobiology of COPD, making it an important target for treatment. To date, many anti-$IL-17$ inhibitors have been developed and successfully used in other inflammatory diseases such as brodalumab (AMG827) for psoriasis. One of such anti-$IL-17$ inhibitors, CNTO6785 was used to treat COPD as part of a phase 2 trial. Unfortunately, there was no difference in the efficacy endpoint in comparison to the placebo, inferring that CNTO6785 is not a successful therapeutic target for COPD(Eich et al., 2017). Very recently, a new target for reducing airway inflammation has been found. G-CSF has been found to attenuate airway inflammation and systemic inflammation along with the reduction in lung tissue destruction in a COPD model(Tsantikos et al., 2018). Therefore, new humanized antibodies targeting these cytokines and biomarker may be beneficial as a therapeutic target against asthma and COPD.

2.4   New treatment strategies for pulmonary inflammation

Current treatments for ARDS and COPD include the use of bronchodilators and corticosteroids. In adults, corticosteroids are supplemented with a low dose of beta-2-agonist. However, the use of corticosteroids has resulted in resistance and hence there is a need to develop new anti-inflammatories. Despite no single asthma gene for a target, proteases have been identified to play a key role(Reed and Kita, 2004). Proteases such as serine proteases and metalloproteases can induce IL-32 and convert IL-1 and IL-18 zymogens to their active form to promote proinflammatory response(Safavi and Farjami, 2011). Other proteases such as cathepsins stimulate $IFN-\gamma$ production. Therefore, one of the strategies in combating inflammation in respiratory disease is by the use of protease inhibitors(Lin et al., 2014). The serine protease inhibitors act by down-regulating $T_h 2$ cytokines and $T_h 17$ cell function and inhibiting $NF-\kappa\beta$ activation in the lung. Upon encountering LPS, DCs upregulate the production of protease inhibitors such as serine

protease inhibitor 6 (Spi6)(Andrew et al., 2008). The protease inhibitors are necessary to protect the DCs from contact-mediated cytotoxicity of the CD8 T lymphocytes(Lovo et al., 2012). Furthermore, thymic stromal lymphopoietin (TSLP) is a protein of the cytokine family involved in maturation of T lymphocytes through activation of antigen presenting cells(He and Geha, 2010; Noh et al., 2016; Reche et al., 2001). TSLP is secreted by epithelial cells and enhances the maturation of CD11c$^+$ DCs(Reche et al., 2001). In the thymus, TSLP activates both CD123$^+$ plasmacytoid and CD11c$^+$ myeloid DCs leading to regulatory T cell production(Hanabuchi et al., 2010). Overexpression of TSLP in the lung leads to severe airway inflammation and airway hyperresponsiveness(Zhou et al., 2005). TSLP is targeted by the antibody Tezepelumab(Corren et al., 2017). It reduced exacerbations in patients with asthma. For a detailed account of TSLP and its role in asthma, see(West et al., 2012). One of the treatment strategies involves the use of LPS inhibitors and statins. But they are not sufficient to down-regulate inflammation.

2.4.1 LPS inhibitors

However, there is no single therapeutic approach capable of culminating LPS induced inflammation completely. E5564 has shown great potential in vivo by blocking LPS induced cytokines and blocks LPS itself. The molecule has been trialled in patients with endotoxemia and has shown successful results in inhibiting all the effects of LPS. However, the immunological tolerance side is not investigated and therefore risks remain in the clinical use of the molecule. Another compound which has been found successful in blocking LPS is TAK-242 *in vitro*. The molecule would need further investigation before clinical use. Furthermore, treatments targeted at $TNF-\alpha$, such as rhynchophilline are available. However, rhynchophilline increases morbidity in mice due to caecal ligation. Other examples include berberine with yohimbine which can modulate the host immune response during endotoxemia in humans. For details on LPS inhibitors, see(Wang et al., 2009).

2.4.2 Statins as anti-inflammatories

Use of statins is another therapeutic approach. Simvastatin has been successfully used in a mouse model of allergic airways disease(Liu, Suh, Yang, Lee, Park and Shin, 2014a).

Statins can reduce expression of activation markers on DCs upon LPS induced maturation(Yilmaz et al., 2006). Therefore, behaving as a potential well-characterised anti-inflammatory agent. Other key treatments which have come to the limelight include the use of anti-IgE(omalizumab) and anti-IL-5(mepolizumab) for treatment of lung inflammation especially asthma(Sy and Siracusa, 2016). Omalizumab acts by reducing FcϵRI expression on basophils and mast cells as well as preventing the binding of IgE to $Fc\epsilon RI$ receptors. The effect of lowered $Fc\epsilon RI$ was observed on DCs which affected their ability to prime naïve T cells towards a T_h2 pathway and secretion of T_h2 cytokines(Prussin et al., 2003) thus preventing inflammation(Schroeder et al., 2009). Treatments with omalizumab result in reduced sputum along with decreased epithelial and subepithelial cells. Other cells such as sub-mucosal B cells and CD4$^+$, CD8$^+$ T lymphocytes are also reduced(Samitas et al., 2015). Treatment with humanized antibodies is not limited to anti-IgE but several other targets such as anti-$IL-4$, $TNF-\alpha$ and $IL-13$. Another approach is to directly deliver anti-inflammatory mediators ($IL-10$, $IL-12$, $IFN-\gamma$) or enhance their rate of production. Unconventional treatments include the use of anti-oxidants shown to have novel anti-inflammatory effects(Braskett and Riedl, 2010).

But none of the currently available treatments gives a greatly improved management of the disease. Nor are they capable of long-term sustainable treatment with fewer side-effects. Very recently, cytokine-induced killer cells (CIK cells) has been used to treat allergic airway inflammation (conventionally used in cancer treatment(Pluangnooch et al., 2017)). These cells could be used for personalised treatments against airway inflammation but need further investigation of the mechanisms involved. The future relies on the development of new anti-inflammatories to be delivered in the lung. However, combinations of multiple pre-clinical therapies can be used to bridge the gap in development of newer anti-inflammatories against LPS induced airway inflammation. The new anti-inflammatories should be capable of providing both an immediate and a sustaining anti-inflammatory effect. One of the possible ways of treatment is by pulmonary nanomedicine.

2.5 Pulmonary Nanomedicine: approaches to delivery and therapeutics

The recent development of surface functionalised nanoparticles have been exploited to conjugate drugs, anti-inflammatories, proteins and other biologically relevant therapeutic molecules. There are several ways by which the essential anti-inflammatories can be attached or conjugated to the nanoparticles(Chakraborty et al., 2017). It is known that inert 50 nm polystyrene nanoparticles conjugated with a neutral amino acid can inhibit allergic airway inflammation. These particles are immunosuppressive and are taken up by the antigen presenting cells while the cell viability is unaffected(Hardy et al., 2012). Nanoparticles can be used to conjugate biologically useful molecules such as therapeutic antibodies, proteins and amino acids. Very recently, amino acid conjugated nanoparticles have gained interest due to their biocompatibility and ease of conjugation. Conjugated nanoparticle carrying a novel molecule of interest can provide a long-lasting response in the lung. This dimension of therapeutics points us to the use of anti-inflammatories providing a sustaining effect in the treatment of inflammation in the lung. Nanoparticles intended for use in vascular delivery have different properties which enable them to be used as anti-inflammatories.

Anti-inflammatories for vascular delivery utilize different types of nano-carriers to carry the drug inside the blood vessels. Nano-carriers include liposomes, dendrimers, antibody-and-polymer drug conjugates, solid lipid and polymeric nanoparticles(Howard et al., 2014). Nanoparticles need to be neutral and under the size of 300 nm for delivery to the vasculature. Recent studies have shown that the hydrodynamic size of the particles is crucial for vascular delivery. Nonspherical carriers have more retention time than spherical counterparts in blood flow. The targets of these nano-carriers include sub-micron particles in blood and endothelial cells for anti-inflammatory delivery. Nanoencapsulation of anti-oxidant enzymes followed by vascular deliver is also possible. Endothelial cells have many uptake mechanisms for anti-inflammatories such as clathrin mediated, caveolae-mediated and non-canonical endocytosis and pinocytosis. Nano-carriers are generally taken up by the endocytic pathway where the nano-carriers target cell adhesion molecules such as E-selectin and VCAM-1. Antibodies binding to such cell adhesion molecules boost anti-oxidant binding, uptake and protective effects in animal models of

LPS-induced inflammation. Nano-carriers on one side are novel agents capable of delivering anti-inflammatories intra-cellularly and on the other hand they accumulate in the microvasculature, kidneys and reticuloendothelial system. For a detailed understanding of nano-carriers and their role in vascular delivery, see(Howard et al., 2014). Therefore, cell adhesion molecules are important to study the behaviour of nano-carriers for drug-delivery.

2.5.1 Significance of cell adhesion molecules for nano-carriers

Since cell adhesion molecules are important for nano-carriers to be endocytosed by the cells, numerous studies have demonstrated the accumulation of biotherapeutics in the pulmonary vasculature. In one such example, antioxidant molecules such as catalase and superoxide dismutase were conjugated to anti-PECAM-1(a cell adhesion molecule) antibody for targeting ROS to alleviate vascular oxidative stress and endothelial inflammation(Han et al., 2011; Shuvaev et al., 2011). In another study, dexamethasone-loaded lysozyme dextran nanogels having affinity for the cell adhesion molecule ICAM-1 was used to ameliorate acute pulmonary inflammation caused by LPS induced ALI(Coll Ferrer et al., 2014). Therefore, target specific delivery is possible using nano-carriers carrying drugs for delivery.

In the treatment of respiratory diseases, the lung provides a large surface area along with a low enzyme-controlled environment so that drugs can be delivered for systemic therapies. However, multiple barriers such as humidity, mucociliary clearance and alveolar macrophages affect the efficacy of drugs(Labiris and Dolovich, 2003). Pulmonary delivery prevents the degradation of the active pharmacophore in the gastro-intestinal tract and the first pass metabolism in the liver. Targeted delivery of drugs into the blood circulating through the lung is complicated due to several anatomical and physiological challenges such as a thin semipermeable epithelium and an extremely thin alveolar-capillary barrier. The size/lumen diameter of the airways can be a challenge as well. Therefore, many molecules tend to deposit into the trachea or the large airways and are unable to reach deep into the alveoli. To overcome such challenges, nanomedicines are the ideal solution for delivery. Exosomes are an excellent example for encapsulation and delivery of anti-inflammatory agents. Exosome encapsulating curcumin has been found to be effective in protecting against LPS induced septic shock(Sun et al., 2010). In one

study, nano-carriers were able to distinguish between inflamed versus healthy tissue. The nano-carriers targeted the cell adhesion molecule PECAM present in the healthy lung but absent from the inflamed lung due to hypoxic vasoconstriction. This lead to the conclusion that intra-organ region-specific delivery of drugs is possible, overcoming local abnormalities of perfusion and permeability.

2.6 An introduction to conjugated nanoparticles

Historically nanoparticles were studied because of their unique chemical and physical properties. They have been classified depending on shape as rods, shells, dots, sheets and composites(Chakraborty et al., 2015; Paul and Robeson, 2008; Pérez-Juste et al., 2005; Wang et al., 2014; Zhongshi et al., 2014). The use of nanoparticles is revolutionizing many industries such as paints and solar cells but is yet to be fully exploited for theranostic applications. Concerns about their safety, and optimizing stable attachment of biologically relevant molecules to these nanoparticles, are limiting rapid progress. One of the most important problems associated with the use of some commonly used pristine metal nanoparticles is the production of reactive oxygen species (ROS) from the inorganic core(Gholami et al., 2015; Inbaraj et al., 2011). Specifically, iron oxide nanoparticles form ROS which leads to lipid peroxidation and DNA damage. Nanoparticle toxicity can be sometimes further related to particle size. For example, metallic bulk gold is inert, but at the nano-scale range (<25 nm) it exhibits catalytic properties useful for Carbon monoxide oxidation(Rodriguez et al., 2014). In addition due to their toxicity to cancer cells in vitro(Pan et al., 2007), gold nanoparticles have been used to treat cancer cells by apoptosis(Selim ME, 2012). However, the toxic effect of the particles is not strictly limited to cancer cells, but can also affect other non-malignant cells, in some cases causing damage to tissue(Abdelhalim, 2011). For example, exposure to carbon nanotubes(Inoue et al., 2009, 2010) and carbon black(Alessandrini et al., 2006; De Haar et al., 2006) nanoparticles <100 nm in the lung exacerbates asthma. Also fine sized particles of TiO_2(Cai et al., 2011), gold(Pan et al., 2007; Selim ME, 2012) and SiO_2(Ariano et al., 2011) in the size range 100 nm-2500 nm show size-dependent toxicity for mammalian cell lines.

Particle size is also important for cellular uptake. Antigen presenting cells (APC) of the immune system, and specifically dendritic cells (DC) and macrophages, are highly

capable of taking up nanoparticles and microparticles from 5nm-10,000 nm(Fifis et al., 2004; Hardy et al., 2012, 2013; Wilson et al., 2015; Xiang et al., 2012, 2006). Other physical aspects like negative charge(He et al., 2010; Verma and Stellacci, 2010), peptide conjugation(Zhao et al., 2002) and alternating hydrophilic-hydrophobic ligands, alter nanoparticle uptake by diverse host cell types. Aside from influencing cellular uptake, particle size also affects their biodistribution into major organs such as liver, kidney, spleen and lung. Indeed particles with size less than 5 nm are normally cleared by the kidney(Soo Choi et al., 2007), while larger particles around usually 50-100 nm end up in the liver(Braet et al., 2007) and particles over 2000 nm tend to accumulate in the spleen(Blanco et al., 2015). Furthermore micrometre-sized particles (2-5 μm) end up in lung capillaries(Liu, Li and Xu, 2014; McVey et al., 2012; Takahashi and Kubo, 2014) and smaller particles (<100 nm) end up in kidney although coatings on particles could hinder the excretion process(Almeida et al., 2011). Other than particle size, another critical factor for nanoparticles is their stability inside the body. Since nanoparticles are in the colloidal range, their stability is dependent on a range of factors with zeta-potential being the most important. An efficient nanoparticle in vivo should not aggregate with serum proteins and antibodies in the blood(Mohr et al., 2014; Moore et al., 2015), evade uptake by antigen presenting cells(Hardy et al., 2012) and finally there should be enough circulation time for the particles to move inside the body(Jin-Wook et al., 2010). Coatings with biocompatible polymers (such as dextran), Poly Ethylene Glycol(PEG) and amino acids can improve their circulation and also prevent them from aggregating inside the body. Therefore, it is not enough to limit the use of nanoparticles *in-vitro* in physiological pH but to evaluate their stability a dynamic media susceptible to rapid pH changes is necessary.

2.6.1 Synthesis of conjugated nanoparticles

Functional groups such as amino(Tiwari et al., 2011), methyl(Larson et al., 2012; Tiwari et al., 2011), carboxy(Wangoo et al., 2008), citrate(Barton et al., 2014) and guanidine(Ballester et al., 2015) are used to functionalize nanoparticles to impart special functional properties. The single amino acids offer both an amino and a carboxyterminal for conjugation of important biomolecules. They also provide higher biocompatibility(Inbaraj et al., 2011) and are designed to overcome some of the challenges

associated with size, bio-distribution, interaction with immune cells and induction of in-flammation(Inbaraj et al., 2011; Pal et al., 2011). The conjugation paradigm uses chemical processes analogous to peptide conjugation utilizing 1-Ethyl-3-(3-dimethylaminopropyl) carbodiimide (EDC)(Fischer, 2010) chemistry or directly with the carboxyl group. The reaction involves an exposed carboxyl group on the surface of the nanoparticle to which EDC reacts to form an ester. This ester intermediate is then attacked by a nucleophile, which is the amino acid to be conjugated. The amino acid is conjugated at the amino terminal and carboxyl group exposed at the surface. Other than using EDC, a spacer molecule of the silane family like (3-Glycidyloxypropyl) trimethoxysilane(GPTMS)(Yan-Ru Zhang and Shi-Li, 2013; Yan-Ru Zhang and Sheng-Qing, 2014) or (3-Aminopropyl) trimethoxysilane can be used to conjugate amino acids. Direct conjugation of amino acids to nanoparticles such as iron oxide(Barick and Hassan, 2012) has been demon-strated by conjugating the amino acid at the time of the nanoparticle formation at a higher reducing temperature.

The amino acid-conjugated nanoparticles are promising as theranostic agents. To the best of our knowledge, they have been used in fabricating biosensors, and for applica-tions such as *in-vivo* imaging as contrast agents, drug delivery, anti-microbial agents and cancer therapy. However, these particles are still vastly underutilized clinically. There are multiple reasons behind their limited usage. One of them being the lack of knowledge on their biodistribution and excretion, as demonstrated by the heavy metal conjugated with amino acids(Han et al., 2016) and the MR contrasting agents(Lee et al., 2010*a*). The high surface area to volume rat-0io of amino acid conjugated nanoparticles offers cheap and efficient surface functionalization alternatives to peptides.

2.7 Factors affecting amino acid conjugated nanoparticle cytotoxicity

Cytotoxicity is the key component that needs to be addressed for translating nanoparti-cles from the lab to the clinic and their effect on human cells is a vast area of research. An important aspect underlying the toxicity of some nanomaterials is the generation of reactive oxygen species (ROS). The overproduction of ROS, mediated by Fenton's

reaction, leads to oxidative stress which in turn causes dysregulation in the physiological redox potentials and ultimately progresses into lipid peroxidation, protein oxidation, and DNA damage. Glutamate is known to prevent oxidative stress(Zabot et al., 2014) and glutamate modified iron oxide nanoparticles(Inbaraj et al., 2011) has displayed high biocompatibility at high concentrations of 1000 μg/ml on human skin fibroblast. Their counterparts, the pristine iron oxide had displayed higher toxicity due to ROS formation. The glutamate capped iron oxide is, therefore, beneficial over the pristine iron oxide nanoparticles in abating the tendency to produce reactive oxygen species.

Gold nanoparticles modified with leucine(Berghian-Grosan et al., 2014) and lysine have less cytotoxicity in comparison to gold nanoparticles modified with glycine and aspartic acid (Figure 2.3E), at a concentration 50 μg/ml (Cai and Yao, 2014). This is contradictory to our preliminary knowledge. We have found glycine modified 50 nm polystyrene particles to be immunosuppressive(Hardy et al., 2012) when taken up by antigen presenting cells whilst their viability remains unaffected. Therefore, the cytotoxicity is related to the particle core and the size of gold nanoparticles (25 nm). At the size range of less than 40 nm, gold nanoparticles have been reported to show a significant amount of cytotoxicity(Pan et al., 2007; Selim ME, 2012; Yen et al., 2009). Pristine gold nanoparticles cause rapid cell death by necrosis(Pan et al., 2007) and hence toxic. Another process may include ROS production, activating stress-dependent signalling pathways(Misawa and Takahashi, 2011). Comparing glycine with histidine and cysteine coated to silver nanoparticles(Shi et al., 2014), it was observed that glycine coated particles were not toxic. Coating with histidine and cysteine, however, favoured cell viability. Over time the histidine coated silver nanoparticles tended to cluster together increasing the hydrodynamic size. It is known that larger particles are rarely taken up by the cells and therefore may have reduced toxicity(Kim et al., 2012).
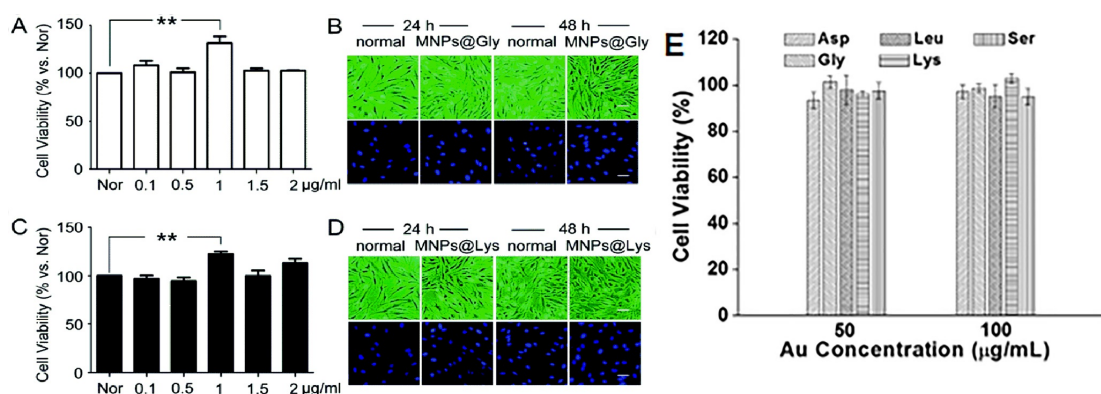
FIGURE 2.3: **Comparison of cytotoxicity of Iron oxide and gold nanoparticles coated with different amino acids.** Gold shows higher cytotoxicity in comparison to magnetic iron oxide nanoparticles. A WST-8 assay of cell viability was used to determine the cytotoxicity of the glycine **(A, B)** and lysine **(C, D)** coated magnetic nanoparticles on bone marrow mesenchymal stem cells. Both the particles induced proliferation of cells rather than death at 1 mg/ml concentration and hence are more biocompatible. At 2 mg/ml, glycine coated particles showed normal cell viability **(A)** which was more for the lysine coated particles **(C)**. The nuclear morphology remained the same for both the particles even after 48 hours of incubation **(B, D)**. But similar glycine and lysine coated gold nanoparticles **(E)** had less cell viability and did not have any proliferative effect on the cancerous KB cells. Reproduced with permission from (Cai and Yao, 2014; Yu et al., 2016) copyright 2014 Elsevier B.V. and The Royal Society of Chemistry 2016.

Particles less than 5 nm tend to accumulate in the nucleus(Huang et al., 2012) whereas particles in the size range 15-40 nm restrict themselves to the cytoplasm(Oh et al., 2011). The ideal size for initial maximum uptake by cells such as dendritic cells (DC) is 50 nm(Hardy et al., 2012), which has been observed with gold(Chithrani et al., 2006), silver(Kettler et al., n.d.) and polystyrene(Hardy et al., 2012) nanoparticles. However, the difference in shape of the non-spherical particles can have a negative impact and may increase the toxicity of gold nanoparticles along with the size(Berghian-Grosan et al., 2014).

Presence of sulfhydryl (–SH) group on cysteine may capture Ag^+ ions released, reducing the chance of cytotoxicity. Silica nanoparticles modified with arginine(Shahabi et al., 2015) are found to be cytotoxic at a concentration of 200 mg/ml. Inhibition of DNA replication and particle size leads to cytotoxicity in bone cells, whereas a relatively shorter doubling time of MG63 cells makes them more biocompatible with the number of particles per cell being very low to induce any cytotoxic effect. Such particles may not have much impact on cancer cell lines which have very high doubling time but could have much observable effect on other cells such as fibroblasts. Furthermore, other cell types like mesenchymal stem cells are very sensitive to culture conditions and are prone to differentiate quickly upon encountering a trigger stimulus such as transient low pH stressor. Interestingly, in context of the cell cycle, the addition of glycine and lysine-modified iron oxide nanoparticles(Yu et al., 2016) at 1 μg/ml, increases the population of cells in S-phase thus promoting the proliferation of mesenchymal stem cells (Figure 2.3B, D). Therefore, these particles show less cytotoxicity in comparison to silica nanoparticles in the earlier study(Shahabi et al., 2015). Low levels of cytotoxicity by amino acid modified iron oxide nanoparticles is not limited to mesenchymal stem cells (Figure 2.3A, C) but is extended to many different cells as discussed in further sections below. In another study, selenium nanoparticles modified with several amino acids(Feng et al., 2014) like lysine, valine, and aspartic acid had shown lower cytotoxicity to human kidney cells (HEK-293) which can be accounted for the fact that these particles have a large size of 120 nm and tend to agglomerate over time.

2.8 Amino acid conjugated nanoparticles for bioimaging

Fluorescent molecular probes are highly useful in applications such as flow cytometry, immunofluorescence staining, and live cell imaging. These techniques utilize the property of the molecules to fluoresce selectively when excited by a certain wavelength of light.

Carbon dots have the property to fluoresce when excited by light of a specific wavelength. The emitted light is dependent on the size of the particles. However, the carbon dots show cytotoxicity(Wang et al., 2011) towards cells, which inhibits their use as fluorescent probes for cell imaging. But recently it was found that carbon dots synthesized using citric acid with amino acids coating such as isoleucine, valine and glycine can have reduced cytotoxicity and have been used as fluorescent bi-colour probes(Sarkar et al., 2015). The authors demonstrated that phosphorous doping induces a red shift, therefore, having a bi-colour probe and that the fluorescent probes have reduced cytotoxicity in HeLa cells. HeLa cells are cancer cells characterized by their fast proliferation unlike other mammalian non-cancerous cell lines such as fibroblasts. It is, therefore, necessary to observe the effect of such particles on a wide range of cells before drawing a conclusion on the cytotoxicity of such ultra-fine particles. This drawback had been addressed partially by Arslan and colleagues upon studying the cytotoxicity of cysteine-capped zinc oxide quantum dots in HEK293 cells(Arslan et al., 2013).The size of the zinc oxide QDs was around 100 nm whereas the carbon quantum dots were 5 nm(Shahabi et al., 2015)(Figure 2.4a-f). Therefore, the smaller size particles appear to be more cytotoxic to cells irrespective of their amino acid coating.
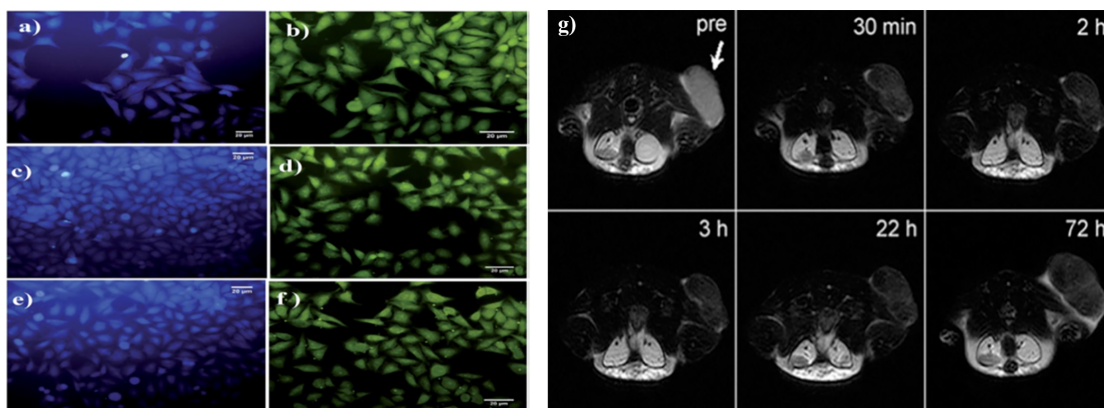
FIGURE 2.4: **Innate fluorescence of amino acid quantum dots and T2 weighted Magnetic Resonance Imaging. (a-f)**Innate fluorescence of amino acid coated carbon dots on HeLa cells. The blue coloured cells are the amino acid coated carbon dots with amino acids isoleucine **(a)**, glycine **(c)** and valine.**(e)**. The green fluorescence is caused by the doping of phosphorous on to the amino acid coated carbon dots with amino acids isoleucine **(b)**, glycine **(d)** and valine **(f)**. Reproduced with permission from (Sarkar et al., 2015), copyright 2015 The Royal Society of Chemistry. **(g)**In-vivo T2 weighted Magnetic Resonance image of amino acid coated iron oxide nanoparticle as a contrasting agent. Images acquired post-injection of 15 mg Fe/kg of poly-aspartic acid coated iron oxide nanoparticles. The particles demonstrated high colloidal stability and were found to be taken up by CT26 tumour cells (at the back of mice) having a low pH environment represented in the image by the arrow. Reproduced with permission from (Lee et al., 2010a), copyright 2010 The Royal Society of Chemistry..

Fluorescent imaging is not limited to cells but has been explored *in-vivo* as well. In a separate study it was shown that amino acids such as aspartic acid, serine and lysine were coated on to upconversion-luminescent nanoparticles made of lanthanides lutetium co-doped with either Ytterbium, Gadolinium or Erbium(Han et al., 2016). The authors demonstrated the accumulation of the particles in the liver and the spleen after 5 hours of the base of tail injection, but have not yet studied their cytotoxicity. Metallic nanoparticles are widely known to be cytotoxic(Berghian-Grosan et al., 2014; Pujalte et al., 2011) and heavy metals used for the process are not excreted by the body, leading to deposition and posing serious effects to the organ. These metals cannot be metabolized by the body(Palasz and Czekaj, 2000; Saturnino et al., 2013) and degradation is not possible(Palasz and Czekaj, 2000). Therefore, tracing the excretion route is essential before use of the particles in *in-vivo* imaging.

2.8.1 Magnetic Resonance Imaging using amino-acid conjugated nanoparticles

The biodegradability of iron oxide nanoparticles(Mazuel et al., 2016) has increased their potential for use as MRI agents. Amino acid coated iron oxide nanoparticles have been used for imaging of tumours and soft tissue. Tumour cells and normal cells both are overall negatively charged due to the presence of phospholipids like phosphatidylserine on the cell membrane. Poly amino acids (such as poly aspartic acid) serve as a coating material for iron oxide nanoparticles and have high colloidal stability in terms of positive zeta potential. Despite a positive zeta potential, the negatively charged tumour cells uptake particles at a low pH environment(Lee et al., 2010*a*). The particles remained in the tumour cells for 3 days without deterioration of the contrasting signal (Figure 2.4g), hence bio-distribution and degradation of such particles would be low. Although the dose of the particles is below lethal concentration, they may have chronic cytotoxicity if not degraded or excreted from the patient's body. Therefore, it is essential to monitor the degradation of such a particle in the body to avoid accumulation in tissues.

A similar particle developed by Yang and colleagues targeted breast cancer cells with anti- HER/neu2 antibody conjugated onto the surface of iron oxide coated poly-aspartic acid nanoparticle(Yang et al., 2010*a*). The authors claimed that the particles have negligible cytotoxicity even at concentrations 1 mg/ml. Due to the presence of iron core,

MR imaging was possible and served as an excellent contrast agent. The only concern would be the size and particle roughness(Vaine et al., 2013). It has been observed that the particle texture is important in eliciting an immune response which will be discussed in detail in the next section.

Other than tumours, poly-aspartic acid coated nanoparticles have been found useful as MR contrasting agents in liver imaging where the core is manganese oxide instead of iron oxide(Xing et al., 2011). The authors demonstrated an increase in the hydrodynamic size of the particles due to the adsorption of serum proteins, which is a key factor in every nanoparticle imaging probes. But the particles are stable colloids as indicated by their negative zeta potential which is also beneficial for the fact that the particles would have low cytotoxicity to the liver cells. To enhance the imaging, bimodal particles with magnetic effect as well as fluorescent properties have been developed(Davide et al., 2013). Such particles have a fluorophore conjugated to an amino acid coating which is on a metal surface the metal being gold or iron oxide nanoparticles. The only disadvantage of these particles would be non-specific signalling due to cleavage of the fluorophore from the particle and hence innate fluorescent properties of particles.

2.9 Effect of nanoparticles on host immunity with emphasis on conjugated nanoparticles

Non-surface functionalized silica particles ranging in size from 30-100 nm have been found to promote lung inflammation mediated by inflammasome activation and $IL-1\beta$ secretion(Kusaka et al., 2014), potentially induced by activation of the MAPK/Nrf2 and $NF-\kappa\beta$ signalling pathways(Guo et al., 2015). By contrast, amino acid coated nanoparticles show little toxicity, and in some cases, are even able to actively prevent damaging inflammatory responses. This has been demonstrated for 50 nm glycine coated nanoparticles, which inhibit acute airway inflammation when taken up by lung dendritic cells (DC)(Hardy et al., 2012). Size is a consideration, and bigger glycine coated 500 nm polystyrene nanoparticles are taken up preferentially by macrophages in the lung which do not promote the same strong anti-inflammatory effect(Hardy et al., 2012, 2013)(Figure 2.1).

At the cellular levels nanoparticle characteristics also highly influence uptake which can be mediated by multiple endocytic mechanisms such as energy-dependent endocytosis through the endosomes and lysosomes (reviewed in (Kim et al., 2006)). Another example of the effects of nanoparticles on the immune system is the use of poly-glutamic acid nanoparticles encapsulating HIV-1 antigen use as vaccines(Akagi et al., 2007) which can lead to DC maturation(Kim et al., 2010*b*), and promote the induction of cytotoxic T cell responses. In addition, the cytotoxicity of nanoparticles is influenced by the charge of their coating and the above-mentioned examples of amino acid coated nanoparticle formulations are all negatively charged. On the other hand, although positively charged particles tend to show increased cytotoxicity(Frohlich, 2012), in some cases these have still been successfully used as vaccine delivery systems(Thomas et al., 2009). Therefore, the issue of charge needs further investigation and a deeper understanding of the specific biological context in which these particles can be used.

So far, we have observed that the amino acid coated nanoparticles are diverse, with existing variations across multiple parameters such as shape, charge, type of amino acid conjugated and route of administration (Table 3). Consequently, these nanoparticles are taken up by a wide variety of organs including spleen(Blanco et al., 2015), lung(Liu, Li and Xu, 2014; McVey et al., 2012; Takahashi and Kubo, 2014) and liver(Braet et al., 2007). It is of interest that some amino acid functionalized particles do have the capacity to localize to multiple organs supporting their potential as MR contrast agents(Sadeghiani et al., 2005). Therefore, nanoparticle size matters when it comes to biodistribution into different organs. However, charge and shape are important aspects to consider as well. The shape of a nanoparticle highly influences its blood vessel fluid dynamics when in circulation. For instance, non-spherical nanoparticles tend to exhibit much better tumbling and lateral drifting characteristics in comparison with their spherical counterparts(Decuzzi et al., 2008). Therefore, non-spherical nanoparticles have an increased chance of particle adherence, binding to the endothelial cell wall and potential extravasation. Charge affects nanoparticles too, by influencing the protein adsorption(Blanco et al., 2015; Saptarshi et al., 2013) and positively charged nanoparticles undergo rapid clearance from the circulation in comparison with their negatively charged counterparts(Arvizo et al., 2011). Indeed, when injecting differently charged gold nanoparticles either intraperitoneal or intravenous in mice, Arvizo and colleagues observed high plasma clearance

for the positive and negatively charged particles. However the neutral and zwitterionic particles exhibited low plasma clearance well after 24h measurements(Arvizo et al., 2011). Overall, finding the optimal combination of nanoparticle properties to use in different medical areas is a challenging task but could lead to exciting new applications in the field of nanoparticle-based drug delivery. For further elucidation, the properties of nanoparticles and their heavy influence on pharmacokinetics and biodistribution has been extensively reviewed by (Blanco et al., 2015). Generally, successfully conjugating antibodies or other specific cell targeting modalities to nanoparticles is needed to support a range of biomedical applications including pulmonary delivery.

2.10 Conjugated nanoparticles as immunomodulators

A deeper insight into how antigen presenting cells work in response to endotoxin and other inflammatory signals would mean newer drug targets and therefore a better way to look at airways inflammation. With the focus shifting towards the immune side of the airway inflammation, new immunomodulators need to be developed.

Currently, natural compounds capable of attenuating inflammation are the subject of intense study. In the coming years, many more will be found which can reduce inflammation. However, an anti-inflammatory compound is not successful until it is translated to clinical use. It has also been suggested to include anti-inflammatory foods in our diet. In this aspect, there are several foods with anti-inflammatory properties such as olive oil, salmon, berries, and tomatoes containing high amounts of functional amino acids. Interestingly, these amino acids are attachable to nano-carriers specifically spherical polystyrene nanoparticles, which are non-biodegradable. Furthermore, it has been found that these amino acid conjugated nanoparticles can inhibit allergic airway inflammation(Hardy et al., 2012, 2013) in an OVA induced asthma mice model. If we combine these amino acids with biodegradable nanoparticles such as with iron oxide for delivery into the lung, it could be used as a sustainable therapeutic and low-cost medication. Therefore these amino acids could be the key to future anti-inflammatories(De Simone et al., 2013).

Antigen presenting cells (APCs) can serve as excellent therapeutic targets. Drugs such

as anti-inflammatories should be able to attenuate inflammation by downregulating activation of the APCs. In doing so, the release of pro-inflammatory mediators will be reduced as a result there will be less injury to the lung. As we develop new ways and treatments to attenuate airway inflammation, the understanding of the role of APCs as therapeutic targets will be vital. Every individual person is unique and therefore needs different methods of treatment and management of the disease. Therefore, personalised medicine and care for individual patients focused at the extent and severity of the disease need to be developed with the APCs in mind.

Considering the developing field of nanotechnology, it is highly likely that cost-effective nanoparticles could be used as therapeutics against airway inflammation. The changing lifestyle of people would also impact the way we look at this disease and therefore a more personalised treatment or care for the affected individuals would be necessary. Currently, the models used to study acute and chronic inflammation are capable of mimicking many but not all aspects of human lung inflammation. Therefore, focusing on the development of advanced disease models to study asthma and COPD would be necessary to investigate the disease from new perspectives. COPD can lead to non-reversible alveolar degradation. Therefore, new strategies to promote tissue remodelling and alveolar reconstruction could open a new field for COPD treatment.

2.11 Research Gaps

Previous data from our lab(Hardy et al., 2013) and others has shown that antigen presenting cells(APCs) in the lung have a preferential uptake of 50 nm particles over 500 nm and that glycine coated polystyrene particles inhibit airway inflammation.

- However, it is currently unknown whether glycine is broadly anti-inflammatory on diverse antigen presenting cells (APCs) beyond alveolar macrophages, especially on BMDCs(key activating APCs).

- It is unclear from our previous studies whether glycine or the particles mediated this effect. Therefore, the role of glycine in attenuating airway inflammation needs to be investigated in greater details.

- Currently, the only mode of administration of glycine is throuugh diet. But, it is not sufficient to be used as an immunomodulator as a significant part is lost by first pass metabolism. Therefore there is a need to develop glycine immunomodulators for pulmonary delivery. The immunomodulators should be capable of both an immediate and sustained anti-inflammatory effect in the lung.

- Develop a non-invasive imaging technique to track pulmonary biodistribution of the immunomodulators and design an on-demand drug delivery system to understand host-immune interaction.

Chapter 3

Materials and Methods

3.1   Materials

Glycine (ReagentPlus® G7126; ≥99% HPLC grade), iron (II) chloride, iron (III) chloride, ammonium persulfate (A3678, ≥98%), ninhydrin (151173, ACS), methacholine (acetyl-β-methacholine chloride ≥98% TLC, A2251) was obtained from Sigma-Aldrich. Sodium chloride was obtained from Merck (106404) and sodium chloride for irrigation was obtained from Baxter. Phosphate buffered saline (PBS) was prepared in-house by dissolving 2.76 g sodium dihydrogen phosphate ($NaH_2PO_4.H_2O$), 11.35 g sodium monohydrogen phosphate anhydrous ($NaHPO_4$) and 43.76 g sodium chloride (NaCl) in 3L milli-Q water and pH adjusted to 7.2, followed by making up the volume to 5 L. Ammonia solution 25% (EMSURE®, ISO, Reag. Ph Eur), hydrochloric acid 37% (EMSURE®, ACS, ISO, Reag. Ph Eur) and absolute ethanol (EMSURE®, ACS, ISO, Reag. Ph Eur) was obtained from Merck. Lactohale200^{TM} was purchased from DFE pharma (product code 585686). For staining nanoparticles taken up by immune cells in the lung, Perl's Prussian Blue was prepared from potassium ferrocyanide (BDH Chemical Ltd) and nuclear fast red (N8002, Sigma Aldrich).

3.2   Buffer and Media Preparation

3.2.1   Phosphate Buffered Saline (PBS)

For preparing a 10X stock of PBS, 22.1 g $NaH_2PO_4.H_2O$ 90.8 g Na_2HPO_4 and 350.4 g NaCl were dissolved in 4 litres of milli-Q water. The pH was adjusted to 7.2-7.4. For preparing a 1x working solution, 10x stock was diluted, 1 in 10 with milli-Q water and pH was further adjusted to 7.2-7.4. Both were sterile filtered under vacuum through a 0.22 μm filter (Merck, Darmstadt, Germany).

3.2.2   ACK lysis buffer

Ammonium chloride potassium (ACK) lysis buffer was prepared by dissolving 8.6 g NH_4Cl, 1.0 g $KHCO_3$ and 0.2 ml 0.5 M ethylenediaminetetraacetic acid (EDTA) was dissolved in 1 litre milli-Q water and the pH was adjusted to 7.2-7.4. The solution was sterile filtered under vacuum through a 0.22 μm filter (Merck, Darmstadt, Germany).

3.2.3 RPMI media

RPMI-1640(Gibco, Gaithersburg, MD, USA) of 450 ml volume was supplemented with 50 ml Fetal Bovine Serum (FBS, Gibco), 10 ml Penicillin (100U/ml final concenctration)/Streptomycin (100 μg/ml, Gibco), 10 ml L-glutamine (4 mM, Gibco), 10 ml HEPES (0.02 M, Gibco), and 2.5 ml β-mercaptoethanol (2ME, 0.1 mM). The supplementary reagents were added by filtering through a 0.22 μm sterile filter on the RPMI media.

3.3   Animals and Ethics

BALB/c female mice (6-8 weeks old) were used for all experiments in chapter 5 and 7. C57BL/6J female mice (6-8 weeks old) was used for experiments in chapter 4 and 5. In chapter 5, C57BL6J was used to understand whether a difference in mouse genotype results in difference in pulmonary inflammation. For chapter 4, a SHIP-1$^{-/-}$ mice in C57BL/6J background were used. For all experiments were maintained in the animal facility at 22-26 °C, 55-75% humidity and a 12/12-hour dark/light cycle with food and water *ad libitum*. All animal work in chapter 5 and 7 was conducted by the approval of Monash University Animal Ethics Committee under ethics No. MARP/2017/117. For chapter 4, all animal work was conduceted by the approval of AMREP Ethics Committee (AEC) under ethics No. All animal ethics are in compliance with the guidelines of the National Health and Medical Research Council (NHMRC) of Australia.

3.4   Bone marrow derived dendritic cell culture

For primary culture of bone marrow derived cells, the tibia, femur and humerus bones were collected from C57BL/6 mice, culled by CO_2 asphyxiation. The bones were cleaned of any tissue and soaked in 80% v/v ethanol for 1 minute. The bones were then placed in a small petri dish containing RPMI1640 medium. Both ends of each bone were removed to expose the bone marrow and placed in a 0.2 ml sterile centrifuge with a hole at the bottom made with 19 Ga needle. The small centrifuge tube containing the bones were placed in a 1.5 ml sterile centrifuge tube and capped. The bone marrow cells were flushed via centrifugation (pulsed to 6000G) and the red cells in pellet were lysed with 3ml of ACK lysis buffer. The cells were dissociated and filtered through a 100 μm strainer, into

a 10 ml centrifuge tube. The cells were centrifuged at 322 G or 1400 RPM for 4 minutes, the pellet was resuspended in 10 ml of complete media and the cells were counted with a haemocytometer. The cells were dispersed in complete RPMI supplemented media with 10 ng/ml GM-CSF at 5.0 x 10^5 cells/ml. In each 6 well plate, 3 ml (1.5 x 10^6 cells)of the cell suspension was added and incubated at 5% CO_2 and 37 °C in an incubator for 3 days. At the third day, 1.5 ml of media was taken out and replaced by fresh complete RPMI supplemented media with 10 ng/ml GM-CSF.

3.5 Cell Harvesting and staining for Flow Cytometry

After incubation of cells for the requisite time, cells were detached from 6 well plates by repeatedly flushing the wells with media and transferring to a 10 ml tube. The remaining attached cells were detached from the plate by adding PBS at 4 °C for 5 minutes, followed by pipetting up-down for collection. The cells were then centrifuged at 322 G or 1400 RPM for 4 minutes and the supernatant was discarded. The cell pellet was suspended in PBS with 2% FBS(FACS buffer) and transferred to a 96 well v-bottom plate(Corning) for antibody staining.

Nonspecific binding was blocked by using FACS buffer(PBS+2% FCS) for 15 minutes. Approximately 1 x 10^6 cells were stained on ice for 20 minutes with combinations of the following antibodies/conjugates(all from BD Pharmigen unless noted).

TABLE 3.1: Antibodies used for flow cytometry in this thesis

Antibody	Clone	Fluorophore	Supplier	Titration
CD11b	M1/70	PE-Cy7	BD Biosciences	500
CD11c	HL3	V450	BD Biosciences	50
CD40	3/23	PE-CF594	BD Biosciences	200
CD80	16-10A1	BV650	BD Biosciences	100
CD86	GL1	PE	BioLegend	200
F4/80	BM8	APC	eBioscience	200
GR-1	RB6-8C5	PerCP-Cy5.5	BD Biosciences	200
MHCII	M5/114/15/2	APC-heFluor 780	eBioscience	500
Zombie Aqua®		V525	BioLegend	500
GlyR $\alpha1+\alpha2$	polyclonal	FITC	Biossusa	50
GlyR $\alpha1$	2E6	IgG2a-κ isotype	Novus Biologicals(Abnova)	1000

Appropriate fluorescence-minus-one controls were used. All dilutions were done in FACS buffer. Cells were protected from light at all times. The acquisition was on LSRII(BD

Biosciences, Franklin Lakes, NJ, USA) or on BD-Fortessa X20 (BD Biosciences) instrument and analysis performed on FlowJo(Tree Star, Ashland, OR).

3.6   Lung function test- Invasive plethysmography

Mice were anaesthetized by i.p administration of ketamine (100 mg/kg body weight) with xylazine (10 mg/kg body weight) using a 26G needle before being subjected to tracheostomy. For tracheostomy procedure, the trachea was exposed by blunt dissection of surrounding muscle tissue followed by a small incision. A 22G steel cannula was inserted in the trachea connected to tubing and tied in place with suture. The tracheostomy cannula tube was attached to the plethysmography machine (Rodent RC site, Elan series, Buxco scientific) which ventilates the lung at normal breathing rate (a video of the procedure is demonstrated in SI video 1). AHR measurements are then taken by flow and pressure sensors in the plethysmography machine in response to increasing (doubling) dose of methacholine (3.125, 6.25, 12.5, 25, 50 mg/mL) (Mch, Acetyl-β-methacholine chloride $\geq$98% TLC, A2251). Physiological baseline data for each mouse were recorded upon administration of PBS which was used as background to normalize data for doubling doses of Mch. The parameters measured include resistance (RS), dynamic compliance (cDyn), maximum dynamic pressure (dPmax), dynamic pleural pressure (dPpl).

3.7   Broncho-alveolar lavage cell counts

Lungs were lavaged using 400 μL sterile, cold PBS followed by 3 further lavages of 300 μL to collect cells. The cells were spun down and resuspended in 200 μL PBS. The cells were counted and centrifuged (200 G or 1100 RPM for 5 minutes) onto a glass slide using a Shandon Cytospin 3 (Thermo Fisher Scientific), stained with Diff-Quik (Merck), and mounted. The slides were scanned using Leica Biosystems at 40X magnification and analyzed using Aperio Imagescope.

3.8   Histology and airway morphometry

Two lobes from both the right and left lung were immersion-fixed in 10% Neutral Buffered Formalin (NBF) followed by routine processing and embedding in paraffin. Using a microtome, lungs were sectioned transversally at the level of the proximal intrapulmonary main axial airway. Sections of 4 μm thickness were cut and placed on glass slides for histology and immunohistochemistry staining. The slides were deparaffinized and hydrated prior to staining. To identify mucus-secreting goblet cells, Alcian blue-periodic acid Schiff (AB-PAS) staining was performed. Alcian blue pH 2.5 was added to slides with hydrated sections; heated in a microwave on high power, for 45 seconds, and were allowed to stand for 2-5 minutes. The slides were washed in running tap water for 5 minutes and rinsed in distilled water. Periodic acid (0.5%) was added and stained for 5 minutes. After staining, the slides were rinsed in distilled water. Schiff's reagent was added, and slides were heated in a microwave on high power for 45 seconds. The slides were left to stand for 2-5 minutes and were washed in running tap water for 5 minutes and rinsed in distilled water. To identify the morphology and architecture of the lung parenchyma, deparaffinized sections were stained with hematoxylin and eosin. The sections were stained with Lillie mayer alum hematoxylin for 4 minutes and were washed in running tap water. The slides were distained in 0.3% acid alcohol and washed under running tap water. The slides were washed in Scott's tap water followed by rinsing the slides in tap water. The slides were then stained with eosin for 2 minutes, dehydrated, cleared and mounted. The slides were scanned using Leica Biosystems at 40X magnification and analyzed using Aperio Imagescope.

3.9   Perl's Prussian Blue counterstained with nuclear fast red for GSPION identification in cells

Perl's Prussian blue was used to identify the iron complex haemosiderin. Haemosiderin has the same iron-oxide core- Fe_2O_3, sharing similarity to our GSPIONs. Hence we utlised the chemistry of the stain to determine uptake by lung immune cells in the lung. The paraffin sections were brought to distilled water and the sections were placed in an equal volume of 2% HCl and 2% Potassium ferrocyanide for 20 minutes. The slides were then washed in distilled water. Following the wash, the slides were counter stained

with nuclear fast red for 10 minutes and washed under tap water. The slides were then dehydrated, cleared, mounted and imaged using an Olympus BX50 microscope. The images obtained were analysed using Aperio Imagescope (Leica Biosystems).

3.10 Immunohistochemical analysis

Sections of lung tissue were stained immunohistochemically to detect and localize IL-1β, IL-6, TNF-α, Glycine receptor α 1 subunit(GlyR-α1) and TSLP expression. IL-1β (1:1500, bs0812R, Bioss antibodies), IL-6 (1:2000, E-AB-40021, Elabscience), TNF-α (1:250, ab6671, Abcam) and thymic stromal lymphopoietin (TSLP, 1:5000, ABT330, Merck) were identified by using rabbit polyclonal antibodies, with kidney and heart sections used for positive control respectively (showed in Supplementary Information Figure). Bound primary antibody was detected using anti-rabbit EnVision (K5007, Dako, Glostrup, Denmark). The chromogen DAB was used, and sections were counterstained with hematoxylin, cleared, mounted and scanned using Leica Biosystems at 40X magnification. The images were analyzed using the positive pixel count algorithm (see section below) of Aperio Imagescope. For one section/mice/group, several sections are identified and scored subtracting the background. The total intensity of the strong positives for each section/mice/group was recorded and statistics were applied.

3.10.1 Positive pixel count algorithm- Aperio Imagescope

The Positive Pixel Count algorithm can be used to quantify the amount of a specific stain (say DAB) present in a scanned slide image. We specify a color say brown for IHC (range of hues and saturation) and three intensity ranges (weak, positive, and strong). For pixels which satisfy the color specification, the algorithm counts the number and intensity–sum in each intensity range, along with three additional quantities: average intensity, ratio of strong/total number, and average intensity of weak+positive pixels. The algorithm aperio uses has a set of default input parameters when first selected these inputs have been pre–configured for Brown color quantification (for IHC calculations) in the three intensity ranges (220–175, 175–100, and 100–0). Pixels which are stained, but do not fall into the positive–color specification, are considered negative stained pixels–these pixels are counted as well, so that the fraction of positive to total stained pixels was

determined. Any background intensity obtained was subtracted from the positive strong pixels in order to normalise and determine true expression/intensity.

3.11 Collagen quantification using Histoindex Genesis 200^{TM}

Formalin-fixed paraffin slides of lung tissue of each group was brought to water after dewaxing and treatment of decreasing alcohol concentrations. Lung tissue sections were scanned on the Genesis 200 (HistoIndex Pte. Lte., Singapore), in which a second harmonic generation (SHG) and two-photon excited fluorescence (TPEF) microscopy was used to visualize collagen deposition in tissue as per Goh and colleagues(George et al., 2019). The instrument was setup involves a laser passes through a pulse compressor (for group velocity dispersion) and an acoustic-optic modulator required for power attentuation. The beam is then diverted by a dichroic mirror, through an objective lens to the lung tissue, where the SHG signal was collected and processed for detection. The magnification of the Genesis 200 system can be adjusted to 10x, 2x, and 40x while other components are not adjustable. The lung sections were laser excited at 780 nm, SHG signals were recorded at 390 nm, and TPEF signals were recorded at 550 nm. The laser power=0.6, TPE and SHG sensitivities 0.8 and 0.7 respectively, with optical fibre bandwidth 11 nm and 88 nm for SHG and TPEF respectively. Images were acquired at 20x fold magnification with 512 pixel x 512 pixel resolution, and each image region was 200 μm x 200 μm. Each section was fully imaged followed by analysis using fibroindexTM image quantification. A region around collagen deposited area was drawn with ten such regions of interest drawn in each slide/lung section/group.

3.12 Fabrication of Glycine-coated Superparamagnetic Iron Oxide Nanoparticles (GSPIONs)

The nanoparticles were synthesized using a modified alkaline co-precipitation method (Barick and Hassan, 2012). $FeCl_3$(5.406 g), $FeCl_2$(1.988 g) in the ratio 2:1 and 1.5 M NaCl were added to 80 mL water in a three-neck flask. The mixture was stirred at 164 G or 1000 rpm under reflux and nitrogen atmosphere at 70 °C. When the temperature reached 70 °C, 30 mL (25%) ammonia solution was added drop-wise using a syringe with

constant stirring. The mixture was left to react for 30 minutes. Then, 4 mL glycine (0.3 g/ml) was added and the temperature was raised to 90 degC and left to react for 1 hour. The particle suspension was then separated with a magnet and the precipitate was washed with MilliQ water six times, by separating the precipitate each time by a magnet. The particle suspension was centrifuged at 13312 G or 9000 rpm for 7 minutes and the supernatant was collected, with the process repeated three times.

3.13   Morphology and Characterization of GSPIONs

The size, structure, and magnetic properties of GSPIONs were characterized by high-resolution transmission electron microscopy (HR-TEM), X-Ray diffraction (XRD) and field dependent magnetization. X-Ray Diffraction (XRD) pattern was recorded on a Rigaku Miniflex diffractometer with CuKα radiation. The crystal structure was analyzed using the Crystallography Open Database (COD). The infrared spectra were recorded in the range of 4000-450 cm^{-1} on a Fourier Transform Infrared Spectrometer (FTIR, Perkin Elmer Spectrum 100 spectrometer). A vibrating sample magnetometer was used to measure the saturation magnetization of the particles under a magnetic field of up to 10 kOe at room temperature. HR-TEM images were acquired by the FEI Tecnai G2 F20 S-TWIN FEGTEM connected to a wide angle Orius SCD200D CCD camera. HR-TEM procedures were conducted in the Monash Centre for Electron Microscopy (MCEM). The average diameter of the particles was measured using Quantax analysis system. The hydrodynamic size of the nanoparticles was measured using a Malvern Nano Zetasizer. Particles were dispersed in PBS and filtered using 0.2 mm syringe filter to remove dust. A probe sonicator (Qsonica, Q2000) was used to break the aggregates of particles by sonicating at 90% amplitude for 5 minutes duration prior to measurement. The cumulant sizes provided by the instrument are reported along with intensity-based distributions. The dip cell was used to measure electrophoretic mobility in PBS. These were converted to zeta potentials by combining Henry's formula with Ohshima's relation as recommended by IUPAC(Delgado et al., 2007; Ohshima, 1995).

3.13.1 Dynamic Light Scattering

Hydrodynamic size of nanoparticles was measured using a zetasizer Nano (Malvern, UK). Nanoparticles were sonicated prior to measurement. The intensity of the peak and size range was recorded for all measurements. To measure zeta-potential on the nanoparticle surface, a dip-cell (ZEN1002) was used to measure electrophoretic mobility in 1mM saline. Then, using Henry's formula with Ohshima's relation as recommended by IUPAC, the zeta-potential was calculated.

3.13.2 Field dependent magnetization to determine superparamagnetism

Field dependent magnetization of uncoated and glycine coated iron oxide nanoparticles was measured at 300 K. The maximum magnetizations of naked and glycine coated iron oxied nanoparticles(at an applied field of 10 KOe) were specifically measured followed by measurement of room temperature magnetization of both naked and glycine coated iron oxide nanoparticles in comparison to bulk Fe_2O_3. A vibrating sample magnetometer was employed for estimation of saturation magnetisation on naked and glycine coated iron oxied nanoparticles with a mass on the order of 15 mg for each type of nanoparticle. Field strengths of up to 8 x 10^5 A/m were with a sweep rate of 1.67 x 10^{-3} Hz. A BH hysteresis loop tracer was utilised for the estimation of magnetic poperties of both samples.

3.13.3 Determining the stability of GSPIONs at various pH

Zeta-potential of nanoparticles was used to measure the stability of nanoparticles in suspension at a range of pH. The GSPIONs were suspended in PBS and sonicated. For the measurement of zeta-potential, a dip-cell was used. The pH of suspended particles in PBS was varied from 1-11. For each pH, a fresh aliquot of particles was used and sonicated prior to pH adjustment. Upon adjustment of the pH, the zeta potential was immediately measured.

3.14 Fabrication of glycine microparticles for encapsulating GSPIONs

Glycine microparticles were fabricated by spray drying using a microfluidic jet spray dryer(Liu et al., 2011*a*; Wu et al., 2011) to produce monodisperse particles. This dryer uses a piezoelectric pulse for droplet generation, rendering even droplets. The dryer uses a nozzle of specific bore diameter. To prevent clogging due to the small nozzle bore, a nozzle with a bore diameter of 100 μm was used as it was found to block below this bore-size. An aqueous solution of 8 wt.% and 18 wt.% glycine was used as precursors for the process. Glycine solution was spray dried at 173 °C inlet drying temperature. Small amounts of the spray-dried glycine powder were placed in a petri plate and were stored under dry condition (¡20% RH) or at humid (76% RH) at room temperature. To reduce the size of glycine micro-carriers, we tried synthesizing them using a commercial spray dryer, Buchi 190 (De Souza et al., 2000) (the detailed procedure can be found in the Appendix 8.2). However, we discontinued using the Buchi 190 spray drier as it produced non-uniform particles (shown in Appendix 8.2). Hence from this point forward when we mention spray-dried glycine microparticles, they were synthesized by the micro-fluidic jet spray dryer.

The GSPIONs were loaded/embedded on to the spherical glycine microparticles. In a typical process, 0.01% (w/v) of GSPION dispersed in DI water was used for loading onto the glycine microparticles for spray drying. These GSPIONS were mixed in an aqueous solution of 17.99 wt.% glycine. The inlet temperature was maintained at 173 °C. The GSPIONs loaded glycine microparticles were kept in a desiccator with silica beads to avoid moisture (as moisture would solubilize the microparticles letting out the nanoparticles).

3.15 Morphology and Characterization of GSPION encapsulated in glycine microparticles

The size, structure and porosity of the microparticles were measured using SEM and X-Ray CT. To determine the size and structure of the particles a FEI Nova NanoSEM 450 FEGSEM was used with a Bruker Quantax 400 X-Ray analysis system. SEM procedures

were conducted in the Monash Centre for Electron Microscopy (MCEM). Images were acquired in both high and low vacuum to obtain high-resolution images at accelerating voltages between 2kV-3kV with spot size 2.0-3.0. To determine the porosity of the microparticles an ultra-high resolution (0.75 microns, Zeiss Xradia XRM520Versa) X-Ray Microscopy Facility (Xradia, Pleasanton, CA, USA) was used for image acquisition in this study. Image projections were acquired by rotating the load-stage 360° around its vertical axis. The frame size of the projections was 1024 × 1024 pixels. Scans were performed at 80kV, 3W with voxel size 0.75 μm. Voxels are defined here as pores. Scanning parameters used for all the samples were kept consistent for comparison. The 2D projections were reconstructed to 3D volumes. The reconstructed images were post-processed using an image processing software Avizo (V9.1.1, FEI, Hillsboro, OR, USA) (al Mahbub and Haque, 2016). Images of microparticles were cropped from the whole apparatus assembly followed by removal of noises using appropriate filters. Subsequently, the solid and void phases (pores) of the image were segmented and the voids were measured.

3.15.1 Quantitative and qualitative analysis of spray-dried glycine microparticles encapsulating GSPIONs

The GSPION loaded onto spray dried glycine microparticles were analysed both by Energy Dispersive Xray (EDX) and Thermogravimetric analysis (TGA) to find the location, behaviour and loading of the nanoparticles in the microparticles. A Bruker Quantax 400 EDX attached to the Nova SEM was used to map C, N, O and Fe at an accelerating voltage of 15kV with WD 5.4 mm. To confirm the loading of the GSPIONs into the microparticles, TGA was performed using a Perkin Elmer STA8000 TGA analyser in between temperatures 50 °C-600 °C. The difference in the degradation profile of the uncoated SPIONs and the GSPION loaded in the microparticles were analysed.

3.15.2 Iron and glycine concentration measurement in GSPION-loaded on to glycine microparticles

Iron concentration is a direct measurement of the efficiency of encapsulation by the spray dried glycine microparticles. Iron concentration was measured by adopting a method of Rad and colleagues (Rad et al., 2007) which utilizes the complex formed by ferric ions with the chloride. A standard curve was created by dissolving ferric nitrate in 5 M HCl

at concentrations from 1-200 μg/ml Fe^{3+} ions. For measuring the concentration of a batch of nanoparticles synthesized, the nanoparticles were dissolved in 5 M HCl and the absorbance at 345 nm based on the standard curve. Ammonium persulfate was dissolved in HCl to oxidize Fe^{2+} ions to Fe^{3+} ions. A microplate reader was used to calculate the absorbance of the assay at 345 nm with a final volume of 100 μl/well.

3.16 Ninhydrin assay to determine glycine chemisorption on nanoparticles

Glycine concentration was measured using a modified ninhydrin assay. An 8% w/v ninhydrin solution was made by dissolving 4 g ninhydrin and dissolving in 50 mL acetone. Standard glycine stock was prepared by dissolving 0.05 g/mL glycine in 1 mL PBS. 50 μL of glycine stock solution was added to the first well and serially diluted to 1/12th of the initial concentration at a final volume of 50 μL. This was used to draw a standard curve to determine the concentration of glycine coated to iron oxide nanoparticles. To determine the concentration of the chemisorbed glycine in the nanoparticles, glycine chemisorbed SPIONs suspended in PBS was used in triplicates. 100 μL of ninhydrin reagent was then added to all the wells. The plate was covered with aluminium foil and incubated in a heating block at 95 °C for 15 minutes. The plate was cooled to RT and 100 μL of 50%v/v ethanol was added. The absorbance was recorded in a micro-plate reader at 570 nm.

3.16.1 Determination of the aerodynamic performance of GSPION loaded on to spray dried glycine microparticles- as excipients

The aerodynamic performance and as a proof of concept for pulmonary delivery excipient use, glycine microparticles as excipient with or without GSPIONs was compared with a commercial excipient Lactohale200^{TM} (lactose-pharmaceutical grade), using a Next Generation Impactor (NGI) (Copley Scientific. Nottingham, UK). A pump was used to disperse the particles in the air stream which could flow through the instrument and impacted on eight consecutive stages of the impactor. A Ventolin® rotahaler® (Allen+hanburys Respiratory care, GlaxoSmithKline) DPI device was attached to the NGI mouthpiece. Four gelatinous capsules (size 3) were used per sample and were

manually loaded with 50 mg of spray-dried glycine microparticles as excipients with or without GSPIONs and compared with lactohale200^{TM}. The powder was discharged from the rotahaler$^®$ into the NGI. Using a critical flow controller TPK2000 (Copley scientific, UK), the airflow was set to 45 L/min for 6 seconds to mimic 4 L of air drawn in human inhalation. After actuation, the contents of the individual stages were washed with 5 ml of PBS and any powder deposit was dissolved and collected. The concentration of glycine was measured by ninhydrin assay against a standard curve with each stage per sample taken in triplicates. Data were analyzed as the fraction of the recovered dose from 50 mg of loaded sample in the capsule (as excipients form the bulk of any capsule). A two-way ANOVA with post-hoc T test was used to find significance in between the different samples at different stages.

3.17 Non-invasive 3D Ultra-short Echo time (UTE) MR lung imaging and biodistribution

For MR imaging mice were anaesthetized with isoflurane (IsoFlo$^®$, Abott Laboratories, North Chicago, IL) in 100% oxygen, and were placed supine with thorax centred with respect to the centre of the small animal radio-frequency coil (RF). A 9.4T Agilent MRI magnet running Bruker imaging hardware was used to obtain all MRI images. Low-resolution multi-slice images were acquired of the lungs in both the transverse and coronal planes using a fast spin echo sequence. Based on the results, a volume of interest (VOI) region encompassing the thorax from the trachea to the diaphragm was positioned. On this region, a non-gated 3D radial UTE sequence(Takahashi et al., 2010) was performed repeatedly with various TEs (0.01, 0.05, 0.1, 0.2, 0.4, 0.6, 0.8, 1.0, 1.2 msec) in fixed scale of receiver gain. The total number of projections was 61214. The other imaging parameters were: 4.0 msec repetition time (TR), 50° flip angle, 353 mm^3 field of view (FOV), 144^3 matrix (isotropic), 100000 Hz spectral bandwidth, and a volume coil 35 mm. Respiration of mice was maintained between 35-45 bpm by controlling isoflurane between 0.5-3%.

3.17.1   MR image processing and quantitative analysis

To measure signal intensity (SI), the lung was segmented for analysis using an open source image processing software (ImageJ). To define the ROIs, pulmonary vessels and trachea were avoided. ROIs such as upper (18.9 mm^2), middle (12.88 mm^2) and lower (19.75 mm^2) for both left and right lung were drawn using the ROI manager tool. The heart (28.18 mm^2) was used as a reference tissue control as the GSPIONs are not systemically circulated upon intranasal administration. Therefore, we do not expect to see any change in SI for both GSPION sensitized or saline (control) groups in the heart. For each TE, a total of 140 slices was imaged from the trachea to the diaphragm. We analyzed from slice 70-80 for SI calculations, as this region displayed the full lung volume without obstruction. SI was quantitated using the measure function of the ROI manager. A T_2 MR calculation was performed using a package developed by Schimdt and colleagues(Schmidt et al., 2004) in each ROI in the slope of the logarithms of noise-corrected SIs versus different TEs(Takahashi et al., 2010). SI of each segment was analysed by the z-axis profile function. The background from the pre-sensitization images was used to analyze the SI in air to provide an estimate of noise in each image(Martin et al., 2008).

3.18   Determination of GSPIONs uptake by lung immune cells

Lung paraffin sections were brought to water and the sections were placed in an equal volume of 2% HCl and 2% potassium ferrocyanide for 20 minutes. The slides were then washed in distilled water. Following the wash, the slides were counterstained with nuclear fast red for 10 minutes and washed under tap water. The slides were then dehydrated, cleared and mounted and imaged using an Olympus BX50 microscope. The images obtained were analysed using Aperio Imagescope (Leica Biosystems).

3.19   Statistical analysis

Statistics were analyzed using GraphPad Prism v6.0 software (GraphPad). Data were analyzed for normal and log-transformed for normality as necessary prior to analysis by

independent t test, ANOVA, or two-way ANOVA with Tukey or Bonferroni post-tests, as appropriate. Differences were considered statistically significant at $p < 0.05$. Group size is included in the figure legend and all values are mean$\pm$SD.

Chapter 4

Immunomodulatory effect of Glycine on Antigen Presenting Cells

4.1 Introduction

I n response to infection and tissue injury, innate immune cells of the body such as dendritic cells(DCs), macrophages and mast cells recognise pathogens and damaged cells by germline-encoded intra-cellular or surface expressed pattern recognition receptors(PRRs). These receptors detect Pathogen − Associated Molecular Patterns(PAMPS) such as bacterial and viral nucleic acids, cell wall components. Toll like receptor family are one of the major PRRs found in cell. When these monocytes and DCs come in contact with a PRR, they express costimulatory molecules for T Lymphocyte activation and are said to be induced or adaptive immune response(Thompson et al., 2011). In a similar way macrophages undergo cell activation in response to LPS or IFN-γ(Dobrovolskaia et al., 2003). When the immature macrophages circulating in the blood come across an infection (bacteria or virus), or bacterial components such as lipopolysaccharide (LPS) they undergo activation. Decrypting these cells of the innate immune system has revealed that the subsets of these cells have specialised in secreting cytokines that have different targets and function. For example, the macrophages secrete pro-inflammatory cytokines which include IL-1β, IL-6, IL-12, TNF-α and IFN$-\gamma$(Thompson et al., 2011). The activation of these cells is induced by IFN$-\gamma$, TLR-4 ligands, IL-4, IL-13 and TGF$-\beta$ but signalling through TLR-4 is not essential but carried out by MyD88 dependent signalling pathway. Prior to adaptive immune response, recognition of infection and triggering inflammatory responses are mediated by Toll like receptors (TLRs)(Pascual et al., 2011) which are a super family of IL-1 receptors. LPS from the gram negative bacterial cell wall is an agonist to TLR4 and is responsible for activation of $NF\kappa\beta$ and MAPK pathway inducing the expression of pro-inflammatory cytokines(Takeda et al., 2003).

Several pathways are implicated in these events, one of which is the PI3K pathway. The PI3K is negatively regulated by lipid phosphatase Src homology 2 domain containing inositol polyphosphate 5-phosphatase 1 (called as SHIP-1) which hydrolyze the 5' phosphate of second messenger phosphatidylinositol 3,4,5 trisphosphate (PIP3) (Figure 4.1). SHIP is necessary for maturation and function of Granular Monocyte Colony Stimulating Factor (GMCSF) induced derived dendritic cells which are matured by TLRs. There is mixed information in the literature about PI3K, whether it is a positive or negative regulator of TLR signaling. In macrophages it is regularly studied as a negative

regulator. Limited studies have been carried out with DCs in the spleen and bone marrow derived DCs(BMDCs) from mice lacking the $p85\alpha$ regulatory subunit of class IA PI3Ks producing more $IL12$ upon stimulation with the TLR ligands such as LPS(Griffiths et al., 2014; Krebs et al., 2012).
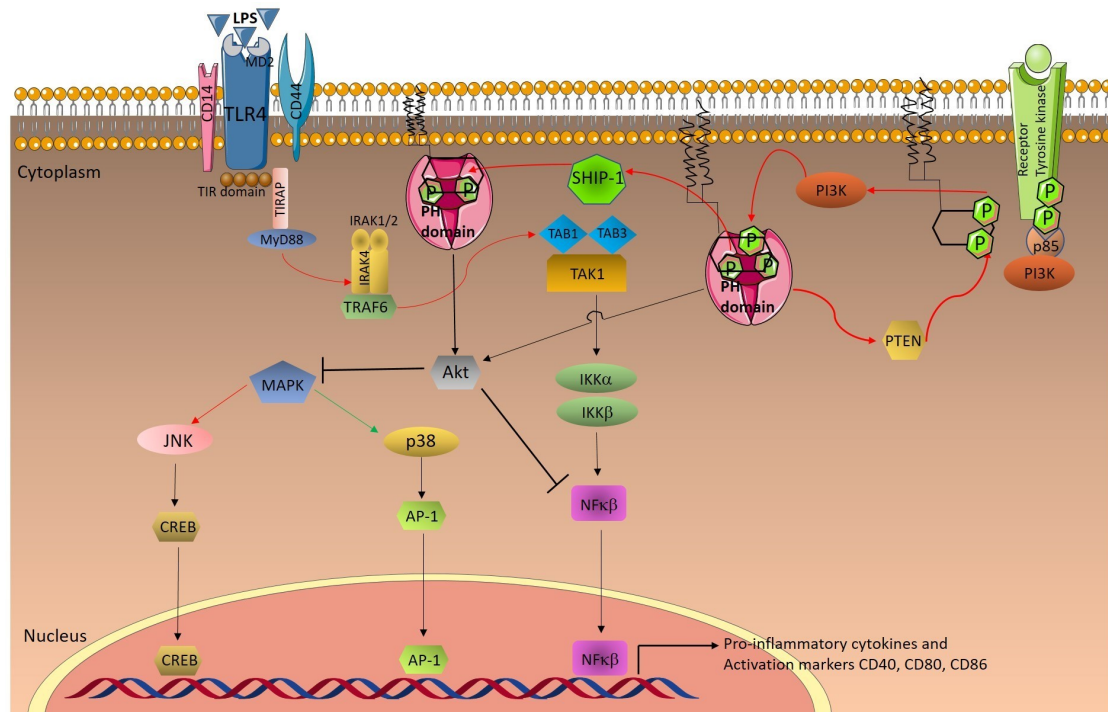
FIGURE 4.1: **Interaction of TLR4 and SHIP-1 in activating pro-inflammatory cytokines and activation markers.** LPS binds to Toll Like Receptor 4(TLR4) and leads to production of Pro-inflammatory cytokines and activation markers such as CD40, CD80 and CD86. PI3k inhibits MyD88 through BCAP. SHIP-1 negatively regulates PI3K which inhibits production of pro-inflammatory cytokines and activation markers in DCs. Figure constructed with reference to (Maxwell et al., 2011)

4.2 Methods

4.2.1 Experimental Design

To demonstrate the role of glycine on LPS stimulated BMDCs, mice bone marrow cells were cultured using GMCSF (please refer to detailed protocol in Chapter 3.5). After experimentation, cells were harvested and analyzed by flow cytometry (please refer to detailed protocol in Chapter 3.6). However, the study design to investigate the role of SHIP$^{-/-}$ on LPS induced BMDCs and macrophages with or without glycine is demonstrated in Figure 4.2 below.
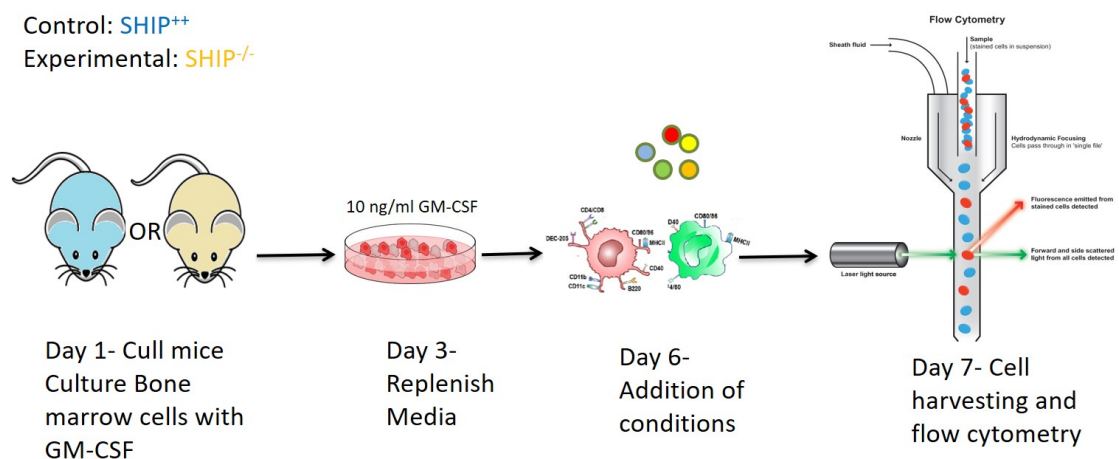
FIGURE 4.2: **Experimental design to investigate the effect of glycine on $SHIP^{+/+}$ and $SHIP^{-/-}$ bone marrow derived dendritic cells and Macrophages**. Cells are cultured with 10 ng/ml GMCSF and media is replenished in day 3 followed by addition of conditions in day 6. Cells are harvested and analysed by flow cytometry at day 7

4.2.2 Glycine receptor staining on BMDCs and GlyR immunohistochemistry on Lung

For staining of glycine receptor on BMDCs and macrophages, GlyRα1+α2-FITC antibody was been used (refer to Table 3.1). For controls, IgG1 at the same concentration as the antibody was used and stained and analysed by flow cytometry following protocol in Chapter 3.5. For immunohistochemistry on paraffin lung and brain cortex sections, the slides were prepared as per detailed protocol in Chapter 3.9 and 3.10. For GlyR α1 staining on lung paraffin sections, GlyRα1 antibody (refer to Table 3.1) was used. For control, IgG2aκ antibody at the same concentration and isotype of GlyR antibody was used to control stain for the background.

4.3 Results

4.3.1 Cell viability is unaffected with glycine

We investigated the overall viability of cells with glycine at concentrations 10 mM and 100 mM by utilizing the *ZombieViolet*$^{\circledR}$ amine reactive fluorescent dye which stains dead cells due to its permeability through compromised membranes. Viability of cells at 10 mM glycine ($83.3 \pm 5.2\%$) which increased to $92.7 \pm 1.4\%$ at 100 mM glycine when compared to untreated cells ($76.8 \pm 3.1\%$) (Figure 4.3). Flow cytometry confirmed that glycine is not cytotoxic to cells and does not interrupt the cell growth process.
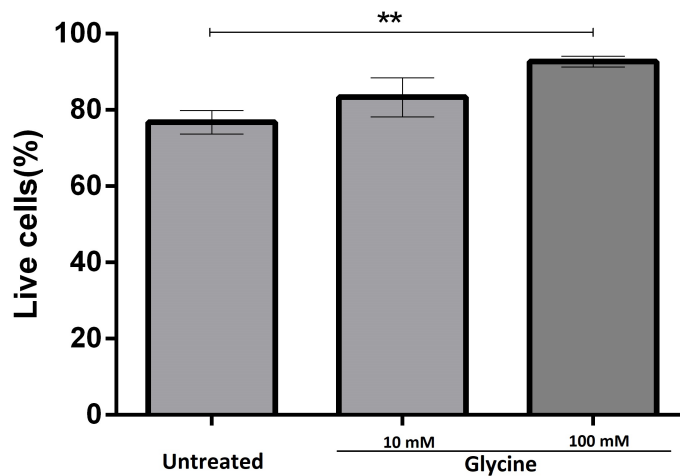
FIGURE 4.3: **Glycine has no cytotoxic effect on cell viability.** Naïve C57BL/6 mice bone marrow cells were cultured with GMCSF and glycine at 10 mM and 100 mM concentrations were added on day 6 of culture followed by harvesting the cells after 24 h. Untreated cells were used as the control. $Mean \pm SD$; n=3/group (each replicate consisting of three mice). $**p < 0.01$.

Since cells were viable at 100 mM glycine we checked the viability of cells at two-fold and three-fold increased glycine concentration. Viability of cells at 200 mM glycine was $76.3 \pm 10.1\%$ and 300 mM was $74.6 \pm 8.7\%$ which is slightly reduced in comparison to untreated cells ($83.1 \pm 2.7\%$) (Figure 4.4). Therefore, it is inferable that glycine can be used at high concentrations on BMDCs albeit small reduction in cell viability. Hence, glycine can be used as an anti-inflammatory compound to down regulate LPS induced activation without affecting cell viability.

4.3.2 LPS induced up-regulation of activation markers on APC is down modulated by glycine

Previous data from our group showed inert glycine coated polystyrene 50 nm nanoparticles do not promote cardiac inflammation or allergic airway inflammation, but coversely inhibit it(Hardy et al., 2012). Therefore, we speculated that glycine may be playing the role in inhibiting inflammation by acting directly on diverse APC, limiting their ability to respond to a pro-inflammatory stimuli, and performed an initial study assessing its effect on different APC subsets generated from bone marrow cell precursors. We analyzed the effect of LPS (10 ng/ml) along with glycine (10 mM and 100 mM) on bone marrow derived dendritic cells (BMDC) ($CD11c^+MHCII^+GR1^-$) and macrophages ($CD11c^-MHCII^+GR1^-CD11b^+F4/80^+$) as gated in Figure 4.5.
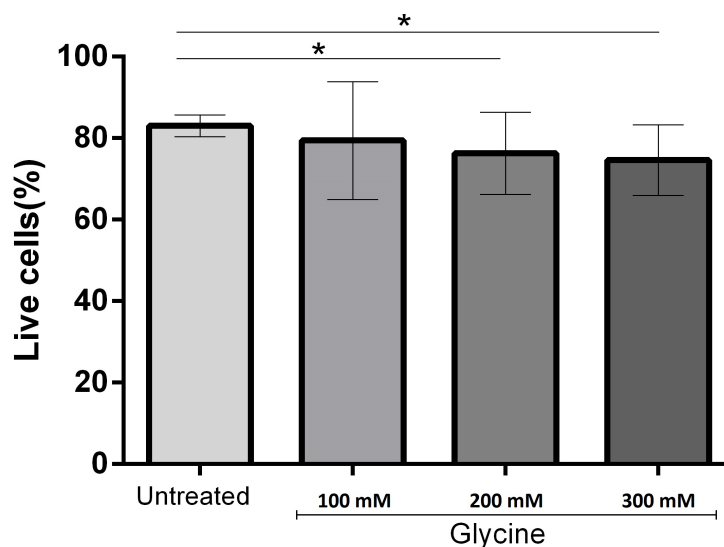
FIGURE 4.4: **Glycine affects cell viability of APCs at two/three fold higher concentration.**Naïve C57BL/6 mice bone marrow cells were cultured with GMCSF and glycine at 100 mM, 200 mM and 300 mM concentrations were added on day 6 of culture followed by harvesting the cells after 24 h. Untreated cells were used as control. There is no difference in cell viability at 100 mM glycine concentration however, there is a slight reduction in cell viability with 200 and 300 mM. $Mean \pm SD$; n=3/group (each replicate consisting of three mice). $*p < 0.5$.

FIGURE 4.5: **Gating stratetgy for analysis of LPS induced activation of activation markers and down modulation by glycine on BMDCs and macrophages.** Bone marrow was isolated from femur and tibia of culled mice followed by culturing with GMCSF. The cells were gated on FSC/side scatter (SSC) followed by gating to exclude doublets. $CD11c^+$ and $MHCII^+$ gating was applied to allow discrimination of $CD11c^+MHCII^+$ BMDCs and $CD11c^-MHCII^+$ macrophages. **(A).** $CD11c^+MHCII^+GR1^-$ BMDCs and **(B).** $CD11c^-MHCII^+GR1^-CD11b^+F4/80^+$ macrophages. FSC-A, FSC pulse area; FSC-H, FSC height; SSC-A, side scatter pulse area; zombie(LIVE/DEAD)

Flow cytometry confirmed that LPS (at a concentration of 10 ng/ml) caused a marked increase in expression of activation markers CD40, CD80, CD86 and MHCII on CD11c$^+$ MHCII$^+$GR1$^-$ BMDCs (Figure 4.6). A significant down modulation of LPS induced activation was seen by incubating in the presence of 100 mM glycine across multiple activation markers: CD40, CD80, CD86 and MHCII. This effect, albeit less pronounced was still observed using 10 mM glycine for the MHCII marker. Neither glycine concentration affected CD86 expression although CD86 is coexpressed with CD80 (Figure 4.6). Similar analysis on $CD11b^+F4/80^+$ macrophages showed significant down modulation of LPS CD40 and MHCII up-regulation by glycine, but no effect on CD80 and CD86 expression. Specifically, glycine at 100 mM was able to down regulate both CD40 and MHCII but at lower concentration(10 mM) failed to do so on CD40 (Figure A.1). This down modulation of costimulatory molecules on activated BMDCs highlights the role of glycine as an anti-inflammatory agent, which further pointed us to investigate whether an increased concentration of glycine could further bring down the activation of costimulatory molecules in response to LPS, down to baseline.
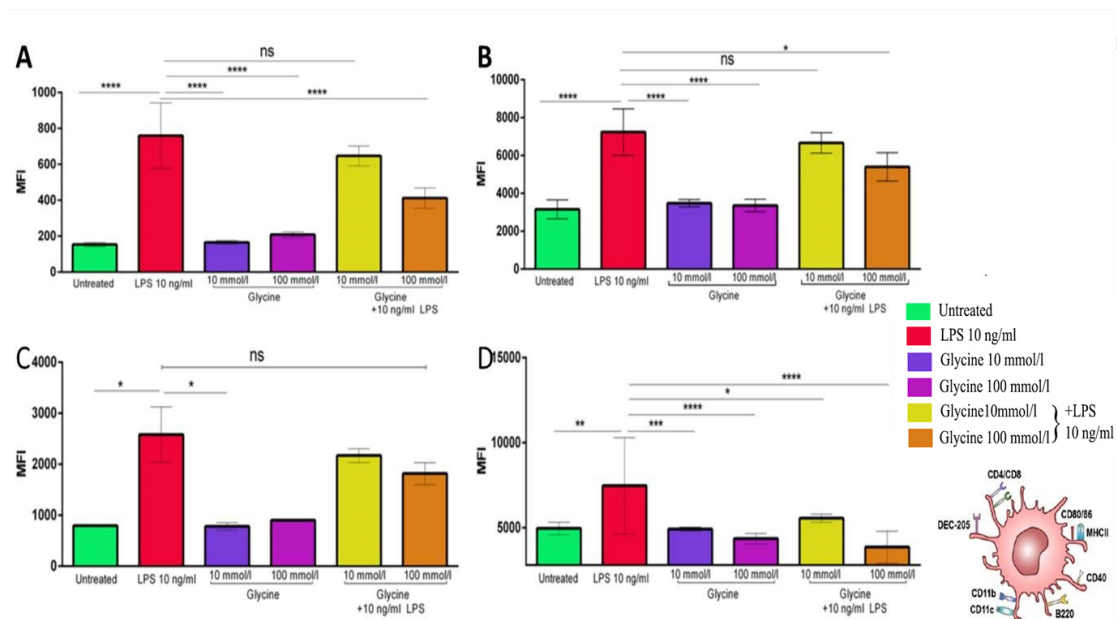
FIGURE 4.6: **Glycine down regulates expression of LPS activated activation markers on BMDCs.** Naïve C57BL/6 mice bone marrow cells were cultured with GMCSF and LPS, glycine conditions added on day 6 of culture and harvested cells after 24 h. Untreated cells were used as control (shown in green). Effect on $CD11c^+MHCII^+GR1^-$ BMDCs as per gating on Figure 4.5A expressing **(A)** CD40, **(B)** CD80, **(C)** CD86 and **(D)** MHCII; $Mean\pm$ SD; n=3/group (each replicate consisting of three mice). ns, non-significant; $*p < 0.1, **p < 0.01, ***p < 0.001, ****p < 0.0001$

To further consolidate our finding we increased the glycine concentration to 200 mM and 300 mM. We also increased the LPS concentration from 10 ng/ml to 1 μg/ml. BMDCs at 200 mM glycine concentration could only down regulate CD40 upon activation by both LPS concentrations. However at 300 mM glycine could significantly down-regulate CD40, CD80 and CD86 for both LPS concentrations. Down modulation observed was down to background levels for CD40 and CD80/86 markers. MHCII showed no effect on either of the glycine concentrations when challenged with LPS (Figure 4.7). The levels of CD40 were significantly low upon challenge with both LPS concentrations which can be attributed to the anti-inflammatory effect of glycine on BMDCs. In this experiment, we additionally were able to analyse separately an important subset of macrophages. In $CD11b^{+}F4/80^{+}$ macrophages, 300 mM glycine could bring down the levels of all the activation markers with both LPS concentrations but could only down-regulate CD86 and not CD80 at 200 mM glycine (Appendix Figure A.2). CD86 activates PI3k which in turn is regulated in a SHIP dependent manner(Kin and Sanders, 2006). Hence in both DC and macrophage subsets, CD40 can be down regulated at a high glycine concentration but CD80/86 demonstrated a selective down-regulation. The selective down regulation of CD86 and not CD80 is discussed in the discussion section following the results supporting the role of glycine in down regulating activation markers in a SHIP dependent manner.
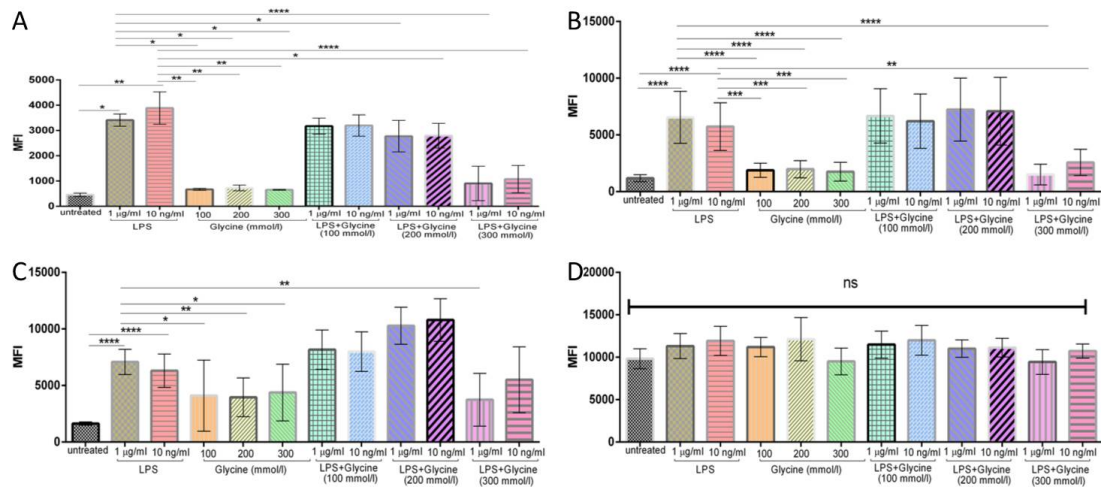
FIGURE 4.7: **Titratable effect of glycine in down-regulating expression of LPS activated activation markers in BMDCs.**Glycine down regulates expression of both 10 ng/ml and 1 μg/ml LPS activated activation markers on BMDCs. Naïve C57BL/6 mice bone marrow cells were cultured with GMCSF and LPS, glycine conditions added on day 6 of culture and harvested cells after 24 h. Untreated cells were used as control. Effect on $CD11c^{+}MHCII^{+}GR1^{-}$ BMDCs as per gating on Figure 4.6A expressing **(A)** CD40, **(B)** CD80, **(C)** CD86 and **(D)** MHCII. $Mean\pm$ SD; n=3/group (each replicate consisting of three mice). *ns, nonsignificant*; $*p < 0.1, **p < 0.01, ***p < 0.001, ****p < 0.0001$

4.3.3 LPS induced up-regulation of activation markers on APCs is down modulated by glycine in a SHIP dependent manner

Bone marrow derived cells from both $SHIP^{+/+}$ and $SHIP^{-/-}$ mice were cultured with GMCSF for differentiation into bone marrow derived dendritic cells (BMDC) characterized as ($CD11c^+MHCII^+GR-1^-$). The effect of LPS (100 ng/ml) and glycine (300mM) was studied on bone marrow derived dendritic cells(BMDCs) from $SHIP^{+/+}$ and $SHIP^{-/-}$ mice. CD40 was up-regulated upon addition of LPS on both $SHIP^{+/+}$ and $SHIP^{-/-}$ BMDCs with a higher up-regulation in $SHIP^{+/+}$ DCs. Upon addition of glycine (300 mM), there was significant down-regulation of CD40 on the $SHIP^{+/+}$ BMDCs but not on $SHIP^{-/-}$ DCs (Figure 4.8A). The same glycine mediated down modulation was also observed on other activation markers CD80 and CD86(Figure 4.8A). The activation of CD80 and CD86 on $SHIP^{+/+}$ BMDCs was higher than $SHIP^{-/-}$ BMDCs. But the attenuation of CD80 and CD86 was observed only on $SHIP^{+/+}$ but not on $SHIP^{-/-}$ BMDCs.
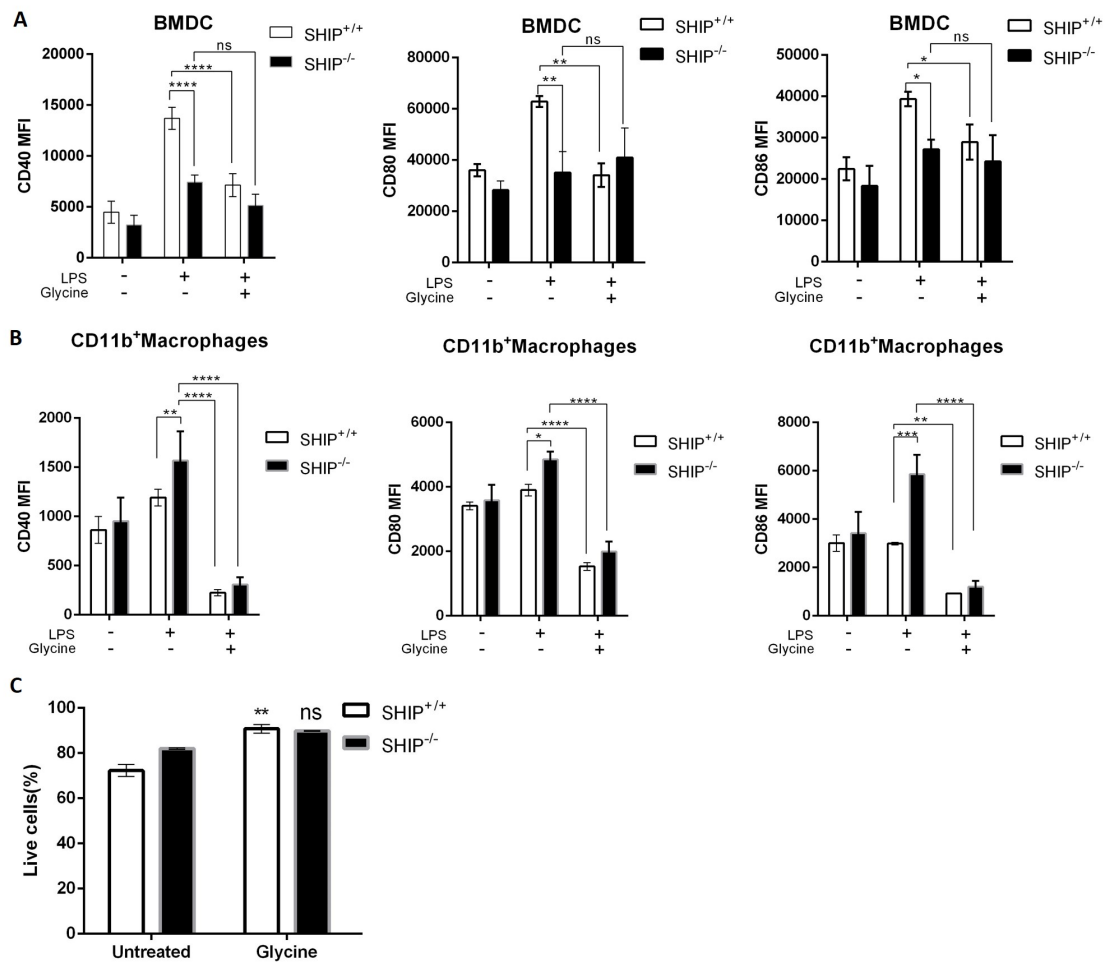
FIGURE 4.8: **Effect of glycine on $SHIP^{+/+}$ and $SHIP^{-/-}$ bone marrow derived dendritic cells and macrophages. (A).** LPS induced up-regulation of CD40 on $SHIP^{+/+}$ and $SHIP^{-/-}$ bone marrow derived dendritic cells. Glycine was able to down modulate the CD40 marker. The down modulation was observed significantly on WT DCs but not on SHIP-1 KO DCs. This showed that glycine signals this down modulation in a SHIP-1 dependent manner. In a similar manner, CD80 and CD86 was upregulated by LPS. Glycine mediated down modulation was observed only on WT BMDCs. **(B).** LPS induced up-regulation of CD40 on $SHIP^{+/+}$ and $SHIP^{-/-}$ CD11b$^+$ bone marrow derived macrophages. Up-regulation of CD40, CD80 and CD86 was more on $SHIP^{-/-}$ than $SHIP^{+/+}$. CD80 and CD86 was also up-regulated on CD11b$^+$ marophages and was down-regulated by glycine. **(C).** Cell viability of $SHIP^{+/+}$ and $SHIP^{-/-}$ cells showing no viability difference in between the two cell types with glycine

In culture, BMDCs is not the only cell type that is induced. There is the presence of some CD11b$^+$ macrophages. The effect was similar on CD11b$^+$ bone marrow derived macrophages. LPS upregulated CD40 on both $SHIP^{+/+}$ and $SHIP^{-/-}$ macrophages and glycine down regulated CD40 on LPS induced $SHIP^{+/+}$ and $SHIP^{-/-}$ macrophages (Figure 4.8B). The effect of up-regulation by LPS was more strong on $SHIP^{-/-}$ than $SHIP^{+/+}$ macrophages. CD80 was up-regulated on $SHIP^{-/-}$ but failed on $SHIP^{+/+}$ macrophages upon stimulation with LPS(Figure 4.8B). CD86 was up-regulated on $SHIP^{-/-}$ but not on $SHIP^{+/+}$ macrophages. Based on our data and that of others, SHIP-1 found in hematopoetic cell acts as a negative regulator of inflammation(Antignano et al., 2010b; Tsantikos et al., 2018). SHIP-1 regulates the NF-$\kappa\beta$ pathway and several other inflammatory pathways involved in producing pro-inflammatory cytokines and activation markers(Pauls and Marshall, 2017; Rauh et al., 2004). SHIP-1 prevents the up-regulation of the activation marker CD40 as confirmed by our data and also in its absence increases CD40 and other activational markers significantly when stimulated with LPS(Antignano et al., 2010a,b). Since, the bone marrow derived cell culture was induced by GMCSF, it leads to a majority of dendritic cell phenotype. However, the effect was consistent in bone marrow derived macrophages.

Glycine showed negligible cytotoxicity at 300 mM on both $SHIP^{+/+}$ and SHIP$^{-/-}$ BMDCs as showed by their cell viability (Figure 4.8C). On both cell types, cell viability was 85$\pm$5 % on glycine treated cells. However, cell viability of glycine treated cells compared to media only (untreated) was higher. To evaluate the effect of glycine co-administered with LPS on BMDCs from both WT and SHIP$^{-/-}$ mice, we measured the mean-fluorescent intensity(MFI) of the marker CD11c. For identifying both DCs and macrophages, the marker CD11c is very important as DCs are CD11c$^+$ while macrophages are CD11c$^-$. We found the expression unchanged for CD11c on both cell types (see Appendix A.3) and hence the down-regulation observed in the activation markers can be attributed to glycine.

4.4 Expression of glycine receptor $\alpha 1$ subunit on BMDCs and lung endothelial cells

Preliminary data suggests that LPS induced activation of BMDCs could be abrogated using the neutral, non-toxic amino acid, glycine. We speculated that this phenomenon is signalled through the glycine receptor (GlyR)(Lynch, 2004). There are several evidence of this neuronal receptor in non-neuronal cells such as in retina, sperm, pancreas, liver, leucocytes, spleen as well as on alveolar macrophages(Van Den Eynden et al., 2009). But the receptor expression on a wide-spectrum of APCs such as bone marrow derived DCs and macrophages is not-known or investigated. Furthermore, we hypothesized that mechanistically glycine would attenuate the effect of LPS by regulating through GlyR in BMDCs and macrophages. Therefore, we investigated the expression of GlyR on human peripheral blood mononuclear cells (PBMCs) to validate the findings by Eynden and colleagues(Van Den Eynden et al., 2009) before investigating the presence of GlyR on bone marrow derived APCs. GlyR$^+$ population of cells on human PBMCS are characterized on the basis of CD3$^+$ (Tcells), CD14$^+$ (monocytes), CD56$^+$ (NK cells) represented in Appendix 8.2, Figure A.4. The mean fluorescence intensity (MFI) of GlyR on these population of cells were compared to the isotype to identify expression of GlyR on PBMCs (and their sub-types).

We investigated for the presence of Glycine receptor in GMCSF induced bone marrow derived cells, alveolar macrophages and lung endothelial cells. The presence or absence of the receptor was confirmed by flow cytometry on BMDCs and by immunohistochemistry on lung resident cells. To investigate the presence of GlyR, BMDCs was gated as $CD11c^+MHCII^+GR-1^-$ and glycine receptor was gated as GlyR vs SSC-A (Figure 4.9A). Bone marrow derived macrophages were gated as $CD11c^-MHCII^+GR-1^-$ followed by $CD11b^+F4/80^+$ (Figure 4.9B). Glycine receptor was gated as GlyR vs SSC-A, with any change from isotype taken as a positive stain. In the figures, expression of the receptor is showed in red, with isotype (in blue), and other antibodies (orange). Glycine receptor expression was identified on these cells with a distinct shift towards a higher log value and separation from the isotype indicated a positive expression of the receptor, observed in BMDCs and BM macrophages(Figure 4.9A,B). The receptor expression was compared on the basis of MFI within different population of cells and was found to be

highly expressed in BMDCs compared to macrophages but could be possible due to less number of available macrophages in culture (Figure 4.9C). However, this indicated that GlyR has a possible expression on macrophages and hence we looked into the lung for its expression.

We investigated for GlyR expression on BMDCs and macrophages under different conditions such as with LPS co-administered with or without glycine. The receptor expression was up-regulated with LPS (1 μg/ml) and down regulated on the addition of glycine (300 mM). The same effect is observed on $CD11c^+$ cells and $CD11b^+F4/80^+$ macrophages (Figure 4.9D). The glycine receptor can become desensitized quickly upon repeated stimulations. Homologous desensitization occurs when a receptor decreases its response to a signalling molecule(in this case, LPS) when the agonist(here glycine) is present in high concentration(Gielen et al., 2015). Neuronal receptors tend to shuffle(LeBrasseur, 2008). The increase in glycine receptor expression on LPS stimulated BMDCs and macrophages is a result of higher glycine receptor shuffling. Since, the cells were incubated for 20 hours which is a long time to have effect, we observe that there is significant up-regulation in LPS due to receptor shuffling. While for glycine which is an agonist to the receptor, at such a high concentration, there is receptor desensitization which leads to abrogation of the receptor shuffling when incubated along with LPS. This is confirmed by the level of expression of the receptor in the untreated sample.
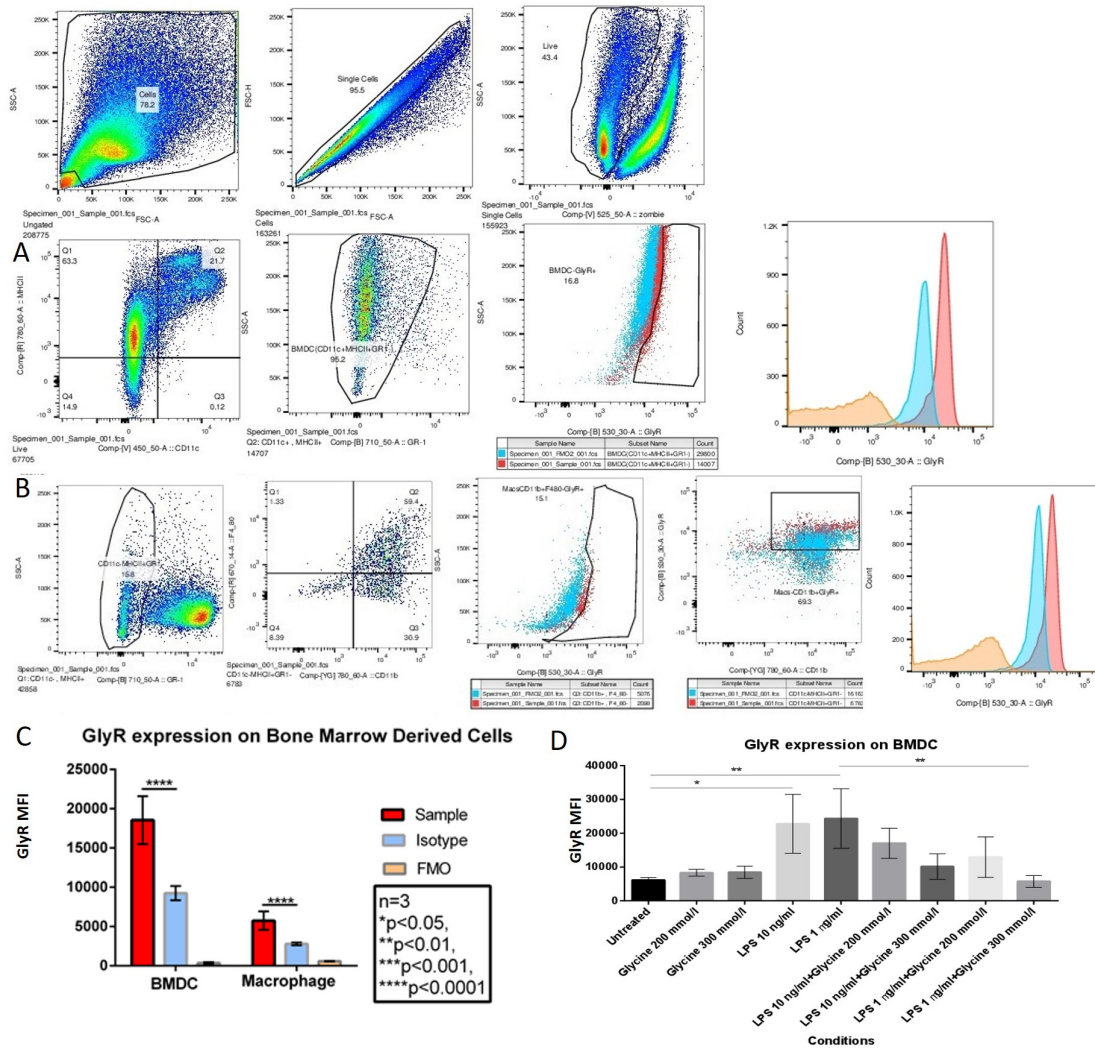
FIGURE 4.9: **Glycine receptor expression on Bone marrow derived dendritic cells and Macrophages**. **(A).** Bone marrow derived dendritic cells were characterised as $CD11c^+MHCII^+GR-1^-$. Glycine receptor(showed in red) was validated against an isotype(showed in blue) of the same antibody. A small shift was observed from the isotype and other phenotypic stains(orange). **(B).** Bone marrow derived macrophages were characterised as $CD11c^-MHCII^+GR-1^-CD11b^+F4/80^+$. Glycine receptor(showed in red) was validated against an isotype(shown in blue) of the same antibody. A small shift was observed from the isotype and other phenotypic stains(orange). n=3/group were stained separately(each replicate consisting of three mice) showed as histograms. **(C).** Bone marrow derived dendritic cells and macrophages were compared in terms of their GlyR expression. Glycine receptor(shown in red) was validated against an isotype(shown in blue) of the same antibody and phenotypic stains(shown in orange). n=3/group were stained separately(each replicate consisting of three mice) and individual un-paired T test was performed. **(D).** GlyR expression upon treatment with LPS and glycine was investigated on Bone marrow derived dendritic cells. Glycine receptor expression increased on inducing by LPS. Glycine receptor expression decreased when glycine was added with LPS.*p< 0.05, **p< 0.01, ***p< 0.001, ****p< 0.0001*

GlyR was found to express on lung endothelial cells(Figure 4.10B) and in the process we identified alveolar macrophages(Figure 4.10B,C(iii)), lymphocytes(Figure 4.10C(i)) and neutrophils (Figure 4.10C(ii))to express the receptor. For controls, Balb/c mice brain cortical sections were used, as GlyR is known to express in the brain cortical region (Figure 4.10A). The stain was compared to the antibody isotype control to acknowledge for any background stain. Using Aperio Imagescope positive pixel count algorithm, GlyR expression in lung sections were quantified.
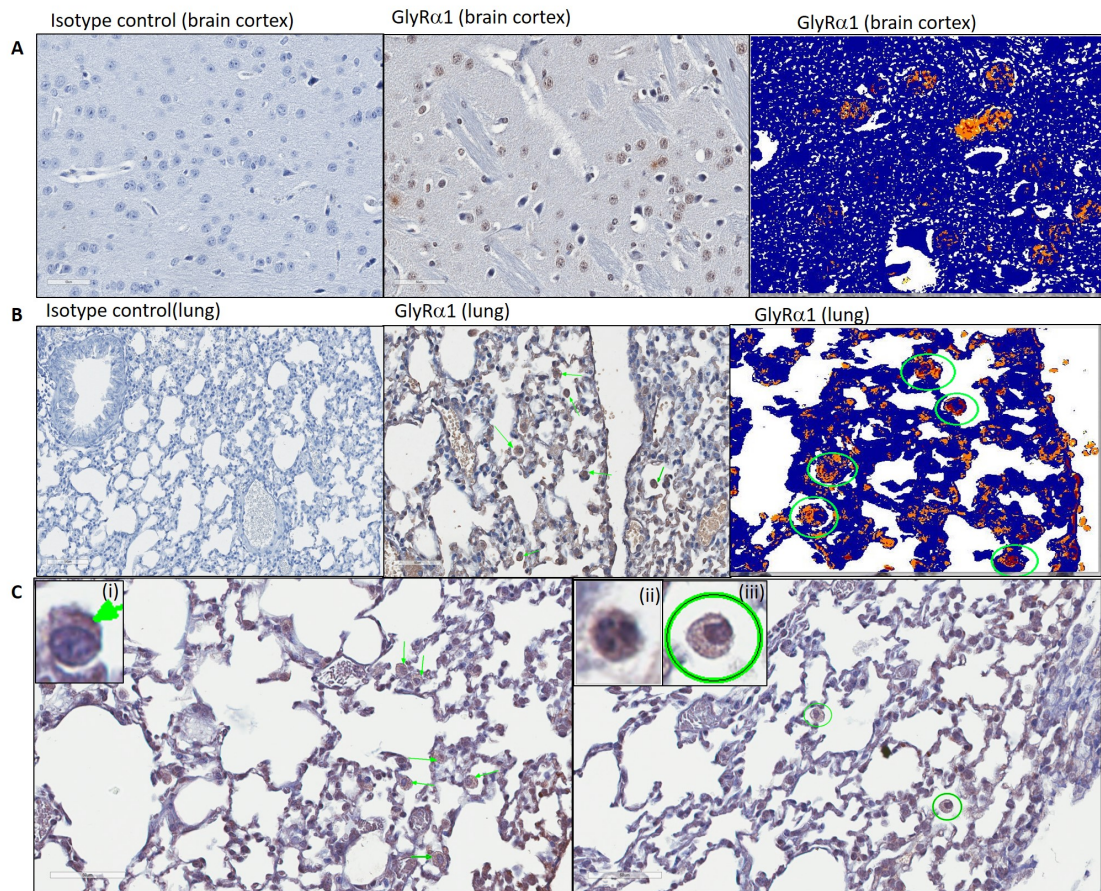
FIGURE 4.10: **GlyR expression on lung endothelial cells and alveolar macrophages.** GlyR expression on paraffin embedded Balb/c mice lung sections was evaluated. **(A).** For positive control, Balb/c mice brain cortex was stained with GlyRα1 antibody and at a similar concentration the isotype was used for staining. By positive pixel algorithm, GlyR expression true stain was identified on brain cortex. **(B).** GlyR expression on lung sections at the same concentration as brain cortex. The arrows and ovals point to different immune cells stained in the process. Aperio positive pixel count algorithm was used to identify true stain which showed different immune cells circled in green. **(C).** Specific staining of different immune cells were identified on the lung sections on the basis of the cell shape and nuclei. **(i)** Lymphocyte, **(ii)** Neutrophil and **(iii)** Alveolar macrophage. Many alveolar macrophages were visible and was confirmed by positive pixel count demonstrated in B.

4.5   Discussion

In context of cell activation, the markers that are looked at up-regulation include CD40, CD80, CD86 and MHCII. LPS upregulated CD40, CD80 and CD86 on MHCII through a TLR4 mediated NF-$\kappa\beta$ signalling(Zhou et al., 2012). LPS triggers the activation of several cytokines such as IL-1β, IL6, TNF$-\alpha$. CD40 is up-regulated in response to TLR9 (CpG) or TLR4(LPS) agonists which occurs by the activation of the p38 MAPK pathway leading to the production of the cytokines IL6, IL12p40(Ma and Clark, 2009). CD80 and CD86 are costimulatory molecules which have been found to have increased expression on LPS stimulated monocytes in non-atopic asthma that secrete cytokines IL5 and IL13(Rutkowski et al., 2003). In addition CD86 activates PI3k while we have seen that glycine mediated downmodulation is in a SHIP dependent manner. SHIP-1 acts via PI3k pathway, therefore affecting CD86 mediated activation. As a result we observe that only CD86 is downregulated but not CD80. In addition, as we found the presence of glycine receptor on BMDCs, Ca-dependent signalling via glycine receptor may prevent the effect on CD80 but not CD86(Podojil and Miller, 2009; Thiel et al., 2010). Similar down regulation has been observed on administration of progesterone which affects the maturation of DC and the activation markers CD80/86 via progesterone receptor or glucocorticoid receptor(Jones et al., 2010). But it is just a hypothesis and beyond the scope of this thesis. Both of these molecules are necessary to maintain the inflammatory process. MHCII molecules are known to present antigen where LPS upregulates their expression in DCs and inhibits IFN$-\gamma$ dependent induction in macrophages(Casals et al., 2007). The difference in MHCII expression across Figure 4.6 and Figure 4.7 can be attributed to different batches of cells from two separate experiments. The baseline expression (untreated group) of MHCII is relatively higher in Figure 4.7. This discrepancy is possible and accountable to batches of cells, culture conditions which varies across different primary DCs cultured (Hennies et al., 2015).

Glycine which is cytoprotective was found to down regulate the activation markers upon LPS stimulation. A significant titratable anti-inflammatory effect of glycine was demonstrated on BMDCs with glycine able to down modulate activation markers activated by LPS at two concentrations ($10 ng/ml$ and $1\mu g/ml$). Glycine reduced the cell viability at high concentrations in comparison to control (media only). But glycine at higher concentration affecting cell viability may be dependent on the duration of incubation and

cell type. The cells we used are primary BMDCs which are affected by multiple factors such as culture conditions. The experiments with SHIP-1 KO BMDCs demonstrated that the cell viability is better with glycine. Hence, glycine may be used at a high concentration to down-modulate activation markers but would require further investigation of its cytotoxicity as it has been seen to vary across different cells. Glycine signals in the nervous system through the hetero-pentameric glycine receptor (GlyR). In non-neuronal cells, GlyR has been found to be expressed in alveolar macrophages, Kupffer cells, T cells, cardiomyocytes and lymphocytes(Van Den Eynden et al., 2009). The receptor is a glycine gated chloride channel. Glycine prevents the increase in $[Ca^{2+}]$ concentration and inhibits the downstream signalling induced by LPS(Hua-dong et al., 2009). More recently it was shown that glycine inhbits TLR4 up-regulation after LPS exposure in Kupffer cells which are similar to macrophages(Xu et al., 2008). Therefore, we think that glycine mediated down modulation of activational markers could be through a functional glycine receptor expressed in these myeloid cells. There has been several other studies on the immunomodulatory effect of glycine such as reducing $TNF\alpha$ in LPS induced monocytes(Spittler et al., 1999) and by down regulating the TLR4 pathway in non-alcoholic hepatitis(Yang et al., 2017). But none of the studies so far addresses the immunomodulatory effect of glycine in down regulating inflammation on myeloid progenitors. The results would be beneficial in understanding the pathway(s) responsible in mediating this effect. To our understanding there is a possible role of GlyR in mediating this effect. Therefore, we also investigated for the receptors presence on different cell types with the help of flow-cytometry and immunohistochemistry (data presented in Appendix 8.2 Figure A.4). There are some evidences of the expression of this receptor on primary APCs such as BMDCs and alveolar macrophages on lung tissue sections. Yet, a further mechanistic study would be necessary to actually answer this question, hence beyond the scope of this thesis. We solely, focus on the beneficial, limited to anti-inflammatory effect of glycine.

SHIP-1 has been demonstrated to be a key regulator of different hematopoetic cell function including activation via the hydrolysis of 5'phosphate from PI3K generated PIP3. In this chapter, we attempted to understand and/or have a mechanistic insight on the role of SHIP-1 in glycine mediated down modulation of LPS induced activation of BMDCs. Comparing bone marrow derived macrophages from $SHIP^{-/-}$ with their controls, WT mice ($SHIP^{+/+}$), we as well as others showed that SHIP-1 is a negative regulator and

that its absence leads to increased inflammation(Maxwell et al., 2011; Tsantikos et al., 2018). The activation is associated with the role of SHIP-1 in inhibiting PI3K which is actively involved in promoting the transcription factor NF-$\kappa\beta$(Rauh et al., 2004). The effect is clear in CD40 and CD86 as CD86 is activated by PI3k. In addition, as a result of calcium influx, costimulatory molecules are upregulated. Glycine signalling via the glycine receptor prevents calcium influx which may be the reason for down regulating inflammation. But similar effects have been seen in LPS mediated liver injury where glycine administration had prevented the effects by preventing calcium influx(Ikejima et al., 1996; Froh et al., 2002).

In general, the role of SHIP-1 after stimulation is established in different myeloid cells such as macrophages(Rauh et al., 2004), neutrophils(Strassheim et al., 2005) and DCs (Antignano et al., 2010b,a). However, the most commendable work by Antignano and colleagues (Antignano et al., 2010b,a) on GMCSF induced BMDCs and describing the role of SHIP in DC proliferation, maturation and activation with TLR agonists has been a milestone work and confirms our findings of LPS stimulated BMDCs and glycine mediated down modulation of the activation markers. DCs being sentinels of the immune system have the primary function of innate immune activation resulting in DC maturation and activation of T cells for adaptive immune responses. The $SHIP^{-/-}$ BMDCs grown in culture with GMCSF, in response to TLR stimulation (with LPS), results in impaired priming of an effective T_H1 response. The activation by LPS is attributed to enhanced activation of PI3K(McGuire et al., 2013; Xia et al., 2018; Saponaro et al., 2012). However, the role of PI3K is still debatable as a positive or negative regulator of TLR induced inflammatory signalling, with a group of researchers considering it to have a positive role(Hattori et al., 2003; Li et al., 2003; Weinstein et al., 2000), while others consider it to have a negative role(Aksoy et al., 2005; Guha and Mackman, 2002; Hazeki et al., 2006). This discrepancy on the role of PI3K arises due to use of different cell types, assay kinetics and relying on different pharmacological inhibitors. Although similar results have been obtained by different groups, the proposed mechanisms are similar to the description by Antignano and colleagues (Antignano et al., 2010b). Considering the down modulation of LPS induced activation, glycine has been known to inhibit NF-$\kappa\beta$ DNA binding capability on Kupffer cells. The presence of GlyR is well established on Kupffer cells as they are the resident macrophages in the liver(Van Den Eynden et al.,

2009). Hence, it can be hypothesized that there is a strong link between LPS/NF-$\kappa\beta$/SHIP/GlyR signalling.

It is known that in mice lacking SHIP-1, there is development of inflammatory lung diseases with features including inflammation, emphysema and small airway fibrosis(Maxwell et al., 2011; Tsantikos et al., 2018). The conditions point out to infiltration of inflammatory cells such as neutrophils and alveolar macrophages. Literature indicates that the Balb/c mice demonstrate a T_H2 response whereas in C57BL/6 mice it is skewed towards a T_H1 response (River and Tessarollo, 2008). However, the degree of inflammation in Balb/c mice is significantly higher than C57BL/6 mice. In Balb/c mice, there is a significant increase of neutrophils, alveolar macrophages in the BALF with higher amounts of pro-inflammatory cytokines. In comparison to Balb/c mice, the C57BL/6 mice shows significantly lower inflammation in the lung(Herz et al., 2004). Therefore, to mimic human ARDS which is the clinical perspective of ALI, we would prefer the use of Balb/c as a model to study ARDS.

The expression of GlyR in the BMDCs and lung need to be understood along with its functional role. However, the little that we found, it may have some role in down regulating LPS induced activation markers on the BMDCs and macrophages. As Eynden and colleagues pointed out that the receptor is expressed in non-neuronal cells(Van Den Eynden et al., 2009), we also agree to certain extent of its expression. The novelty of the finding is in GlyR expression on primary cells of myeloid lineage (BMDCs and macrophages). However, to say with certainty a follow up study is required with the other subunits of the receptor. Study of the receptor function with or without glycine and LPS is mandatory to understand the pathway(s) involved in mediating this effect. But, it is too extensive in itself and diverts away from the key theme of developing a new immunomodulator for airway inflammation.

4.6 Summary

The anti-inflammatory effect of glycine in bone marrow derived APC subsets such as DCs, was demonstrated for the first time. Glycine showed a titratable anti-inflammatory effect on BMDCs upon LPS stimulation. Cell viability was unchanged at 100 mM glycine but

reduced minimally for higher 200 mM and 300 mM concentration. Therefore, glycine can be used to down modulate inflammation and there is a possibility that the effect is mediated in a SHIP dependent manner. We also found the presence of non-neuronal glycine receptor but its functional role in mediating glycine's anti-inflammatory effect is an area for future investigation and is beyond the scope of this thesis. However, the little that we have understood is that, there is a strong link between glycine signalling through GlyR/SHIP/PI3K/NF-$\kappa\beta$. Therefore, we hypothesize that by preventing $[Ca^{2+}]$ influx, glycine is able to inhibit NF-$\kappa\beta$ binding to DNA, thereby preventing transcription. Therefore, with this established *in-vitro* BMDC model, we propose the anti-inflammatory role of glycine in general, and intend to use it for attenuating airway inflammation in a model of ARDS.

Chapter 5

Role of Glycine in attenuating airway inflammation

5.1 Introduction

Acute respiratory distress syndrome (ARDS) is characterized by pulmonary edema, refractory hypoxemia with an increased lung stiffness and impaired carbon dioxide elimination. Current treatments includes the use of bronchodilators with corticosteroids(Chakraborty et al., 2018). In adults, this is augmented by a short-acting β-2 agonist which is currently considered as the gold standard therapy. These drugs reduce infiltration of neutrophils, eosinophils and pro-inflammatory cytokines. One important factor which causes ARDS is the presence of endotoxins such as lipopolysaccharide (LPS) from the cell wall of gram-negative bacteria. LPS exposure causes airway inflammation which is characterized by airway hyperresponsiveness (AHR), airway epithelial mucus production and allergen specific T_h2 cytokines in lung-draining lymph nodes(Manni et al., 2016). LPS binds to the Toll Like Receptor 4(TLR4) expressed on airway smooth muscle cells. Therefore, the effect of LPS on airway resistance can be explained by the direct activation of airway smooth muscle cells(Schwartz et al., 2001; de Souza Xavier Costa et al., 2017; Weifeng et al., 2016). Even though there are various compounds claiming to be anti-inflammatory (Grommes et al., 2012; Baudish et al., 2016; Sadikot R et al., 2017; Chang et al., 2018; Tu et al., 2017; Liu, Suh, Yang, Lee, Park and Shin, 2014b), none of the therapies currently available (including LPS inhibitors, statins, glucocortecoids, β-nitrostyrene derivates and glitazones) can attenuate acute LPS mediated inflammation and AHR in a clinical setting(Gross and Barnes, 2017). These compounds are capable of reducing pulmonary inflammation but have immunological tolerance thereby increasing the risk for clinical use(Wang et al., 2009). In addition, there are several side-effects associated with these compounds such as impaired growth in children, increased blood pressure and triglycerides, decreased bone mineral density, skin thinning, bruising, cataracts, chest pain, obesity, mitogenic, rhabdomyolysis(Dahl, 2006; Moghadam-Kia and Werth, 2010; Carruthers et al., 2008; Patricia et al., 2008; Catapano et al., 2015) along with the problem of resistance to cortecosteoids(Barnes, 2013). With the advancement of immunotherapies there may be newer possibilites and reducing adverse effects for long term clinical use(Cova et al., 2017).

Currently, natural compounds capable of attenuating inflammation are the subject of intense study. However, very limited information is available on their use in reducing pulmonary inflammation and improving lung function. Several foods with anti-inflammatory

properties such as olive oil, salmon, berries, and tomatoes contain high amounts of amino acids. Glycine, the smallest amino acid has been used in ingestible form for the treatment of colitis(Tsune et al., 2003; Liu, Wang and Hu, 2017). A previous study from our group has also found glycine coated polystyrene nanoparticles instilled into the lung in a murine model can inhibit allergic airway inflammation(Hardy et al., 2012). The contribution of glycine itself to this effect was not investigated. The potential anti-inflammatory properties of glycine when administered directly into the lung has not been investigated for any inflammatory disease, including ARDS.

In this chapter we explore for the first time glycine as a novel neutral anti-inflammatory compound to attenuate airway inflammation and specifically as a novel treatment for ARDS.Glycine has negligible side-effects and consumable by lactose intolerant and hyperglycemic patients. To achieve these aims, we induced ARDS (acute phase) in mice using lipopolysaccharide (LPS) and then investigated the effect of glycine in modulating this acute phase reposnses across multiple combined immunological and functional respiratory parameters. These have included the attenuation of pulmonary inflammation assessed through invasive plethysmography, tissue immunohistochemistry of pro-inflammatory cytokines, morphometry of lung parenchymal damage, cellular influx in broncho-alveolar lavage fluid(BALF) and collagen evaluation. The results indicate that mechanistically the beneficial effects of glycine treatment that we observe on ARDS are mediated by its regulation of lung associated immune cells.

5.2 Methods

5.2.1 Experimental Design

ARDS/ALI was induced in mice by sensitization with LPS (from E.coli K12, Invivogen) according to previously established protocols (Donovan et al., 2015; Bozinovski et al., 2012). In brief, mice were anesthetized by inhalation of isoflurane at 0.5-1 L/min with 3% oxygen prior to sensitization. Mice were sensitized intranasally with LPS (5 μg in 50 μL) in 0.9% saline for irrigation(vehicle) with or without glycine (100mM in 50 μL) in 0.9% saline (vehicle) or with 0.9% saline (vehicle only). For each experimental group 6 mice were sensitized as per the methodology outlined in Figure 5.1. The tail of each mice/group was marked in order to maintain the order of sensitization and determining their cull time point.
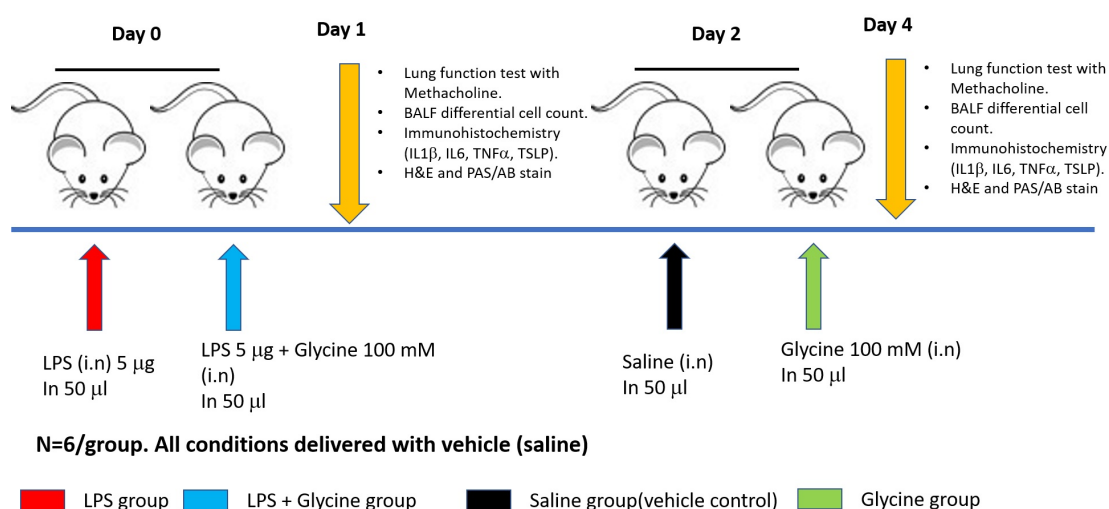
FIGURE 5.1: **Study design to investigate effect of glycine in attentuating pulmonary inflammation**. Intranasal administration of LPS was used to induce ARDS and glycine (100 mM) was used as treatment. Post 24 hours of sensitization, invasive-plethysmography was performed along with immunohistochemistry and histological staining of lung sections to determine damage to tissue and BALF cells were quantified.

5.3 Results

5.3.1 Glycine reduces airway resistance and improves lung function

The effect of LPS on the induction of AHR to methacholine (MCh) was evaluated in mice after 24 h of LPS administration. MCh is a non-selective muscarinic receptor agonist in the parasympathetic nervous system, used to diagnose bronchial hyperreactivity which is a hallmark of airway inflammatory diseases. Respiratory resistance (RS) is the resistance of the respiratory tract to airflow during inhalation and expiration. RS was significantly higher in LPS sensitized mice in concentrations of 25 and 50 mg/ml in comparison to vehicle controls (Figure 5.2A). Glycine (only) in vehicle did not show an increase in resistance and was comparable to baseline. Glycine co-administration in LPS sensitized groups, showed a dramatic decrease in resistance in comparison to LPS (only) sensitized groups. This decrease in resistance brought resistance levels back to baseline (saline only) groups.

The $cDyn$ measures the stiffness of the lung. LPS (only) sensitization reduced $cDyn$ of the lung significantly and substantially (by 50%) from MCh doses beyond 6.25 mg/ml in comparison to vehicle control(Figure 5.2B). By contrast, both glycine (alone) and LPS sensitized groups that had glycine co-administered showed no difference on $cDyn$ values and were at par with baseline saline values. There was no decrease with increasing MCh doses indicating that the elasticity of the lung was normal. The reduced $cDyn$ values in LPS group indicates the presence of emphysematous change. The low values of $cDyn$ also indicate loss of alveolar and elastic tissue which agrees to our lung morphometry demonstrated in forthcoming sections. Glycine administration in LPS sensitized mice was therefore able to prevent the functional lung changes associated with the pathology of ARDS.

Other parameters which are of clinical relevance such as the $dPmax$(Figure 5.2C) and $dPpl$(Figure 5.2D) demonstrated a high pressure in MCh doses 12.5, 25 and 50 mg/ml in comparison to vehicle controls. However, both glycine (alone) and treatment group sensitized with LPS showed reduced pressure and were comparable to baseline values. The reduced pressure in the lung with glycine indicates that there are more alveoli for gaseous exchange and the lung is less injured. The findings are further supported in the coming sections.
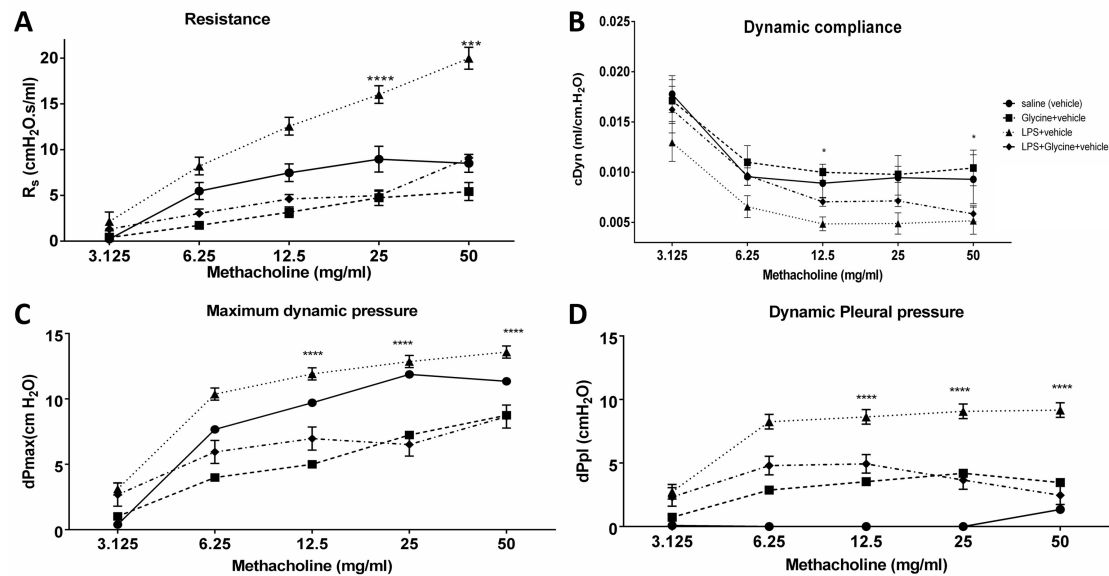
FIGURE 5.2: **Invasive plethysmography results showing different parameters of lung function on the effect of glycine in LPS induced ARDS**. The different experimental groups demonstrated are saline (control), LPS, glycine (only) and LPS along with glycine (treatment) group. **(A).** Glycine reduced resistance (Rs) which was increased by LPS. The increase in resistance was compared to saline (baseline levels).; **(B).** Reduced dynamic compliance(cDyn) with LPS which is improved and remains at par with saline levels; **(C).** Increased dynamic pressure(dPmax) in lung with LPS which is lowered with glycine; **(D).** LPS increased dynamic Pleural pressure(dPpl) with glycine treatment reducing it significantly. All comparisons are made between LPS induced ARDS group versus glycine treatment group. LPS induced group is significant in all parameters in comparison to vehicle (saline). N=6 mice/group, Mean$\pm$SEM. A 2-way ANOVA was used to determine the significance between LPS group vs LPS+glycine group. $****p < 0.0001$, $***p < 0.001$, $*p < 0.5$

5.3.2 Glycine reduces pro-inflammatory cytokines and improves signs of emphysematous change

The expression of pro-inflammatory cytokines $IL-1\beta$, IL-6 and TNF was investigated locally in lung tissues specifically around the smaller airways and lung parenchyma (Figure 5.3). For positive controls, the antibodies listed in chapter 3.10 and isotype of the antibodies (as negative control) were used to stain known tissue section such as heart and kidney (see results in Appendix 8.2). For this purpose, ten sections per mouse lung were selected using the positive pixel count algorithm avoiding muscle tissues. In these sections, the algorithm quantifies the amount of positive stain present in that section of the tissue and represents the data with different intensities (using heat maps) as well as the background. The background is subtracted from the positive stain intensity and recorded as total intensity of strong positive. It was found that LPS administration induced the expression of all the pro-inflammatory cytokines in the tissues. However, the production of IL-6(Figure 5.3B) was three-fold and TNF (Figure 5.3C) 1.5-fold more than that of $IL-1\beta$(Figure 5.3A). Glycine (alone) showed comparable cytokine expression levels to background (vehicle) for $IL-1\beta$, IL-6 but displayed some TNF upregulation. Glycine administration in LPS sensitized mice dramatically reduced the expression of pro-inflammatory cytokines compared to LPS alone, by four-fold ($IL-1\beta$), three-fold (IL-6) and two-fold (TNF). Many immunce cell types involved in producing pro-inflammatory cytokines inflammation across different organs. Many of them, such as Kupffer cells (liver), alveolar macrophages(Fogarty et al., 2004), neutrophils have been demonstrated to have glycine-gated chloride channels which are hetero-pentameric glycine receptors (GlyR) expressed in their cell membrane(Wilson and Wynn, 2009). We investigated the presence of this receptor in the lung parenchyma, especially of inflammatory cells. We confirmed the expression of GlyR (α1 subunit) on endothelial cells as well as on inflammatory cells including neutrophils and alveolar macrophages (see chapter 4, Figure 4.10). In addition, the expression of GlyR has been seen in non-neuronal cells such as PBMCs(Van Den Eynden et al., 2009). We investigated GlyR expression on PBMCs to confirm our findings of the receptor on lung parenchyma and endothelial cells (data shown in 8.2).
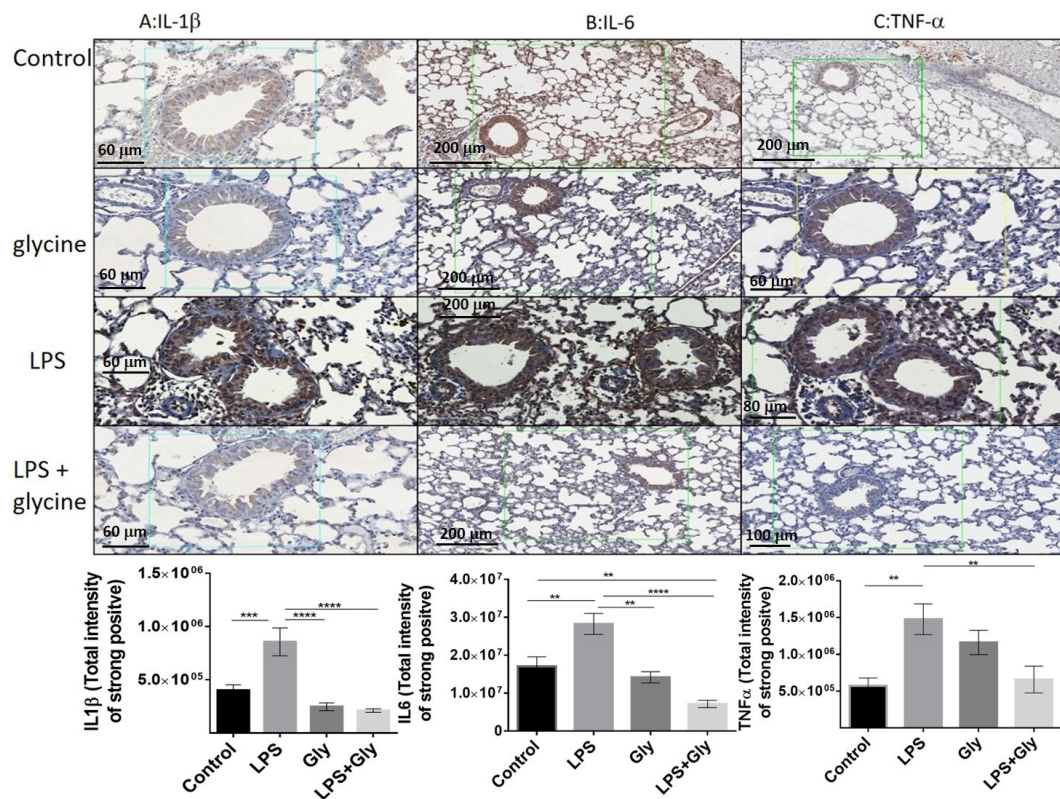
FIGURE 5.3: **Expression of pro-inflammatory cytokines in lung tissue showing airway and lung parenchyma**. The different experimental groups demonstrated are saline (control), LPS, glycine (only) and LPS along with glycine (treatment) group. **(A).** Increased expression of IL-1β in comparison to saline (control) in LPS induced ARDS group, while glycine reduced the expression to baseline levels (that of control); **(B).** LPS increased expression of IL-6 which was reduced significantly by glycine. IL-6 was significantly lower in glycine only group in comparison to LPS suggesting its strong anti-inflammatory role; **(C).** Expression of TNF-α was reduced significantly in comparison to LPS but was at par to saline (control) levels. N=6 mice/group, Mean±SEM. A 2-way ANOVA with post-hoc t test was used to determine the significance in between different groups. Each group was quantified for strong positive expression by analyzing 10 sections/lung/group. $****p < 0.0001$, $***p < 0.001$, $**p < 0.01$.

The increased production of IL-6 and TNF is associated with increased mucus secretion by goblet cells around the larger airways(Neveu et al., 2009; Lora et al., 2005). Therefore, we quantified the presence of goblet cells to evaluate the effect of glycine in controlling the production of mucus. The number of goblet cells per 100 μm of large airway basement membrane per lung section was recorded. The number of goblet cells in the LPS sensitized mice (Figure 5.4A) was 15 times more than the vehicle control. Glycine (alone) was comparable to vehicle only with negligible goblet cells and reduced the number of cells by 67% on mice sensitized with LPS. In LPS sensitized mice, signs of emphysema were observed. Signs of emphysema were measured by indirect quantification of factors such as alveolar area (Figure 5.4B), alveolar septation count (Figure 5.4C), airway area (Figure 5.4D) and alveolar count. Alveolar area was measured by averaging the area of ten alveoli per 1 mm^2 of area of the section. The alveolar area was six times more than vehicle treated mice, in LPS sensitized group which was reduced by 73%. The presence of small alveoli signifies more alveoli for normal gaseous exchange. Alveolar septation count was measured by drawing a 1 mm line and counting the number of alveolar septae intersecting that line. It was found that the number of alveolar septa decreased by 47% in LPS sensitized mice indicating large but a smaller number of alveoli. This was increased as per baseline levels with glycine. In a similar manner, the number of alveoli (counted per 1 mm^2 area of 2 sections per lung) was reduced by 62% in comparison to vehicle treated mice. This agrees with the reduced number of alveolar septa. Interestingly, in LPS sensitized mice, the airway area had increased by four-fold and when LPS sensitized mice were treated with glycine the airway area remained normal and of comparable size to that of vehicle treated mice.
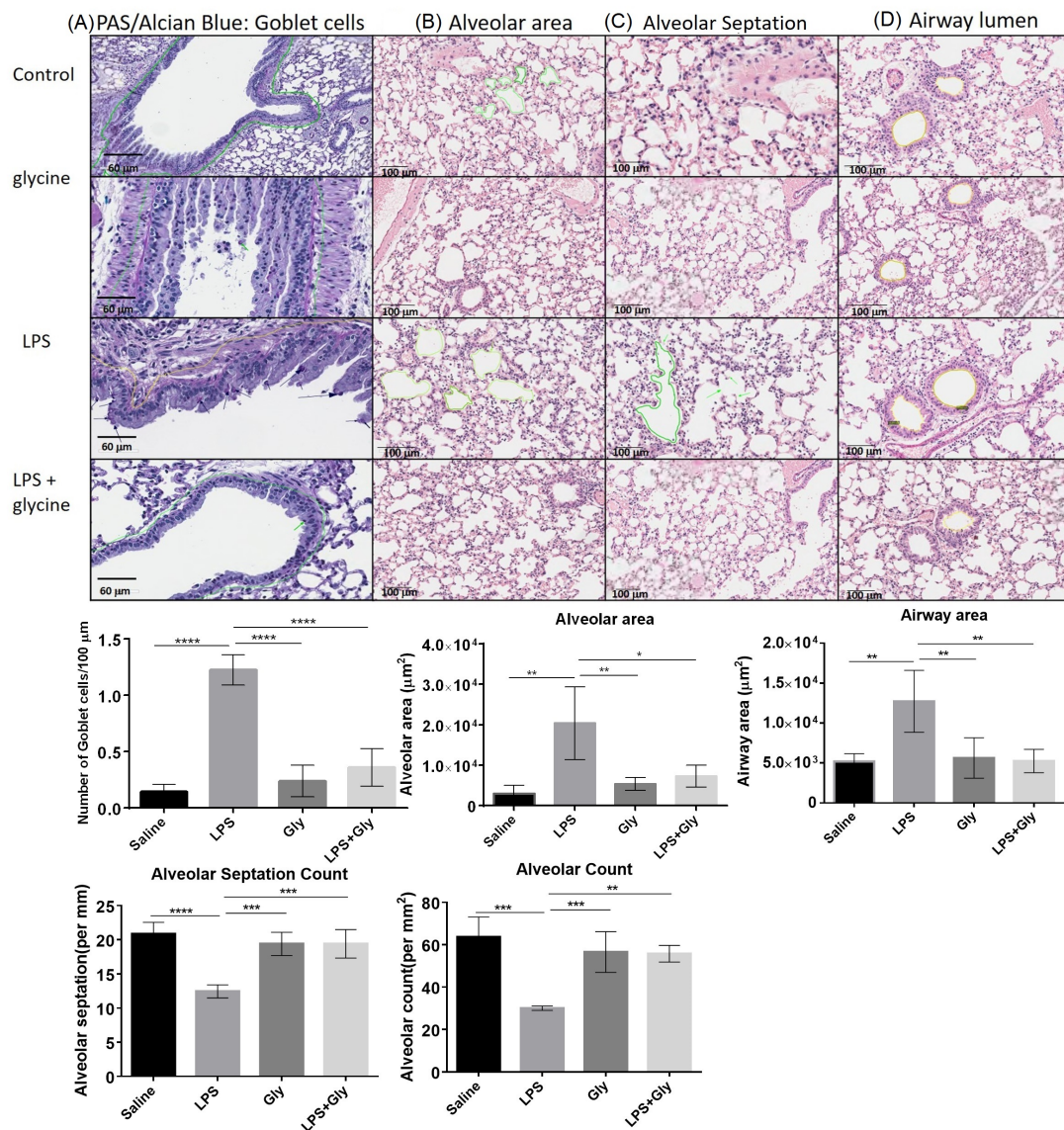
FIGURE 5.4: **LPS increases goblet cells and damage to lung parenchyma**. The different experimental groups demonstrated are saline (control), LPS, glycine (only) and LPS along with glycine (treatment) group. **(A).** PAS/Alcian blue stained airways and lung parenchyma showing goblet cells (indicated by arrows) counted per 100 μm of airway. An increased number of goblet cells were found on LPS induced mice and was significantly low in glycine treated group; **(B).** Alveolar area of 10 alveoli per 1 mm^2 for 2 sections/lung/group showed large alveolar area in LPS induced group which was at par saline (control) group with glycine treatment; **(C).** Number of alveolar septa per 1 mm was reduced in LPS induced group indicating large alveoli, reduced number of alveoli per mm^2 with broken alveolar septa showed by arrow; **(D).** Airway lumen area per lung section/per group was measured and it was found increased in LPS induced group in comparison to saline (control) group. N=6 mice/group, Mean±SEM. A 2-way ANOVA with post-hoc t test was used to determine the significance in between different groups. Each group was quantified for strong positive expression by analyzing 10 sections/lung/group. $****p < 0.0001$, $***p < 0.001$, $**p < 0.01$ and $*p < 0.5$.

5.3.3 Glycine reduces neutrophil mediated lung injury

Mice sensitized with LPS mounted a strong response, reflected by increased neutrophils ($1x10^6$ cells) and alveolar macrophage ($5x10^5$ cells) frequency (Figure 5.5A). The number of neutrophils was reduced by 45% and alveolar macrophage by 60% in mice treated with LPS and glycine, compared to LPS alone. Furthermore, there were negligible neutrophils detectable in glycine (only) treated mice and the levels of naïve alveolar macrophages were same as that of the vehicle only. We also investigated the presence of monocytes/-macrophages and lymphocytes in the BAL fluid. The BAL fluid is the washing of the lung to collect the cells present in order to understand the types of cells present by cytospots. In all the groups, the number of eosinophils were very low and insignificant. As expected, LPS administration caused an increased in overall cellularity drivern primarily by substantial and significant increases in neutrophil and macrophage numbers, and a concomitant decrease in lymphocytes. The presence of a high number of neutrophils explains the presence of emphysema, lung injury and high *Rs* value leading to a low compliance in these mice. Whereas, glycine by itself had little effect on cellularity or its composition compared to the control saline group, when glycine was given to LPS sensitized mice it reduced overall cellularity and macrophage numbers back to baseline levels, as well as substantially reducing LPS induced neutrophilia. The reduction in neutrophils caused by glycine was also accompanied by significant increase in lymphocytes.
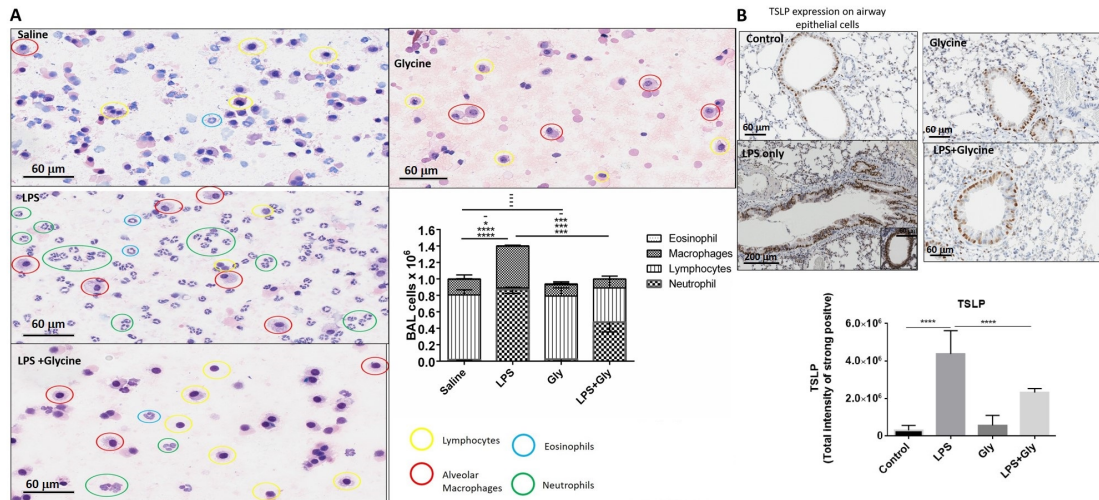
FIGURE 5.5: **Cytospin images of BALF showing differential cell count of different leucocytes and TSLP expression**. **(A).** Influx of neutrophil(green) and alveolar macrophages(red) in LPS induced ARDS and increased lymphocytes(yellow) in glycine treatment group; N=6 mice/group, Mean±SEM. A 2-way ANOVA with post-hoc t test was used to determine the significance in between different groups. Each group was quantified for strong positive expression by analyzing 10 sections/lung/group. $****p < 0.0001, ***p < 0.001$ and $*p < 0.5$, - non-significant. **(B).** TSLP expression in airway epithelial cells in LPS group is higher in comparison to saline(control) as well as glycine and LPS+glycine group attributing to neutrophilic influx. (**B-Inset**) A small airway in LPS group showing over-expression of TSLP. Expression of TSLP was five fold higher than saline control while it was significantly reduced by coadministration of glycine. N=6 mice/group, Mean±SEM. A 2-way ANOVA with post-hoc t test was used to determine the significance in between different groups. Each group was quantified for strong positive expression by analyzing 4 airways/lung section/group. $****p < 0.0001$.

We further investigated the reason behind the infiltration of neutrophils and therefore, investigated the epithelial cell derived cytokine thymic stromal lymphopoietin (TSLP) expression around the airways (Figure 5.5B). We found a five-fold higher expression of TSLP in LPS sensitized mice than that of vehicle controls. Although there was expression of the protein in glycine (alone), yet it was significantly less compared to the LPS sensitized group. In addition, co-administration of LPS with glycine reduced TSLP expression significantly by three folds, although it was higher than vehicle (saline) controls. The damage in the epithelial membrane therefore accounts for the increase in neutrophils leading to injury, and glycine was able to prevent the overexpression of TSLP.

5.3.4 Glycine treatment of LPS induced ARDS leads to early collagen fibre deposition in lung tissue

Generally, acute phase of ALI lead to lung fibrosis. The most prevalent technique available to detect collagen is by Masson trichrome staining. However, it detects collagen at a high level of deposition which is not suitable to ALI models which usually display very little collagen deposition at early stages. Therefore, we utilized Histoindex which uses second harmonics generation to detect collagen fibres as fine as 100 nm (Figure 5.6). The difference in tissue electron excitation leads to auto-fluorescence of collagen type I (SHG: green 390 nm) and tissue (TPE: red 780 nm). After scanning the tissue sections, we evaluated the presence of collagen in terms of mean fluorescent intensity as means of quantitating collagen presence around airways. It was found that LPS leads to an increase in early collagen deposition which is not affected by glycine coadministration. Glycine (only) treated mice, has similar levels of collagen in lung to vehicle controls. Therefore, whilst glycine decreases TSLP expression leading to reduced neutrophilia it does not prevent early collagen deposition induced by LPS.
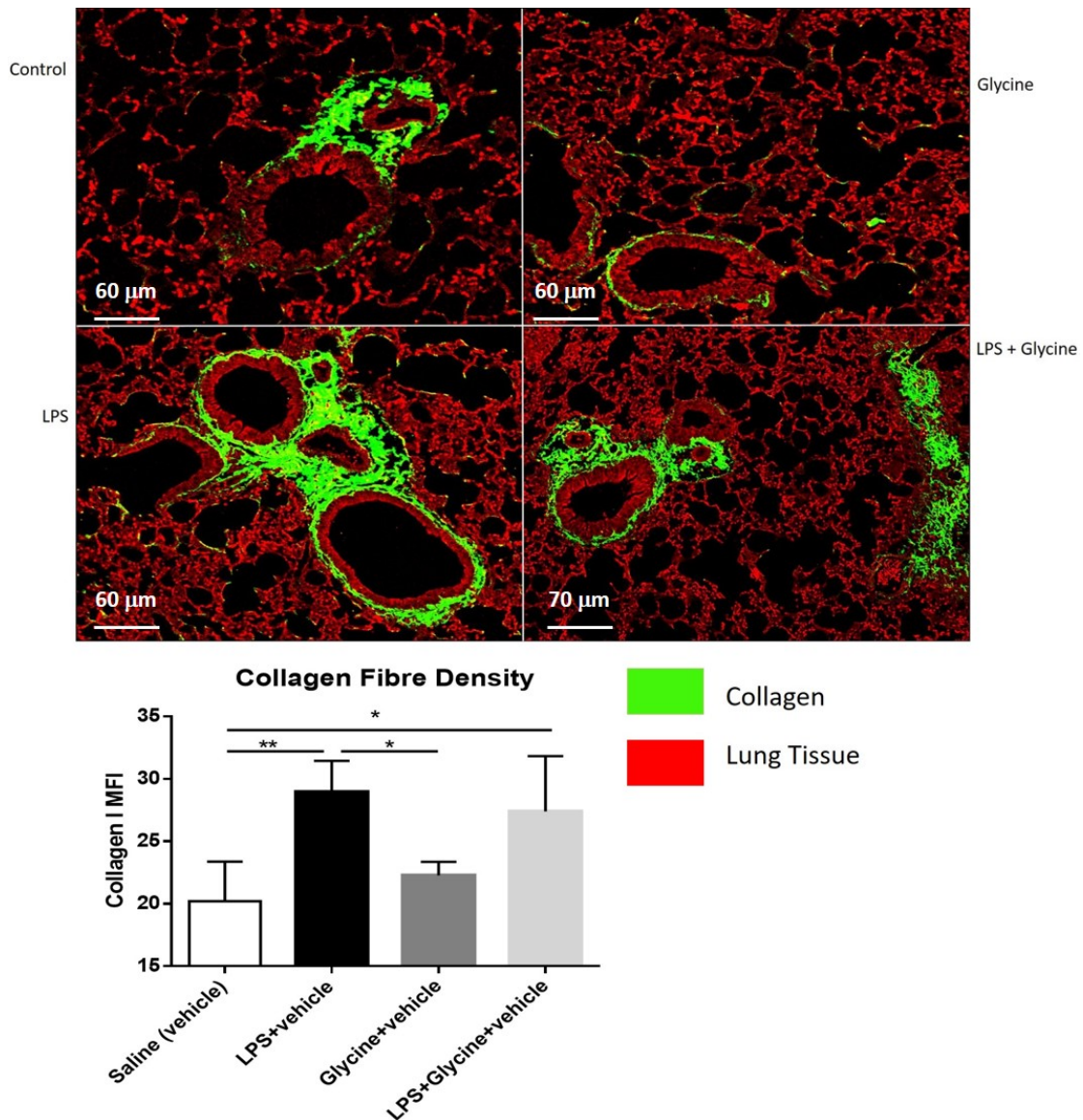
FIGURE 5.6: **Collagen deposition in lung tissue. Collagen fibre density was quantified by histoindex 200 using second harmonic generation laser**. Collagen(green) was distinguished from lung parenchyma (red) on the basis of their structural difference. For each lung section/group, the area around the airways were selected for ROI along with any interstitial collagen deposited. The mean fluorescence intensity(MFI) was evaluated for each of the ROI and was normalized with background levels of collagen found in control group. The MFI is a direct correlation between the presence of collagen and tissue density. N=6 mice/group, Mean±SEM. A 2-way ANOVA with post-hoc t test was used to determine the significance in between different groups. Each group was quantified for MFI of collagen by analyzing 10 ROI/lung section/group. $**p < 0.01$ and $*p < 0.5$.

5.4 Discussion

The theory that diet has an influence on asthma has been established on fatty acids and minerals. However, there is no correlation higher fasting concentrations of amino acids in plasma with asthma. However, there is a significant inverse correlation of plasma glycine levels and that of asthma. This protective effect on asthma could be potentially attributed to glycine controlling intracellular oxidation status(Fogarty et al., 2004). We demonstrate for the first time, that glycine behaves directly as a novel anti-inflammatory compound in the lung in attenuating ARDS by reducing neutrophil infiltration and preventing the increase of alveolar macrophages. In doing so, glycine also reduced resistance to breathing and improves lung function. Glycine promotes a revival of lymphocyte numbers establishing a lung environment closer to its homeostatic state, and potentially permissive to heal from LPS injury. The deposition of collagen in interstitial space and around the airways has also been observed as a result of lung healing(Wilson and Wynn, 2009). In a 24 hour acute model, collagen quantification is difficult with currently available staining procedures (Masson's trichrome), but is achievable using the laser based second generation harmonics which identifies collagen structural features. Herein we show glycine attenuated airway inflammation whilst allowing the augmented collagen deposition caused by LPS.

In our previous studies glycine conjugated to non-biodegradable polystyrene nanoparticles was able to attenuate airway inflammation(Hardy et al., 2012). But whether the particles or the glycine mediated this effect was unclear. Therefore, we investigated the potential anti-inflammatory role of glycine administered into the lung in the context of its potential to attenuate ARDS, given current anti-inflammatory treatments are largely ineffective with adverse effects during acute ARDS in the clinical setting(Dahl, 2006; Moghadam-Kia and Werth, 2010; Catapano et al., 2015). Our results suggest that glycine indeed can act to down regulate acute inflammation in the lung. Glycine was able to reduce airway resistance and improve the dynamic compliance, which can be attributed to its ability to inhibit the production of TNF and superoxide anions induced by substance such as LPS(Vargas et al., 2017).

In this model of ARDS, intense accumulation of inflammatory cells (especially neutrophils) in the alveolar and interstitial space; increased pro-inflammatory cytokines

in the tissue such as ($IL-1\beta$, IL-6, TNF) and is reviewed by Matute-Bello and colleagues(Matute-Bello et al., 2008). TNF is a key early mediator of pulmonary inflammation, where LPS is implicated and is known to have microbicidal activities(Chakraborty et al., 2018). Release of TNF from inflammatory cells leads to lung tissue damage and oxidative stress as well as involved in alveolar macrophage activation(Parameswaran and Patial, 2010). Reduction in serum TNF in rats intravenously injected with LPS has also been observed in rats fed a diet enriched with glycine(Wheeler et al., 2000; Ikejima et al., 1996). Another pro-inflammatory cytokine $IL-1\beta$ has been known to cause pulmonary inflammation characterized by neutrophil and alveolar macrophage infiltration; which explains the high number of these cells in our BALF(Lappalainen et al., 2005). The T_h1 cytokine $IL-1\beta$, found in lung tissue is attributed to secretion by alveolar macrophages. High frequency of alveolar macrophages, therefore, explains the high expression of $IL-1\beta$ in LPS sensitized group. Interestingly, we found relatively higher number of mucus secreting goblet cells in our LPS group. It is well established that alveolar macrophages and neutrophils secrete IL-6 when stimulated with LPS(de Souza Xavier Costa et al., 2017; Chakraborty et al., 2018). IL-6 secretion leads to activation of airway mucin synthesis. Not only IL-6, even $IL-1\beta$ is known to activate MUC5AC promoter in airway epithelial cells which also leads to increased mucin expression through ROS generation with neutrophil elastases enhancing mucin production(Harris et al., 2007). IL-6 also plays a causative role in determining an increase in airway resistance which supports our finding of an increase in airway resistance with LPS and a decrease upon glycine coadministration(Alessandro, 2013). The reduced resistance observed in glycine (only) group (Figure 5.2) in comparison to saline can be attributed to role of glycine role in preventing mucus production by limiting the local release of pro-inflammatory mediators IL-1β, IL-6 and TNF-α(Voynow and Rubin, 2009; Vargas et al., 2017). The reduced production of pro-inflammatory cytokines by glycine is supported in other diseases and organs(Liu, Wang and Hu, 2017; Cruz et al., 2008; Alarcon-Aguilar et al., 2008; Tsune et al., 2003) but we show for the first time it is a potent local immunomodulator in the lung, with potential utility in the therapeutic treatment of ARDS.

We also investigated another aspect of ARDS which includes pulmonary edema and parenchymal injury and our results comply with several other studies reviewed by Mühlfeld and Ochs(Muhlfeld and Ochs, 2013). We evaluated and analyzed lung morphology in a semi-quantitative manner for signs of emphysema and edema, such as the increase

in alveolar area, airway area with reduced number of alveoli and thick walls. The effects are due to hypertropic and hyperplastic mucus glands as well as due to infiltration of alveolar macrophages, neutrophils and cytotoxic T lymphocytes(Chakraborty et al., 2018). Similar damage to the lung has been observed by Costa and colleagues(de Souza Xavier Costa et al., 2017). The epithelial injury (observed by TSLP expression), possibly caused as a result of infiltration of neutrophils into the alveolar lumen, exposes the basement membrane which becomes prone to bacterial action. Similar up-regulation of TSLP has been observed by Yanlu and colleagues upon stimulation with LPS (Zhang et al., 2012). It also indicates that the elevation of TSLP results in activation of TLR4/MyD88 pathway leading to release of pro-inflammatory cytokines IL-1β, IL-6 and TNF (Minye et al., 2017). Co-administration of glycine has demonstrated the reduction in expression of TSLP as well as these pro-inflammatory cytokines, therefore highlighting glycine's anti-inflammatory role in attenuating airway inflammation through inhibition of TSLP mediated pro-inflammatory cytokine activation in the airways. In addition, one of the mechanisms of injury and tissue damage can be recognized as neutrophil-dependent injury. Accumulation of neutrophils in alveolar lumen gets activated leading to ROS and pro-inflammatory cytokine production. Our observations comply with this mechanism where we observed a higher neutrophilic influx and expression of pro-inflammatory cytokines. In addition, there is increased septal breaks along with thickened alveolar septa pointing towards a neutrophil mediated diffused alveolar damage. Glycine is established to suppress LPS induced activation of cultured neutrophils and their ROS production by directly affecting glycine-gated chloride channels(Wheeler et al., 2000). In addition, glycine has also been reported to be able to reduce IL-17 expression from T_H17 cells, a cytokine essential for neutrophilic recruitment at mucosal surface. The reduction in ROS and neutrophilic influx therefore can be attributed in preventing tissue damage(Vargas et al., 2017).

Reduced production of pro-inflammatory cytokines can be attributed to glycine acting via the GlyR to inhibit their production, as previously shown in rats intravenously injected with LPS(Wheeler et al., 2000). It was also notable that, in addition to the influx of neutrophils and alveolar macrophages, lymphocytes and monocytes were found to be reduced after LPS exposure. Resolution of inflammation is a complex process, however, the fact that glycine prevented the depletion of lymphocytes even after LPS exposure points out to effects on multiple cells types. Glycine is also known to blunt

agonist-induced calcium influx in lymphocytes and can induce immunosuppressive effects(Wheeler et al., 2000).

Animal models of ARDS can reproduce similar mechanism to the human disease. However, since the lung injury generally resolves in two weeks, the underlying healing capability of lung tissue may not be well represented. The effects as early as 24 hours are also important in studying ARDS healing in a greater detail. Recovery in ARDS leads to lung fibrosis as a result of healing, but this is controversial and variable(de Souza Xavier Costa et al., 2017). The advent of pulmonary fibrosis is a result of latent expression of $TGF - \beta$ in the early stages and is facilitated by $IL - 1\beta$ in an IL-17A dependent manner(Wilson et al., 2010). In humans, collagen deposition (fibrosis) is analyzed solely as a late tissue response. However, in ARDS there is an increased procollagen levels during onset of ARDS (<48 hours) post injury. Furthermore, pro-inflammatory cytokines, such as $IL - 1\beta$ and TNF, are regarded as fibrogenic and result in substitution of collagen type III with type I during ongoing phase of ARDS. Costa and colleagues have nicely demonstrated that there is an increased collagen build up in lung tissue 5 weeks post LPS mediated injury but the data shows very limited collagen in their 24 hour model. We attribute this to the detection method used. In the same 24 hour model, we found using Histoindex comparable levels of expression of collagen. Histoindex determines collagen on structural basis by the pattern of fibres, and reflectance of the laser. Therefore, unlike conventional histochemistry, it is capable of detecting fibres as low as 100 nm thickness. Our data are in agreement with Costa and colleagues(de Souza Xavier Costa et al., 2017), in suggesting that ARDS onset and recovery leads to collagen deposition. However, in a model of ARDS, which effects the lung parenchyma, our data shows an interesting result, taking into account that Balb/c mice used in this model are generally thought to be resistant to pulmonary fibrosis(Walkin et al., 2013; de Souza Xavier Costa et al., 2017). In addition to glycine being able to attenuate airway inflammation, it contributes to collagen deposition. For instance, glycine is required for the formation of collagen and glutathione produced by glutathione synthetase, augmenting anti-oxidant enzyme activities suitable for collagen deposition(Fogarty et al., 2004).

5.5   Summary

In summary, the results show that glycine can directly reduce inflammation by preventing neutrophil influx and increase of alveolar macrophages. Glycine improved pulmonary function and prevented damage of lung parenchyma by reducing the expression of pro-inflammatory cytokines from airway epithelial cells. Post injury, we showed that the lung resorts to a healing state with recruitment of lymphocytes and deposition of fine collagen fibres which were not possible to be measured previously using conventional histochemical techniques, given the method utilised staining of fibres of higher thickness and density. Hence, glycine can be used in a clinical setting without any adverse effects.

Chapter 6

To develop Glycine immunomodulators for pulmonary delivery

6.1   Introduction

The pulmonary route of drug delivery enables targeting of both local area and systemic circulation by escaping the first pass metabolism (loss of a fraction of drug in the gut and liver before entry into systemic circulation). In addition, the method provides improved stability in the solid state and relatively low product cost. Drug loss is prevented by the large alveolar surface area, thin epithelium, and high vascularization of the lungs, which also maximize drug absorption. The most recent delivery system involves the use of surface functionalized nanoparticles. These particles has gained significance due to bioavailibility of the drug and interaction with cells of the immune system such as alveolar macrophages and neutrophils(van Rijt et al., 2014). With the development of nanoparticle-mediated pulmonary drug delivery, there are advanced strategies such as modification in particle characteristics to change the way they carry and release drug after administration. However, the administration of these nanoparticles poses several problems. Current challenges with pulmonary delivery of nanoparticles include size(Rogueda and Traini, 2007), cytotoxicity, biodegradability, particle instability due to aggregation and/or particle-particle interaction(Yang et al., 2008), triggering pro-inflammatory pathways, and many more(Chakraborty et al., 2017). One of the major problem with the use of non-biodegradable nanoparticles is the production of reactive oxygen species (ROS) and autophagy leading to apoptosis of cells (Anozie and Dalhaimer, 2017). Moreover, accumulation of non-biodegradable or slowly degrading particles causes chronic inflammation in the region of accumulation(Medina et al., 2007) leading to a preference of biodegradable nanoparticles are for pulmonary delivery(Aragao-Santiago et al., 2016).

In addition to these challenges, anatomical barriers such as narrower airway lumen and airway mucus poses a problem. Nearly 25% of ultrafine particles (size < 100 nm) are cleared from the lung by mucociliary function in the airways. This is followed by a slower process in the lung periphery, mediated by antigen presenting cell such as alveolar macrophages(Moller et al., 2008). In COPD patients and smokers, the mucociliary clearance mechanism is impaired due to pulmonary inflammation, airway remodelling resulting in mucus hypersecretion. The mechanism for incomplete mucociliary clearance can be explained by particle displacement due to surface forces by surfactants on top of the mucus layer and periciliary fluid towards the epithelium. Moreover, discontinuities

in the mucus layer is caused by the anti-inflammatory (demonstrated in chapter 4 and 5) amino acid glycine(Wei et al., 2005), by reducing local pro-inflammatory mediators which promote mucus production(Vargas et al., 2017). Therefore, glycine has a beneficial use in preventing airway mucus secretion (which increases extensively in airway inflammation).

Inhalable biodegradable nanoparticles suspensions, administered by nebulization has been a growing trend in the pharmaceutical industry(Dailey et al., 2003). However, it has several drawbacks including inconvenience of bulk device, variability in droplet size (due to nebulizer difference), low delivery efficiency and possibility of damage to the active ingredient due to the high shear force(Yang et al., 2015). Therefore, biodegradable nanoparticle delivery with glycine microparticles as a dry powder is ideal due to its ease of administration, convenient portability, bulk production and the anti-inflammatory role glycine preventing mucus hypersecretion (established in chapter 5). Glycine can also be used as an excipient, which is advantageous in terms of cost, availability, low hygroscopicity, excellent physical stability, water solubility along with a sweet taste(Rowe et al., 2013; Chongprasert et al., 2001). In addition, glycine improves insulin sensitivity along with reduction of alterations induced by hyperglycemia(Nuttall et al., 2002; Alvarado-Vásquez et al., 2003) by inhibition of oxidative processes(Alvarado-Vásquez et al., 2003) and has numerous therapeutic benefits such as in treatment of inflammatory bowel disease(Liu, Wang and Hu, 2017; Tsune et al., 2003), schizophrenia(Javitt et al., 2001) and rheumatoid arthritis(Li et al., 2001). For the formulation of glycine microparticles to encapsulate the biodegradable nanoparticles (for use as excipients and anti-inflammatories), several methods such as spray-drying and freeze drying can be employed(Wei et al., 2005). Albeit spray drying of glycine to produce anti-inflammatory, microparticle based excipients has not been developed before. Spray drying is a favorable method for development of inhalable dry powder(Nandiyanto and Okuyama, 2011; Yang et al., 2015) due to its scalability, adaptability, cost, encapsulation efficiency(Sou et al., 2016). In addition, micro-fluidic jet-spray drying generates uniform, monodisperse particles with higher stability and nanoparticle entrapment capability(Lin et al., 2017; Wu et al., 2011). Glycine has been used to encapsulate antibiotics for inhalation previously. However, the spray-dryer used (Buchi 290) generates non-uniform, agglomerates of spray-dried powder due to aerosolization of glycine. Instead, even microparticle formation was observed in the advanced micro-fluidic jet spray dryer which uses a piezo-electric

droplet generator(Lin et al., 2017, 2015; Liu et al., 2011*b*). Using the micro-fluidic jet spray drier, we can alter the particles' physicochemical properties including size, distribution, density, shape, morphology without aggregation issues of nanoparticles(Seville et al., 2007), as the nanoparticles are suspended in bulk excipient (glycine for example).

In this chapter, the feasibility of using a micro-fluidic jet spray dryer to produce inhalable nanoparticles in glycine microparticles imparting anti-inflammatory properties for pulmonary delivery was investigated. Although the use of glycine as a freeze-dried excipient is known in the literature(Wei et al., 2005; Rowe et al., 2013; Chongprasert et al., 2001; Wang, 2000), however, the influence of spray-dried glycine microparticles as an excipient and its anti-inflammatory role has never been studied. Biodegradability of nanoparticles play an important role in clinical use as they do not accumulate in tissue. Iron oxide nanoparticles have the property of biodegradability unlike other non-metallic nanoparticles(Chakraborty et al., 2017). Coating with amino acids prevents the production of reactive oxygen species making them ideal candidates for use as pulmonary delivery vehicles. Therefore, in this study we synthesized biodegradable super-paramagnetic iron oxide nanoparticles surface functionalized with glycine (GSPIONs), as immunomodulators for use with spray-dried glycine microparticles. The characterization of the spray-dried immunomodulators in the form of microparticles were evaluated in terms of their aerodynamic properties and GSPIONs encapsulation capability. This work provides a foundation for the use of spray-dried glycine microparticles containing biodegradable nanoparticles for the treatment of respiratory diseases (being anti-inflammatory) and development of immunomodulators.

6.2 Results and Discussion

Iron oxide nanoparticles were coated with glycine by alkaline co-precipitation method. After synthesis of GSPIONs, the nanoparticles were characterized and their ability for use as pulmonary delivery agents were evaluated.

6.2.1 Morphology and characterization of glycine coated iron oxide nanoparticles (GSPIONs)

For characterization, the size of the nanoparticles was measured by TEM. The synthesized glycine coated iron oxide nanoparticles (GSPIONs) were dispersed with a narrow standard deviation (SD) with an average size of 12 ± 5 nm (Figure 6.1A). The electron diffraction pattern shows sharp rings which corresponds to peaks found by XRD analysis. XRD analysis revealed the formation of crystalline metastable cubic γFe_2O_3 structure (Figure 6.1B). The presence of eight characteristic sharp and intense peaks such as (311) confirmed the formation of crystalline nanoparticles with signature peaks at (620) and (533), which is consistent with maghemite. Taking Bragg's law (Equation (6.1)) into account, the interplanar spacing d_{hkl}, corresponding to the (311) plane, can be calculated with its peak position to d_{hkl}=2.476$\mathring{A}$. Upon applying the results from Equation (6.1) in Equation (6.2), the lattice constant α= 8.212$\mathring{A}$ was determined which agrees with the value reported in literature (maghemite, α=8.3457$\mathring{A}$) (Cervellino et al., 2014).

$$d_{hkl} = \frac{\lambda}{2sin\theta} \tag{6.1}$$

$$d_{hkl} = \frac{a}{\sqrt{h^2 + k^2 + l^2}} \tag{6.2}$$

The electron diffraction pattern (Figure 6.1A) and the HRTEM image of GSPIONs also confirmed the degree of crystallinity of their constituents. The electron diffraction pattern can be indexed to crystalline reflections, such as (220), (311), (400), (422), (511), (440), (620) and (533) of spinel cubic γFe_2O_3 structure, which is consistent with the XRD result. The degree of crystallinity is likely a result of extended crystal growth time during synthesis and the interactions of the amino acid (which was added at a later stage).
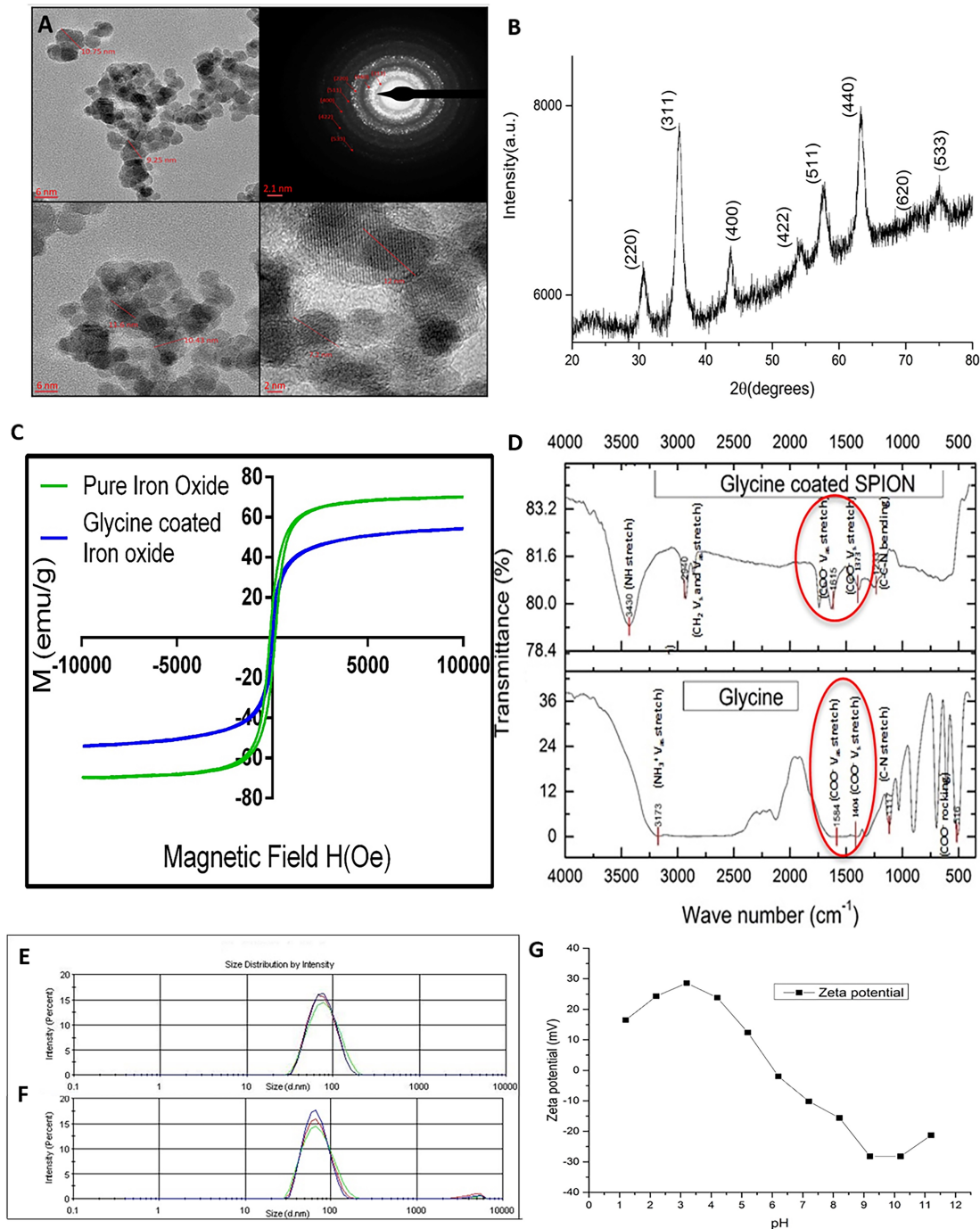
FIGURE 6.1: **Characterization of GSPIONs**. **(A).** HRTEM images of GSPIONs with average 12±5 nm diameter and their electron diffraction pattern; **(B).** XRD spectra of GSPIONs showing eight characteristic peaks and two signature peaks at (620), (533) corresponding to maghemite ($\gamma - Fe_2O_3$); **(C).** Field dependent magnetization plots of iron oxide nanoparticles and GSPIONs at 300 K showing superparamagnetic behavior; **(D).** FTIR spectra of glycine alone (showing V_s and V_{as} COO^- bands) and GSPIONs with corresponding functional groups shown in red between wave number 450-4000 cm^{-1}; **(E).** Hydrodynamic sizes of GSPIONs and **(F).** SPIONs with a poly-dispersity index of 0.146 and 0.259 respectively; **(G).** Zeta potential of GSPIONs varying with pH.

The initial products of the reaction (Fe_2O_3), enhanced the capability for growth/re-organization in an ordered manner, resulting in crystalline nanoparticles as has been previously observed for synthesis in the presence of glycine(Barick and Hassan, 2012). Figure 6.1C shows the field dependent magnetization plots of citrate stabilized iron oxide nanoparticles and glycine coated nanoparticles measured at 300 K. The glycine coated iron oxide nanoparticles exhibit superparamagnetic behaviour without magnetic hysteresis and remanence at 300K, whereas that of the citrate stabilized pure iron oxide nanoparticles exhibit hysteresis. This transition from ferro or ferrimagnetic behaviour to superparamagnetic behaviour at room temperature was attributed to glycine chemisorption. The maximum magnetizations of citrate stabilized and glycine coated iron oxide nanoparticles (at an applied field of 10 KOe) were found to be 70.09 and 54.42 emu/g respectively. It was observed that the room temperature magnetization of glycine coated iron oxide nanoparticles was reduced to 88% respectively of the bulk Fe_2O_3. Hence, the glycine coated iron oxide nanoparticles demonstrate super-paramagnetic behaviour and we refer to them as GSPIONs.

To evaluate the success of glycine chemisorption onto iron oxide nanoparticles, IR spectroscopy and CHN analysis was utilised. Figure 6.1D shows FTIR spectra of GSPIONs and glycine with their corresponding peak assignments in the wave number ranging from 450-4000 cm^{-1}. The absorption bands for glycine were found to be resolved properly as it is a zwitterionic compound. However, that of GSPIONs are broad. There is a shifting of NH^{3+} V_{as} stretching in pure glycine to (NH) and CH_2 stretching vibration at 3430 cm^{-1} and 2940 cm^{-1} respectively in the coated sample. Stretching vibration in pure glycine at 1117 cm^{-1} shifted to a bending $C–C-N$ vibration at 1233 cm^{-1} and absence of COO^- rocking vibration in glycine coated sample. The V_s and V_{as} stretching bands of COO^- group of glycine are shifted from 1404 to 1373 cm^{-1} and 1584 to 1615 cm^{-1} along with a wave number separation of Δ=242 cm^{-1} between V_s COO^- and V_{as} COO^-. This type of covalent bonding suggests that glycine is chemisorbed onto the surface of the nanoparticles through carboxylate groups with freely exposed amine $(-NH_2)$ groups. The exposed amine groups interact with water forming hydrogen bonds whereas the carboxylate groups strongly coordinate to iron cations(Wang et al., 2006). Stabilization of the GSPIONs was also carried out by electrostatic repulsive forces originating from the ionization of the surface groups.

To validate the presence of glycine on SPIONs CHN analysis was performed which quantifies the elemental presence of the elements carbon (C), hydrogen (H) and nitrogen (N) in a sample. Therefore, we utilized this method in order to find the presence as well as quantify the number of glycine molecules chemisorbed per nanoparticle on to the surface of GSPIONs (see Apendix 8.2, Table 2). Glycine has 2 carbons, 5 hydrogens and one nitrogen. Hence nitrogen was used as the element to evaluate the number of glycines chemisorbed. The particles show themselves as a cubic lattice and their diameter varies from 4.5 to 12 which we had seen in HR-TEM micrographs using Quantax analysis. Therefore, glycine content is estimated by a function of the nitrogen content and size of the particles as proposed below and calculated using Wolfram Alpha$^{\circledR}$ (shown in Appendix 8.2 Figure C.4)

Number of glycine molecules per particle =

$$\int\limits_{a=4.5}^{12} 6a^2 \int\limits_{18.39}^{22.61} \frac{N}{14} dN da$$

a, the side length of the cube where the side length ranges from 4.5 nm to 12 nm.

N, percent of nitrogen.

resulting in an estimated average 20.2 x 10^3 glycine molecules chemisorbed in each particle.

The initial focus of the development of the nanoparticles was to have a hydrodynamic diameter around 50 nm. It is shown from a previous study that size of nanoparticles around 50 nm, plays a key role in uptake by antigen presenting cells in the lung(Hardy et al., 2012). Therefore, the initial challenge was to synthesize glycine coated iron oxide nanoparticles within the size range of 50 nm with a low poly-dispersity index (PDI). Dynamic light scattering (DLS) measurements such as the hydrodynamic size of the particles were measured over 8 replicates using a Malvern Zetasizer. The pristine citrate stabilized SPIONs size had an average diameter of 65.8 $\pm$ 30 nm (Figure 6.1E) with a PDI of 0.259. On the other hand, the glycine coated SPIONs showed a diameter of 84.19 $\pm$ 18 nm (Figure 6.1F) with a PDI of 0.146 indicating monodispersity of the nanoparticles. The difference in the size can be correlated to the coating of glycine as verified by HR-TEM EDX (12 $\pm$ 5 nm)(shown in Appendix 8.2, Figure C.1F). Furthermore, DLS

measurement indicates that these particles existed as aqueous colloidal suspensions with the presence of associated and hydrated organic layers. We investigated the charge of the glycine coated SPIONs in a range of different pH. Figure 6.1G shows the zeta potential (ζ) measurements of glycine coated SPIONs at pH 1-11. The particles have net positive charge at pH<6.0 and negative surface charge at pH>7.0. Therefore, the pH of zero-point charge was determined to be around 6.0. This difference in their charge can be attributed to the degree of ionization of zwitterionic glycine observed at different pH. The efficiency of chemisorption of glycine onto nanoparticles was found to be 37.8% calculated by extrapolation from a ninhydrin standard curve (shown in Appendix 8.2, Figure C.1E). The GSPIONs are biodegradable as iron oxide nanoparticles are broken down through the endosomes (Mazuel et al., 2016) and are non-toxic to cells even at higher concentrations of 400 μg/ml (Ghasempour et al., 2015). The biodegradability of these particles is an advantage, as after degradation, iron can reach the blood stream and is useful for the body.

6.2.2   Generation of uniform, mono-disperse glycine microparticles by microfluidic jet spray drying

Commercially available glycine powder has a size ranging from 450-600 μm and is bipyramidal in shape (see Appendix 8.2 Figure C.1A1,A2). The microparticles generated by the microfluidic jet spray dryer were around 60$\pm$10 μm and were monodisperse, porous and uniform. However, the size of the microparticles is very large in comparison to the ideal size needed for pulmonary delivery(upper respiratory tract $< 5\mu m$, lower respiratory tract $1 - 5\mu m$ and alveoli $< 1\mu m$)(van Rijt et al., 2014) but, similar to D_{50} values of excipients like lactohale200^{TM}. The particles were therefore characterized based on their surface morphology and structure having anti-inflammatory properties of glycine as well as the ideal size for use as excipients.

Spray-dried glycine microparticles displayed a spherical shape for all samples (Figure 6.2A-D). Crystalline glycine particles produced by cooling or evaporation produces particles which are needle-like, bipyramidal or plate like(Lin et al., 2015) and hence may cause irritation in the respiratory tract upon use as excipients. However, the bipyramidal shape of the particles (commercially available glycine powder, see 8.2, Figure C.1A)

has transformed to a spherical shape due to the process of spray drying in order to produce monodisperse particles(Lin et al., 2015, 2017). Microparticles with different feed concentrations (8 wt.% and 18 wt.%) of glycine, displayed similar sizes around 60 μm for the final spherical dry powder formed. The spray dried microparticles with 18 wt.% glycine concentration was dense with a single hole at the point of droplet disengagement (Figure 6.2A, B). The microparticles spray-dried with 8 wt.% glycine concentration displayed a hollow microsphere (Figure 6.2C) and a coral-like structure as reported here and previously(Lin et al., 2015) unlike random shaped particles of lactohale200^{TM}. Furthermore, XRD data of the glycine microparticles-based excipients without GSPIONs shows three peaks indicating the extent of crystallinity (shown in Appendix 8.2, Figure C.2A). When these microparticles were stored at 76% relative humidity (RH), they became more porous and coral-like (Figure 6.2D) indicating that and increase in moisture would lead to disintegration of the particle. The inlet temperature also played a major role in spray drying. At an elevated temperature of 185 °C, the crystal formed was in large blocks compared to those spray dried at 173 °C. When the velocity of air during the spray drying process was increased to 400 ms^{-1}, several striations were observed under immersion mode (ultra-high resolution) of the microscope (Figure 6.2E). The crystals joined to form the microparticles and is like a cenosphere (hollow shell-like) (Figure 6.2D, 2-3). Therefore, the 18 wt.% feed concentrations were discontinued and for the rest of the experiments, spray-dried glycine microparticle-based excipients were formed with 8 wt.% feed concentration and the excipient microparticles were stored under 76% RH in order to generate a high degree of porosity. The pores are induced into the particles by humidity treatment due to internal flow of glycine by capillary forces exerted on the condensing water as observed by us previously(Lin et al., 2015). The introduction of porosity is a key feature for these microparticles-based excipient, rendering them hollow, ceonospheric for improved aerodynamic performance unlike solid, dense lactohale200. Humidity treatment induces partial dissolution of glycine and then subsequent recrystallization. This phenomenon is important in order to generate discontinuities in the mucus layer as well as to disengage the GSPIONs after impact of subsequent periciliary flow towards the smaller airways and subsequntly into the peripheral lung. The free energy is proportionally related to crystal area, and therefore small crystal grains tend to grow into larger ones with the ultrafine grains showed in high resolution SEM images (Figure 6.2E) forming larger crystal grains(Lin et al., 2015). The size of the microparticles was large for use as a carrier/delivery-vehicle to the alveoli and the peripheral airways, hence

we used them as excipients to get past the oropharyngeal region in order to protect the GSPIONs from the mucus layer.
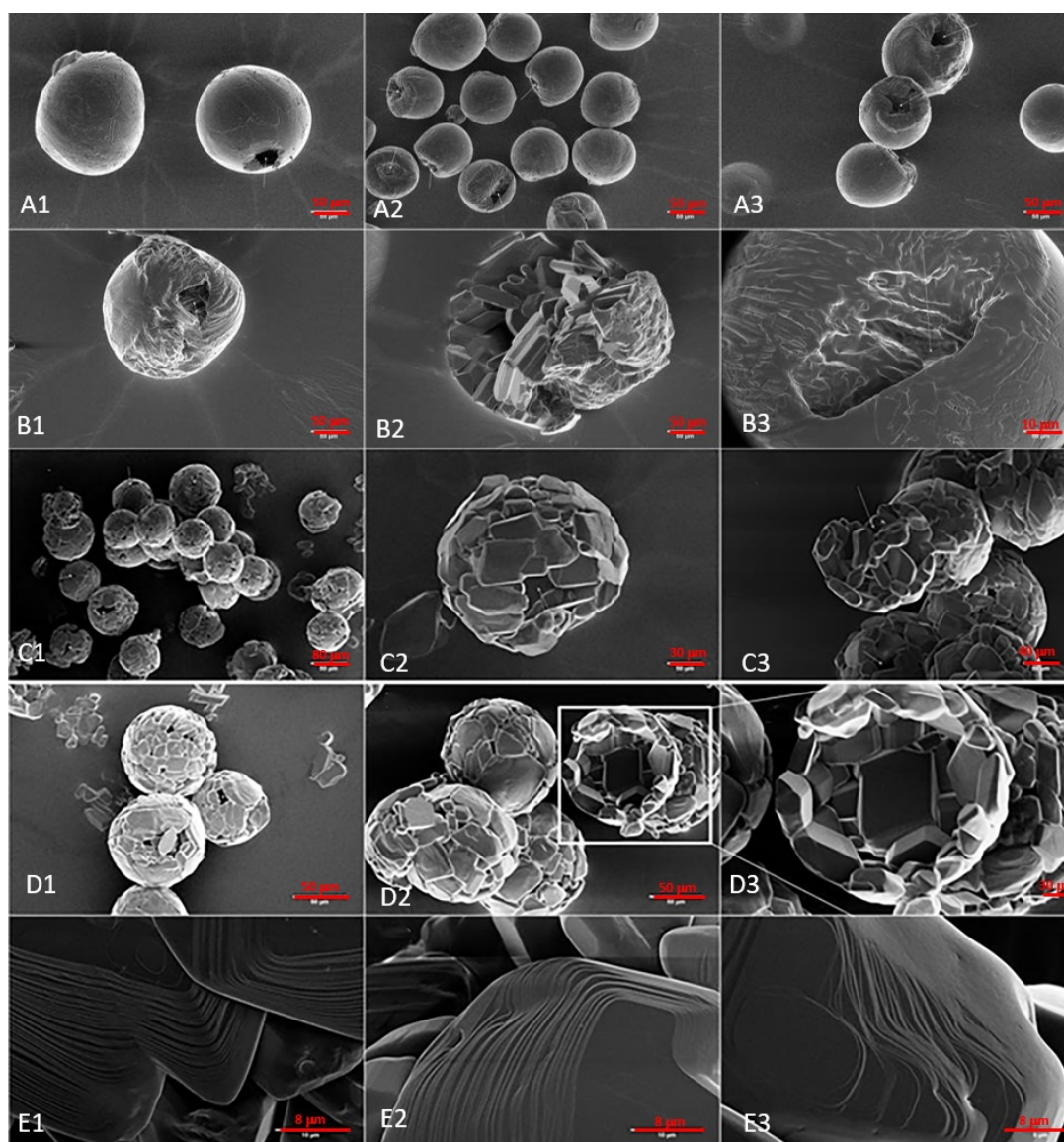
FIGURE 6.2: **SEM images of spray-dried glycine microparticle-based excipient synthesized using a microfluidic jet spray drier. (A).** Glycine microparticles synthesized with a feed concentration of 18 wt.% showing similar spherical shape, uniform but **(B).** dense, monodispersed having a single large pore; **(C).** Glycine microparticles synthesized with a feed concentration of 8 wt.% showing crystalline, spherical, uniform microparticles with **(D).** a hollow core (cenospheric) along with a highly porous surface; **(E).** High resolution image of the microparticle surface showing striation (wave and ridges).

6.2.3 Characteristic features for spray-dried glycine microparticle-based excipients for pulmonary delivery of GSPIONs

GSPIONs with hydrodynamic size 84.19 ± 18 nm were loaded at a concentration of 200 μg/ml onto 8 wt.% glycine feed concentration in order to generate microparticle-based excipients. The spray dried microparticles encapsulating GSPIONs were uniform with low standard deviation (Figure 6.3A). Upon dissolving the microparticle-based excipients containing the GSPIONs in PBS and quantifying for their iron content, we found the iron concentration to be 2.45 μg/ml. These spray dried glycine microparticles appeared to be hollow inside (Figure 6.3B). The "coral-like" surface of the microparticle-based excipient changed to a rough surface due to the presence of GSPIONs (Figure 6.3C). We next evaluated the aerodynamic performance of the microparticles-based excipient. The xRay CT reconstituted 3D images of the glycine microparticles-based excipients containing the GSPIONs (Figure 6.3D) showed the presence of pores (pointed by arrows) on the outer surface (Figure 6.3D1) along with a high degree of uniformity in their size (Figure 6.3D). Moreover, when we observed the cross-section of these microparticles, we found that due to the GSPIONs presence, there was a presence of longitudinal pores (showed by arrows) making the particles very light and aerodynamically efficient (Figure 6.3D2, Supplementary video 2a). We compared our spray-dried glycine microparticle-based excipient with commercial Lactohale 200^{TM} for aerodynamic performance which are defined in terms of its porosity, equivalent spherical diameter and aerodynamic volume. We found that our microparticles have a median porosity of 29%, 570361 μm^3 volume and 80 μm aerodynamic diameter. In Lactohale200^{TM}, the pores were not detected at our voxel size due to the dense nature of lactohale (see supplementary video 2b) which also explains its early deposition in the respiratory tract. Lactohale particles were of non-uniform shape with high poly-dispersity index, making it difficult to calculate the spherical diameter and aerodynamic volume (data therefore not shown). The MSDS of Lactohale 200^{TM} indicates a physical diameter ($d_{50} = 50 - 100\mu m$) A summary of the comparison between GSPIONs loaded on to glycine microparticles-based excipients versus that of the same excipient without GSPIONs are shown in Appendix 8.2, Table 1.
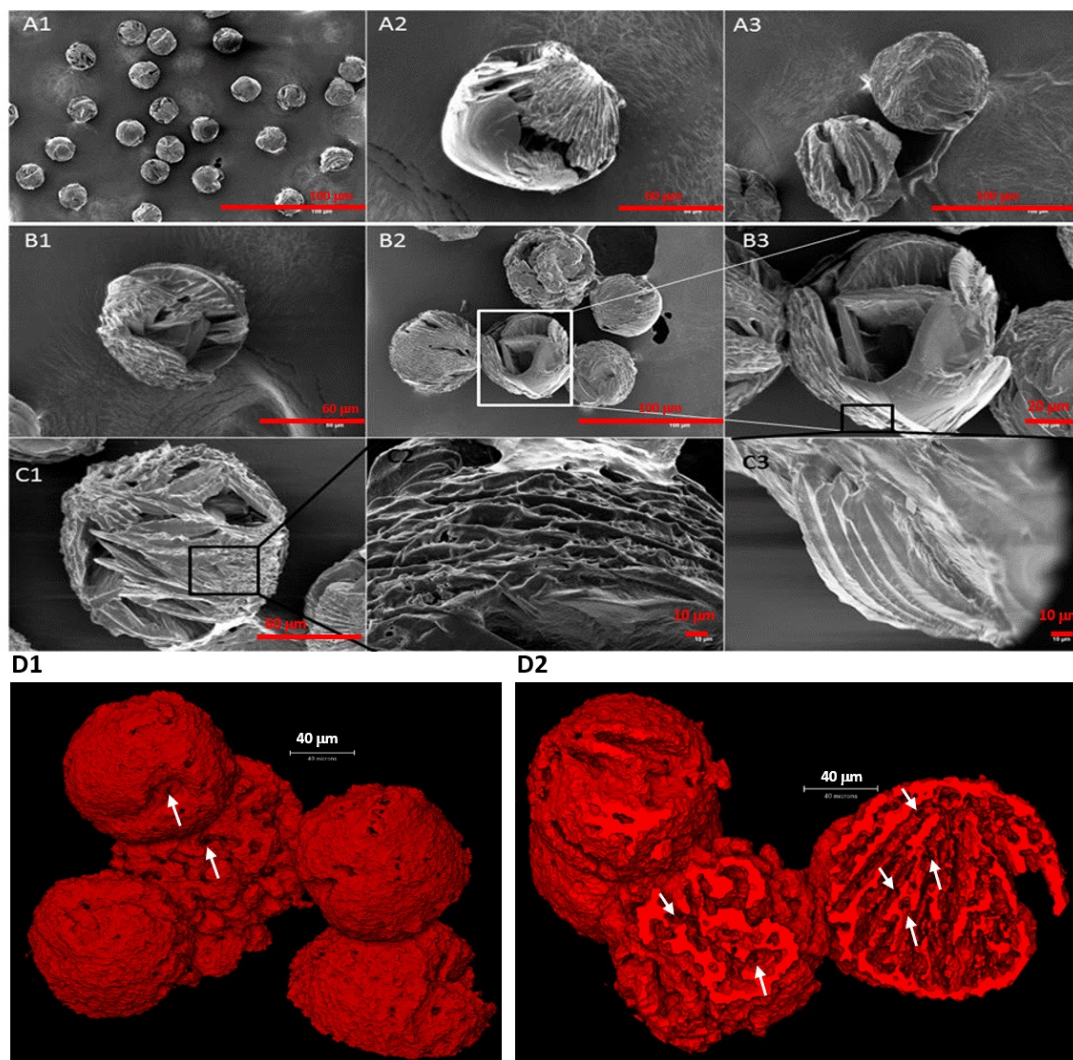
FIGURE 6.3: **GSPIONs loaded on to spray-dried glycine microparticles-based excipients. (A).** The average size ranged from 60-80 μm with both smooth and uneven surface morphology. The spherical structure of the microparticles was maintained. There were several cracks on the crystal (A3). **(B).** The glycine microparticles-based excipient was found to be rough from inside with wall like growth inside the hollow microsphere (B3). **(C).** On higher magnification, wave like structure (C2) was observed on the surface which is due to GSPION deposition with ridges marked by high velocity air (C3). **(D).** XRay CT 3D reconstituted images of the GSPION loaded on to glycine microparticle-based excipient showing pores (white arrows) by a voxel size of 0.75 μm with (D2) the presence of a highly porous core showing longitudinal pores upon looking into their cross-sections. Inset showing the narrow particle size distribution confirming their uniformity and monodisperse nature. Three representative particles were used for measurement and statistical analysis.

We also evaluated the location of the GSPIONs using EDX (to validate our XRay CT data) and investigated whether the glycine microparticles used as an excipient shields the GSPIONs from degrading by thermogravimetric analysis. Whether the protective effect of glycine microparticles is extended to other APIs coated on SPIONs, is beyond the scope of this thesis. On examination of the location of the GSPIONs by EDX (Figure 6.4A- inset) it was observed that the particles were located mainly on the inside. Due to simultaneous effect of drying and crystallization there is formation of wave like structure (Figure 6.3B) and ridges (Figure 6.3C)(Islam and Langrish, 2010). Since glycine is an amino acid, the presence of carbon, nitrogen, oxygen was mapped using the EDX (showed in Figure 6.4A, Appendix 8.2 Figure C.2). However, the microparticles were unstable at a high accelerating voltage of 15 kV (probably due to heat) for EDX therefore the inside of the microspheres could not be mapped. It can be said that due to fast evaporation there is a bubble formation in the core where the nucleation starts to take place with the GSPIONS serving as a nucleus and concentrating at the core with larger crystal formations (Figure 6.3B2-3).

TGA confirmed the loading of the GSPIONs on to the spray-dried glycine microparticles-based excipients. A comparative analysis of spray dried glycine microparticles-based excipients loaded with GSPIONs, empty glycine microparticles, and GSPIONs by itself were carried out (Figure 6.4B). GSPIONs showed negligible weight loss in between 50 °C – 600 °C (the range of temperature analyzed). A two-stage degradation was visible in glycine microparticles and GSPION loaded glycine microparticles. The excipient concentration of glycine used at 8 wt.% yields 26% residue due to coke formation under N_2 atmosphere because of pyrolysis. The GSPIONs loaded glycine microparticles had a significant change of weight in between 180 °C – 220 °C which can be due to physisorbed water, making the dissolution of the excipient ideal upon encountering mucus. Both empty and GSPION loaded glycine microparticles-based excipients showed stability from 200 °C - 240 °C. There is less mass loss in GSPION loaded glycine microparticles, in comparison to empty glycine microparticles. This signifies that the GSPIONs are protected from degradation by the spray-dried microparticles and serves well as excipient. Moreover, the degradation from 300 °C to 450 °C was quite significant as there is release of several gaseous hydrocarbons. TThis also demonstrates that the GSPIONs are protected by the glycine microparticles from degrading. The presence of the GSPIONs

at the core is also confirmed as the GSPIONs themselves have a very small weight loss of 5%. This also confirmed the presence of coating of glycine on the SPION surface.
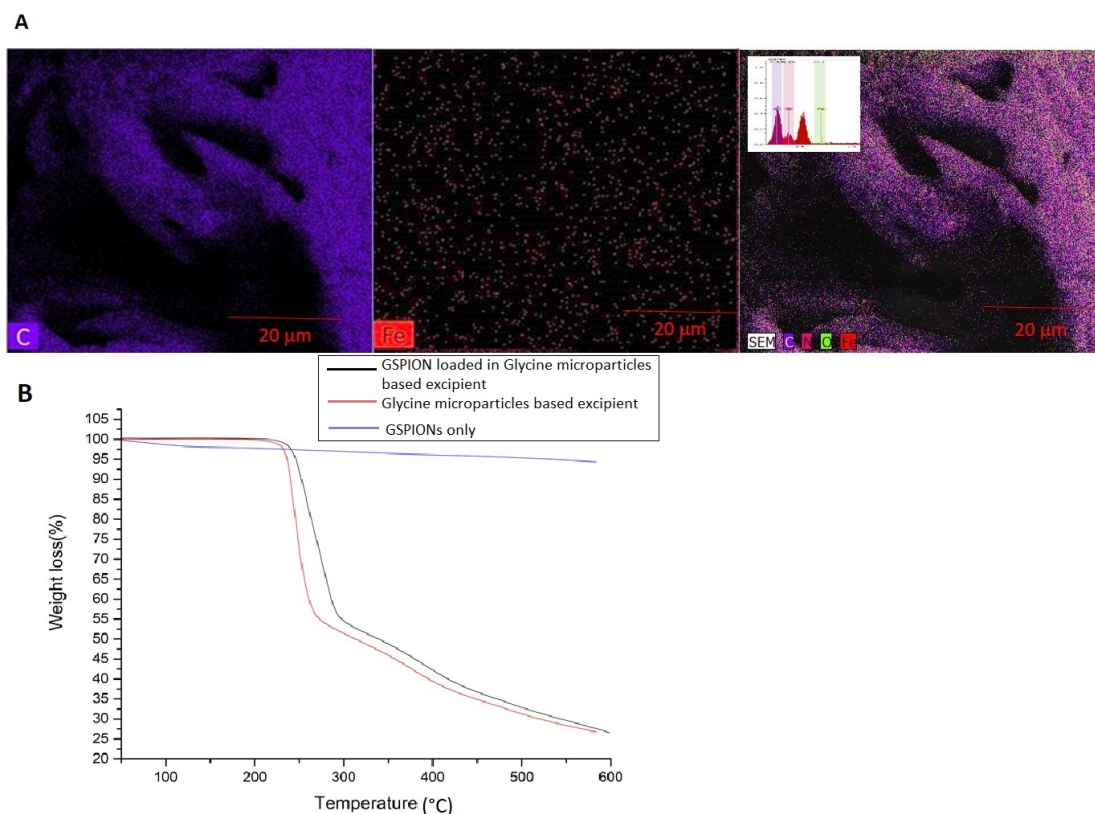
FIGURE 6.4: **Distribution of GSPIONs loaded in spray dried glycine microparticles-based excipients**. **(A).** The location of the GSPIONs was determined by EDX mapping for iron and other elements such as carbon, nitrogen, oxygen. In panel A, the first EDX map shows carbon (in purple) which is attributed to carbon present in glycine. The second map shows iron (in red), which is present relatively at low abundance on the surface. The third map shows carbon(in purple), nitrogen(orange), oxygen(green) and iron (in red). Furthermore, the presence of iron is also confirmed by the peak intensity of the different elements present (inset); **(B).** Thermogravimetric analysis showing stability and protective nature of glycine microparticles-based excipients loaded with GSPIONs (in black), the spray dried glycine microparticles-based excipients only (in red) and the GSPIONs alone (in blue). There was negligible change in mass for GSPIONs only. Whereas, the mass difference of GSPIONs in glycine microparticles were more which is attributed to the protective nature of the microparticles on the GSPIONs.

6.3   Further Discussion

The optimum location to deposit the drug largely depends on the disease type. For example, drug delivery to the upper airways is needed for asthma while for alveolar lung diseases such as COPD and fibrosis it needs to be delivered deep in the lung(van Rijt et al., 2014). In general particles of size greater than 5 μm are deposited in the trachea while that between 1-5 μm are largely phagocytosed and less than 1 μm(Carvalho et al., 2011) are deposited in the alveoli(Paranjpe and Müller-Goymann, 2014) for uptake by immune cells. We utilized this principle to design our inhalable spray-dried glycine microparticle-based excipient to carry GSPION in order to protect them from mucociliary clearance. Due to the porosity and aerodynamic performance of the microparticles, they can be delivered to the upper airways past the oropharyngeal region. The GSPIONs due to their nano-size and glycine coating do not aggregate due to charge-based repulsion. The GSPIONs are carried to the alveoli by periciliary fluid movement along the airway. In addition, glycine in the literature has been reported to prevent mucus hypersecretion. The dissolution and high solubility of the glycine micoparticle-based excipient would result in mucus discontinuity (as well as our data, see chapter5.3.2), leading the nanoparticles to reach the periphery. The coating with glycine yielded crystalline superparamagnetic particles which was transformed from ferro or ferri-magnetic iron oxide nanoparticles(Barick and Hassan, 2012). This decrease in magnetization can be attributed to the combined effect of the nano-core size and (large surface to volume ration) and robust coating of glycine molecules on their surface (quenching of magnetic moment by electron exchange between coating and surface atoms)(Mikhaylova et al., 2004). Recent studies with iron oxide nanoparticles have showed that TEM size of 10 nm are ideal for uptake by macrophages(Feng et al., 2018) especially alveolar macrophages(Katsnelson et al., 2012) and our GSPIONs are in the TEM size range of 12 ± 5 nm.

There are several challenges in delivering therapeutics to lung alveoli using nanoparticles especially in patients with respiratory diseases. In general, uncoated iron oxide nanoparticles tend to crash out of solution/agglomerate (Chakraborty et al., 2017). But coating the particles with glycine stabilizes them and makes them ideal for conjugating drugs/compounds or use as is for pulmonary delivery. The low PDI of 0.146 of the glycine coated nanoparticles leads to a monodisperse suspension and therefore stable in comparison to that of pristine iron oxide nanoparticles (PDI 0.249). The coating

results in inter-particle repulsion causing them to stay in solution preventing agglomeration. The surface functionalization is important to prevent the particles in ameliorating pulmonary inflammation. It is known that pristine nanoparticles without surface modification in the same size range of 30-100 nm promotes lung inflammation mediated by inflammasome activation and $IL - 1\beta$ secretion (Kusaka et al., 2014). Therefore, glycine coated particles will be advantageous from the clinical perspective. Furthermore, the coating with glycine results in a hydrodynamic size ideal for uptake by cells in the lung(Hardy et al., 2012, 2013). Particles less than 5 nm accumulate in the nucleus while that of 15-40 nm restrict themselves to the cytoplasm. On the other hand, particles in the size range 100-233 nm are prevented to enter the cell(Chakraborty et al., 2017), thus our GSPIONs with HRTEM size 12±5 nm and hydrodynamic size 84.19±18 nm are ideal both for functional and mechanistic studies as well as pulmonary delivery of therapeutics.

Another problem associated with delivery of nanoparticles is instability in different biological environments. The airway epithelium has an excellent defense mechanism to remove infectious particles from inhaled air and thereby preventing infection in the lung. The lung pH is highly maintained by $H^+ - K^+$ ATPase, vacuolar type H^+ ATPase as well as HCO_3^- conduction from the CFTR Cl^- channels(Fischer and Widdicombe, 2006). Our result shows a great stability of the glycine coated nanoparticles in a wide range of pH. At both ends of the pH scale the zeta-potential increases which could be due to the development of partial charge in chemisorbed glycine leading to its stability.

6.4 Summary

In summary, our data suggests that spray-dried glycine microparticles synthesized using a micro-fluidic jet spray dryer could be used as an ideal excipient in pulmonary delivery of functionalized nanoparticles. The glycine excipients are porous, aerodynamically stable, monodisperse and uniform which is advantageous over other available commercial excipients in terms of availability, cost of production, ease of encapsulation, homogeneity, hygroscopicity and most important preventing mucus clearance for pulmonary delivery. Using this excipient to encapsulate functionalized super-paramagnetic iron oxide nanoparticles coated with glycine (GSPIONs) is beneficial for use as carriers for pulmonary delivery. The GSPIONs are of a hydrodynamic size ideal for uptake by lung

resident immune cells. In acute inflammatory lung diseases such as Acute Respiratory Distress Syndrome (ARDS), the main infiltrating cells are the neutrophils and alveolar macrophages. Our GSPIONs are taken up by these lung resident cells and hence we propose the use of these biodegradable nanoparticles for mechanistic studies of pulmonary inflammation and conjugating or using them as immunomodulators in respiratory diseases. Overall, these data demonstrate that spray-drying can be used to design inhalable, biodegradable microparticle-based excipient system for protecting and/or encapsulating functional nanoparticles for pulmonary delivery. It also increases our understanding of nanoparticle uptake by immune cells in the lung and provides future directions to utilize these nanoparticles as immunomodulators in the attenuation of airway inflammation. Our findings provide new insights into spray-drying of amino acids to design uniform, monodisperse excipients capable of passing the oropharyngeal region for pulmonary drug delivery and supports the hypothesis to deliver inhalable immunomodulatots in the lung periphery without entrapment in the mucus.

Chapter 7

Delivery of immunomodulators-Proof of Principle

7.1 Introduction

Discovery of new drug targets has become essential due to the diversity of diseases and alleviating resistance to drugs. Therapeutic interventions targeting specific cells are being developed to treat respiratory diseases. Nanoparticles are capable of pulmonary drug delivery, albeit there has been concern in the literature that some of them may promote lung pathology, since a number of man-made and environmental nanoparticles cause asthma exacerbations(Inoue et al., 2009, 2010; Alessandrini et al., 2006; De Haar et al., 2006), and are associated with size dependent cytotoxicity in mammalian cells(Pan et al., 2007; Cai et al., 2011; Vedantam et al., 2013; Ariano et al., 2011). Nanoparticle size is also important in terms of nanoparticle distribution in the lung(van Rijt et al., 2014) and plays a major role in their overall systemic clearance and biodistribution. Usually, particles with a size of less than 5 nm are cleared by the kidneys(Soo Choi et al., 2007), whilst 50-100 nm particles lodge in the liver(Braet et al., 2007). Often bigger micron-sized particles end up in the spleen(Blanco et al., 2015). However, coating the particles modulate their excretion(Almeida et al., 2011). Some nanoparticles are cytotoxic(Pan et al., 2007; Cai et al., 2011; Vedantam et al., 2013; Ariano et al., 2011) related in some cases with additional other physicochemical aspects such as charge(He et al., 2010; Verma and Stellacci, 2010). For pulmonary delivery, unless particles are highly porous with aerodynamic features to support delivery; they end up in lung capillaries(Liu, Li and Xu, 2014; McVey et al., 2012). Targeting nanoparticles for uptake by alveolar macrophages has recently been shown to be useful in intervention to treat respiratory diseases(Rahul et al., 2017), and given their central role in the control of many disease of the lung, it is likely to be useful across multiple disease. However, since uptake by alveolar macrophages of pro-inflammatory or toxic nanoparticles and microparticles including those made from some form of silica and asbestos, can lead to pulmonary fibrosis and neoplasia(Nakayama, 2018). It will be useful to develop nanoparticle scaffolds that do not trigger potentially damaging inflammatory pathways during particle uptake. The uptake of diverse type of nanoparticles and microparticles in the lung by a range of subtypes of endocytic cells, has been recently extensively reviewed (Chakraborty et al., 2018).

The charge on the nanoparticle surface is another critical determinant of its stability *in-vivo*, therefore, as well as size, the zeta-potential of the particles is also important(Moore

et al., 2015). For instance, the coating on the particles' surface can enhance their circulation time in the body by preventing efficient uptake by antigen presenting cells(Mohr et al., 2014), or precluding aggregation due to a biological fluid such as serum or mucus(Walkey et al., 2012; Lai et al., 2009). However, it is not necessary that the coating on the nanoparticle surface will always affect the charge. In fact, the component coated on the particle surface determines the immune response. For example, poly-l-lysine coated nanoparticles are ineffective in inducing mucosal immunity versus that of chitosan coated(Marasini et al., 2017). Overall, amino acid coatings can be used to improve the biocompatibility, size and biodistribution as well as potential interaction with immune cells, making them ideal molecules for conjugating of nanoparticles for therapeutic and diagnostic applications(Inbaraj et al., 2011; Chakraborty et al., 2017). Therefore, the coating on the particle along with its core, will both be significant when designing particles for pulmonary delivery.

Different coatings which can help modify the biodistribution of the particles *in-vivo* include polyethene glycol, dextran and amino acids(Chakraborty et al., 2017) which contain methyl, amino, carboxy functional groups. Amino acids possess both amino and carboxy terminals due to their zwitterionic nature. The availability of two functional groups is beneficial as one can be utilised for attachment of drugs and other molecules while the other is accessible to the nanoparticle. For diagnostic application, iron oxide nanoparticles have been proved to be successful in Magnetic Resonance Imaging (MRI) of tumours and soft tissues(Lee et al., 2010*b*; Yang et al., 2010*b*) and its biodegradable nature prevents accumulation in tissues(Mazuel et al., 2016). Coating of iron oxide nanoparticles with poly-aspartic acid leads to a charged surface aiding to their uptake by tumour cells and enhancing their ability to provide tumor contrast(Lee et al., 2010*b*). The advantage of MRI over fluorescent probes and/or nanoparticles is the localization of the signal within tissue, MRI can image deep within the body while fluoresce is limited in penetration by tissue scattering of the emitted light. Additionally, the fluorescent probe can be cleaved from the nanoparticle leading to a false positive signal. Biodegradable nanoparticles with super-paramagnetic properties are useful as MR contrast agents as the core of the particle is responsible for image contrast(Yang et al., 2010*b*) with improvement in contrast when two adjacent areas have difference in signal intensity (SI).Contrast difference is required to differentiate between normal anatomy from pathology. Therefore, signal intensity on an MR image is governed by many factors including the tissue

characteristics, proton density and type of sequence used(Bloem et al., 2018).

Despite the recent advancements in biomedical imaging especially MRI of tumours(Lee et al., 2010b; Yang et al., 2010b) and soft tissues such as liver(Xing et al., 2011), non-invasive lung imaging is difficult and MR imaging of the lung is not well established. The potential to improve lung MR imaging is extensive. Pulmonary inflammation is a hallmark in many respiratory disease in which cells such as neutrophils and alveolar macrophages are the key players in regulating inflammation. An unmet need would be in tracking functional immune regulatory lung cells, such as alveolar macrophages and neutrophils. There is fundamental need to understand nanoparticle biodistribution in the lung to inform clinical utilization of thse particles. A key problem with current lung MR imaging is due to the hollow nature of the lung, comprising of air and negligible hydrogen protons, which are required for standard MR imaging(Altes et al., 2007). In addition, the lung is not a static organ as it is consistently under a rhythm of inhalation-exhalation further complicating the imaging. To overcome this problem, we used a non-invasive 3D ultra-short echo time (UTE) MR imaging sequence in order to nullify respiratory and cardiac motion(Takahashi et al., 2010). With near zero echo times such as ultra-short echo time sequence, have shown utility for the assesment of non-cell lung carcinoma and pulmonary edema(Johnson et al., 2013). In order to study nanoparticle biodistribution, we synthesized and delivered intranasally, super-paramagnetic iron oxide nanoparticles coated with the amino acid glycine (GSPIONs) to investigate the uptake by cells resident in the lung. Glycine is the simplest, neutral amino acid, it does not induce inflammation and being small it minimizes extending ligand arms with functional groups helping control nanoparticle size. We demonstrate for the first time the biodistribution of GSPIONs within the lung of mice following inhalation using a 9.4T magnet and a non-invasive 3D ultra-short echo time (UTE) MR imaging sequence previously developed by Takahashi and colleagues(Takahashi et al., 2010). Utilizing $\gamma - Fe_2O_3$ core of the nanoparticles, we were able to show selective nanoparticle uptake by specific alveolar macrophages and neutrophils. We measured airway resistance and local pro-inflammatory cytokine induction in the lung after GSPION administration and were able to confirm the particles were not inflammatory. The data shows a promising safety profile for nanoparticles coated in this neutral amino acid and a useful base to further explore applications for potential clinical use.

7.2 Methods

7.2.1 Experimental design

Glycine immunomodulators were developed by conjugating glycine on to biodegradable super-paramagnetic iron oxide nanoparticles. Mice were intranasally given either GS-PION or control (0.9% saline, vehicle only). Mice were anaesthetized using isoflurane (IsoFlo®, Abbott Laboratories, North Chicago, IL) in 100% oxygen; and either GSPI-ONs (200 µg/ml) or control (0.9% saline, vehicle only) were intranasally administered. GSPIONs were suspended in either 100 mM glycine or saline. MR imaging was performed prior to sensitization and 24 hours after sensitization (detailed protocol in chapter 3.17). For GSPION sensitized group (n=5) and control (vehicle: 0.9% saline) (n=3) mice were analyzed. The experimental design is demonstrated in Figure 7.1 below. After MR imaging and measurement of lung function (see chapter 3.6), mice were culled and lungs were subjected to Perl's prussian blue staining (refer to chapter 3.9) to locate the GPSIONs. Lung architecture was also evaluated by staining with Hematoxylin and Eosin (see chapter 3.8). Other organs such as liver, heart and spleen were checked for the presence of GSPIONs (shown in Appendix 8.2).
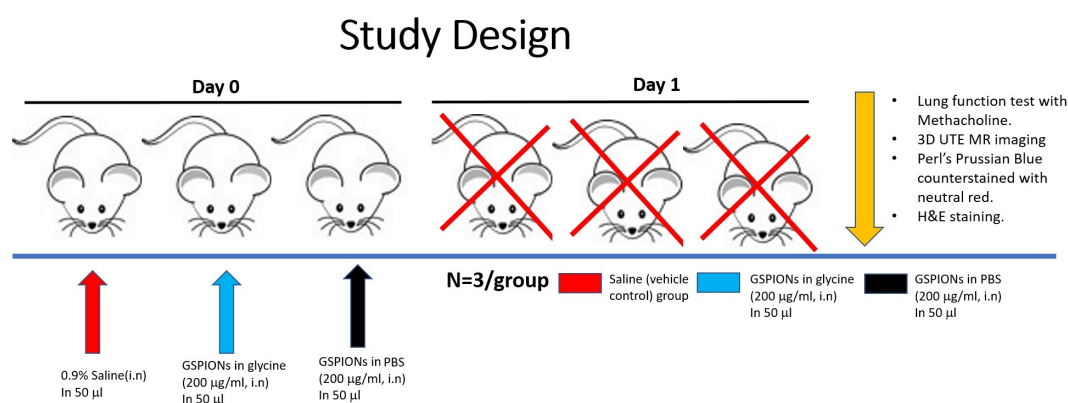
FIGURE 7.1: **Study design showing sensitization of mice with GSPIONs(200 µg/ml) suspended in PBS or glycine and saline (control)**. Mice were sensitized with GPSIONs(immunomodulators) suspended in either 0.9% saline or 100 mM glycine and compared to saline (control). After 24 hours of sensitization, mice were subjected to 3D UTE MR imaging, lung function test, Perl's prussian blue counter stained with neutral red to stain GSPIONs and lung architecture stained using Hematoxylin and Eosin staining.

7.3 Results

7.3.1 Glycine immunomodulatories are capable of pulmonary delivery

The NGI dispersion data for glycine microparticles with and without GPSIONs as well as the commercial excipient Lactohale200^{TM} are plotted in Figure 7.2. The emitted fraction of lactohale 200^{TM} (78±1 %) was higher than the glycine microparticles alone (56±1 %) but were comparable to that of GSPIONs loaded on to glycine microparticles (74±1 %). The fraction of recovered powder at each stage were similar between Lactohale 200^{TM} and our GSPIONs loaded glycine microparticles are comparable to Lactohale excipient. Inspection of the NGI data showed that, majority of the particles deposited in stages 1-5. The microparticles deposited beyond stage 5 were almost negligible and beyond the detection limit of the assay (data not shown). Spray dried glycine microparticles without GSPIONs majorly deposited in between stage 1 and 2 and limited availability was observed in between stage 3-5. When we compared spray dried glycine microparticles with GSPIONs to that of lactohale 200^{TM} at individual stages, it was found that at stage 1,2 and 4, there is no significant difference in their deposition between lactohale 200^{TM} and GSPIONs loaded on to glycine microparticles, hence comparable as excipients. The glycine microparticles without the GSPIONs were significantly less deposited across all the stages. The glycine microparticles were found to be highly porous (29% porosity from X-Ray CT data), crystalline (Figure 6.3D2), wave-ridge, "coral-like", cenospheric (hollow core) microcarriers with aerodynamic diameter (80±10 μm, from 3D reconstruction of XRay CT images) generated during spray drying with GSPIONs.
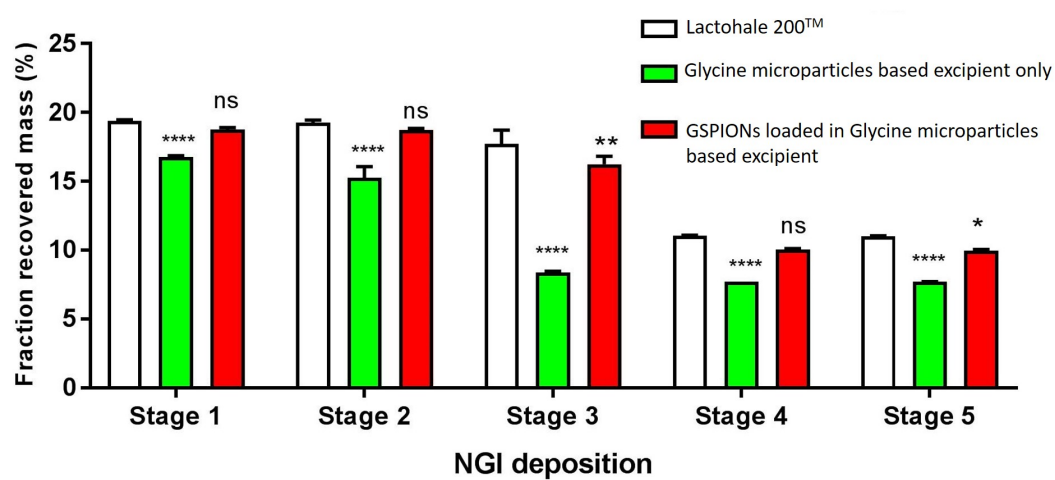
FIGURE 7.2: **Next Generation Impactor recovery of glycine micrparticles at different stages**. Distribution of glycine microparticless loaded with or without GSPIONs in comparison to commercial excipient Lactohale200^{TM} collected from the next generation impactor at various stages. Data represented as Mean±SD with n=4 and 3 assay replicates/stage.

At a flow rate of 45 L/min which is the normal inspiratory flow rate in a human(with a pulmonary disease such as COPD or fibrosis), the microparticles carrying the GSPI-ONs demonstrate a proof of concept that they are able to travel longer whereas the microparticles alone are carried less due to reduced porosity although both the structures show spherical morphology. Processing of the NGI data also allowed us to compare between the mass median diameter of the microparticles (80 ± 10 μm) in comparison to large physical diameters ($d_{50} = 50 - 100\mu$m) values of commercial Lactohale 200^{TM}. The aerodynamic size of the GSPION loaded onto glycine microparticles and the d_{50} value of lactohale 200^{TM} coincide and can be correlated with the NGI deposition at the different stages. Therefore, the microparticles are comparable as excipients with similar aerodynamic performance and capable of pulmonary administration of the GSPIONs. The fabricated glycine microparticles have better aerodynamic performance despite of having large geometric diameter because of their low densities. The low density of glycine (8 wt.%) used as feed concentration to generate the microparticles, owed to cenospheric, highly porous morphologies, causes their aerodynamic diameter to lie within the range for effective depositions past the oropharyngeal region. In addition, the solubility of glycine microparticles (240 mg/ml) was higher than that of lactohale (190 mg/ml) at 25 °C, owing to its porous nature and availability of physiosorbed water.

7.3.2 GSPIONs are distributed throughout the lung and shows T2* relaxivity in lung

Typical ultra-short echo time (UTE) images of the lungs in mice instilled with saline or GSPIONs at nine different echo-times (TEs) ranging from ultrashort (0.01 msec) to conventional (1.2 msec) are shown in Figure 7.3A. The images were not degraded by motion artefacts. Signal intensity (SI) was consistent within the cardiac muscle which we used the heart as an internal imaging control. The signal intensity for GSPION sensitized mice was lower(Pusnik et al., 2016) in comparison to saline treated mice (Figure 7.3B) for any TE. In general, the GSPIONs showed a reduction in signal intensity consistent with the effects of iron oxide nanoparticles and the coating did not effect it (shown in Appendix 8.2). For determining the SI in lung parenchyma, the lung was segmented into upper, middle and lower regions.
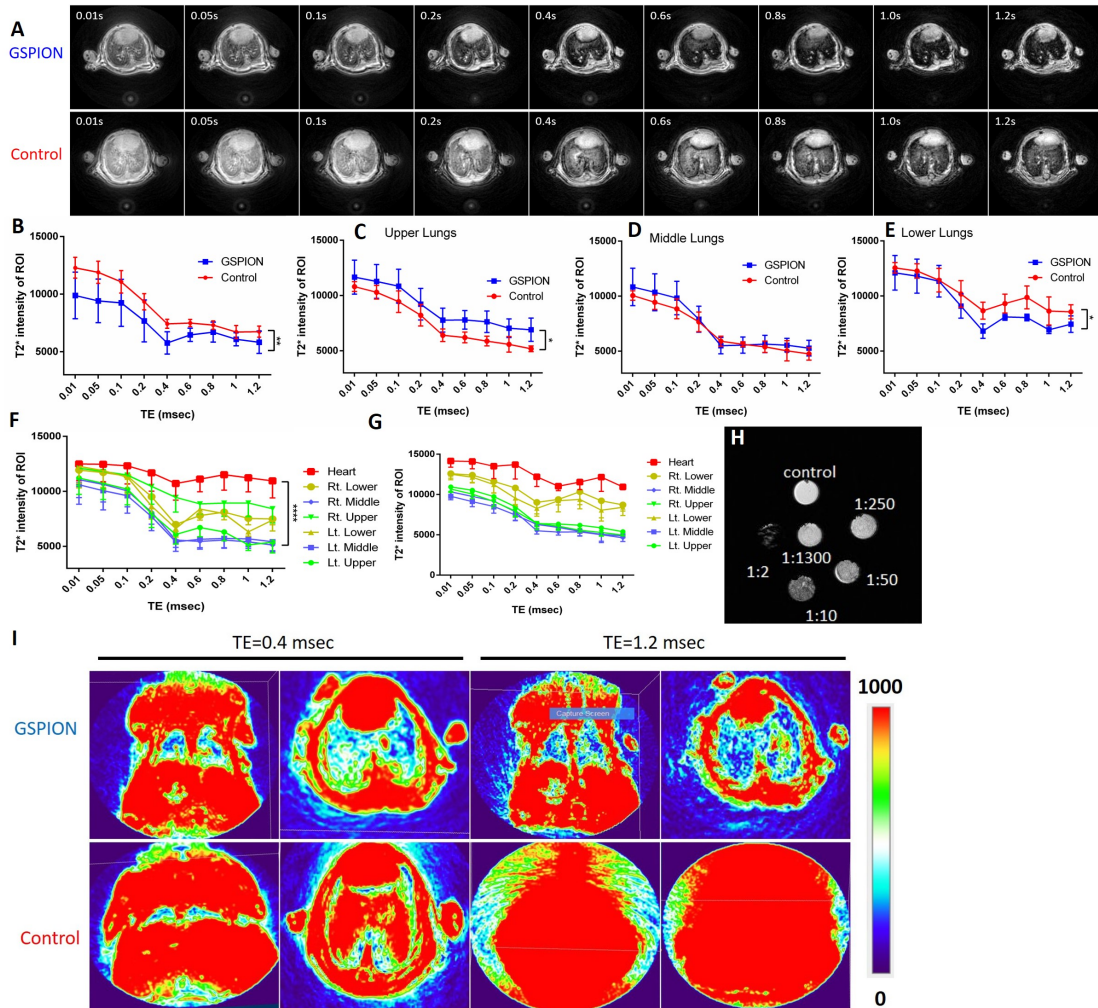
FIGURE 7.3: **Non-invasive 3D UTE MR imaging of the lung for biodistribution**. All MR images are at slice 71. **(A).** GSPION vs Control (0.9% saline) sensitized mice imaged at different TEs. **(B).** T2* signal intensity for all lung segments in GSPION vs saline (control) groups. **(C).** T2* signal intensity of the upper lung region for GSPION vs control (saline) groups. **(D).** T2* signal intensity of the middle lung region for GSPION vs control (saline) groups. **(E).** T2* signal intensity of the lower lung region for GSPION vs control (saline) groups. **(F).** T2* signal intensity of heart (control) in comparison to different lung segment in both left(Lt.) and right (Rt.) lobes of the lung in GSPION group. **(G).** T2* signal intensity of heart (control) in comparison to different lung segment in both left(Lt.) and right (Rt.) lobes of the lung in saline group. **(H).** T2* signal intensity of different GSPION dilutions (concentrations) showing relaxivity and darkening due to GSPIONs presence. **(I).** 3D UTE volumetric rendering of GSPION sensitized and control mice at ultra-short TE 0.4 msec and conventional TE 1.2 msec. The decrease in the heat map corresponds to tissue whereas the increase corresponds to GSPIONs increasing the relaxivity.

Interestingly, the SI for control (saline treated) mice was lower than GSPION sensitized mice in the upper segment of the lungs, did not change in the middle segment and was reduced in the lower segments (Figure 7.3C, D and E). The pattern of SI decreases for the GSPION group showed a gradual decrease from the upper segment to the lower segment, indicating a higher concentration of particles in the lower alveolar regions. Upon comparing the different segments of the lung with heart (control), the SI for each individual segment was lower than the heart (Figure 7.3F) for any TE. The GSPIONs were evenly distributed between the left and right lobe of the lung as the SI was consistent irrespective of the lung lobe. The control (saline) group showed very similar SI between lobes(Figure 7.3G). Increasing concentrations of GSPIONs decreased SI when embedded in agarose(Figure 7.3H). The dark patches in the lung parenchyma are consistent with the biodistribution of GSPIONs following inhalation (Figure 7.3A,I) but not visible in saline controls (Figure 7.3I).

7.3.3 Selective localization of GSPIONs in the lung within alveolar macrophages and neutrophils

In airway inflammatory diseases such as Acute Respiratory Distress Syndrome (ARDS), asthma and COPD, the airway walls become thickened due to remodeling of all resident cellular components at the wall, as well as infiltration of macrophages, neutrophils and cytotoxic T lymphocytes. The inflammatory cells such as neutrophils and alveolar macrophages release cytokines such as IL-8 and TNF leading to tissue damage (Chakraborty et al., 2017). Therefore, drugs target these cells in attenuating airway inflammation. To validate whether our GSPIONs can deliver therapeutics for interacting with these inflammatory cells, we sensitized mice with GSPIONs intranasally followed by staining the lung sections with Perl's Prussian blue in order to identify if lung resident immune cells take up these particles. GSPIONs were delivered intranasally by suspending either in PBS (as recovered from reaction) or in glycine and compared to saline (vehicle control) followed by invasive plethysmography, H & E and Perl's Prussian blue staining (Figure 7.4A). GSPIONs were taken up by different immune cells as they stained blue due to Perl's Prussian blue stain (Figure 7.4B). The cells are circled (in green) taking up the particles and are absent in the saline (control) group which is attributed to the absence of particles. Specifically, alveolar macrophages and neutrophils were found to take up the GSPIONs (Figure 7.4B inset) and was confirmed by Perl's Prussian blue positive stain of

the spleen. The GSPIONs were not found in the heart or liver (see Appendix8.2, Figure C.3), indicating their localization in the lung. The lung parenchyma showed no signs of damage to the parenchyma or the airways, when compared to saline (Figure 7.4C and Appendix Figure C.3A). By invasive plethysmography, lung resistance was measured for all the groups. It was found that GSPIONs suspended in glycine showed lower resistance in comparison to GSPIONs suspended in PBS. However, the resistance of GSPIONs in PBS was comparable to saline (control).
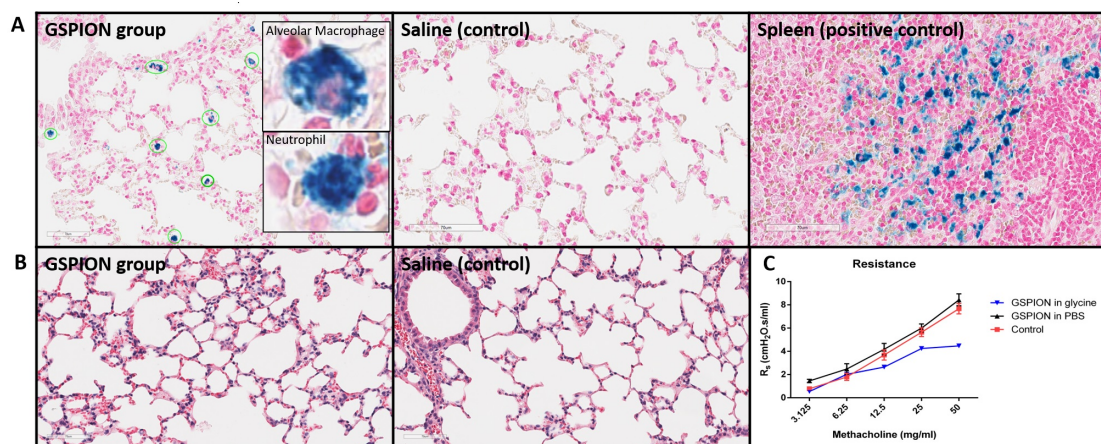
FIGURE 7.4: **Therapeutic efficacy of GSPIONs in lung**. **(A).** Perls Prussian blue counter stained with neutral red to determine uptake by immune cells in the lung for GSPIONs and saline group and spleen showing positive stain. **(B).** Hematoxylin and Eosin stain showing lung parenchyma in both GSPION and saline (control) group. **(C).** Lung resistance measured by invasive plethysmography in GSPIONs suspended in glycine and PBS in comparison to control.

The coating of the SPIONs with glycine as a model compound served in a way to identify the efficacy of interaction by lung resident cells and confirms the hypothesis that nanoparticles in the periphery are cleared by alveolar macrophages. The spray-dried glycine microparticles was developed to protect these nanoparticles from mucociliary clearance by providing protection. As seen from our results in chapter 4 and 5, glycine is anti-inflammatory and can be used to reduce mucus production although the microparticles have size and structure comparable to the excipient, lactohale200^{TM}. We found that this microparticle-based excipient was able to get past the oropharyngeal region as needed but could not reach the terminal airways or the alveolar airspace. However, as we hypothesized that the use of this spray-dried glycine microparticle will lead to discontinuity in the mucus preventing mucociliary clearance has been successfully demonstrated by these GSPIONs. We found that the GSPIONs are not deposited in the terminal airways but are present in the alveoli. This consolidates our hypothesis that glycine coating prevents aggregation by particle-particle interaction as well as abrogating mucociliary expulsion of the particles by preventing airway mucus hypersecretion. The most significant finding was that both neutrophils and alveolar macrophages (identified in the lung section by their nuclear morphologies) has taken up the GSPIONs (Figure 7.4A inset-stained in blue). Therefore, the use of these nanoparticles for delivering glycine as immunomodulators in airway diseases without the problem of nanoparticle disintegration can facilitate targeting alveolar macrophages and neutrophils which are elevated in ARDS and confirmed by our elevated levels of the cells in the BALF before.

7.3.4 GSPIONs do not induce pro-inflammatory cytokines

Expression of pro-inflammatory cytokines IL-1β, IL-6, TNF was investigated upon administration of GSPIONs suspended in PBS or glycine and compared to control (vehicle) into the lung (Figure 7.5). In each section/mice/group, ten regions were selected using the positive pixel count algorithm avoiding muscles to quantify the amount of positive stain for each of these cytokines as heat maps to represent the different intensity of expression. The background was subtracted from the positive pixel intensity and recorded as intensity of strong positive. Expression of pro-inflammatory cytokines in both GSPIONs suspended in PBS or glycine did not elicit an immune response resulting in a higher expression compared to saline. Parallel studies with LPS by contrast showed clear and significant cytokine upregulation (data shown in Figure 5.3). The background expression

of IL-1β was comparatively lower to that of IL-6 and TNF in all groups. The unchanged expression of pro-inflammatory cytokines clearly indicates that these GSPIONs, unlike naked iron oxide nanoparticles do not initiate an inflammatory reaction(Liu et al., 2018; S et al., 2017). Therefore, these GSPIONs offer a potentially useful new platform for the development clinical applications such as in diagnostics and therapeutics.
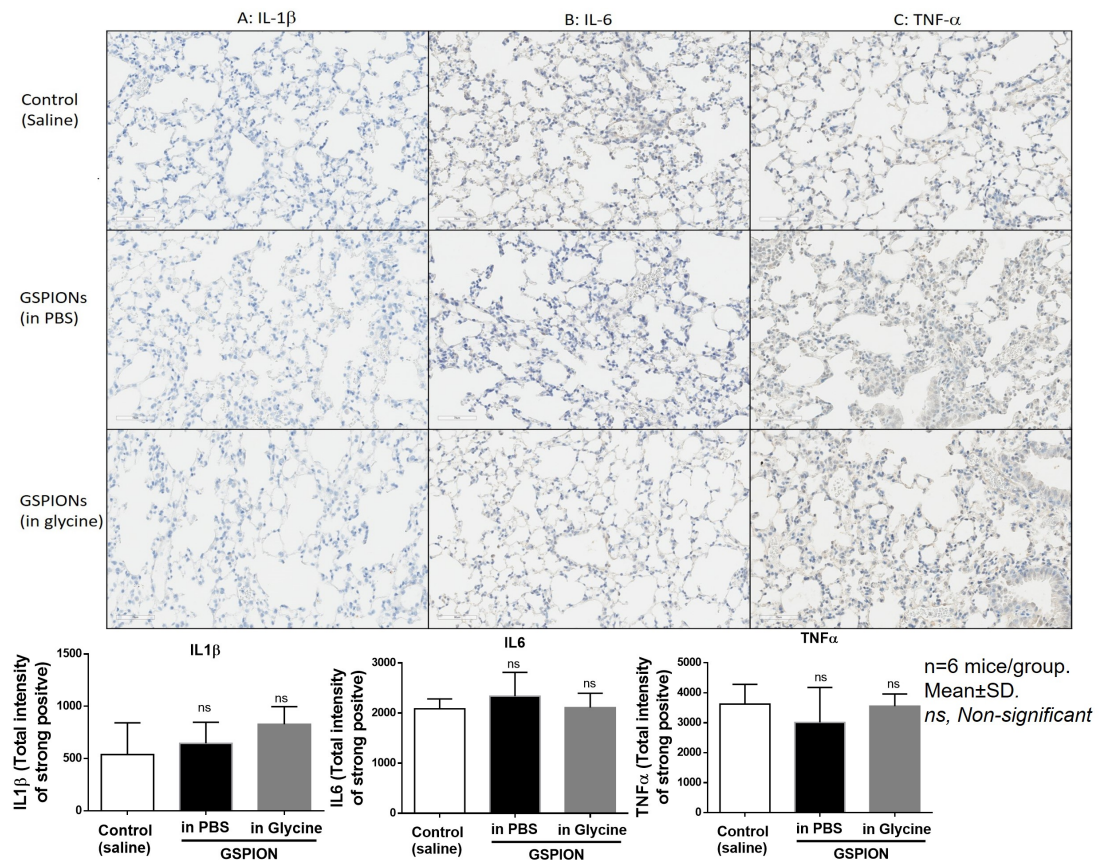
FIGURE 7.5: **GSPIONs do not increase expression of pro-inflammatory cytokines in lung parenchyma.**. In comparison to control (saline), expression of proinflammatory cytokines, **(A).** IL-1β, **(B).** IL-6 and **(C).** TNF; was unchanged along with negligible damage in the lung parenchyma. For positive controls, heart and kidney sections were stained by the same pro-inflammatory cytokines and IgG (as negative control), in the same concentration of the antibody used here (shown in Appendix 8.2 Figure B.1). Scale bars represent 70 μm. N=6 mice/group, Mean $\pm$ SEM. A one-way ANOVA with post-hoc T-test was used to determine the significance in between different groups. Each group was quantified for strong positive expression by analyzing 10 sections/lung/group. *ns, non-significant.*

7.4 Discussion

Properties of nanoparticles such as size, shape and charge are very important for interaction with immune cells. Regarding nanoparticle size in pulmonary delivery, dense microparticles (>5 μm) are deposited in the trachea while in between 1-5 μm are phagocytosed(Carvalho et al., 2011), but nanoparticles with size less than 1 μm end up in the alveoli (Paranjpe and Müller-Goymann, 2014). These nanoparticles are then taken up by endocytic cells that are present in the lung such as alveolar macrophages and neutrophils. These in turn are changed in number under diverse environmental challenges, such as infections or pollution, or due to the presence of cancer. Our nanoparticles have a hydrodynamic size of approximatelt 84.19 $\pm$ 18 nm which is ideal for reaching the lung alveoli during pulmonary delivery and the MRI as well as histology data suggest the particles reach the lower levels of the lung within the alveoli spaces. Our GSPIONs could be useful to enable the development of diagnostic and therapeutic agents for targeting the alveoli in diverse diseases, with COPD and fibrosis as obvious candidates. Very recently, it has been demonstrated that macrophages (especially alveolar macrophages) take up iron oxide nanoparticles with an average size range (measured by TEM) of 10 nm(Feng et al., 2018; Katsnelson et al., 2012). Our GSPIONs are of the size 12 $\pm$ 5 nm as measured by TEM (see section 6.2.1), and we show they are taken up by alveolar macrophages and neutrophils. The assembly of nanoparticles observed on our DLS measurement of the hydrodynamic size can be attributed to the presence of NaCl during synthesis and washing, increasing the solvation layer around the particles. Furthermore, the coating with glycine was advantageous as it prevented the agglomeration unlike naked iron oxide nanoparticles, while at the same time being a useful inert coating for use in patients with diabetes(Chakraborty et al., 2017). Although a very minute amount of glycine is being coated on to the nanoparticles yet it has several advantages for future clinical use. Glycine is known to be sweet and improves insulin sensitivity along with a reduction of symptoms induced by hyperglycemia(Nuttall et al., 2002; Alvarado-Vásquez et al., 2003), albeit at higher concentration than what we coated our nanoparticles. Our GSPIONs do not escalate inflammation unlike other naked nanoparticles in the size range of 30-300 nm(Kusaka et al., 2014). In addition, nanoparticles within 5 nm often accumulate in the nucleus of cells, while that of 15-40 nm end up in the cytoplasm(Chakraborty et al., 2017). Overall, the GSPIONs are ideal for further development of therapeutic applications in the lung, aiming to reach deep alveoli, without by themselves inducing

inflammation.

Nanoparticles not only are useful for tumour ablation, but are also useful as imaging agents, although there is a significant gap in knowledge regarding organ-specific imaging. Magnetic resonance imaging of lung is limited due to the low density of H-protons in air and a relative lack of water. The problem can be avoided with 3D ultra-short echo time MR imaging. 3D UTE MRI adequately generated signal from lung parenchyma that was decreased by the presence of GSPIONs and showed that GSPIONs could be delivered and used as novel diagnostic agents due to their distribution into the alveolar spaces along with stratification within lobes. Some studies have reported reduced relaxivity of super-paramagnetic nanoparticles upon cellular uptake(Klug et al., 2010; Gossuin et al., 2009), but our functionalised glycine coated GSPIONs continue to reduce signal intensity 24 hour after administration when histology results suggest they are taken up by phagocytic cells. The results thus far demonstrate this non-invasive technique can determine GSPION distribution in the healthy lung. The results would be useful for diagnosis of respiratory diseases where emphysema and oedema are observed. In addition, our results demonstrate for the first time for glycine coated biodegradable nanoparticles, a volumetric differentiation of nanoparticle distribution when standardised to cardiac tissue, which can segregate their biodistribution depending on the signal intensity observed in the lung slices. Future studies may test the potential range of applications against diverse lung diseases including lung cancer, infectious diseases, asthma and COPD. For example, this differentiation may be useful in future applications for determining drug delivery, and for identifying lung-lobe specific targets in diseases such as asthma (where the upper airways and lobes are targeted) or COPD and lung fibrosis (where the lower lobes are affected)(van Rijt et al., 2014).

Our results using GSPIONs show them to be localized *invivo* within alveolar macrophages and neutrophils. It clearly indicates that cells responsible for pro-inflammatory cytokines secretion leading to pulmonary inflammation could be targeted using these GSPIONs. In addition, macrophages have elevated plasticity, and can be useful as therapeutic targets. For example, in a tumour micro-environment macrophages play a pro-tumoral role and are classified as tumour associated macrophages(Lichtenstein et al., 2010) which are directly associated with cancer (Chakraborty et al., 2018). Tumor associated macrophages

(TAMs) in the resting phase secrete immune-suppressive cytokine IL-10 while during activation by LPS, they secrete proinflammatory cytokines IL-1β, IL-6 and TNF. Successful interaction of our GSPIONs with alveolar macrophages is a suggestive indication that GSPION uptake by TAMs may also be developed as a tool to help inhibit malignant cell growth. This potential is supported by recent findings in lung adenocarcinoma, where uptake by alveolar macrophages of apoptotic drugs resulted in alveolar macrophage depletion leading to tumour reduction(Ponzoni et al., 2018). In other diseases such as COPD, characterized by increased alveolar macrophages leading to epithelial thickening and emphysema, the GSPIONs may be similarly useful in attenuating inflammatory conditions. The negligible resistance of GSPIONs which is similar to control (saline) leads to the use of these GSPIONs as immunomodulators ideal for clinical use in contrast to other nanoparticles(Kusaka et al., 2014). The lack of alteration of lung function after GSPIONs instillation can be attributed to ablation of alveolar macrophages and neutrophils as it did not elicit an increase in pro-inflammatory cytokines IL-1β, IL-6 and TNF. The unchanged pro-inflammatory cytokines and uptake by neutrophils and alveolar macrophages points out their significant use in therapies for respiratory diseases such as COPD and acute respiratory distress syndrome (ARDS). In regard to ARDS, an increased neutrophil inflammation is observed due to IL-33 being secreted by the neutrophils themselves and augmenting it by alveolar macrophages(Chakraborty et al., 2018). Uptake of our GSPIONs by neutrophils as well as macrophages indicates an additional potential use of these nanoparticles in abrogating neutrophilic influx in the alveolar space, preventing further inflammation and also combatting against the already present alveolar macrophages from expressing co-stimulatory molecules. Therefore, for therapeutic and diagnostic interventions, GSPIONs are a new potentially useful candidate complying with current pharmacotherapeutic considerations for use as pulmonary delivery agents targeting a cohort of immune cells relevant to multiple diseases.

7.5 Summary

In summary, we created GSPION nanoparticles preferentially taken up by neutrophils, and alveolar macrophages in the lung. These nanoparticles do not end up in liver, spleen or heart within 24h of our investigation and hence can be used for pulmonary delivery

as immunomodulators which can escape the first pass metabolism. The core of the GS-PIONs is crystalline with a size ideal for distribution into deep alveoli in the lung. In addition, the magnetic core is potentially useful for applications such as magnetic hyperthermia therapy. The core has magnetic resonance due to which we were able to utilize a short-echo time for imaging the lung. In-depth analysis pointed out that these GSPIONs are delivered to the lower lobes than the upper lobes. The GSPIONs suspended in glycine showed negligible resistance to breathing in comparison to controls and hence offering a useful formulation for targeting immune cells without provoking respiratory changes or inflammation, and hence supporting non-invasive imaging of the lung. Preferential uptake of the GSPIONs by alveolar macrophages and neutrophils suggests their use in targeting of these cells in therapeutic interventions in diseases involving these cells, such as in cancer, COPD, fibrosis and many infections. Furthermore, unaltered lung function by GSPIONs highlights their potential utility as lung delivery vehicles. The capability of these GSPIONs for clinical use across different aspects will govern the new therapeutic modality for both diagnostics (magnetic resonance imaging), therapeutics (targeted, cell-specific delivery and interaction), and perhaps also theranostics.

Chapter 8

Conclusion and Recommendations

8.1 Conclusions

I n this thesis, we addressed the need of developing an immunomodulator to attenuate airway inflammation, specifically acute respiratory distress syndrome (ARDS). One of the main contributions of our work is the use of the neutral, smallest amino acid glycine as an anti-inflammatory agent in attenuating airway inflammation including ARDS. We were able to develop glycine coated super-paramagnetic iron oxide nanoparticles for the use as immunomodulators capable of pulmonary delivery. In addition, to the immunomodulatory role, we demonstrated for the first time the use of glycine conjugated biodegradable SPIONs in magnetic resonance imaging of the lung. The method will be highly useful in clinical practice for diagnosis and treatment of respiratory diseases owing to limited contrast agents, techniques and water molecules available in the lung.

For the first aim, we investigated whether glycine alters the cell viability and affects the expression of co-stimulatory molecules across a range of concentration from 1 mM to 300 mM on BMDCs. Glycine did not affect cell viability up to 100 mM but slightly reduced cell viability at high concentrations of 200 and 300 mM. LPS increased the expression of co-stimulatory molecules CD40, CD80 and CD86 in compliance to literature (Zhou et al., 2012). We found that glycine reduced LPS induced activation markers (CD40, CD80 and CD86) at a concentration of 100 mM, and the effect was titratable up to baseline with glycine at a concentration of 300 mM. We also found that SHIP-1 is essential in mediating this effect. The role of SHIP-1 is involved in Akt/PI3K pathway, therefore, it is hypothesized that glycine mediated downregulation of activation markers is possibly down-modulated involving a SHIP-1 signalling inhibiting PI3k (see figure 4.1). In addition to the requirement of SHIP-1 we also found evidence of expression of a neuronal receptor (GlyR) on the lung especially on alveolar macrophages and monocytes. In similar context to Eynden and colleagues(Van Den Eynden et al., 2009) we also found GlyR expression on endothelial cells and alveolar macrophages and confirmed the expression to be true using positive control staining of mouse brain tissue (see Figure 4.10). As demonstrated in chapter 4 Figure 4.9, there is a sign of expression of the receptor on mice BMDCs, monocytes, alveolar macrophages (Figure 4.10C) and human PBMC subsets- $CD3^+$, $CD14^+$, $CD56^+$ (see Appendix Figure A.4). However, the functionality and molecular characteristics of the receptor still needs to be validated and is beyond the scope of this work.

For the second aim, we investigated the potential of glycine in reducing airway inflammation. We found glycine was able to reduce resistance to breathing caused by LPS and improved lung stiffness as well as several other parameters of lung function. In LPS induced mice, where LPS is administered intra-nasally, there is usually an increased airway resistance and decreased dynamic compliance. In a clinical setting, these results are useful for evaluating positive end-expiratory pressure (PEEP) for diagnosing and treatment of airway inflammatory diseases. In LPS sensitized mice, we found a surge of pro-inflammatory cytokines (IL-1β, IL-6, TNF-α) as anticipated. Glycine reduced the levels of these cytokines to baseline which correlates its anti-inflammatory role established in chapter 4. In addition, it makes our hypothesis clear that glycine has a role in preventing $NF - \kappa\beta$ to bind to DNA as $NF - \kappa\beta$ is required for production of these cytokines(Sheller et al., 2009; Lawrence, 2009; Jones et al., 2005). The induction of pro-inflammatory cytokine IL-1β and $NF - \kappa\beta$ resulted in neutrophil infiltration(Jones et al., 2005) along with increased alveolar macrophages showing their activation due to LPS. Glycine reduced and prevented further neutrophil influx preventing lung damage and reduced the number of alveolar macrophages. Interestingly, the reduced numbers of lymphocytes were brought to baseline by glycine inducing healing. In terms of the lung resorting to a healing state, the signs of collagen deposition consolidate that LPS and glycine (combined), increases collagen deposition whereas glycine itself does not induce collagen deposition.

For the third aim, to develop an immunomodulator capable of exerting an immediate as well as a sustaining anti-inflammatory effect, we developed glycine coated superparamagnetic iron oxide nanoparticles enclosed in glycine microparticles. The glycine coated SPIONs were used as theranostic agents to target the lung periphery, while the bigger glycine microparticles provided an immediate anti-inflammatory effect (as demonstrated in chapter 5 by reducing mucus producing goblet cells) and preventing mucociliary clearance. In addition, the size of the bigger glycine microparticles, together with their aerodynamic properties enabled their use as excipients comparable to Lactohale200^{TM}. The synthesized nanoparticles were characterised in terms of size, charge, stability, crystallinity, surface coating and their ability for uptake by lung immune cells were evaluated. We clearly demonstrated that glycine coated SPIONs were taken up by alveolar macrophages and neutrophils in the lung. In addition, we also found that

these particles do not end up in the liver, heart, kidney or spleen, making them useful immunomodulatory agents for clinical use. The glycine microparticles developed were spherical, cenospheric, monodisperse, porous with aerodynamic properties comparable to the commercial excipient Lactohale200^{TM}. With reference to our results in chapter 5, we therefore recommend the use of spray-dried glycine microparticles not only for their size and aerodynamic properties but for their anti-inflammatory and mucus abrogating role.

For the final aim, we demonstrated for the first time, the use of glycine coated SPI-ONS in magnetic resonance imaging of the lung. Using GSPIONs and 3D UTE MR imaging we developed a non-invasive lung imaging useful for clinical diagnosis of respiratory diseases. Our results demonstrated that GSPIONs are delivered more on the lower alveolar regions owing to its smaller size and can be used as good MR contrast agents. In addition, their residence time was longer (24 hours measured), successive imaging is possible without any surgical procedure. Owing to super-paramagnetic property of GSPION, the nanoparticles were useful as novel contrast agents and was beneficial for understanding the particle biodistribution after pulmonary delivery. The final aim of the thesis was to provide a proof of concept for the pulmonary delivery of the immunomodulators. We demonstrate the pulmonary delivery of glycine coated SPIONs and show that the aerodynamic properties, structure and features of the spray-dried glycine microparticles comply for as excipients (preventing mucociliary clearance) but not for delivery into the lung periphery.

8.2 Limitations and Future Recommendations

The results obtained in this work clearly demonstrates the ability of glycine in attenuating airway inflammation, along with several limitations. However, there are numerous questions which have been raised but left to be answered. Investigation of these questions would further enhance the understanding of glycines' role in attenuating airway inflammation. Considering the immunomodulatory role of glycine demonstrated in chapter 4, we need to focus on the glycine receptor and its role in mediating this effect. We had some insight that GlyR and SHIP-1 may play some role in mediating the anti-inflammatory

effect but is beyond the scope of this thesis. It is possible that glycine inhibits LPS mediated activation through a metabolic regulator such as mTOR(Katholnig et al., 2013). Macrophage activation through metabolic reprogramming is orchestrated by metabolites such as α ketoglutarate and is dependent on the amino acid glutamine (Liu, Wang, Li, Chao, Teav, Christen, Di Conza, Cheng, Chou, Vavakova, Muret, Debackere, Mazzone, Huang, Fendt, Ivanisevic and Ho, 2017). In a similar way affecting mTOR mediated response for down regulating inflammation has been possible with other amino acids such as leucine(Ananieva et al., 2016). Other possible pathways of inhibition could be through inhibition of $NF - \kappa\beta$ DNA binding. The presence of GlyR expression observed in the lung endothelial cells and alveolar macrophages clearly points out that there is a relation between glycine reducing the pro-inflammatory cytokines via inhibition of $NF - \kappa\beta$ pathway. In addition to GlyR mediated signalling the possible role and involvement of SHIP-1 and other mechanistic pathways needs to be explored in more detail. For better understanding and elucidation of glycine's role in the lung, we need to investigate its role in our ARDS model in SHIP$^{-/-}$ mice. It will enrich our knowledge of the pathway(s) through which glycine signals in the lung in attenuating inflammation. The established anti-inflammatory role of glycine was then used to investigate in an *in-vivo* model of airway inflammation.

To better understand the role of glycine in attenuating inflammation, it is recommended to use glycine in other models of airway inflammation. Models such as the OVA model of chronic inflammation or house dust mite (HDM) model of inflammation would provide useful information and insight in glycine's use in combatting chronic inflammation. Since, glycine has been found to reduce signs of emphysema, it is hypothesized that glycine may be useful in the treatment of COPD. Currently, the models available for COPD include active smoking of mice for a long period in order to induce emphysema in lungs. Glycine may act as a protective compound or could be useful to reverse emphysema in lung. We demonstrated signs of collagen deposition by LPS and glycine together, but, addressed it in an acute model. The deposition of collagen may increase with the increase of duration of LPS induced inflammation. Supplementary data showed in Appendix, points out the relationship between TGF-β in LPS+glycine group, which clearly suggests that glycine leads to lung healing. A thorough understanding of the pathway involved is therefore necessary. One of the limitations of this ARDS model, was intranasal glycine delivery. As a recommendation for chronic models requiring regular

glycine administration, nebulization of glycine is a good solution. In addition, FACS analysis of the different cells in the BAL with activation markers will yield an extensive knowledge of the exact phenotype of neutrophils, DCs, macrophages and lymphocytes in the lung. This would increase and consolidate our idea of the different roles of the various cells in mitigating this effect.

One of the best ways to deliver drugs is by pulmonary delivery as it escapes the first pass metabolism. In doing so, a significant amount of drug loss is prevented, and the dose can be calculated accurately. The sole idea for the development of an immunomodulator was to have a dual role upon administration in the lung. The capability of the immunomodulator was supposed to provide with an immediate and a sustained anti-inflammatory effect in the lung. Nanoparticles are capable of delivery to the lung and are well established. We synthesized glycine conjugated super-paramagnetic iron oxide nanoparticles as means of glycine delivery for a sustained effect. Iron oxide was chosen to impart biodegradability and its super-paramagnetism has been showed useful in chapter 7. The nanoparticles have been encapsulated in inhalable dry powder synthesized by spray drying glycine. The synthesized inhalable glycine microparticles have been demonstrated capable of pulmonary delivery by mechanical means using a NGI and evaluating its aerodynamic performance. It is a limitation that due to the extensiveness of this work we could not actually administer the spray dried glycine microspheres containing GSPIONs in models of ARDS. Therefore, it is recommended to use these GSPIONs in glycine microspheres in ARDS mice models and evaluate the immuneimprinting of these particles. The results will provide a deep insight into spray dried amino acid microspheres as DPI and would also answer the many questions associated with GSPIONs delivery in the lung.

Upon establishing GSPIONs as immunomodulators for pulmonary delivery of glycine, we resorted to understand it's biodistribution, interaction and tracking the nanoparticles in the lung. In addition, the core of the nanoparticles being super-paramagnetic and iron oxide helped us in identifying particle uptake by immune cells by histochemical analysis. The nanoparticles being super-paramagnetic has significant magnetic susceptibility and therefore we utilised this aspect for imaging the particles in the lung to determine biodistribution. In due course, using these biodegradable GSPIONs and 3D UTE MR imaging sequences, biodistribution of drugs can be targeted as well as lung impact could be measured. Due to the extensiveness of this work, we could not differentiate between

a healthy versus a diseased lung using these nanoparticles. As a recommendation, we propose the use of these GSPIONs for non-invasive MR imaging to identify patients with respiratory disease. This would open a new field for respirologists, assuring patient comfort and easier diagnosis of respiratory disease which was earlier not possible.

Awards, Scholarships and Conferences

The following awards and scholarships have been received in the course of this research work.

Awards

- People's choice Best Presentor award, for Oral Presentation in Nanobiotechnology Symposium 2016, organized by University of Western Australia, December 2016.

- Best Presentation award, for Oral Presentation in 6th Annual Monash University Chemical Engineering Conference in Melbourne, October 2016.

Scholarships and Travel Grants

- Travel Scholarship for the European Respiratory Society Congress (ERS 2018), Paris in September 2018, sponsored by Monash Post-Graduate Association (MPA).

- Travel Grant for the Post-Graduate Symposium by European Molecular Biology Limited (EMBL), Brisbane in November 2018, sponsored by EMBL, Australia.

- Co-funded Monash Graduate Scholarship and Monash International Postgraduate Research Scholarship, October 2015-April 2019, sponsored by Monash University.

- Invited Oral presentation at Pre-clinical imaging symposium, December 2018, organised by Monash Biomedical Imaging.

Conferences

- Polychromatic Panel Design Theory and Practical Workshops for Flow cytometry, organised by BD Biosciences, Melbourne in February 2016.

- Nanobiotechnology Symposium 2016, organised by University of Western Australia, Perth, in December 2016.

- BD Horizon^{TM} Global Tour, organised by BD Biosciences, Melbourne, in April 2017.

- European Respiratory Society Congress (ERS2018) in Paris, September 2018.

- Post-Graduate Symposium 2018, organised by European Molecular Biology Limited (EMBL), Australia, Brisbane, November 2018.

- Monash Biomedical Imaging symposium, organised by Monash Biomedical Imaging, Melbourne, in December 2018.

- Advancing the boundaries of High Parameter Flow Cytometry, BD Biosciences, Melbourne, in March 2019.

Miscallenous

- Chemical Engineering Post-Graduate Association (CEPA) 6th, 7th, 8th Annual-conference in October 2016, 2017, 2018.

- Cutting Edge Journal Club Presentation on High impact publications in the field of respiratory diseases, organised by Central Clinical School, Monash, twice a year from 2016-2019.

- Participated in Three-minute thesis competition organised by Central Clinical school in 2017, Department of Chemical Engineering in 2017, Monash University.

Appendix A
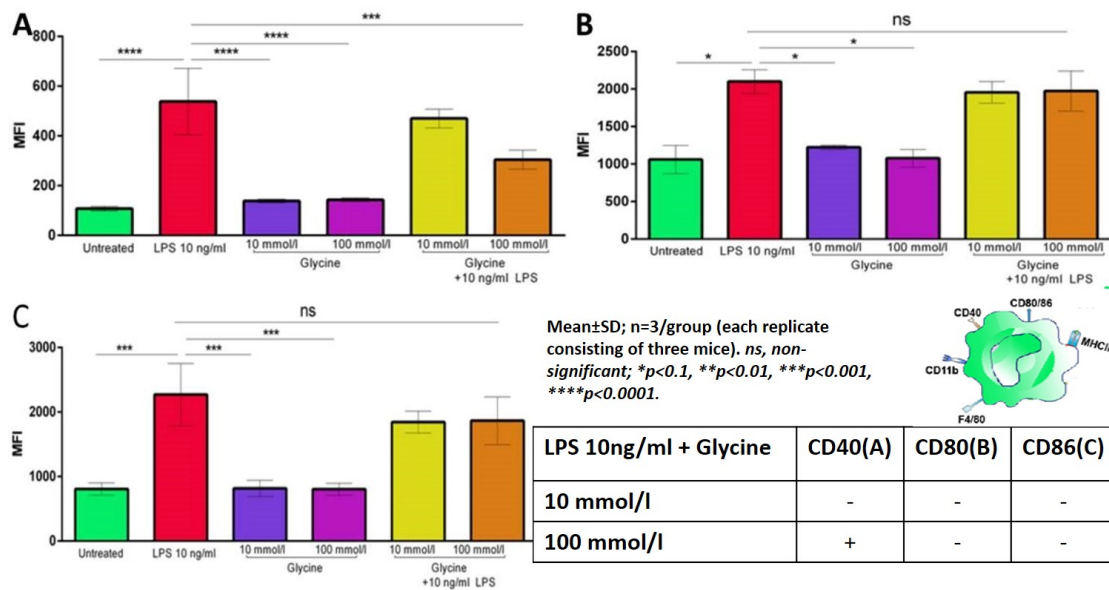
FIGURE A.1: **Glycine down regulates expression of LPS activated activation markers on Bone maroow Derived macrophages.** Naïve C57/BL6 mice bone marrow cells were cultured with GMCSF and LPS, glycine conditions added on day 5 of culture and harvested cells after 24 h. Untreated cells were control (shown in green). Effect on $CD11c^-MHCII^+GR1^-CD11b^+$ macrophages as per gating on Figure 4.5B expressing **(A).** CD40, **(B).** CD80 and **(C).** CD86; $Mean\pm$ SD; n=3/group (each replicate consisting of three mice). ns, non-significant; $*p < 0.1, **p < 0.01, ***p < 0.001, ****p < 0.0001$
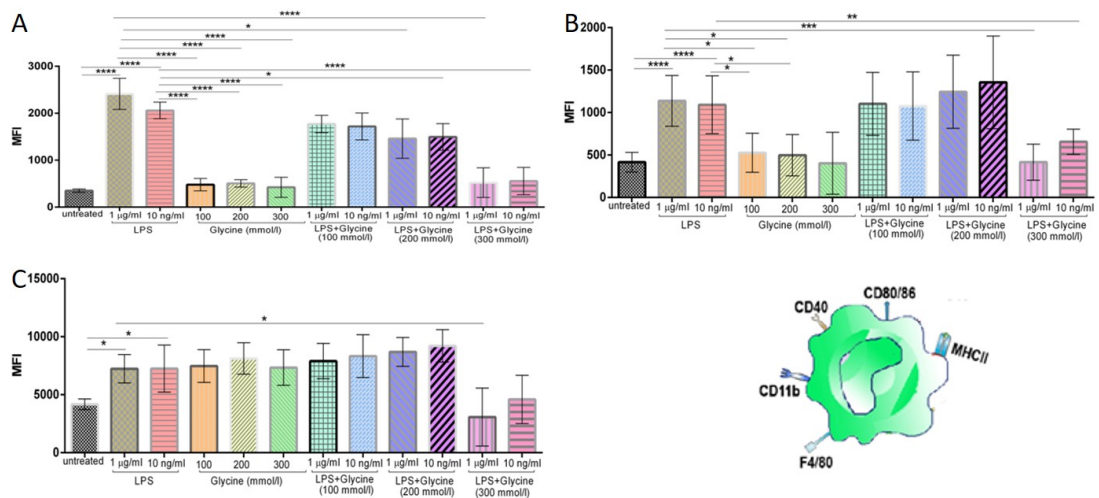
FIGURE A.2: **A higher glycine down regulates expression of LPS mediated activation markers on Bone marrow Derived macrophages.** Naïve C57/BL6 mice bone marrow cells were cultured with GMCSF and LPS, glycine conditions added on day 6 of culture and harvested cells after 24 h. Untreated cells were used as control (shown in green). Effect on $CD11c^-MHCII^+GR1^-CD11b^+$ macrophages as per gating on Figure 4.5B expressing **(A).** CD40, **(B).** CD80 and **(C).** CD86; $Mean\pm$ SD; n=3/group (each replicate consisting of three mice). ns, non-significant; $*p < 0.1, **p < 0.01, ***p < 0.001, ****p < 0.0001$
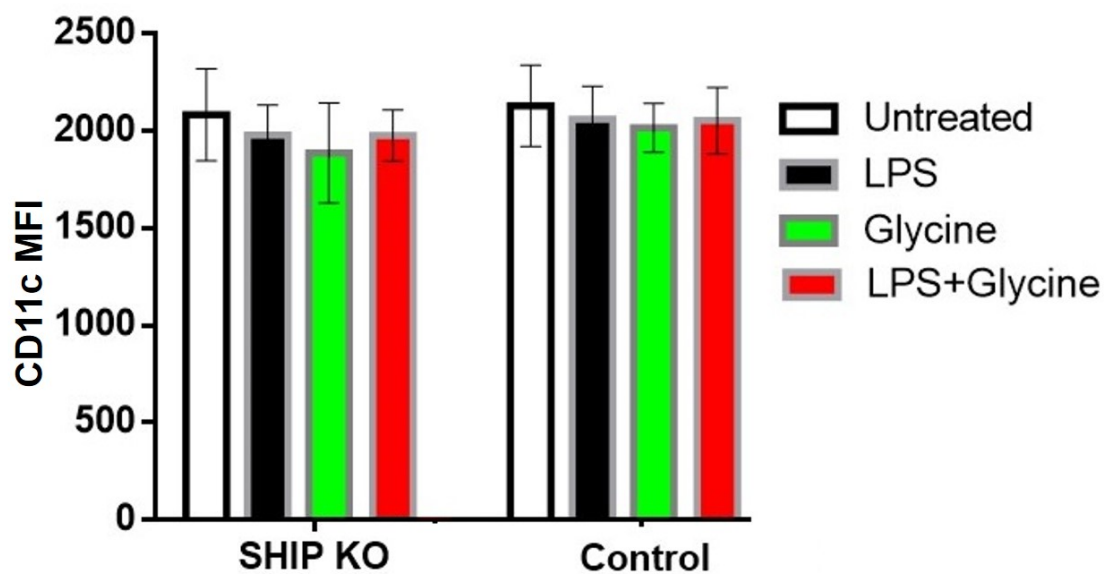
FIGURE A.3: **CD11c expression remains unchanged on Bone marrow derived cells from both WT and SHIP$^{-/-}$ mice upon addition of different conditions.** To confirm the effect of glycine and LPS co-administered and alone, we measured the MFI of the marker CD11c as its expression forms the backbone for gating CD11c$^+$ DCs and CD11c$^-$ macrophages on both WT and SHIP$^{-/-}$ mice. We found the expression unchanged even upon addition of different experimental conditions on both mice.

Presence of Glycine receptor in Peripheral Blood Mononuclear Cells(PBMCs)

We investigated the expression of GlyR on human peripheral blood mononuclear cells (PBMCs) to validate the findings by Eynden and colleagues(Van Den Eynden et al., 2009).PBMCs were gated as lymphocytes based on their Forward and side scatter. The lymphocytes were further gated into 3 subsets CD3$^+$(T cells), CD14$^+$(Monocytes), CD56$^+$(NK cells) (Figure A.4A-D). Glycine receptor expression(red) was validated with respect to isotype(blue). The receptor expression was compared in different cells present under lymphocytes(graph-Figure A.4A-C).
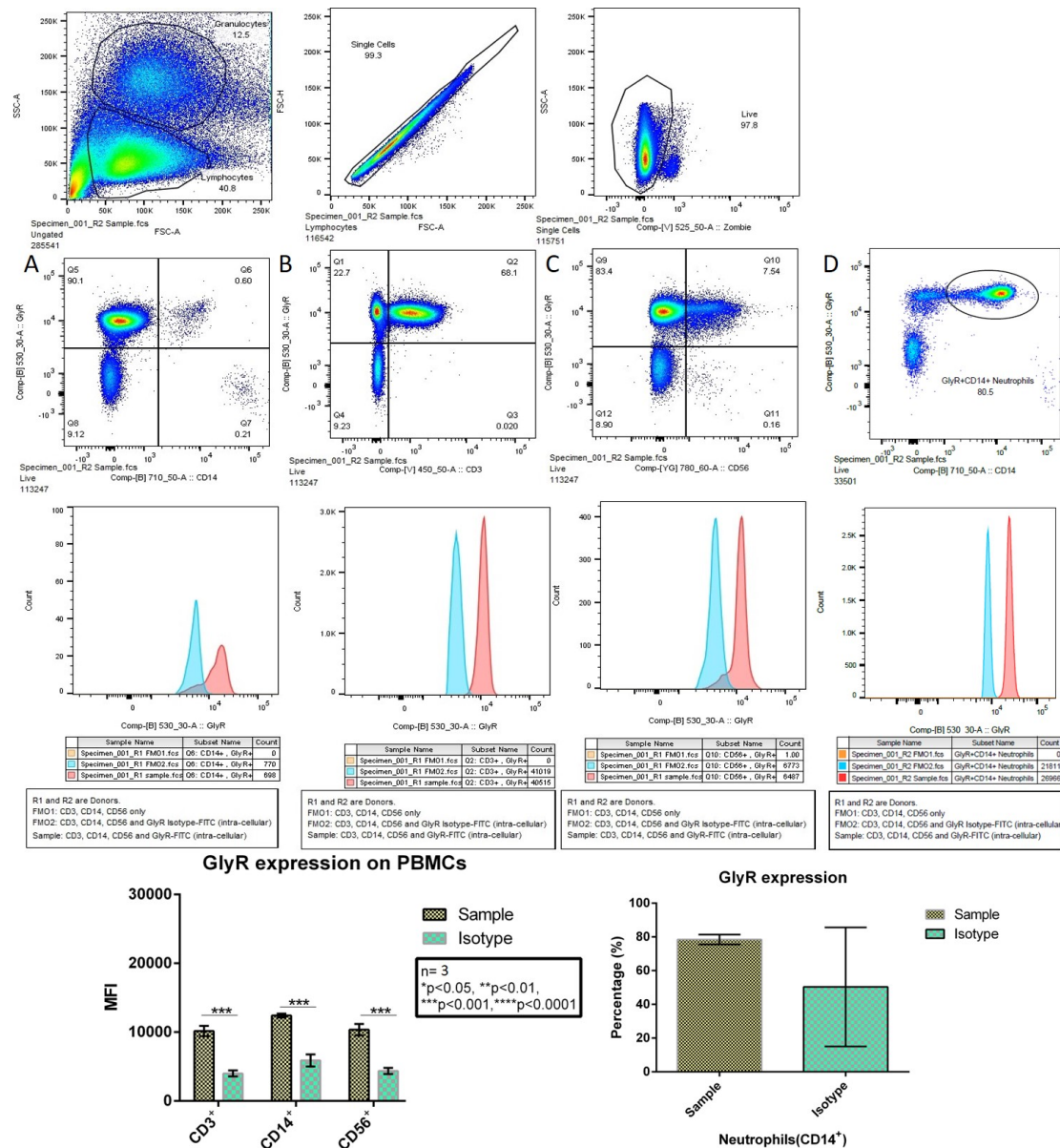
FIGURE A.4: **Glycine receptor expression on human peripheral blood mononuclear cells (PBMCs)**. PBMCs were isolated from three donors and was stained for CD3, CD14 and CD56 vs Glycine receptor (GlyR) expression. Glycine receptor(showed in red) was validated against an isotype(showed in blue) of the same antibody. A small shift was observed from the isotype. Cells were gated on the basis of FSC-A and SSC-A for lymphocytes and neutrophils excluding debris. This was followed by a doublet exclusion and gating on live cells (zombie-selection). Glycine receptor vs. the different markers were gated in quadrant plots. Flow panels: **(A).** CD14$^+$ monocytes, **(B).** CD3$^+$ T cells, **(C).** CD56$^+$ NK cells and **(D).** CD14$^+$ Neutrophils. The relative expression (MFI) was plot against the isotype.

Appendix B

For confirming expression of pro-inflammatory cytokines by immunohistochemical staining on lung sections as positive, the same antibody was used to stain mice organ sections which are positive as per the antibody MSDS. The isotype of the antibody at the same dilution was used to identify background (if any) and was also stained in the same tissue section to designate it as the negative control (Figure B.1). Pro-inflammatory cytokines such as IL-1β(1:1500, bs-0812R, Bioss antibodies) with positive control kidney, IL-6 (1:2000, E-AB-40021, Elabscience) with positive control heart and TNF-α (1:250, ab6671, Abcam) with positive control heart were stained with the primary antibodies and detected as outlined in chapter 3.10 and counterstained with hematoxylin. For isotype control IgG was used for all the pro-inflammatory cytokines but at the same concentration as that of the positive control.
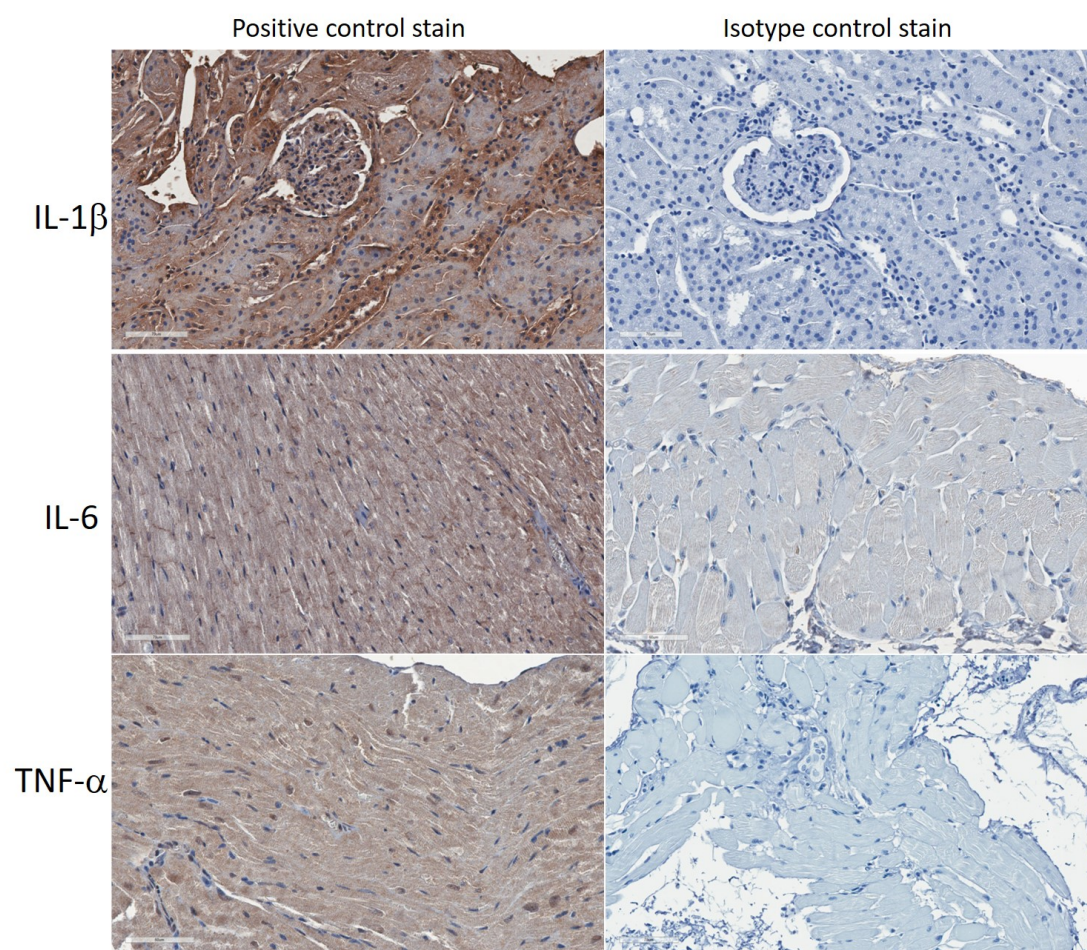
FIGURE B.1: **Expression of pro-inflammatory cytokines as positive control on tissues other than lung**. IL-1β, IL-6 and TNF-α was stained on kidney and heart tissues respectively as positive control for their expression. IgG was used as isotype control and served to determine the background and negative stain.

Appendix C

Synthesis of Glycine micro-carriers using Buchi 190 spray dryer

Initially glycine microparticles were synthesized by spray drying using a Buchi 190 spray dyer, with feed concentration 18 wt.% (Figure C.1B) and 8 wt.% (Figure C.1C, D). The dryer produced non-uniform, dense, microparticles of 10 ± 4 μm size, using both feed concentration of 18 wt.% glycine (Figure C.1B) and 8 wt.% glycine (Figure C.1C,1-3). These particles were relatively dense and exhibit large discrepancy in their shape from pyramidal to random shapes (Figure C.1B,2-3). Ideally, this particle size is suitable for pulmonary delivery. But, they are not uniform and hence the loading can vary, which could result in the delivery of uneven dose.
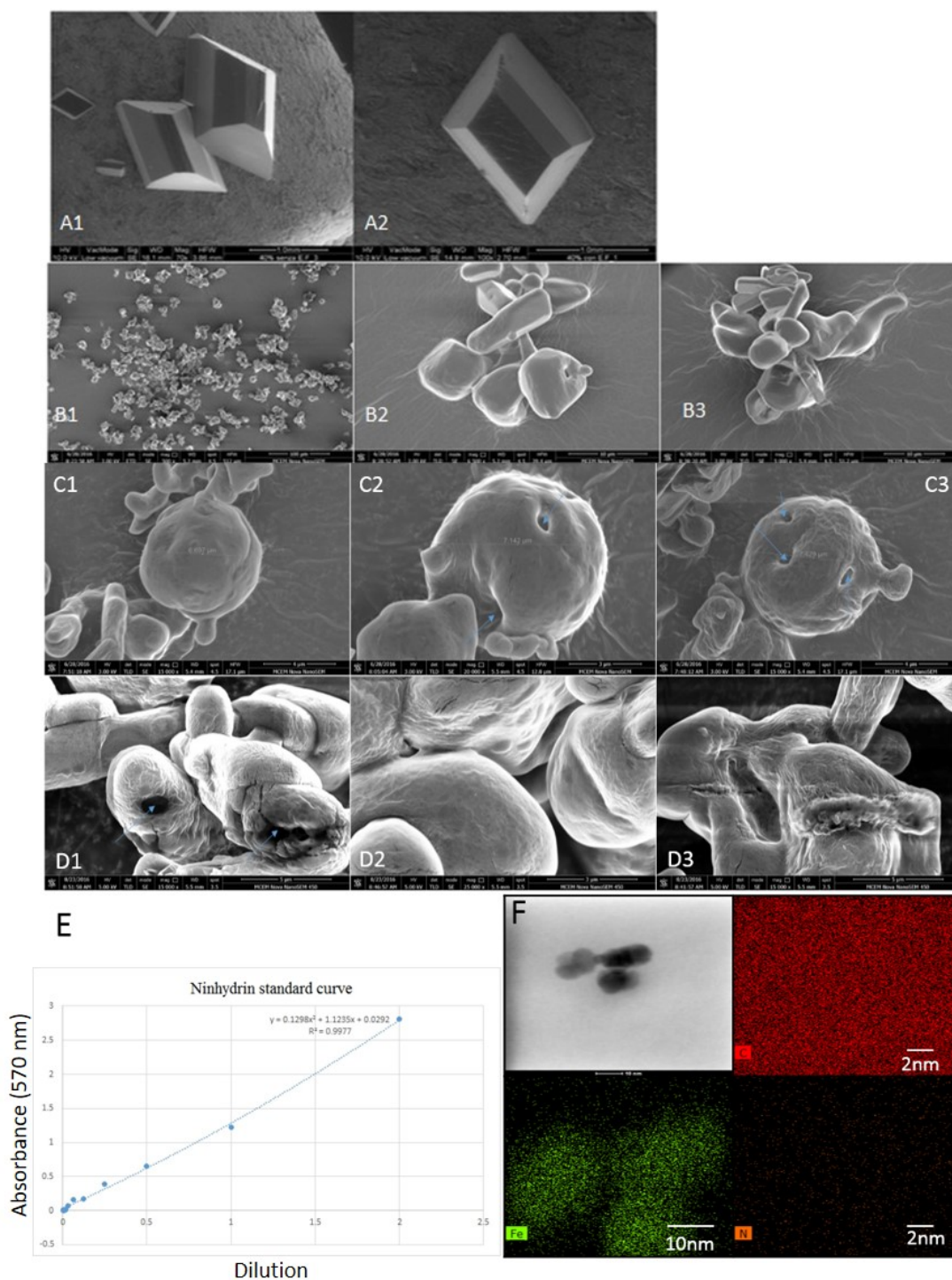
FIGURE C.1: **Microcarriers produced in Buchi 190 spray dryer and glycine coating on GSPION**. **(A).** Commercially available glycine powder showing bipyramidal shape and 450 μm size; **(B).** spray-dried glycine micro-carriers with 18wt.% glycine feed concentration showing random shape and dense morphology; **(C).** Spray-dried glycine micro-carriers with 8 wt.% glycine feed concentration showing random shape with pores (showed by arrows); **(D).** High-resolution SEM images of 8 wt.4% glycine feed solution spray dried using Buchi 190 showing dense structure without internal pores; **(E).** Ninhydrin standard curve to determine glycine concentration; **(F).** HRTEM-coupled with EDX to determine coating of glycine showing Fe, N(from glycine in a single particle at 2 nm) and carbon(single particle at 2 nm)
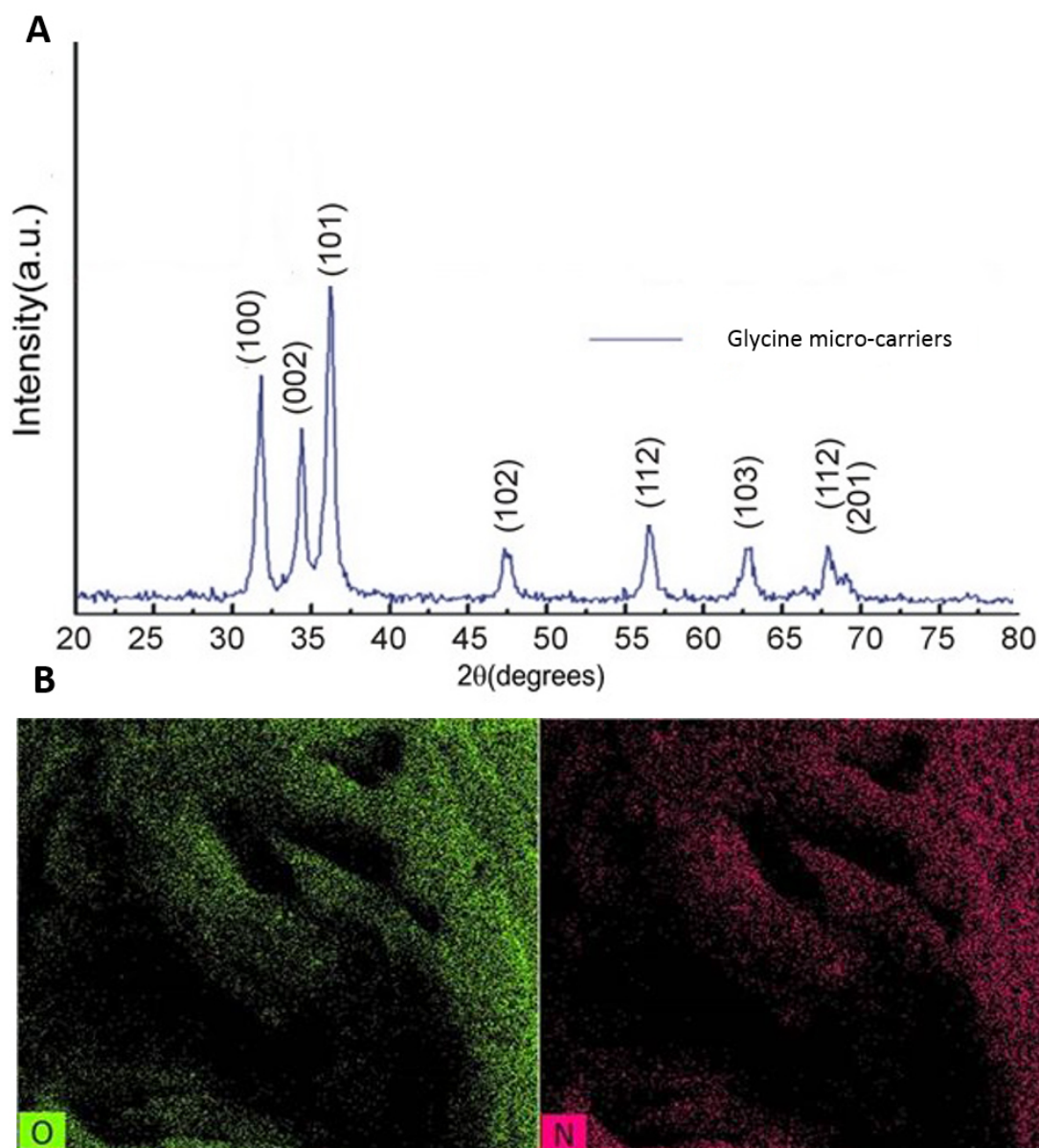
FIGURE C.2: **Glycine X-Ray diffraction spectra (XRD) and map of Energy dispersive X-Ray (EDX) of oxygen and nitrogen in glycine**. **(A).** XRD spectra with signature peaks at (100), (002) and (101) of spray-dried glycine micro-carriers showing crystallinity of the synthesized microcarriers; **(B).** High resolution SEM coupled with EDX for mapping oxygen and nitrogen on surface of the spray dried glycine microcarriers.
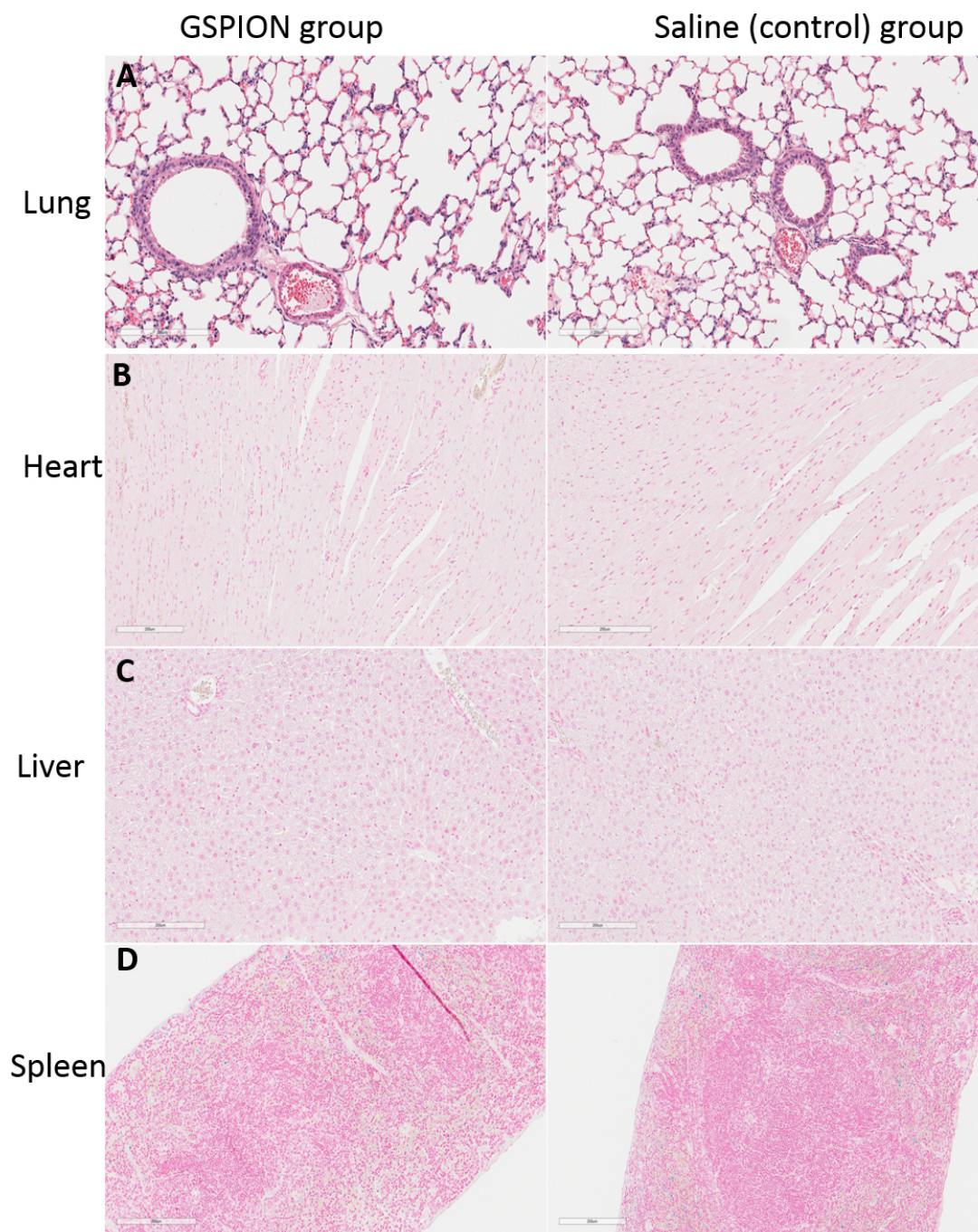
FIGURE C.3: **H and E staining of lung tissue showing no damage and Perls prussian blue counterstained with nuclear fast red showing absence of GS-PIONs in different tissues**. **(A).** Hematoxylin and Eosin staining of lung sections in GSPION and saline sensitized group showing no damage to lung parenchyma or the airway; **(B).** Perl's Prussian blue counterstained with nuclear fast red in heart sections of mice sensitized with GSPIONs and saline showing no deposition of GSPIONs in heart; **(C).** Perl's Prussian blue counterstained with nuclear fast red in liver sections of mice sensitized with GSPIONs and saline showing no deposition of GSPIONs in liver; **(D).** Perl's Prussian blue counterstained with nuclear fast red of spleen section. Spleen is a positive control for Perl's Prussian blue stain as red blood cells are broken down in spleen releasing haemoglobin which has iron. The few blue stains observed are in both the GPSION and saline groups. This confirms the positive staining of the stain and the ability to stain for GSPIONs in the lung.

TABLE 1: Morphometry analysis of Glycine micro-carriers and Lactohale200^{TM} for three representative particles per sample.

Sample	Particle Z-axis position	Volume (μm³)	Equivalent spherical diameter (μm)	Porosity(%)
	460-555	305227.401	BD 83.55	29.45
Glycine microcarriers	456-556	271511.45	80.45	29.7
	500-598	295580.39	82.66	29.2
	393-524	495553.36	98.2	28.7
Lactohale200^{TM}	419-540	523816.03	100.03	29.44
	415-536	537571.69	100.9	29.38

TABLE 2: Elemental percentage composition of C,H and N

Sample	%N	%C	%H
Glycine coated SPION	19.10	33.15	6.94
	19.22	33.16	6.94
Pure Glycine	18.38	32.04	6.81
	18.40	31.76	6.68

integrate (6a^2N)/14 dadN a from 4.5 to 12, N from 18.39 to

Definite integral:

$$\int_{18.39}^{22.61} \int_{4.5}^{12} \frac{6a^2 N}{14} \, da \, dN = 20\,229.4$$

© Wolfram Alpha LLC—A Wolfram Research Company. Use and redistribution subject to Wolfram|Alpha TOU at wolfram.com/termsofuse
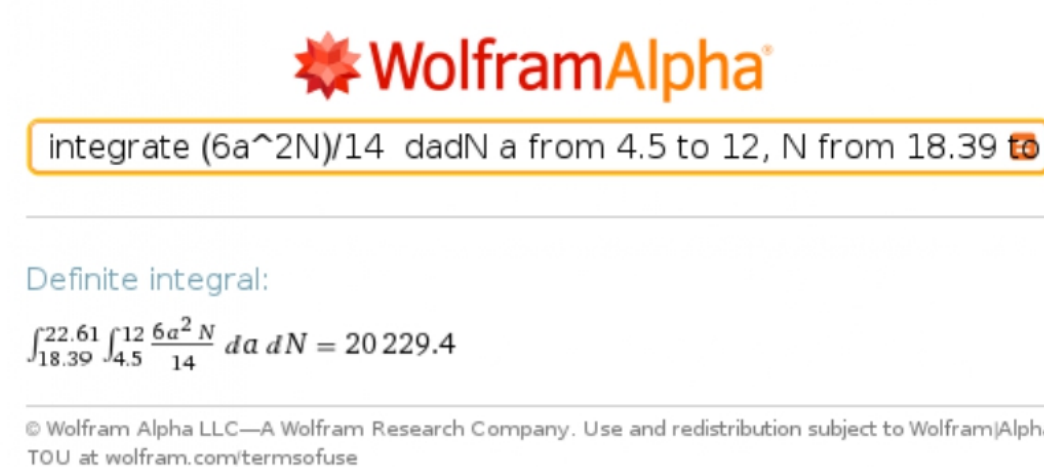
FIGURE C.4: **Calculation for glycine conjugation on SPIONs**. Wolfram Alpha$^{\circledR}$ was used to determine the number of glycine molecules conjuagted per nanoparticle.

Appendix D

Amino Acid Functionalized Inorganic Nanoparticles as Cutting-Edge Therapeutic and Diagnostic Agents

Amlan Chakraborty,[†,‡] Jennifer C. Boer,[‡] Cordelia Selomulya,[†] and Magdalena Plebanski*[,§,‡]

[†]Department of Chemical Engineering and [§]Monash Institute of Medical Engineering, Monash University, Clayton, Victoria 3800, Australia

[‡]Department of Immunology and Pathology, Central Clinical School, Monash University, Melbourne, Victoria 3004, Australia

ABSTRACT: The field of medical diagnostics and therapeutics is being revolutionized by nanotechnology, from targeted drug delivery to cancer immunotherapy. Inorganic nanoparticles are widely used, albeit problems with agglutination, cytotoxicity, free radical generation, and instability in some biological environments limits their utility. Conjugation of biomolecules such as peptides to the surface of nanoparticles can mitigate such problems, as well as confer specialized theranostic (therapeutic and/or diagnostic) properties, useful across biomedical applications such as vaccines, drug delivery, and *in vivo* imaging. Coating with amino acids, rather than peptides, offers further a highly cost-effective approach (due to their ease of purification and availability), but is currently an underutilized way to decrease toxicity and enhance stability. Amino acid molecules are small (<200 Da) and have both positive and negative charge groups (zwitterionic) facilitating charge-specific molecule binding. Additionally, amino acids exert by themselves some useful biological functions, with antibacterial and viability enhancing properties (for eukaryotic cells). Overall particle size, nanoparticle core, and the specific amino acid used to functionalize their surface influence their biodistribution, and their effects on host immunity. In this review, we provide for the first time an overview of this emerging field, and identify gaps in knowledge for future research.
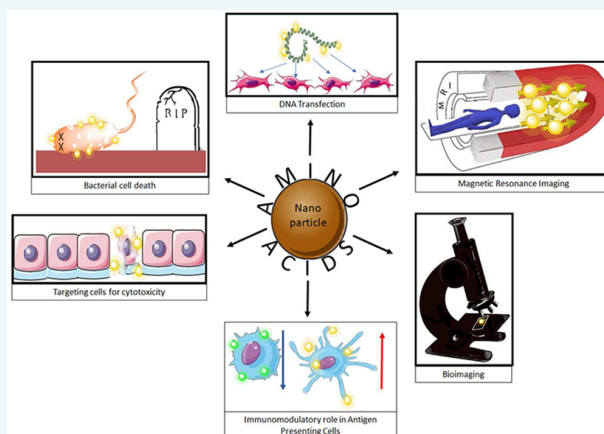
1. INTRODUCTION

Historically nanoparticles have been studied because of their unique chemical and physical properties. They have been classified depending on shape as rods, shells, dots, sheets, and composites.[1−5] The use of nanoparticles is revolutionizing many industries such as paints[6] and solar cells[7] but is yet to be fully exploited for theranostic applications. Concerns about their safety, and optimizing stable attachment of biologically relevant molecules to these nanoparticles, are limiting rapid progress. One of the most important problems associated with the use of some commonly used pristine metal nanoparticles is the production of reactive oxygen species (ROS) from the inorganic core.[8,9] Specifically, iron oxide nanoparticles form ROS which leads to lipid peroxidation and DNA damage.[9] Nanoparticle toxicity can be sometimes further related to particle size. For example, metallic bulk gold is inert, but at the nanoscale range (<25 nm) it exhibits catalytic properties useful for carbon monoxide oxidation.[10] In addition due to their toxicity to cancer cells *in vitro*,[11] gold nanoparticles have been used to treat cancer cells by apoptosis.[12] However, the toxic effect of the particles is not strictly limited to cancer cells, but can also affect other nonmalignant cells, in some cases causing damage to tissue.[13] For example, exposure to carbon nano-tubes[14,15] and carbon black[16,17] nanoparticles <100 nm in the lung exacerbates asthma. Also, fine-sized particles of TiO_2,[18] gold,[11,12,19] and SiO_2[20] in the size range 100−2500 nm show size-dependent toxicity for mammalian cell lines.

Particle size is also important for cellular uptake. Antigen presenting cells (APC) of the immune system, and specifically dendritic cells (DC) and macrophages, are highly capable of taking up nanoparticles and microparticles from 5 nm to 10,000 nm.[21−26] Other physical aspects like negative charge,[27,28] peptide conjugation,[29] and alternating hydrophilic−hydrophobic ligands[30] alter nanoparticle uptake by diverse host cell types. Aside from influencing cellular uptake, particle size also affects their biodistribution into major organs such as liver, kidney, spleen, and lung. Indeed particles with size less than 5 nm are normally cleared by the kidney,[31] while larger particles around usually 50−100 nm end up in the liver[32] and particles over 2000 nm tend to accumulate in the spleen.[33] Furthermore,
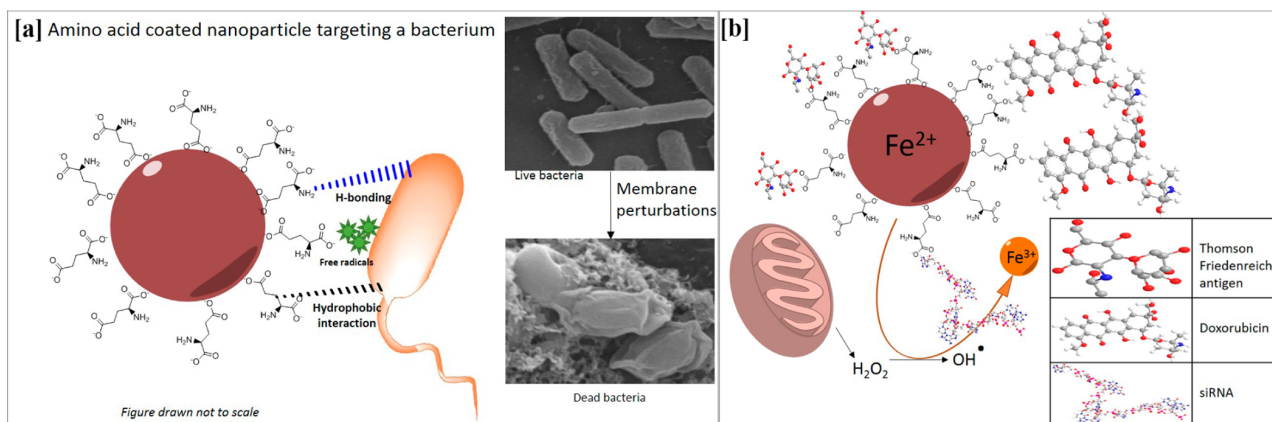
Figure 1. (a) Amino acid conjugated nanoparticles showing different interactions with bacteria. The amino acid conjugated to the nanoparticle can interact by hydrogen bonding between the (N) of amine in amino acid and (O) of the cell surface carboxyl group. Hydrophobic interaction between carbon chains of amino acid and a methyl group on the bacterial cell wall. These interactions can lead to free radical generation which can cause membrane perturbations (pores in the membrane). Due to perturbations, there is oozing out of the bacterial cytoplasm leading the cell to death due to loss of proteins, nucleic acids, and cell structural rigidity. (b) Antigen, drug conjugated to amino acid coated nanoparticles. The particles can conjugate the TF antigen, therapeutic siRNA, and the drug doxorubicin. The cellular mitochondrion releases hydrogen peroxide which by fentons reaction oxidizes iron(II) to iron(III) leading to a hydroxyl free radical generation. These free radicals and reactive oxygen species induce apoptosis to cancer cells by activation of caspase 8 and 9. Delivery of siRNA and doxorubicin by using these nanoparticles as vehicles has been found successful in delivering the payload which can induce apoptosis selectively in cancer cells.

micrometer-sized particles (2−5 μm) end up in lung capillaries[34−36] and smaller particles (<100 nm) end up in kidneys although coatings on particles could hinder the excretion process.[37] Other than particle size, another critical factor for nanoparticles is their stability inside the body. Since nanoparticles are in the colloidal range, their stability is dependent on a range of factors with zeta-potential being the most important. An efficient nanoparticle *in vivo* should not aggregate with serum proteins and antibodies in the blood[38,39] or evade uptake by antigen presenting cells[22] and finally there should be enough circulation time for the particles to move inside the body.[40] Coatings with biocompatible polymers (such as dextran), poly(ethylene glycol) (PEG), and amino acids can improve their circulation and prevent them aggregating inside the body. Therefore, it is not enough to limit the use of nanoparticles *in vitro* in physiological pH; to evaluate their stability, a dynamic media susceptible to rapid pH change is necessary.

Functional groups such as amino,[41] methyl,[42,41] carboxy,[43] citrate,[44] and guanidine[45] are used to functionalize nanoparticles to impart special functional properties. The single amino acids offer both an amino and a carboxy-terminal for conjugation of important biomolecules. They also provide higher biocompatibility[9] and are designed to overcome some of the challenges associated with size, biodistribution, interaction with immune cells, and induction of inflammation.[9,46−49] The conjugation paradigm uses chemical processes analogous to peptide conjugation utilizing 1-ethyl-3-(3-(dimethylamino)-propyl) carbodiimide (EDC)[50] chemistry or directly with the carboxyl group. The reaction involves an exposed carboxyl group on the surface of the nanoparticle to which EDC reacts to form an ester. This ester intermediate is then attacked by a nucleophile, which is the amino acid to be conjugated. The amino acid is conjugated at the amino terminal and carboxyl group exposed at the surface. Other than using EDC, a spacer molecule of the silane family like (3-glycidyloxypropyl) trimethoxysilane (GPTMS)[51,52] or (3-aminopropyl) trimethoxysilane can be used to conjugate amino acids. Direct

conjugation of amino acids to nanoparticles such as iron oxide[53] has been demonstrated by conjugating the amino acid at the time of the nanoparticle formation at a higher reducing temperature.

The amino acid conjugated nanoparticles are promising as theranostic agents. To the best of our knowledge, they have been used in fabricating biosensors, and for applications such as *in vivo* imaging as contrast agents, drug delivery, antimicrobial agents, and cancer therapy. However, these particles are still vastly underutilized clinically. There are multiple reasons behind their limited usage. One of them being the lack of knowledge on their biodistribution and excretion, as demonstrated by the heavy metal conjugated with amino acids[54] and the MR contrasting agents.[55] The high surface area to volume ratio of amino acid conjugated nanoparticles offers cheap and efficient surface functionalization alternatives to peptides. In this review, we will critically investigate the reported applications of amino acid conjugated nanoparticles in various fields of medical science, and identify the gaps in knowledge, as well as review the impact of critical factors such as toxicity, pro-inflammatory properties and biodistribution, on their *in vivo* behavior and potential clinical applicability.

2. RECENT DEVELOPMENTS OF AMINO ACID FUNCTIONALIZED NANOPARTICLES AS ANTIMICROBIAL AGENTS

The most common concern when introducing medical devices or nanotechnology based theranostics in a clinical scenario is potential contamination leading to sepsis. In this context several types of amino acid modified nanoparticles such as iron oxide,[56] gold,[47] and titanium dioxide[57] nanoparticles could be very useful as they have demonstrated antimicrobial properties. These particles have a metallic core with the amino acid conjugated to the surface, which interact by hydrophobic and hydrogen bonding with the bacterial cell wall (Figure 1a). The metallic core liberates free radicals, which delineates in part how their antiseptic properties operate. Other excellent

Table 1. Amino Acid Conjugated Nanoparticles and the Bacteria They Target/Capture/Kill

nanoparticle core	amino acid conjugated	bacterial gram stain	bacteria target/capture/killed	ref
Iron oxide	Lysine, arginine	Positive	*Bacillis subtilis*	56
		Negative	*Escherichia coli* 15597	
	Glutamate	Negative	*E. coli*	9
Gold	Phenylalanine, leucine	Negative	*Streptococcus aureus, Bacillis subtilis*	47
		Negative	*E. coli, Pseudomonas aurgenosa*	
Titanium dioxide	Glycine	Negative	*E. coli*	57
Silver	Tyrosine, tryptophan	Positive	*Listeria monocytogenes*	48
		Negative	*E. coli*	

antibacterial agents are N-doped carbon nanosheets[1] and to a lesser extent graphene oxide sheets, but the cytotoxicity of such compounds has not been addressed so far on human cells.

When using amino acid conjugated nanoparticles, the isoelectric point is an important aspect that defines their stability and capability to interact with bacteria. Gram-positive and Gram-negative bacteria have their isoelectric point between pH 1.5 to 4.5 due to the presence of ionized phosphoryl and carboxylate group on their cell walls. In an early study, positively charged lysine and arginine conjugated iron oxide nanoparticle could capture both Gram-positive and -negative bacteria.[56] More recently, negatively charged glutamate coated nanoparticles inhibited the growth of Gram-negative *E. coli*.[9] To understand the bacterial growth inhibition, positively charged amino acid(lysine) coated iron oxide nanoparticles were used at pH 6.[56] At pH 6, lysine has a positive charge with its isoelectric point at 9.74. In these conditions, multiple interactions can be responsible for the adsorption of the particles, e.g., hydrogen bonding between the nitrogen of amine group in the amino acids and the oxygen of the cell surface carboxyl group (Figure 1a). There is also a chance of hydrophobic interaction between carbon chains of amino acids with methyl groups on the bacterial surface. Therefore, the charge on the amino acid may play an essential role in the interaction of the nanoparticles with the bacterial cell wall. However, the negatively charged bacterial cell wall would be repulsive to the particles coated with negatively charged glutamate.[9] It is, therefore, questionable how the bacterial cell wall interacted with the particles despite being repulsive. Overall the binding of the above-mentioned amino acid conjugated nanoparticles to bacteria has a bactericidal effect irrespective of their cell wall properties (Table 1), benchmarked using the minimum inhibitory concentration (MIC). The MIC of the particles was found to be 128 μg/mL in comparison to 8 μg/mL of commercial antibiotic cefaclor. This may have resulted in limiting the media for bacterial growth. In addition, glutamate is known for its antibacterial properties.[58] Determination of MIC value on multiple replicates is subjected to measurement errors. Development of assay based experiments such as using resazurin[59] could support the hypothesis. In addition, nanoparticles such as iron oxide nanoparticles aggregate[60] readily when water dries in the environment. Soft agar is porous and the porosity depends on the concentration of agar used for polymerization of the matrix. The polymerization occurs between agar and water leading to the solidification of the matrix with pores. Diffusion of the antibiotic through the pores is responsible for the bacterial killing. In the case of nanoparticles it is not possible for the particles to migrate and is therefore questionable. The cellular cytotoxicity of these particles[9] is discussed in the next section. The nanoparticles conjugated with amino acids are therefore able to target, capture, and kill bacteria (Table 1).

Phenylalanine and leucine have been utilized to construct cyclic synthetic peptides which then were conjugated to gold nanoparticles.[47] When these particles were used against Gram-positive bacteria, membrane depolarization (cytoplasmic efflux) and perturbations (morphological changes) were observed (Figure 1a). Similar effects of antibacterial activity of glycine modified titania nanoparticles[57] had been seen against *E. coli*. These nanoparticles irradiated in the blue wavelength may generate free radicals and/or oxidizing species. We think it is related to N-doping[61] by glycine causing bacterial cell death (Figure 1a). It is interesting to note that glycine also shows antibacterial properties.[62] However, the activity of these particles was not observed in the green wavelength which could be due to the production of oxygen singlets at a low energy blue irradiation.[63] Further experiments with white light are essential before drawing a conclusion of the antibacterial behavior of such neutral amino acid coated nanoparticles.
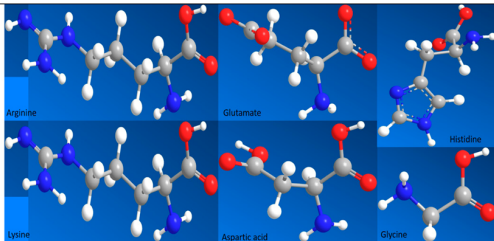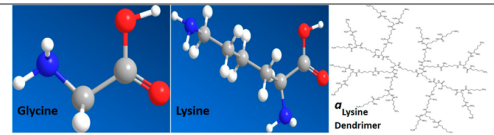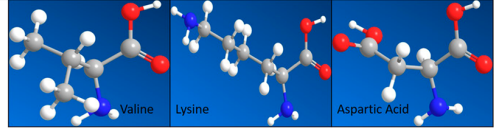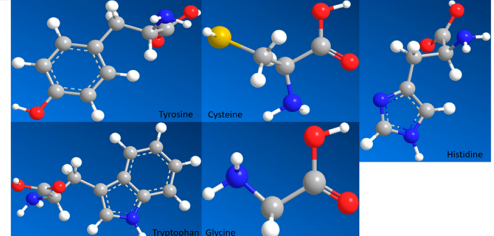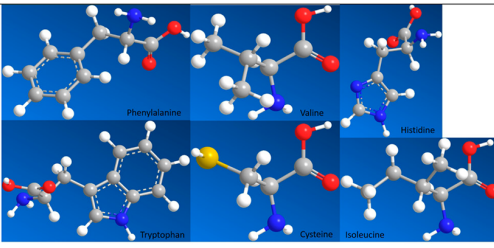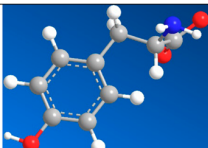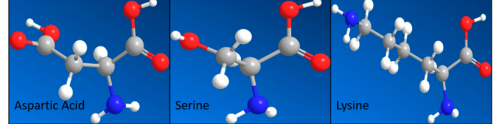
In one study, silver nanoparticles were modified with aromatic amino acids tyrosine and tryptophan[48] to test their antibacterial property. It was observed that the MIC of these particles was significantly low in comparison to pristine silver nanoparticles upon treatment to both Gram-positive and negative bacterium. However, the authors claimed that the antibacterial activity of the particles was due to silver cations penetrating the cell, but it is known that both tyrosine[64] and tryptophan[65] are antibacterial. The amino acids may interact with the bacterial cell wall by their phosphorus or sulfur molecules leading to morphological and metabolic changes. To the best of our knowledge, the plausible reason could be the generation of free radicals and hydrophobic interaction of the aromatic ring of the amino acid (Table 2) with the methyl group on the bacterial surface. It is, therefore, apparent that the amino acid conjugated to the particle surface is the critical element underlying the ability of nanoparticles to exert antibacterial behavior. We suggest the use of these nanoparticles to treat antibiotic resistant bacteria. Antimicrobial resistance is a huge area and is outside the scope of this review, but for recent developments one may refer to Singer and colleagues,[66] Allahverdiyev and colleagues,[67] Anderson, and Hughes.[68]

3. RAPID INTERNALIZATION OF AMINO ACID CONJUGATED NANOPARTICLES INDUCES APOPTOSIS

There are different approaches toward cancer treatment although the available therapies have significant side-effects like loss of hair, inflammation, and the harming of normal healthy cells. Current progress aims to translate effective molecular candidates for use in the clinic.

Amino acids serine and threonine have been conjugated to gold nanoparticles,[69] and this scaffold is used to indirectly

Table 2. Nanoparticle Core Properties and Quantitative Structure Activity Relationship (QSAR) of the Conjugated Amino Acids Side Chain Descriptors[b]

Nanoparticle core	Core properties	Structure of amino acid conjugated	QSAR[76]	
			Electronic Charge Index (ECI)	Isotropic Surface Area (ISA)
Iron oxide	Paramagnetic, biodegradable,		Lysine-0.53 Arginine-1.69 Glutamate-1.31 Glycine-0.02 Histidine-0.56 Aspartic Acid-1.25	Lysine-102.78 Arginine-52.98 Glutamate-30.19 Glycine-19.93 Histidine-87.38 Aspartic Acid-18.46
Gold	Surface plasmon resonance (SPR), hyperthermia, catalyst		Glycine-0.02 Lysine-0.53	Glycine-19.93 Lysine-102.78
Selenium	Antioxidant, antibacterial, semiconductor		Valine-0.07 Lysine-0.53 Aspartic acid-1.25	Valine-120.91 Lysine-102.78 Aspartic acid-18.46
Silver	SPR, antibacterial properties, thermal and electrical conductivity, metal enhanced fluorescence (MEF), surface enhanced Raman Scattering (SERS)		Tyrosine-0.72 Tryptophan-1.08 Glycine-0.02 Histidine-0.56 Cysteine-0.15	Tyrosine-132.16 Tryptophan-179.16 Glycine-19.93 Histidine-87.38 Cysteine-78.51
Quantum dots	LED, photodetectors, photovoltaics		Phenylalanine-0.14 Tryptophan-1.08 Histidine-0.56 Cysteine-0.15 Isoleucine-0.09 Valine-0.07	Phenylalanine-189.42 Tryptophan-179.16 Histidine-87.38 Cysteine-78.51 Isoleucine-149.77 Valine-120.91
Graphene oxide	Antibacterial, Field Effect Transistors[77], supercapacitor,	Tyrosine	Tyrosine-0.72	Tyrosine-132.16
Lanthanides	Luminescent		Aspartic acid-1.25 Serine-0.56 Lysine-0.53	Aspartic acid-18.46 Serine-19.75 Lysine-102.78

[a]Reproduced with permission from ref 78, copyright The Royal Society of Chemistry 2012. [b]Color of atoms in amino acid structures: Hydrogen (white), Carbon (gray), Nitrogen (blue), Oxygen (red), Sulfur (yellow). QSAR from ref 76; Antibacterial Field Effect Transistors from ref 77.

172

conjugate the Thomsen Friedenreich (TF) antigen (Figure 1b). The TF antigen is known to bind the anti-apoptotic protein Gal3. In Gal3⁺ carcinomas, it was found that threonine modified particles had fourfold apoptotic activity over serine. This effect could be due to more conjugation of threonine than serine. Another possibility could be the effect of an electron donating methyl group on threonine which is inducing the apoptosis.[70] Similar effects have been seen with histidine modified gold nanoparticles acting on cancer cells, as well as on mouse fibroblast.[71] An alternative to gold nanoparticles is histidine coated silver nanoparticles which are of low toxicity.[72] The apoptotic effect on cancer cells is due to the smaller size and shape of the particles, which promotes rapid internalization resulting in killing the cells. Therefore, particle core and size may also play a role in modulating the activation of the extrinsic pathway of apoptosis (Table 3).

Iron oxide nanoparticles modified with glycine[8] at a higher concentration (100 μg/mL) promoted only limited apoptosis in Hep-G2 cancer cells. The apoptosis occurs due to release of reactive oxygen species by Fentons reaction (Figure 1b) causing cell membrane damage followed by cell death. The medium RPMI-1640 has glycine at 0.01 g/mL and was not accounted for. Glycine is essential for cellular maintenance and a key ingredient in the medium for cell survival. Therefore, it is possible that the effect observed could be an artifact. Unreacted iron may get endocytosed causing a cytotoxic effect. Selenium nanoparticles modified with valine, lysine, and aspartic acid have clearer anticancer potential. The effect of the particles was studied against breast cancer cells MCF-7, cervical cancer HeLa, and liver cancer Hep G2. Lysine modified selenium particles[73] were found to induce apoptosis, which involved the activation of both caspase 8 and caspase 9. The activation of caspases 8 and 9 indicated the activation of both Fas and mitochondria-mediated apoptosis. The activation of the caspases could be due to an increase in reactive oxygen species (by Fentons reaction) inside the cells. Lysine which has twice as many amino functional groups can induce ROS (Table 2). The internalized particles are located in acidic lysosomes inside the cell. Inside the lysosomes, the amino acid becomes protonated due to the acidic pH. Due to this protonation, production of ROS becomes possible by Fentons reaction.

Doxorubicin is a chemotherapeutic drug for killing cancer cells. Doxorubicin (Figure 1b) was successfully administered to cancer cells by a carrier-mediated process as demonstrated by Yang and colleagues.[74] They utilized histidine modified iron oxide nanoparticles for the delivery of doxorubicin. The acidic pH in endosomes results in histidine ionization leading to doxorubicin release. This opens further improvements of the process as only 6.8 wt % of doxorubicin could be loaded. The mechanism for the preferential uptake of these particles by cancer cells, and not by normal cells which also have endosomes, is still unclear. Conjugation of siRNA (Figure 1b) to nanoparticles for inducing apoptosis has also been made possible and is very useful when the presence of a negative charge on siRNAs interferes with their proper delivery into cells. For example, survivin, an anti-apoptotic protein found in the human gastric cancer cell line MGC-803, is responsible for early entry into the cell cycle. Wang and colleagues showed that via the formation of tryptophan passivated carbon dots,[4] it was possible to deliver siRNA against survivin. The particles down-

regulated survivin-expression in MGC-803 cells and induced apoptosis. The uptake was achieved due to the modification of the carbon dots with the amino acid tryptophan as dopant and polyethylimine as a coating material, which promotes hydrophilic interactions with the cell membrane.

Magnetic nanoparticles have also been used in the context of tumor cell biology. For example, the surface functionalization of magnetic nanoparticles with aspartic acid has been correlated with tumor cell growth inhibition, which is influenced by the induction of pro-inflammatory macrophage polarization in tumor tissues.[75] Many other exciting applications are expected to emerge in the rapidly moving cancer therapeutics and diagnostics field which are beyond the scope of this review.

4. CYTOTOXICITY IS DEPENDENT ON NANOPARTICLE SIZE, SHAPE, AND CAPACITY TO INDUCE ROS

Cytotoxicity is the key component that needs to be addressed for translating nanoparticles from the lab to the clinic, and their effect on human cells is a vast area of research (Table 3). An important aspect underlying the toxicity of some nanomaterials is the generation of reactive oxygen species (ROS). The overproduction of ROS, mediated by Fenton's reaction, leads to oxidative stress which in turn causes a dysregulation in the physiological redox potentials and ultimately progresses into lipid peroxidation, protein oxidation, and DNA damage. Glutamate is known to prevent oxidative stress,[79] and glutamate modified iron oxide nanoparticles[9] have displayed high biocompatibility at high concentrations of 1000 μg/mL on human skin fibroblast. Their counterparts, the pristine iron oxide, had displayed a higher toxicity due to ROS formation. The glutamate capped iron oxide is, therefore, beneficial over the pristine iron oxide nanoparticles in abating the tendency to produce reactive oxygen species.

Gold nanoparticles modified with leucine[82] and lysine have less cytotoxicity in comparison to gold nanoparticles modified with glycine and aspartic acid (Figure 2e), at a concentration 50 μg/mL.[80] This is contradictory to our preliminary knowledge. We have found glycine modified 50 nm polystyrene particles to be immunosuppressive[22] when taken up by antigen presenting cells while their viability remains unaffected. Therefore, the cytotoxicity is related to the particle core and the size of gold nanoparticles (~25 nm). At the size range of less than 40 nm, gold nanoparticles have been reported to show a significant amount of cytotoxicity.[11,12,83] Pristine gold nanoparticles cause rapid cell death by necrosis[11] and are hence toxic. Another process may include ROS production, activating stress-dependent signaling pathways.[84] By comparing glycine with histidine and cysteine coated to silver nanoparticles,[72] it was observed that glycine coated particles were not toxic. Coating with histidine and cysteine, however, favored cell viability. Over time the histidine coated silver nanoparticles tended to cluster together increasing the hydrodynamic size. It is known that larger particles are rarely taken up by the cells and therefore may have reduced toxicity.[85]

Particles less than 5 nm tend to accumulate in the nucleus,[86] whereas particles in the size range 15−40 nm restrict themselves to the cytoplasm.[87] The ideal size for initial maximum uptake by cells such as dendritic cells (DC) is 50 nm,[22] which has been observed with gold,[88] silver,[89] and polystyrene[22] nanoparticles. However, the difference in shape

Table 3. Summary of Problems and Solutions Associated with Amino Acid Conjugated Nanoparticles

nanoparticle core	amino acid(s) conjugated	function	references	problems associated[a]	solutions to problems[b]
Iron oxide and pristine iron oxide	Lysine, arginine, glutamate, glycine, histidine, aspartic acid	1. Antibacterial activity 2. Biocompatibility 3. Apoptosis—preferential uptake by cancer cells 4. Transfection of cells 5. Magnetic Resonance Imaging 6. MR contrasting agent 7. Vaccine carriers	9,56 98,81 8 91 119 55,130 97	1. Same charge resulting in repulsion. 2. Limiting media for bacterial growth due to excess particles. 3. Experimental design was not enough to answer the questions raised. 4. Agglomeration of nanoparticles in soft agar. 5. Cytotoxicity. 6. Reduced bioavailability of nutrients for the cells. 7. Reason behind preferential uptake by cancer cells is not understandable. 8. Toxicity of polyethylimine. 9. Low biodistribution, elimination and degradation. 10. Size and roughness.	1. Investigating neutral and positively charged amino acids. 2. Resazurin assay instead of soft-agar method. 3. Experiments need to be carried out on noncarcinoma cell lines 4. Studies on particle uptake mechanism need to be done. 5. Other compounds/spacer molecules necessary for attachment of amino acids 6. Degradation of the particles needs investigation. 7. Down regulation of immune response may be necessary 8. May be useful for delivery of therapeutic antibodies but not for long-term drug delivery.
Gold	Peptide, glycine, lysine and its dendrimer	1. Transfecting DNA 2. Attachment of drugs	95,94 138	1. Glycine failed but lysine could transfect. Large particles cannot enter cells. 2. Localization of the particles are at the nucleus and may affect cell division	1. Fluorophore tagged experiments are necessary to find the location of the particles post transfection. 2. Less cytotoxic as the particles are large and interact with the cell membrane proteins. 3. Experiments determining the cell growth are essential. Other basic amino acids such as arginine and histidine needs to be tested
Selenium	Valine, lysine, aspartic acid	Apoptosis	73	ROS generation leading to cell death	
Quantum dots	Phenylalanine, tryptophan, histidine, cysteine, isoleucine, valine and glycine	1. Transfection of siRNA 2. Detection of thyroxin 3. Bioimaging by bicolor probes	49 46 113	1. Cytotoxicity. 2. Charge neutralization of cysteine leads to thyroxine zinc interaction is yet to be established. 3. Role of cysteine modification is not highlighted. 4. Salts, proteins, hormones and other compounds may influence thyroxin detection from fortified saliva.	1. Sulfhydryl groups cause cytotoxicity which needs to be curbed. 2. Aromatic amino acids as an alternative to cationic surfactants. 3. Quantification of the levels of thyroxine based on a standard curve is essential. 4. Several clinical experiments need to be done. 5. The particles need to be tested on a wide range of cells before drawing a conclusion.
Graphene oxide	Tyrosine	Detection of dopamine	102	1. Salts, antibodies in sera needs to be accounted. 2. Electrostatic interaction between particles	1. Aromatic amino acids may interact with graphene and therefore can detect lower concentrations of analyte.
Lanthanides doped with ytterbium, gadolinium or erbium	Aspartic acid, serine, lysine	Cytotoxicity	117	1. Cytotoxicity untested. 2. Deposition can lead to serious effect on organs	1. Tracing the excretion route is essential
Poly(glutamic acid) and phenylalanine	OVA, HIV-1 antigen	Immune response	126,129	dendritic cell activation and T_c cell response	1. TLR9 antagonist to limit the activation of DC. Mechanism needs investigation

[a]Problems associated with the nanoparticles in translation to clinic such as cytotoxicity, aggregation, experimental shortcomings, and other drawbacks. [b]Possible solutions we suggest to overcome these problems to bridge the gap between laboratory and clinical use.
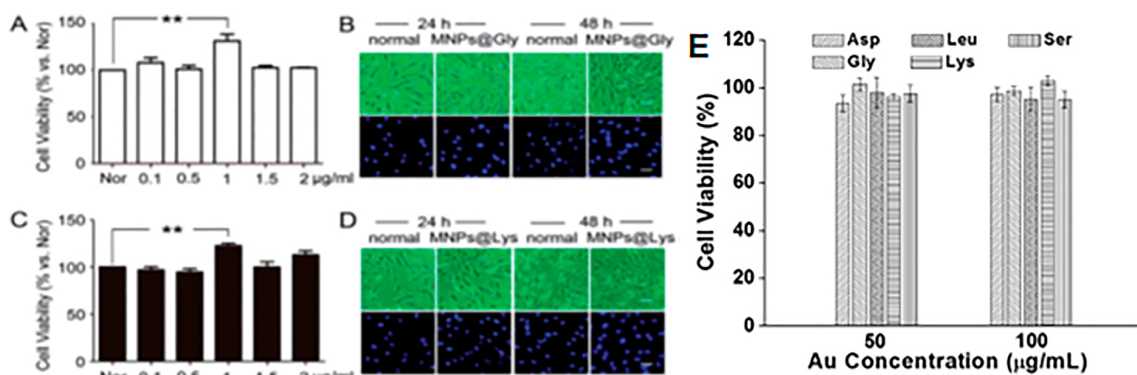
174

Figure 2. Comparison of cytotoxicity of iron oxide and gold nanoparticles coated with different amino acids. Gold shows a higher cytotoxicity in comparison to magnetic iron oxide nanoparticles. A WST-8 assay of cell viability was used to determine the cytotoxicity of the glycine (A, B) and lysine (C, D) coated magnetic nanoparticles on bone marrow mesenchymal stem cells. Both particles induced proliferation of cells rather than death at 1 mg/mL concentration and hence are more biocompatible. At 2 mg/mL, glycine coated particles showed normal cell viability (A) which was more for the lysine coated particles (C). The nuclear morphology remained the same for both the particles even after 48 h of incubation (B, D), but similar glycine and lysine coated gold nanoparticles (E) had less cell viability and did not have any proliferative effect on the cancerous KB cells. Reproduced with permission from ref 80, copyright 2014 Elsevier B.V.; and ref 81, copyright The Royal Society of Chemistry 2016.

of the nonspherical particles can have a negative impact and may increase the toxicity of gold nanoparticles along with size.[82]

The presence of sulfhydryl (−SH) group on cysteine (Table 2) may capture Ag$^+$ ions released, reducing the chance of cytotoxicity. Silica nanoparticles modified with arginine[90] are found to be cytotoxic at a concentration of 200 mg/mL. Inhibition of DNA replication and particle size leads to cytotoxicity in bone cells, whereas a relatively shorter doubling time of MG63 cells makes them more biocompatible with the number of particles per cell being very low to induce any cytotoxic effect. Such particles may not have much impact on cancer cell lines, which have very high doubling time, but could have much observable effect on other cells such as fibroblasts. Furthermore, other cell types like mesenchymal stem cells are very sensitive to culture conditions and are prone to differentiate quickly upon encountering a trigger stimulus such as transient low pH stressor. Interestingly, in the context of cell cycle, the addition of glycine and lysine-modified iron oxide nanoparticles[81] at 1 μg/mL increases the population of cells in S-phase thus promoting the proliferation of mesenchymal stem cells (Figure 2b,d). Therefore, these particles show less cytotoxicity in comparison to silica nanoparticles in the earlier study.[90] Low levels of cytotoxicity by amino acid modified iron oxide nanoparticles is not limited to mesenchymal stem cells (Figure 2a,c) but is extended to many different cells as discussed in further sections below. In another study, selenium nanoparticles modified with several amino acids[73] like lysine, valine, and aspartic acid had shown lower cytotoxicity to human kidney cells (HEK-293) which can account for the fact that these particles have a large size of 120 nm and tend to agglomerate over time.

5. GENE, THERAPEUTIC SIRNA, PROTEIN, AND DRUG DELIVERY

Molecular biologists use several methods such as electroporation, heat shock of competent cells, ultrasound, ballistic delivery, and focused laser for DNA transfection in the cell.[91] Lysine is known to be an excellent binder of DNA and hence DNA bound particles have low cytotoxicity. Polylysine bound nanoparticles transfecting DNA is a huge area and is outside the

scope of this review, but for general interest one may refer to Jin and colleagues[92] and Cherif and colleagues.[93]

Gene delivery using lysine as a dendrimer (Figure 3a)[94] coated to gold nanoparticles is a noteworthy example and has
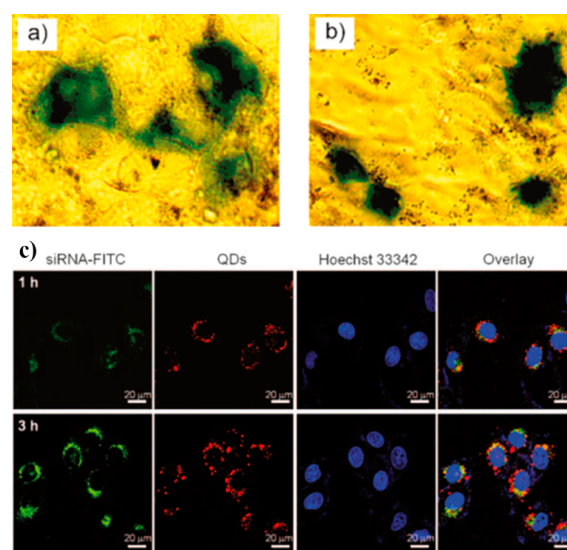
Figure 3. (a,b) Production of β-galactosidase cleaving X-Gal upon transfection of β-Gal gene in Cos-1 cells. The blue colored product signifies the successful transfection of Cos-1 cells with the β-Gal gene which produces the enzyme β-galactosidase capable of cleaving X-Gal. The process was possible with lysine coated (b) and lysine dendrimer (a) nanoparticles but not with glycine coated nanoparticles. Reproduced with permission from ref 94, copyright 2008 American Chemical Society. (c) HeLa cells take up amino acid coated quantum dots carrying siRNA. Green fluorescence increasing with time signifies the siRNA uptake along with the amino acid coated QD uptake after 3 h. The Hoechst 33342 stains DNA in the nucleus (shown in purple). The overlay image suggests active siRNA binding the DNA and the localization of the QDs at the nucleus, which suggests the therapeutic potential of amino acid coated QDs. Reproduced with permission from ref 49, copyright 2011 Wiley-VCH Verlag GmbH&Co. KGaA, Weinheim.
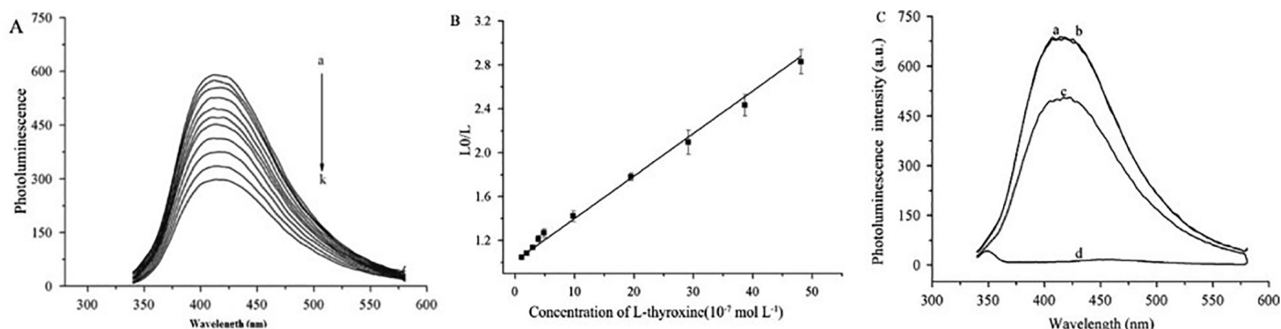
Figure 4. Detection of thyroxine using cysteine coated ZnS quantum dots. Photoluminescence emission spectra of cysteine-capped ZnS quantum dots used as probes (A) at various concentrations ranging from (a) 0 to (k) 4.0×10^{-6} mol L^{-1}; and (B) Stern−Volmer-type standard calibration curve for the detection of thyroxine. (C) In clinical sample, such as saliva, the particles could detect as low as 4.0×10^{-6} mol L^{-1}. Photoluminescence quenching was observed when thyroxine was present (c) with respect to saliva in water (d) and saliva in probe suspension (b). Reproduced with permission from ref 46, copyright 2014 Elsevier B.V.

been compared with single molecule coating of lysine (Figure 3b).[95] Lysine dendrimer gold nanoparticles (Table 2) showed an increased efficiency of transfection in comparison to the pristine lysine molecule coated gold nanoparticles (Figure 3b). When glycine coated gold nanoparticles were used, they were incapable to transfect the β-gal gene. Therefore, the positively charged lysine could bind the negatively charged DNA to transfect DNA into the Cos-1 cells. The reason being the neutral charge of glycine at pH 7.4 and hence unable to bind to DNA. In addition, the lysine coated gold nanoparticles left the cell viability unaltered and hence causing very low cytotoxicity. This is accounted for by the large size of the particles (93−233 nm). Reports suggest that particles of such portly size are unable to enter the cell[96] and fluorophore tagged experiments are hence necessary to identify the location of the particles.

Polyethylenimine coated magnetic nanoparticles for DNA delivery is reported widely.[97] Similar work was carried out with iron oxide nanoparticles coated with arginine as synthesized by Theerdhala and colleagues.[98] Transfection under the influence of an external magnet with amino acid modified magnetic nanoparticles would be less cytotoxic in comparison to currently available techniques. Interestingly CdSe/ZnSe quantum dots (Figure 3c) coated with amino acids phenyl-alanine, tryptophan, histidine, and cysteine[49] can carry siRNA inside the cells. A negative charge often reduces gene silencing effects by nonspecific protein adsorption onto the complex. Cysteine coated particle toxicity is due to the sulfhydryl group[99] which is absent for the other amino acids (Table 2). Change of pH due the particles lead to protonation or deprotonation of the endosome respectively and thus the endosome ruptures by proton sponge effect. Overall the particles were more toxic to cancer cells than normal cells and were found clustered in the cytoplasm in multiple pinosomes (Figure 3c). This has been portrayed with cysteine coated particles and clarifies that several answers as size and charge are essential for the delivery of siRNA.

6. TOWARD SENSING FOR DIAGNOSTIC APPLICATIONS

Hormones, proteins, enzymes, and other biomarkers are quantified in a pathology lab every day. The prevalent methods involve time-consuming, reagent exhaustive process and require good skills to generate repetitive reliable data.

The thyroid hormone thyroxine is essential for active metabolism. Thyroxine has been quantified[46] using cysteine-

capped zinc sulfide quantum dots at a concentration as low as 9.5×10^{-7} mol L^{-1} (Figure 4a,b).[46] It was observed that the cysteine modified quantum dot photoluminescence was quenched upon addition of thyroxine (Figure 4a) due to cysteine charge neutralization leading to thyroxine−zinc interaction.

Problems associated with clinical samples such as separating cells, salivary thyroxine (Figure 4c), proteins, hormones, antibodies (cysteine−cysteine sulfhydryl group interaction) in blood, amino acids, and salts may hamper the detection. The quantification of thyroxine in the patient sample can be quantified by interpreting from a standard curve (Figure 4b) of the fluorescence quenching by known amounts of thyroxine. Although the particles seem promising for applications as successful diagnostics agents, several clinical experiments need to be done.

Dopamine is a neurotransmitter associated with the central nervous system and change in its concentration can lead to Parkinson's disease and Huntington's disease. Exhaustive work has been carried out for dopamine sensing with detection limits as low as 100 nM.[100] One may refer to the current trends in dopamine sensing for in-depth understanding, illustrated by Jackowska and colleagues,[101] but in one unique study, tyrosine functionalized graphene oxide nanoparticles could detect dopamine levels as low as 2.8×10^{-7} molL^{-1} [102] comparable to N-doped graphene sheets.[100] One might suggest that for detection at physiological pH, negatively charged amino acids could be used, although the problems highlighted with thyroxine detection need to be kept in mind. The aromatic rings of graphene and tyrosine (Table 2) together may act as a high electron-withdrawing group facilitating low detectable limits. Therefore, further tests with other aromatic amino acids are necessary.

Ascorbic acid is an antioxidant balancing oxidative stress in the body of clinical significance. A biosensor developed using N-acetyl-cysteine coated core/shell/shell CdTe/CdS/ZnS quantum dots could detect ascorbic acid with limits as low as 1.8 nM in urine samples.[103] Other components such as salts, amino acids, and nucleotides, which might influence detection, were also taken into consideration, but not proteinuria. Although the reason behind the use of a modified cysteine residue for coating is still unclear, we think it could be the effect of the electron withdrawing nature of the acetyl group leading to drawing of electrons from the conduction band of the ZnS shell.
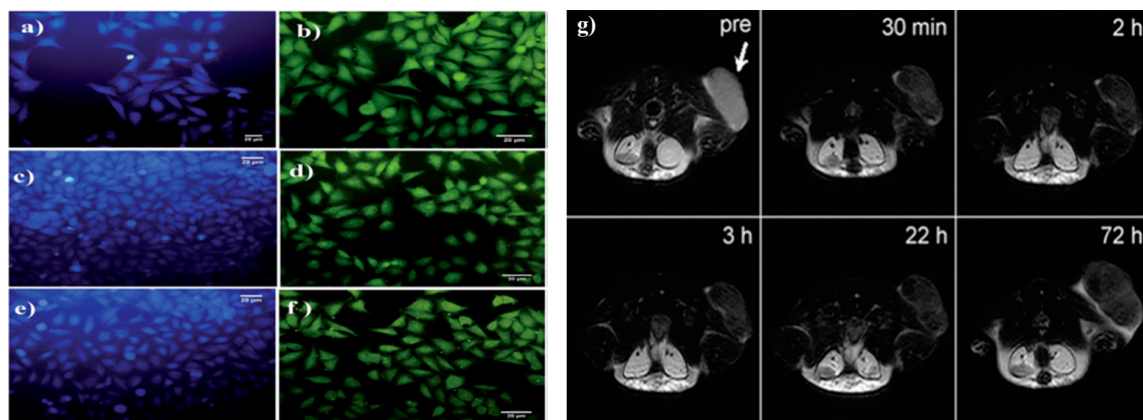
Figure 5. (a−f) Innate fluorescence of amino acid coated carbon dots on HeLa cells. The blue colored cells are the amino acid coated carbon dots with amino acids isoleucine (a), glycine (c), and valine (e). The green fluorescence is caused by the doping of phosphorus on to the amino acid coated carbon dots with amino acids isoleucine (b), glycine (d), and valine (f). Reproduced with permission from ref 113, copyright 2015 The Royal Society of Chemistry. (g) In vivo T2 weighted magnetic resonance image of amino acid coated iron oxide nanoparticle as a contrasting agent. Images acquired post-injection of 15 mg Fe/kg of poly(aspartic acid) coated iron oxide nanoparticles. The particles demonstrated high colloidal stability and were found to be taken up by CT26 tumor cells (at back of mice) having a low pH environment represented in the image by the arrow. Reproduced with permission from ref 55, copyright 2010 The Royal Society of Chemistry.

Similar particles could detect glutathione at a concentration as low as 2.49 ng/mL.[104] Glutathione is important in diseases like HIV, Parkinson's disease, and Alzheimer's disease making it significant for clinical detections. The results are significant in determining serum glutathione levels and can be used clinically. However, the presence of cysteine in the analyte could impact the detection because of similar structure of cysteine (Table 2). The interaction of mercury and N-acetyl cysteine is unclear. Recently it had been demonstrated that asparagine coated gold nanoparticles can be novel substitutes to EDC-NHS modified gold nanoparticles.[105] Such particles were demonstrated to be immune sensors when conjugated with the Anti-CA125 antibody. CA125 is a cancer antigen which is used to diagnose ovarian cancer.[106] The sensor is sensitive beyond 500 IU/mL of CA125 biomarker, which can be of clinical relevance.

Nonfluorescent amino acid conjugated nanoparticles serving as detecting probes for clinically relevant molecules are rare. However, there are several other conjugated nanoparticles which can detect C-Reactive Protein (CRP), virus, and biologically relevant molecules. For example, Perez and colleagues made iron oxide nanoparticles conjugated with HSV-1 and ADV-5 antibodies for detection of both Herpes Simplex Virus (HSV) and Adenovirus (ADV).[107] These magnetic viral sensors could detect as low as 5 viral particles in 10 μL by using NMR and MRI technologies. This is advantageous over conventional ELISA and PCR methods. In another study, C-Reactive Protein (CRP), an useful biomarker of inflammation in human could be detected using anti-CRP antibody conjugated nanoparticles at a detection limit of 0.12 μg/mL.[108] The authors use a competitive method to determine the presence of CRP in serum samples. The method is robust as a linear range of CRP concentration can be detected. Use of gold nanoparticles in detection of thrombin, aflatoxins, free radicals, and bacteria has been reviewed elsewhere and is beyond the scope of this review.[41] Gold nanoparticles exhibit surface plasmon resonance property and Raman signature spectra which enables the detection of the species mentioned before. Another unique study revealed the enhancement of fingerprints using anti-L-amino acid antibody conjugated gold nanoparticles.[109] The presence of phenylalanine in fingerprints

was detected as it was used as a hapten for the antibody development. For further details about applications of such nanoparticles in the biological system, one may refer to a number of other articles.[110,111]

In short, despite the use of some nonfluorescent nanoparticles as detecting probes, the basic principle of detection of clinically relevant molecules relies mostly on the quenching of fluorescence. This is either carried out by the analyte in question or by another molecule, which curbs the fluorescence caused by the analyte molecule. In both cases, amino acid conjugated nanoparticles (mostly cysteine and its modifications) play the role to detect or quench the fluorescence. Therefore, a successful diagnostic agent should be able to combat the problems identified along with detecting the target analyte at a wide concentration range (Table 3).

7. BIOIMAGING WITH EMPHASIS ON MRI

Fluorescent molecular probes are highly useful in applications such as flow cytometry, immunofluorescence staining, and live cell imaging. These techniques utilize the property of the molecules to fluoresce selectively when excited by a certain wavelength of light.

Carbon dots have the unique property to fluoresce when excited by light of a specific wavelength. The emitted light is dependent on the size of the particles. However, the carbon dots show cytotoxicity[112] toward cells, which inhibits their use as fluorescent probes for cell imaging. Recently, however, it was found that carbon dots synthesized using citric acid with amino acids coating such as isoleucine, valine, and glycine can have reduced cytotoxicity and have been used as fluorescent bicolor probes.[113] The authors demonstrated that phosphorus doping induces a red shift, therefore having a bicolor probe, and that the fluorescent probes have reduced cytotoxicity in HeLa cells. HeLa cells are cancer cells characterized by their fast proliferation, which is not consistent with other mammalian noncancerous cell lines such as fibroblasts. It is, therefore, necessary to observe the effect of such particles on a wide range of cells before drawing a conclusion on the cytotoxicity of such ultrafine particles. This drawback had been addressed partially
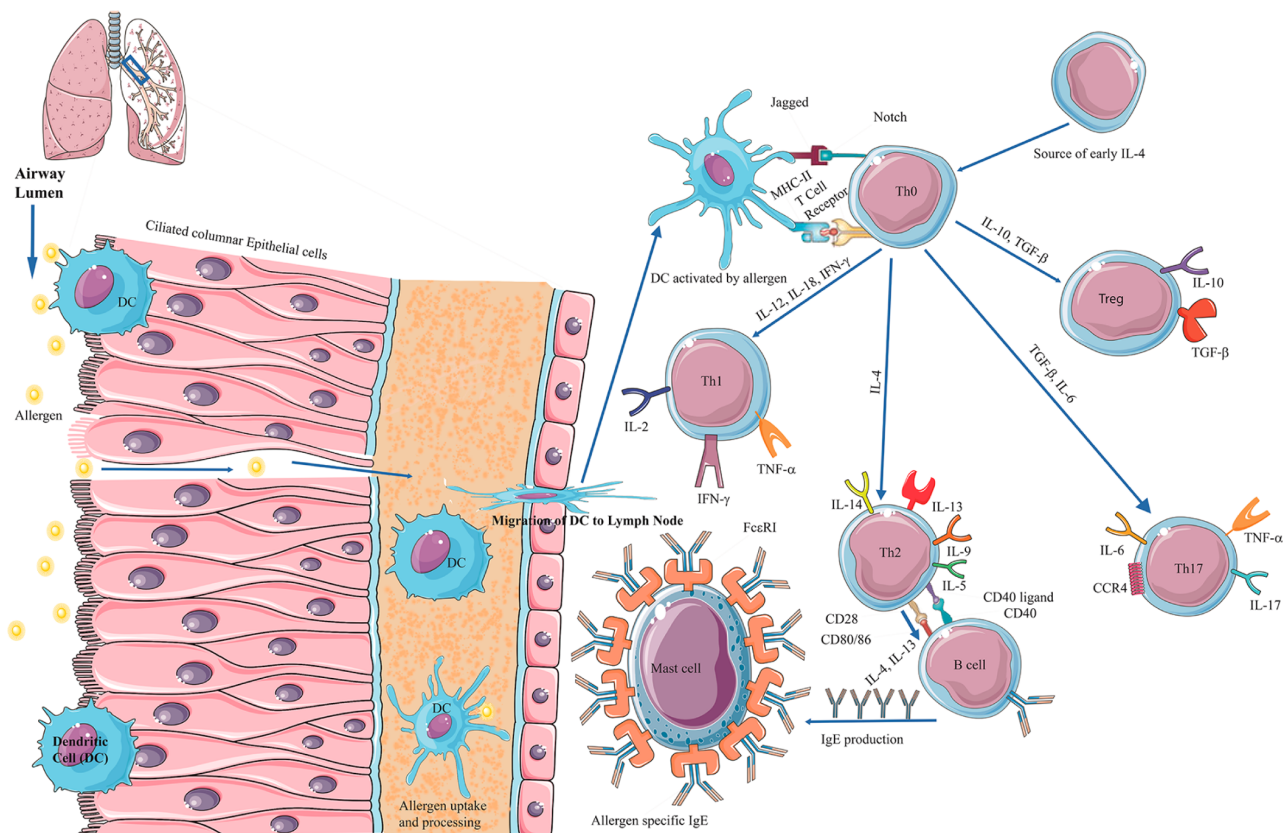
Figure 6. Inflammation and airway sensitization by nanoparticles. Allergens such as nanoparticles are captured by patrolling immature dendritic cells (DCs) in the airway lumen and becomes activated. The mature DCs then migrate to the regional lymph node (LN) through disrupted epithelium or cell tight junctions. At the LN they present the processed allergen by MHCII to naïve T cells. The naïve T cells acquire the characteristics of T_H2 cells by the interaction of MHCII and jagged receptor on activated DC to TCR and Notch receptor respectively on naïve T cells. Two important T_H2 pro-inflammatory cytokines IL-4 and IL-13 lead to ligation of costimulatory molecules CD40 and CD80/86 on T_H2 cells with CD40 L and CD28 on B cells, respectively, as well as upregulation of the markers. The activation leads the B cells to produce allergen-specific IgE which binds to the high-affinity receptor FCεRI on tissue-resident mast cells. The process sensitizes them to respond when the host is later exposed to the same allergen.

by Arslan and colleagues upon studying the cytotoxicity of cysteine-capped zinc oxide quantum dots in HEK293 cells.[114] The size of the zinc oxide QDs was around 100 nm,[114] whereas the carbon quantum dots were 5 nm[90] (Figure 5a−f). Therefore, the smaller sized particles appear to be more cytotoxic to cells irrespective of their amino acid coating.

Fluorescent imaging is not limited to cells but has been explored *in vivo* as well. In a separate study it was shown that amino acids such as aspartic acid, serine, and lysine were coated onto upconversion-luminescent nanoparticles made of lanthanides lutetium codoped with either ytterbium, gadolinium, or erbium.[54] The authors demonstrated the accumulation of the particles in the liver and the spleen after 5 h of the base of tail injection, but have not studied their cytotoxicity yet. Metallic nanoparticles are widely known to be cytotoxic[82,115] and heavy metals used for the process are not excreted by the body, leading to deposition and posing serious effects to the organ. These metals cannot be metabolized by the body,[116,117] and degradation is not possible.[116] Therefore, tracing the excretion route is essential before use of the particles in *in vivo* imaging.

7.1. Magnetic Resonance Imaging Using Poly(aspartic acid)-Coated Nanoparticles. The biodegradability of iron oxide nanoparticles[118] has increased their potential for use as MRI agents. Amino acid coated iron oxide nanoparticles have

been used for imaging of tumors and soft tissue. Tumor cells and normal cells both are overall negatively charged due to the presence of phospholipids like phosphatidylserine on the cell membrane. Poly(amino acid)s (such as poly(aspartic acid)) serve as a coating material for iron oxide nanoparticles and have high colloidal stability in terms of positive zeta potential. Despite the positive zeta potential, the negatively charged tumor cells take up particles in a low pH environment.[55] The particles remained in the tumor cells for 3 days without deterioration of the contrasting signal (Figure 5g); hence biodistribution and degradation of such particles would be low. Although the dose of the particles is below lethal concentration, they may have chronic cytotoxicity if not degraded or excreted from the patient's body. Therefore, it is essential to monitor the degradation of such particles in the body to avoid accumulation in tissues.

A similar particle developed by Yang and colleagues targeted breast cancer cells with anti- HER/neu2 antibody conjugated onto the surface of iron oxide coated poly(aspartic acid) nanoparticles.[119] The authors claimed that the particles have negligible cytotoxicity even at concentrations 1 mg/mL. Due to the presence of iron core, MR imaging was possible and served as an excellent contrast agent. The only concern would be the size and particle roughness.[120]

Other than tumors, poly(aspartic acid)-coated nanoparticles have been found useful as MR contrasting agents in liver imaging where the core is manganese oxide instead of iron oxide.[121] The authors demonstrated an increase in the hydrodynamic size of the particles due to adsorption of serum proteins, which is a key factor in every nanoparticle imaging probes. However, the particles are stable colloids as indicated by their negative zeta potential which is also beneficial for the particles having low cytotoxicity to the liver cells. To enhance the imaging, bimodal particles with magnetic effect as well as fluorescent properties have been developed.[122] Such particles have a fluorophore conjugated to an amino acid coating which is on a metal surface, the metal being gold or iron oxide nanoparticles. The only disadvantage of these particles would be nonspecific signaling due to cleavage of the fluorophore from the particle and hence innate fluorescent properties of particles as discussed earlier.[103,46,104,112]

8. EFFECT OF NANOPARTICLES ON HOST IMMUNITY WITH EMPHASIS ON CONJUGATED PARTICLES

Non-surface-functionalized silica particles ranging in size from 30 to 100 nm have been found to promote lung inflammation mediated by inflammasome activation and IL-1β secretion,[123] potentially induced by activation of the MAPK/Nrf2 and NF-$\kappa\beta$ signaling pathways.[124] By contrast, amino acid coated nanoparticles show little toxicity and, in some cases, are even able to actively prevent damaging inflammatory responses. This has been demonstrated for 50 nm glycine coated nanoparticles, which inhibit acute airway inflammation when taken up by lung dendritic cells (DC).[22] Size is a consideration, and bigger glycine coated 500 nm polystyrene nanoparticles are taken up preferentially by macrophages in the lung which do not promote the same strong anti-inflammatory effect[22,23] (Figure 6).

At the cellular levels nanoparticle characteristics also highly influence uptake which can be mediated by multiple endocytic mechanisms such as an energy-dependent endocytosis through the endosomes and lysosomes (reviewed ref 125).

Another example of the effects of nanoparticles on the immune system is the use of poly(glutamic acid) nanoparticles encapsulating HIV-1 antigen use as vaccines[126] which can lead to DC maturation[127] and promote the induction of cytotoxic T cell responses. In addition, the cytotoxicity of nanoparticles is influenced by charge of their coating, and the above-mentioned examples of amino acid coated nanoparticle formulations are all negatively charged. On the other hand, although positively charged particles tend to show increased cytotoxicity,[128] in some cases these have still been successfully used as vaccine delivery systems.[129] Therefore, the issue of charge needs further investigation and a deeper understanding of the specific biological context in which these particles can be used.

So far, we have observed that the amino acid coated nanoparticles are diverse, with existing variations across multiple parameters such as shape, charge, type of amino acid conjugated, and route of administration (Table 3). Consequently these nanoparticles are taken up by a wide variety of organs including spleen,[33] lung,[34−36] and liver.[32,130] It is of interest that some amino acid functionalized particles do have the capacity to localize to multiple organs supporting their potential as MR contrast agents.[130] As mentioned in the introduction of this review size matters when it comes to biodistribution of nanoparticles into different organs. However, charge and shape are important aspects to consider as well. The

shape of a nanoparticle highly influences its blood vessel fluid dynamics when in circulation. For instance, nonspherical nanoparticles tend to exhibit much better tumbling and lateral drifting characteristics in comparison with their spherical counterparts.[131] Therefore, nonspherical nanoparticles have an increased chance of particle adherence, binding to the endothelial cell wall, and potential extravasation. Charge affects nanoparticles too, by influencing the protein adsorption[33,132] and positively charged nanoparticles undergo rapid clearance from the circulation in comparison with their negatively charged counterparts.[133] Indeed, when injecting differently charged gold nanoparticles either intraperitoneal or intravenous in mice, Arvizo and colleagues observed high plasma clearance for the positively and negatively charged particles. However, the neutral and zwitterionic particles exhibited low plasma clearance well after 24 h measurements.[133] Overall, finding the optimal combination of nanoparticle properties to use in different medical areas is a challenging task but could lead to exciting new applications in the field of nanoparticle-based drug delivery. For further elucidation, the properties of nanoparticles and their heavy influence on pharmacokinetics and biodistribution has been extensively reviewed by Blanco et al.[33]

Generally, successfully conjugating antibodies or other specific cell targeting modalities to nanoparticles is needed to support a range of biomedical applications such as sensing and diagnosis, targeted delivery of small molecule drugs, and cancer therapy.[134−137]

9. CONCLUSION

Amino acid conjugated particles show promise as components of devices and nanotechnology products for clinical use. Development of probes to detect clinical analytes at low concentrations *in vitro* leads the way in this field, but should not be the only focus. Therapeutics, imaging, and diagnostics are some of the areas where these particles could have extensive use. As the field evolves, more *in vivo* applications are expected to emerge. The issues addressed in this review may help support the design of effective surface functionalized particles for such specific *in vivo* biological applications, with a focus on biocompatibility as being related to a combination of size and charge (the latter potentially modified by the coating amino acid). The consideration of the amino acid used in functionalizing is also essential for trapping ROS and preventing cytotoxicity. Biodistribution and subsequent excretion of injected probe nanoparticles is important in imaging. As well as providing additional *in vivo* stability, biocompatibility, and capacity for additional surface modifications, amino acid conjugated nanoparticles are emerging as immunomodulatory agents themselves, as illustrated by the discovery of nanoparticles capable of inhibiting the elicitation of inflammatory lung diseases such as asthma. This new area needs further investigation into the mechanism of action, and range of nanoparticles and amino acids capable of mediating such novel effects.

■ AUTHOR INFORMATION

Corresponding Author

*E-mail: magdalena.plebanski@monash.edu.

ORCID ◉

Magdalena Plebanski: 0000-0001-6889-3667

Author Contributions

Amlan Chakraborty reviewed the literature, developed the manuscript and the figures with supervision from Magdalena Plebanski, Cordelia Selomulya, and Jennifer C. Boer. All authors revised, edited, and proofread the manuscript.

Notes

The authors declare no competing financial interest.

■ ACKNOWLEDGMENTS

■ REFERENCES

(1) Chakraborty, A., Patni, P., Suhag, D., Saini, G., Singh, A., Chakrabarti, S., and Mukherjee, M. (2015) N-doped carbon nanosheets with antibacterial activity: mechanistic insight. *RSC Adv.* 5, 23591−23598.

(2) Paul, D. R., and Robeson, L. M. (2008) Polymer nanotechnology: Nanocomposites. *Polymer* 49, 3187−3204.

(3) Pérez-Juste, J., Pastoriza-Santos, I., Liz-Marzán, L. M., and Mulvaney, P. (2005) Gold nanorods: Synthesis, characterization and applications. *Coord. Chem. Rev.* 249, 1870−1901.

(4) Wang, Q., Zhang, C., Shen, G., Liu, H., Fu, H., and Cui, D. (2014) Fluorescent carbon dots as an efficient siRNA nanocarrier for its interference therapy in gastric cancer cells. *J. Nanobiotechnol.* 12, 1−12.

(5) Zhongshi, L., Xingui, L., Yegui, X., and Shunying, L. (2014) 'Smart' gold nanoshells for combined cancer chemotherapy and hyperthermia. *Biomed. Mater.* 9, 025012.

(6) Kaiser, J. P., Diener, L., and Wick, P. (2013) Nanoparticles in paints: A new strategy to protect façades and surfaces? *J. Phys.: Conf. Ser.* 429, 012036.

(7) González, D. M., Körstgens, V., Yao, Y., Song, L., Santoro, G., Roth, S. V., and Müller-Buschbaum, P. (2015) Improved Power Conversion Efficiency of P3HT: PCBM Organic Solar Cells by Strong Spin−Orbit Coupling-Induced Delayed Fluorescence. *Adv. Energy Mater.* 5, 1401770.

(8) Gholami, A., Rasoul-amini, S., Ebrahiminezhad, A., Seyed Hassan, S., and Ghasemi, Y. (2015) Lipoamino Acid Coated Superparamagnetic Iron Oxide Nanoparticles Concentration and Time Dependently Enhanced Growth of Human Hepatocarcinoma Cell Line (Hep-G2). *J. Nanomater.* 2015, 1.

(9) Inbaraj, B. S., Kao, T. H., Tsai, T. Y., Chiu, C. P., Kumar, R., and Chen, B. H. (2011) The synthesis and characterization of poly(γ-glutamic acid)-coated magnetite nanoparticles and their effects on antibacterial activity and cytotoxicity. *Nanotechnology* 22, 075101.

(10) Rodriguez, P., Plana, D., Fermin, D. J., and Koper, M. T. M. (2014) New insights into the catalytic activity of gold nanoparticles for CO oxidation in electrochemical media. *J. Catal.* 311, 182−189.

(11) Pan, Y., Neuss, S., Leifert, A., Fischler, M., Wen, F., Simon, U., Schmid, G., Brandau, W., and Jahnen-Dechent, W. (2007) Size-Dependent Cytotoxicity of Gold Nanoparticles. *Small* 3, 1941−1949.

(12) Selim, ME H.A. (2012) Gold Nanoparticles Induce Apoptosis in MCF-7 Human Breast Cancer Cells. *Asian Pacific Journal of Cancer Prevention* 13, 1617−1620.

(13) Abdelhalim, M. A. K. (2011) Exposure to gold nanoparticles produces cardiac tissue damage that depends on the size and duration of exposure. *Lipids Health Dis.* 10, 205.

(14) Inoue, K.-i., Koike, E., Yanagisawa, R., Hirano, S., Nishikawa, M., and Takano, H. (2009) Effects of multi-walled carbon nanotubes on a murine allergic airway inflammation model. *Toxicol. Appl. Pharmacol.* 237, 306−316.

(15) Inoue, K.-i., Yanagisawa, R., Koike, E., Nishikawa, M., and Takano, H. (2010) Repeated pulmonary exposure to single-walled carbon nanotubes exacerbates allergic inflammation of the airway: Possible role of oxidative stress. *Free Radical Biol. Med.* 48, 924−934.

(16) Alessandrini, F., Schulz, H., Takenaka, S., Lentner, B., Karg, E., Behrendt, H., and Jakob, T. (2006) Effects of ultrafine carbon particle inhalation on allergic inflammation of the lung. *J. Allergy Clin. Immunol.* 117, 824−830.

(17) De Haar, C., Hassing, I., Bol, M., Bleumink, R., and Pieters, R. (2006) Ultrafine but not fine particulate matter causes airway inflammation and allergic airway sensitization to co-administered antigen in mice. *Clin. Exp. Allergy* 36, 1469−1479.

(18) Cai, K., Hou, Y., Hu, Y., Zhao, L., Luo, Z., Shi, Y., Lai, M., Yang, W., and Liu, P. (2011) Correlation of the Cytotoxicity of TiO2 Nanoparticles with Different Particle Sizes on a Sub-200-nm Scale. *Small* 7, 3026−3031.

(19) Vedantam, P., Huang, G., and Tzeng, T. R. J. (2013) Size-dependent cellular toxicity and uptake of commercial colloidal gold nanoparticles in DU-145 cells. *Cancer Nanotechnol.* 4, 13−20.

(20) Ariano, P., Zamburlin, P., Gilardino, A., Mortera, R., Onida, B., Tomatis, M., Ghiazza, M., Fubini, B., and Lovisolo, D. (2011) Interaction of Spherical Silica Nanoparticles with Neuronal Cells: Size-Dependent Toxicity and Perturbation of Calcium Homeostasis. *Small* 7, 766−774.

(21) Fifis, T., Gamvrellis, A., Crimeen-Irwin, B., Pietersz, G. A., Li, J., Mottram, P. L., McKenzie, I. F., and Plebanski, M. (2004) Size-dependent immunogenicity: therapeutic and protective properties of nano-vaccines against tumors. *J. Immunol.* 173, 3148−3154.

(22) Hardy, C. L., LeMasurier, J. S., Belz, G. T., Scalzo-Inguanti, K., Yao, J., Xiang, S. D., Kanellakis, P., Bobik, A., Strickland, D. H., Rolland, J. M., et al. (2012) Inert 50-nm Polystyrene Nanoparticles That Modify Pulmonary Dendritic Cell Function and Inhibit Allergic Airway Inflammation. *J. Immunol.* 188, 1431−1441.

(23) Hardy, C. L., LeMasurier, J. S., Mohamud, R., Yao, J., Xiang, S. D., Rolland, J. M., O'Hehir, R. E., and Plebanski, M. (2013) Differential Uptake of Nanoparticles and Microparticles by Pulmonary APC Subsets Induces Discrete Immunological Imprints. *J. Immunol.* 191, 5278−5290.

(24) Wilson, K. L., Xiang, S. D., and Plebanski, M. (2015) Montanide, Poly I: C and nanoparticle based vaccines promote differential suppressor and effector cell expansion: a study of induction of CD8 T cells to a minimal Plasmodium berghei epitope. *Front. Microbiol.* 6, 29.

(25) Xiang, S. D., Fuchsberger, M., Karlson, T. D. L., Hardy, C. L., Selomulya, C., and Plebanski, M. Nanoparticles, Immunomodulation and Vaccine Delivery. In *Handbook of Immunological Properties of Engineered Nanomaterials*; World Scientific, 2012; pp 449−475.

(26) Xiang, S. D., Scholzen, A., Minigo, G., David, C., Apostolopoulos, V., Mottram, P. L., and Plebanski, M. (2006) Pathogen recognition and development of particulate vaccines: Does size matter? *Methods* 40, 1−9.

(27) He, C., Hu, Y., Yin, L., Tang, C., and Yin, C. (2010) Effects of particle size and surface charge on cellular uptake and biodistribution of polymeric nanoparticles. *Biomaterials* 31, 3657−3666.

(28) Verma, A., and Stellacci, F. (2010) Effect of Surface Properties on Nanoparticle−Cell Interactions. *Small* 6, 12−21.

(29) Zhao, M., Kircher, M. F., Josephson, L., and Weissleder, R. (2002) Differential Conjugation of Tat Peptide to Superparamagnetic Nanoparticles and Its Effect on Cellular Uptake. *Bioconjugate Chem.* 13, 840−844.

(30) Verma, A., Uzun, O., Hu, Y., Hu, Y., Han, H.-S., Watson, N., Chen, S., Irvine, D. J., and Stellacci, F. (2008) Surface-structure-regulated cell-membrane penetration by monolayer-protected nanoparticles. *Nat. Mater.* 7, 588−595.

(31) Soo Choi, H., Liu, W., Misra, P., Tanaka, E., Zimmer, J. P., Itty Ipe, B., Bawendi, M. G., and Frangioni, J. V. (2007) Renal clearance of quantum dots. *Nat. Biotechnol.* 25, 1165−1170.

(32) Braet, F., Wisse, E., Bomans, P., Frederik, P., Geerts, W., Koster, A., Soon, L., and Ringer, S. (2007) Contribution of high-resolution

correlative imaging techniques in the study of the liver sieve in three-dimensions. *Microsc. Res. Tech. 70*, 230−242.

(33) Blanco, E., Shen, H., and Ferrari, M. (2015) Principles of nanoparticle design for overcoming biological barriers to drug delivery. *Nat. Biotechnol. 33*, 941−951.

(34) Liu, H., Ding, L., Zhang, Y., and Ni, S. (2014) Circulating endothelial microparticles involved in lung function decline in a rat exposed in cigarette smoke maybe from apoptotic pulmonary capillary endothelial cells. *Journal of Thoracic Disease 6*, 649−655.

(35) McVey, M., Tabuchi, A., and Kuebler, W. M. (2012) Microparticles and acute lung injury. *American Journal of Physiology - Lung Cellular and Molecular Physiology 303*, L364−L381.

(36) Takahashi, T., and Kubo, H. (2014) The role of microparticles in chronic obstructive pulmonary disease. *Int. J. Chronic Obstruct. Pulm. Dis. 9*, 303−314.

(37) Almeida, J. P. M., Chen, A. L., Foster, A., and Drezek, R. (2011) In vivo biodistribution of nanoparticles. *Nanomedicine 6*, 815−835.

(38) Kristin Mohr, M. S., Baier, G., Schöttler, S., Okwieka, P., Tenzer, S., Landfester, K., Mailänder, V., Schmidt, M., and Meyer, R. G. (2014) Aggregation Behavior of Polystyrene-Nanoparticles in Human Blood Serum and its Impact on the in vivo Distribution in Mice. *Journal of Nanomedicine and Nanotechnology 5*, 193.

(39) Moore, T. L., Rodriguez-Lorenzo, L., Hirsch, V., Balog, S., Urban, D., Jud, C., Rothen-Rutishauser, B., Lattuada, M., and Petri-Fink, A. (2015) Nanoparticle colloidal stability in cell culture media and impact on cellular interactions. *Chem. Soc. Rev. 44*, 6287−6305.

(40) Yoo, J., Chambers, E., and Mitragotri, S. (2010) Factors that Control the Circulation Time of Nanoparticles in Blood: Challenges, Solutions and Future Prospects. *Curr. Pharm. Des. 16*, 2298−2307.

(41) Tiwari, P., Vig, K., Dennis, V., and Singh, S. (2011) Functionalized Gold Nanoparticles and Their Biomedical Applications. *Nanomaterials 1*, 31.

(42) Larson, T. A., Joshi, P. P., and Sokolov, K. (2012) Preventing Protein Adsorption and Macrophage Uptake of Gold Nanoparticles via a Hydrophobic Shield. *ACS Nano 6*, 9182−9190.

(43) Wangoo, N., Bhasin, K. K., Mehta, S. K., and Suri, C. R. (2008) Synthesis and capping of water-dispersed gold nanoparticles by an amino acid: Bioconjugation and binding studies. *J. Colloid Interface Sci. 323*, 247−254.

(44) Barton, L. E., Auffan, M., Bertrand, M., Barakat, M., Santaella, C., Masion, A., Borschneck, D., Olivi, L., Roche, N., Wiesner, M. R., et al. (2014) Transformation of Pristine and Citrate-Functionalized CeO2 Nanoparticles in a Laboratory-Scale Activated Sludge Reactor. *Environ. Sci. Technol. 48*, 7289−7296.

(45) Ballester, M., Jeanbart, L., de Titta, A., Nembrini, C., Marsland, B. J., Hubbell, J. A., and Swartz, M. A. (2015) Nanoparticle conjugation enhances the immunomodulatory effects of intranasally delivered CpG in house dust mite-allergic mice. *Sci. Rep. 5*, 14274.

(46) Khan, S., Carneiro, L. S. A., Romani, E. C., Larrudé, D. G., and Aucelio, R. Q. (2014) Quantification of thyroxine by the selective photoluminescence quenching of l-cysteine−ZnS quantum dots in aqueous solution containing hexadecyltrimethylammonium bromide. *J. Lumin. 156*, 16−24.

(47) Pal, S., Mitra, K., Azmi, S., Ghosh, J. K., and Chakraborty, T. K. (2011) Towards the synthesis of sugar amino acid containing antimicrobial noncytotoxic CAP conjugates with gold nanoparticles and a mechanistic study of cell disruption. *Org. Biomol. Chem. 9*, 4806−4810.

(48) Shankar, S., and Rhim, J.-W. (2015) Amino acid mediated synthesis of silver nanoparticles and preparation of antimicrobial agar/silver nanoparticles composite films. *Carbohydr. Polym. 130*, 353−363.

(49) Zhao, M. X., Li, J. M., Du, L., Tan, C. P., Xia, Q., Mao, Z. W., and Ji, L. N. (2011) Targeted Cellular Uptake and siRNA Silencing by Quantum-Dot Nanoparticles Coated with β-Cyclodextrin Coupled to Amino Acids. *Chem. - Eur. J. 17*, 5171−5179.

(50) Fischer, M. J. E. Amine Coupling Through EDC/NHS: A Practical Approach. In *Surface Plasmon Resonance: Methods and Protocols*, Mol, N. J., and Fischer, M. J. E., Eds.; Humana Press: Totowa, NJ; 2010; pp 55−73.

(51) Zhang, Y. R., and Shen, S. L. (2014) A dual function magnetic nanomaterial modified with lysine for removal of organic dyes from water solution. *Chem. Eng. J. 239*, 250.

(52) Zhang, Y. R., and Wang, S. Q. (2013) A novel water treatment magnetic nanomaterial for removal of anionic and cationic dyes under severe condition. *Chem. Eng. J. 233*, 258.

(53) Barick, K. C., and Hassan, P. A. (2012) Glycine passivated Fe3O4 nanoparticles for thermal therapy. *J. Colloid Interface Sci. 369*, 96−102.

(54) Han, G.-M., Jiang, H.-X., Huo, Y.-F., and Kong, D.-M. (2016) Simple synthesis of amino acid-functionalized hydrophilic upconversion nanoparticles capped with both carboxyl and amino groups for bimodal imaging. *J. Mater. Chem. B 4*, 3351−3357.

(55) Lee, H. J., Jang, K.-S., Jang, S., Kim, J. W., Yang, H.-M., Jeong, Y. Y., and Kim, J.-D. (2010) Poly(amino acid)s micelle-mediated assembly of magnetite nanoparticles for ultra-sensitive long-term MR imaging of tumors. *Chem. Commun. 46*, 3559−3561.

(56) Jin, Y., Liu, F., Shan, C., Tong, M., and Hou, Y. (2014) Efficient bacterial capture with amino acid modified magnetic nanoparticles. *Water Res. 50*, 124−134.

(57) Senna, M., Myers, N., Aimable, A., Laporte, V., Pulgarin, C., Baghriche, O., and Bowen, P. (2013) Modification of titania nanoparticles for photocatalytic antibacterial activity via a colloidal route with glycine and subsequent annealing. *J. Mater. Res. 28*, 354−361.

(58) Newsholme, P. (2001) Why Is l-Glutamine Metabolism Important to Cells of the Immune System in Health, Postinjury, Surgery or Infection? *Journal of Nutrition 131*, 2515S−2522S.

(59) Sarker, S. D., Nahar, L., and Kumarasamy, Y. (2007) Microtitre plate-based antibacterial assay incorporating resazurin as an indicator of cell growth, and its application in the in vitro antibacterial screening of phytochemicals. *Methods 42*, 321−324.

(60) Hotze, E. M., Phenrat, T., and Lowry, G. V. (2010) Nanoparticle Aggregation: Challenges to Understanding Transport and Reactivity in the Environment. *J. Environ. Qual. 39*, 1909−1924.

(61) Duan, X., Ao, Z., Sun, H., Zhou, L., Wang, G., and Wang, S. (2015) Insights into N-doping in single-walled carbon nanotubes for enhanced activation of superoxides: a mechanistic study. *Chem. Commun. 51*, 15249−15252.

(62) Minami, M., Ando, T., Hashikawa, S.-n., Torii, K., Hasegawa, T., Israel, D. A., Ina, K., Kusugami, K., Goto, H., and Ohta, M. (2004) Effect of Glycine on Helicobacter pylori In Vitro. *Antimicrob. Agents Chemother. 48*, 3782−3788.

(63) Różanowska, M., Wessels, J., Boulton, M., Burke, J. M., Rodgers, M. A. J., Truscott, T. G., and Sarna, T. (1998) Blue Light-Induced Singlet Oxygen Generation by Retinal Lipofuscin in Non-Polar Media. *Free Radical Biol. Med. 24*, 1107−1112.

(64) Joondan, N., Jhaumeer-Laulloo, S., and Caumul, P. (2014) A study of the antibacterial activity of l-Phenylalanine and l-Tyrosine esters in relation to their CMCs and their interactions with 1,2-dipalmitoyl-sn-glycero-3-phosphocholine, DPPC as model membrane. *Microbiol. Res. 169*, 675−685.

(65) Haug, B. E., and Svendsen, J. S. (2001) The role of tryptophan in the antibacterial activity of a 15-residue bovine lactoferricin peptide. *J. Pept. Sci. 7*, 190−196.

(66) Singer, A. C., Shaw, H., Rhodes, V., and Hart, A. (2016) Review of Antimicrobial Resistance in the Environment and Its Relevance to Environmental Regulators. *Front. Microbiol. 7*, 1 DOI: 10.3389/fmicb.2016.01728.

(67) Allahverdiyev, A. M., Kon, K. V., Abamor, E. S., Bagirova, M., and Rafailovich, M. (2011) Coping with antibiotic resistance: combining nanoparticles with antibiotics and other antimicrobial agents. *Expert Rev. Anti-Infect. Ther. 9*, 1035−1052.

(68) Andersson, D. I., and Hughes, D. (2010) Antibiotic resistance and its cost: is it possible to reverse resistance? *Nat. Rev. Microbiol. 8*, 260−271.

(69) Biswas, S., Medina, S. H., and Barchi, J. J., Jr (2015) Synthesis and cell-selective antitumor properties of amino acid conjugated

tumor-associated carbohydrate antigen-coated gold nanoparticles. *Carbohydr. Res. 405*, 93−101.

(70) Shin, O.-H., Mar, M.-H., Albright, C. D., Citarella, M. T., da Costa, K.-A., and Zeisel, S. H. (1997) Methyl-group donors cannot prevent apoptotic death of rat hepatocytes induced by choline-deficiency. *J. Cell. Biochem. 64*, 196−208.

(71) Joseph, D., Tyagi, N., Geckeler, C., and Geckeler, K. E. (2014) Protein-coated pH-responsive gold nanoparticles: Microwave-assisted synthesis and surface charge-dependent anticancer activity. *Beilstein J. Nanotechnol. 5*, 1452−1462.

(72) Shi, J., Sun, X., Zou, X., and Zhang, H. (2014) Amino acid-dependent transformations of citrate-coated silver nanoparticles: Impact on morphology, stability and toxicity. *Toxicol. Lett. 229*, 17−24.

(73) Feng, Y., Su, J., Zhao, Z., Zheng, W., Wu, H., Zhang, Y., and Chen, T. (2014) Differential effects of amino acid surface decoration on the anticancer efficacy of selenium nanoparticles. *Dalton Transactions 43*, 1854−1861.

(74) Yang, H.-M., Lee, H. J., Park, C. W., Yoon, S. R., Lim, S., Jung, B. H., and Kim, J.-D. (2011) Endosome-escapable magnetic poly(amino acid) nanoparticles for cancer diagnosis and therapy. *Chem. Commun. 47*, 5322−5324.

(75) Zanganeh, S., Hutter, G., Spitler, R., Lenkov, O., Mahmoudi, M., Shaw, A., Pajarinen, J. S., Nejadnik, H., Goodman, S., Moseley, M., et al. (2016) Iron oxide nanoparticles inhibit tumour growth by inducing pro-inflammatory macrophage polarization in tumour tissues. *Nat. Nanotechnol. 11*, 986−994.

(76) Collantes, E. R., and Dunn, W. J. (1995) Amino Acid Side Chain Descriptors for Quantitative Structure-Activity Relationship Studies of Peptide Analogs. *J. Med. Chem. 38*, 2705−2713.

(77) Sindrilaru, A., Peters, T., Wieschalka, S., Baican, C., Baican, A., Peter, H., Hainzl, A., Schatz, S., Qi, Y., Schlecht, A., et al. (2011) An unrestrained proinflammatory M1 macrophage population induced by iron impairs wound healing in humans and mice. *J. Clin. Invest. 121*, 985−997.

(78) Liu, X., Rocchi, P., and Peng, L. (2012) Dendrimers as non-viral vectors for siRNA delivery. *New J. Chem. 36*, 256−263.

(79) Zabot, G. P., Carvalhal, G. F., Marroni, N. P., Hartmann, R. M., da Silva, V. D., and Fillmann, H. S. (2014) Glutamine prevents oxidative stress in a model of mesenteric ischemia and reperfusion. *World Journal of Gastroenterology: WJG 20*, 11406−11414.

(80) Cai, H., and Yao, P. (2014) Gold nanoparticles with different amino acid surfaces: Serum albumin adsorption, intracellular uptake and cytotoxicity. *Colloids Surf., B 123*, 900−906.

(81) Yu, Z.-Z., Wu, Q.-H., Zhang, S.-L., Miao, J.-Y., Zhao, B.-X., and Su, L. (2016) Two novel amino acid-coated super paramagnetic nanoparticles at low concentrations label and promote the proliferation of mesenchymal stem cells. *RSC Adv. 6*, 10159−10161.

(82) Berghian-Grosan, C., Olenic, L., Katona, G., Perde-Schrepler, M., and Vulcu, A. (2014) l-Leucine for gold nanoparticles synthesis and their cytotoxic effects evaluation. *Amino Acids 46*, 2545−2552.

(83) Yen, H.-J., Hsu, S.-h., and Tsai, C.-L. (2009) Cytotoxicity and Immunological Response of Gold and Silver Nanoparticles of Different Sizes. *Small 5*, 1553−1561.

(84) Misawa, M., and Takahashi, J. (2011) Generation of reactive oxygen species induced by gold nanoparticles under x-ray and UV Irradiations. *Nanomedicine 7*, 604−614.

(85) Kim, T.-H., Kim, M., Park, H.-S., Shin, U. S., Gong, M.-S., and Kim, H.-W. (2012) Size-dependent cellular toxicity of silver nanoparticles. *J. Biomed. Mater. Res., Part A 100A*, 1033−1043.

(86) Huang, K., Ma, H., Liu, J., Huo, S., Kumar, A., Wei, T., Zhang, X., Jin, S., Gan, Y., Wang, P. C., et al. (2012) Size-Dependent Localization and Penetration of Ultrasmall Gold Nanoparticles in Cancer Cells, Multicellular Spheroids, and Tumors in Vivo. *ACS Nano 6*, 4483−4493.

(87) Oh, E., Delehanty, J. B., Sapsford, K. E., Susumu, K., Goswami, R., Blanco-Canosa, J. B., Dawson, P. E., Granek, J., Shoff, M., Zhang, Q., et al. (2011) Cellular Uptake and Fate of PEGylated Gold Nanoparticles Is Dependent on Both Cell-Penetration Peptides and Particle Size. *ACS Nano 5*, 6434−6448.

(88) Chithrani, B. D., Ghazani, A. A., and Chan, W. C. W. (2006) Determining the Size and Shape Dependence of Gold Nanoparticle Uptake into Mammalian Cells. *Nano Lett. 6*, 662−668.

(89) Kettler, K., Krystek, P., Giannakou, C., Hendriks, A. J., and de Jong, W. H. (2016) Exploring the effect of silver nanoparticle size and medium composition on uptake into pulmonary epithelial 16HBE14o-cells. *J. Nanopart. Res. 18*, 182.

(90) Shahabi, S., Treccani, L., and Rezwan, K. (2015) Amino acid-catalyzed seed regrowth synthesis of photostable high fluorescent silica nanoparticles with tunable sizes for intracellular studies. *J. Nanopart. Res. 17*, 1−15.

(91) Yang, P., Singh, J., Wettig, S., Foldvari, M., Verrall, R. E., and Badea, I. (2010) Enhanced gene expression in epithelial cells transfected with amino acid-substituted gemini nanoparticles. *Eur. J. Pharm. Biopharm. 75*, 311−320.

(92) Jin, L., Zeng, X., Liu, M., Deng, Y., and He, N. (2014) Current Progress in Gene Delivery Technology Based on Chemical Methods and Nano-carriers. *Theranostics 4*, 240−255.

(93) Cherif, M. S., Mbanefo, E. C., Shuaibu, M. N., Kodama, Y., Avenido, E. F., Campos-Alberto, E., Mizukami, S., Camara, F., Helegbe, G. K., Kikuchi, M., et al. (2016) Human-applicable dendrigraft poly-l-lysine-based nanoparticle-coated Plasmodium yoe-lii-transamidase DNA vaccine is immunogenic and protective as the polyethylenimine-based formulation. *J. Bioact. Compat. Polym. 31*, 334−347.

(94) Ghosh, P. S., Kim, C.-K., Han, G., Forbes, N. S., and Rotello, V. M. (2008) Efficient Gene Delivery Vectors by Tuning the Surface Charge Density of Amino Acid-Functionalized Gold Nanoparticles. *ACS Nano 2*, 2213−2218.

(95) Ghosh, P. S., Han, G., Erdogan, B., Rosado, O., Krovi, S. A., and Rotello, V. M. (2007) Nanoparticles Featuring Amino Acid-function-alized Side Chains as DNA Receptors. *Chem. Biol. Drug Des. 70*, 13−18.

(96) Barua, S., and Mitragotri, S. (2014) Challenges associated with Penetration of Nanoparticles across Cell and Tissue Barriers: A Review of Current Status and Future Prospects. *Nano Today 9*, 223−243.

(97) Nawwab Al-Deen, F. M., Selomulya, C., Kong, Y. Y., Xiang, S. D., Ma, C., Coppel, R. L., and Plebanski, M. (2014) Design of magnetic polyplexes taken up efficiently by dendritic cell for enhanced DNA vaccine delivery. *Gene Ther. 21*, 212−218.

(98) Theerdhala, S., Bahadur, D., Vitta, S., Perkas, N., Zhong, Z., and Gedanken, A. (2010) Sonochemical stabilization of ultrafine colloidal biocompatible magnetite nanoparticles using amino acid, l-arginine, for possible bio applications. *Ultrason. Sonochem. 17*, 730−737.

(99) Xia, Y.-S., and Zhu, C.-Q. (2009) Interaction of CdTe nanocrystals with thiol-containing amino acids at different pH: a fluorimetric study. *Microchim. Acta 164*, 29−34.

(100) Suhag, D., Singh, A., Chattopadhyay, S., Chakrabarti, S., and Mukherjee, M. (2015) Hydrothermal synthesis of nitrogen doped graphene nanosheets from carbon nanosheets with enhanced electro-catalytic properties. *RSC Adv. 5*, 39705−39713.

(101) Jackowska, K., and Krysinski, P. (2013) New trends in the electrochemical sensing of dopamine. *Anal. Bioanal. Chem. 405*, 3753−3771.

(102) Wang, X., Zhang, F., Xia, J., Wang, Z., Bi, S., Xia, L., Li, Y., Xia, Y., and Xia, L. (2015) Modification of electrode surface with covalently functionalized graphene oxide by l-tyrosine for determination of dopamine. *J. Electroanal. Chem. 738*, 203−208.

(103) Huang, S., Zhu, F., Xiao, Q., Su, W., Sheng, J., Huang, C., and Hu, B. (2014) A CdTe/CdS/ZnS core/shell/shell QDs-based "OFF-ON" fluorescent biosensor for sensitive and specific determination of l-ascorbic acid. *RSC Adv. 4*, 46751−46761.

(104) Tan, X., Yang, J., Li, Q., and Yang, Q. (2015) Detection of glutathione with an "off-on" fluorescent biosensor based on N-acetyl-l-cysteine capped CdTe quantum dots. *Analyst 140*, 6748−6757.

(105) Raghav, R., and Srivastava, S. (2016) Immobilization strategy for enhancing sensitivity of immunosensors: L-Asparagine−AuNPs as a promising alternative of EDC−NHS activated citrate−AuNPs for antibody immobilization. *Biosens. Bioelectron. 78*, 396−403.

(106) Coussy, F., Chéreau, E., Daraï, E., Dhombres, F., Lotz, J. P., Rouzier, R., and Selle, F. (2011) Intérêt du dosage du CA 125 dans la prise en charge du cancer de l'ovaire. *Gynécologie Obstétrique & Fertilité* 39, 296−301.

(107) Perez, J. M., Simeone, F. J., Saeki, Y., Josephson, L., and Weissleder, R. (2003) Viral-Induced Self-Assembly of Magnetic Nanoparticles Allows the Detection of Viral Particles in Biological Media. *J. Am. Chem. Soc.* 125, 10192−10193.

(108) Tsai, H. Y., Hsu, C. F., Chiu, I. W., and Fuh, C. B. (2007) Detection of C-Reactive Protein Based on Immunoassay Using Antibody-Conjugated Magnetic Nanoparticles. *Anal. Chem.* 79, 8416−8419.

(109) Spindler, X., Hofstetter, O., McDonagh, A. M., Roux, C., and Lennard, C. (2011) Enhancement of latent fingermarks on non-porous surfaces using anti-l-amino acid antibodies conjugated to gold nanoparticles. *Chem. Commun.* 47, 5602−5604.

(110) De, M., Ghosh, P. S., and Rotello, V. M. (2008) Applications of Nanoparticles in Biology. *Adv. Mater.* 20, 4225−4241.

(111) Riu, J., Maroto, A., and Rius, F. X. (2006) Nanosensors in environmental analysis. *Talanta* 69, 288−301.

(112) Wang, Y., Anilkumar, P., Cao, L., Liu, J.-H., Luo, P. G., Tackett, K. N., Sahu, S., Wang, P., Wang, X., and Sun, Y.-P. (2011) Carbon dots of different composition and surface functionalization: cytotoxicity issues relevant to fluorescence cell imaging. *Exp. Biol. Med.* 236, 1231−1238.

(113) Sarkar, S., Das, K., Ghosh, M., and Das, P. K. (2015) Amino acid functionalized blue and phosphorous-doped green fluorescent carbon dots as bioimaging probe. *RSC Adv.* 5, 65913−65921.

(114) Arslan, O., Singh, A. P., Belkoura, L., and Mathur, S. (2013) Cysteine-functionalized zwitterionic ZnO quantum dots. *J. Mater. Res.* 28, 1947−1954.

(115) Pujalté, I., Passagne, I., Brouillaud, B., Tréguer, M., Durand, E., Ohayon-Courtès, C., and L'Azou, B. (2011) Cytotoxity and oxidative stress induced by different metallic nanoparticles on human kidney cells. *Part. Fibre Toxicol.* 8, 10.

(116) Palasz, A., and Czekaj, P. (2000) Toxicological and cytophysiological aspects of lanthanides action. *Acta Biochim. Pol.* 47, 1107−1114.

(117) Saturnino, C., Bortoluzzi, M., Napoli, M., Popolo, A., Pinto, A., Longo, P., and Paolucci, G. (2013) New insights on cytotoxic activity of group 3 and lanthanide compounds: complexes with [N, N,N]-scorpionate ligands. *J. Pharm. Pharmacol.* 65, 1354−1359.

(118) Mazuel, F., Espinosa, A., Luciani, N., Reffay, M., Le Borgne, R., Motte, L., Desboeufs, K., Michel, A., Pellegrino, T., Lalatonne, Y., et al. (2016) Massive Intracellular Biodegradation of Iron Oxide Nanoparticles Evidenced Magnetically at Single-Endosome and Tissue Levels. *ACS Nano* 10, 7627−7638.

(119) Yang, H.-M., Park, C. W., Woo, M.-A., Kim, M. I., Jo, Y. M., Park, H. G., and Kim, J.-D. (2010) HER2/neu Antibody Conjugated Poly(amino acid)-Coated Iron Oxide Nanoparticles for Breast Cancer MR Imaging. *Biomacromolecules* 11, 2866−2872.

(120) Vaine, C. A., Patel, M. K., Zhu, J., Lee, E., Finberg, R. W., Hayward, R. C., and Kurt-Jones, E. A. (2013) Tuning Innate Immune Activation by Surface Texturing of Polymer Microparticles: The Role of Shape in Inflammasome Activation. *J. Immunol.* 190, 3525−3532.

(121) Xing, R., Zhang, F., Xie, J., Aronova, M., Zhang, G., Guo, N., Huang, X., Sun, X., Liu, G., Bryant, L. H., et al. (2011) Polyaspartic acid coated manganese oxide nanoparticles for efficient liver MRI. *Nanoscale* 3, 4943−4945.

(122) Perego, D., Masciocchi, N., Guagliardi, A., Manuel Dominguez-Vera, J., and Galvez, N. (2013) Poly(amino acid) functionalized maghemite and gold nanoparticles. *Nanotechnology* 24, 075102.

(123) Kusaka, T., Nakayama, M., Nakamura, K., Ishimiya, M., Furusawa, E., and Ogasawara, K. (2014) Effect of Silica Particle Size on Macrophage Inflammatory Responses. *PLoS One* 9, e92634.

(124) Guo, C., Xia, Y., Niu, P., Jiang, L., Duan, J., Yu, Y., Zhou, X., Li, Y., and Sun, Z. (2015) Silica nanoparticles induce oxidative stress, inflammation, and endothelial dysfunction in vitro via activation of the MAPK/Nrf2 pathway and nuclear factor-κB signaling. *Int. J. Nanomed.* 10, 1463−1477.

(125) Kim, J.-S., Yoon, T.-J., Yu, K.-N., Noh, M. S., Woo, M., Kim, B.-G., Lee, K.-H., Sohn, B.-H., Park, S.-B., Lee, J.-K., et al. (2006) Cellular uptake of magnetic nanoparticle is mediated through energy-dependent endocytosis in A549 cells. *J. Vet Sci.* 7, 321−326.

(126) Akagi, T., Wang, X., Uto, T., Baba, M., and Akashi, M. (2007) Protein direct delivery to dendritic cells using nanoparticles based on amphiphilic poly(amino acid) derivatives. *Biomaterials* 28, 3427−3436.

(127) Kim, H., Uto, T., Akagi, T., Baba, M., and Akashi, M. (2010) Amphiphilic Poly(Amino Acid) Nanoparticles Induce Size-Dependent Dendritic Cell Maturation. *Adv. Funct. Mater.* 20, 3925−3931.

(128) Fröhlich, E. (2012) The role of surface charge in cellular uptake and cytotoxicity of medical nanoparticles. *Int. J. Nanomed.* 7, 5577−5591.

(129) Thomas, C., Gupta, V., and Ahsan, F. (2009) Influence of surface charge of PLGA particles of recombinant hepatitis B surface antigen in enhancing systemic and mucosal immune responses. *Int. J. Pharm.* 379, 41−50.

(130) Sadeghiani, N., Barbosa, L. S., Guedes, M. H. A., Chaves, S. B., Santos, J. G., Silva, O., Pelegrini, F., Azevedo, R. B., Morais, P. C., and Lacava, Z. G. M. (2005) Magnetic resonance of polyaspartic acid-coated magnetite nanoparticles administered in mice. *IEEE Trans. Magn.* 41, 4108−4110.

(131) Decuzzi, P., Pasqualini, R., Arap, W., and Ferrari, M. (2009) Intravascular Delivery of Particulate Systems: Does Geometry Really Matter? *Pharm. Res.* 26, 235.

(132) Saptarshi, S. R., Duschl, A., and Lopata, A. L. (2013) Interaction of nanoparticles with proteins: relation to bio-reactivity of the nanoparticle. *J. Nanobiotechnol.* 11, 26.

(133) Arvizo, R. R., Miranda, O. R., Moyano, D. F., Walden, C. A., Giri, K., Bhattacharya, R., Robertson, J. D., Rotello, V. M., Reid, J. M., and Mukherjee, P. (2011) Modulating Pharmacokinetics, Tumor Uptake and Biodistribution by Engineered Nanoparticles. *PLoS One* 6, e24374.

(134) Arruebo, M., Valladares, M., and González-Fernández, Á. (2009) Antibody-Conjugated Nanoparticles for Biomedical Applications. *J. Nanomater.* 2009, 24.

(135) Fay, F., and Scott, C. J. (2011) Antibody-targeted nanoparticles for cancer therapy. *Immunotherapy* 3, 381−394.

(136) Goodall, S., Jones, M. L., and Mahler, S. (2015) Monoclonal antibody-targeted polymeric nanoparticles for cancer therapy − future prospects. *J. Chem. Technol. Biotechnol.* 90, 1169−1176.

(137) Mitragotri, S., Burke, P. A., and Langer, R. (2014) Overcoming the challenges in administering biopharmaceuticals: formulation and delivery strategies. *Nat. Rev. Drug Discovery* 13, 655−672.

(138) Parween, S., Ali, A., and Chauhan, V. S. (2013) Non-natural Amino Acids Containing Peptide-Capped Gold Nanoparticles for Drug Delivery Application. *ACS Appl. Mater. Interfaces* 5, 6484−6493.

Insights into endotoxin-mediated lung inflammation and future treatment strategies

Amlan Chakraborty, Jennifer C. Boer, Cordelia Selomulya, Magdalena Plebanski & Simon G. Royce

Taylor & Francis
Taylor & Francis Group

REVIEW

Check for updates

Insights into endotoxin-mediated lung inflammation and future treatment strategies

Amlan Chakraborty [a,b], Jennifer C. Boer[b], Cordelia Selomulya[a], Magdalena Plebanski[b,c] and Simon G. Royce[d,e]

[a]Department of Chemical Engineering, Monash University, Clayton, Australia; [b]Department of Immunology and Pathology, Central Clinical School, Monash University, Melbourne, Australia; [c]School of Health and Biomedical Sciences and Enabling Capability platforms, Biomedical and Health Innovation, RMIT University, Melbourne, Australia; [d]Central Clinical School, Monash University, Clayton, Victoria, Australia; [e]Department of Pharmacology, Monash University, Clayton, Australia

ABSTRACT

Introduction: Airway inflammatory disorders are prevalent diseases in need of better management and new therapeutics. Immunotherapies offer a solution to the problem of corticosteroid resistance.

Areas covered: The current review focuses on lipopolysaccharide (Gram-negative bacterial endotoxin)-mediated inflammation in the lung and the animal models used to study related diseases. Endotoxin-induced lung pathology is usually initiated by antigen presenting cells (APC). We will discuss different subsets of APC including lung dendritic cells and macrophages, and their role in responding to endotoxin and environmental challenges.

Expert commentary: The pharmacotherapeutic considerations to combat airway inflammation should cost-effectively improve quality of life with sustainable and safe strategies. Selectively targeting APCs in the lung offer the potential for a promising new strategy for the better management and treatment of inflammatory lung disease.

1. Introduction

Inflammatory lung diseases such as asthma and chronic obstructive pulmonary disease (COPD) are very common with over 4 million deaths per year [1]. Apart from rising levels of pollution, other factors such as bacteria, irritants, avian-derived proteins, and agricultural dusts can lead to inflammation of the airway. The lung is a non-sterile organ as it is in direct contact with the outside environment including bacteria. Their cell walls are composed of lipopolysaccharide (LPS), hence this is a major contributor to the development of airway inflammation [2,3]. However, immune recognition and response to LPS also play a role in the defense against invading Gram-negative bacteria. Antigen presenting cells (APCs) in the lung, such as alveolar macrophages (AMs) and dendritic cells (DC), express a class of receptors called Toll-like receptors (TLRs). LPS binds to TLR4 with support from the protein MD-2, forming a complex enabling the adapter protein MyD88 to signal further downstream. MyD88 activates a cascade of proteins which leads to the activation of the nuclear transcription factor NF-κβ. The activation of NF-κβ leads to the production of inflammatory mediators such as interleukin IL-6, IL-1β, tumor necrosis factor α (TNF-α) which have microbicidal activities. AMs express many pattern recognition receptors (pathogen-associated molecular patterns [PAMPs]) and are able to phagocytose bacteria. They are also involved in preventing access of lung DCs to bacteria and further limit the antigen presenting response of these DCs. Other than bacteria, viral infections including rhinovirus, can lead to inflammation in the

lung. The infection leads to severe wheezing episodes and recurrent episodes of asthma. Viral infection-mediated lung inflammation is beyond the scope of this review but is reviewed by Woodlands and Wang et al. [4,5].

The TLR agonist LPS is known to increase airway hyper-responsiveness (AHR) [6]. AHR is defined by an exaggerated response of the airways to nonspecific stimuli, which results in airway obstruction and contraction of airways triggered by bronchospasm. Inflammation of the airways is characterized by AHR, airway epithelial mucous production, and allergen-specific Th2 cytokines in the lung-draining lymph nodes [7]. These processes are orchestrated by APCs such as DCs and macrophages (Mφs). AHR is a key feature in diseases such as asthma and COPD. Asthma is a form of bronchial disorder caused by inflammation of the bronchi. It is characterized by spasmodic contraction of airway smooth muscle, difficulty breathing, wheezing, and coughing. COPD on the other hand is characterized by poorly reversible airway obstruction, which is confirmed by spirometry, and includes obstruction of the small airways (chronic obstructive broncholitis), emphysema, which leads to air trapping and shortness of breath in response to physical exertion [8]. Asthma and COPD are differentiated by the inflammation type, cause, and extent. If the airway inflammatory process occurs in the peripheral lung wall, it signifies COPD, whereas inflammation in the airways of the central and distal areas of the lung is observed mostly in asthma. The pathophysiology of COPD involves an increased number of goblet cells, mucous gland hyperplasia, fibrosis,

and reduction of small airways (peripheral airways) accompanied by narrowing [9]. In the central and distal airways of the lung, there is upregulation of Th2 cytokines and inflammatory cells [10]. Bronchoscopic sampling has been limited to proximal airways of the lung. Therefore, studies with the distal airways (i.e. small airways) are limited. When airway inflammation becomes chronic in asthma, it leads to airway remodeling, characterized by airway fibrosis, epithelial damage, and smooth muscle hyperplasia [11].

Moreover, in many respects, such as respiratory symptoms, asthma and COPD are quite similar. COPD involves increased aging of the lungs and an aberrated repair mechanism driven by oxidative stress. Potential factors that lead to the development of these diseases could have inherited or atopic component or acquired. Whilst many patients have demonstrated a family history of the diseases, no single gene responsible showing Mendelian inheritance has been identified. There is a stronger predisposition of the disease or be acquired due to environmental factors including ultrafine particulates in air [12], large farm animals [13], cigarette smoking [14], house dust mites [15], and endotoxins from Gram-negative bacteria [16]. Non-atopic causes of asthma include viral and bacterial respiratory infections. Endotoxin such as LPS can mediate other diseases such as osteoarthritis [17], congestive heart disease, and coronary artery disease [18].

In airway inflammatory disease such as asthma, impaired breathing due to bronchoconstriction leads to repeated/routine exacerbations which impacts human health. Therefore, not only availability of anti-inflammatory drugs but proper management is essential. Current treatments include the use of bronchodilators and anti-inflammatory drugs such as corticosteroids (e.g. prednisone, beclomethasone, fluticasone) and cromolyn in pediatric therapy. In adults, an inhaled corticosteroid with a low dose of short-acting beta-2-agonist is used as a gold standard therapy. An alternative therapy uses leukotriene-receptor agonist combined with long-acting beta-2-agonist. These drugs reduce eosinophil and neutrophil infiltration as well as the secretion of pro-inflammatory cytokines. But the prolonged use of these drugs may cause adverse effects such as impaired growth in children, decreased bone mineral density, skin thinning, bruising, and cataracts [19]. Furthermore, the usage of these anti-inflammatory drugs and bronchodilators has led to the development of resistance and hence requires the development of new anti-inflammatories associated with systemic or oral administration [20].

Novel anti-inflammatories would cater to the pharmacotherapeutic considerations and give both an immediate and sustaining effect without having adverse side effects. In this review, we discuss on endotoxin-mediated inflammation in the lung and the mechanisms which are pivotal. Endotoxin involves different cells of the immune system in generating a response. Therefore, we explore the two most important APCs, DCs and Mφs along with their subsets, to gain an insight at the cellular level in the development of therapeutics. With the knowledge of the immune cells and endotoxin-mediated inflammation, we finally introduce new strategies for therapeutics including better management and treatment of lung disease.

2. Inflammation of the airway

Inflammation is a phenomenon of the body in the form of an immediate response to triggers like tissue injury, infection by pathogens, or by noxious chemicals [21]. Based on the duration of response, inflammation is characterized by acute and chronic inflammation. Acute inflammation is generally short term with an early (IgE-mediated hypersensitivity type I reaction) and late phase reaction associated with Th2 cells [22]. Acute inflammation lasts for around 2 days, and symptoms are dependent on the region of inflammation such as bronchial smooth muscle contraction [23] due to various types of airway allergens. On the other hand, chronic inflammation lasts for over 6 months. Chronic inflammation is a feature of both asthma and COPD. In patients with COPD, it has been found that IL-33 is responsible for chronic inflammation and leads to enhanced secretion of pro-inflammatory cytokines [24]. Similarly, IL-33 is responsible for increased AHR, inflammation, and remodeling in asthma [25]. However, persistent exposure to a certain allergen results in the recruitment of cells of the innate and adaptive immune response to the site of exposure [22]. The nature of inflammation is different in asthma and COPD. In asthma, the nature of inflammation is driven by the infiltration of eosinophils and CD4+ T cells, whereas in COPD, it is mostly driven by neutrophils and CD8+ T cells [26]. The chronic inflammation in asthma is alluded to frequent wheezing episodes with increased AHR and coughing, whereas in COPD, it is more of limited airflow to the lung.

The most obvious effect observed with airway inflammation is the recruitment of eosinophils. Th2 lymphocytes release interleukin 5 (IL-5) which attracts, activates, and stimulates eosinophils, therefore, perpetuating the inflammatory response [27]. In inflammatory response, the airway walls become thickened due to hypertrophic and hyperplastic mucus glands as well as infiltration of Mφs, neutrophils, and cytotoxic T lymphocytes (CTLs) as well as proliferation of resident structural cells in the chronic setting [28,29]. Cytokines such as interleukin 8 (IL-8) and TNF-α are released by the inflammatory cells leading to tissue damage and oxidative stress. The entry of an allergen is associated with a complex response in the host as different immune cells play their role in dealing with the allergen. The understanding of the cells and the cytokines they produce can serve as therapeutic targets. Therefore, we need to gain insight on how airway inflammation takes place after allergen entry.

2.1. Mechanistic insights in airway inflammation

The airway lumen contains mucous for the entrapment of dust particles but is still exposed to antigens (bacteria and its cell wall component, LPS) which are processed by the submucosal DCs leading to activation and migration to lymph nodes. The immune response to acute inflammation sensitizes the mast cells in the individual due to the production of IgE specific to the antigen (Figure 1). Although the response is seen in the mast cell, the TH2 cytokines actively play a role in activating the B cells for the production of the antigen-specific IgE [22]. The sensitization releases mediators including amines like histamines and serotonin. This series of steps induces bronchoconstriction of
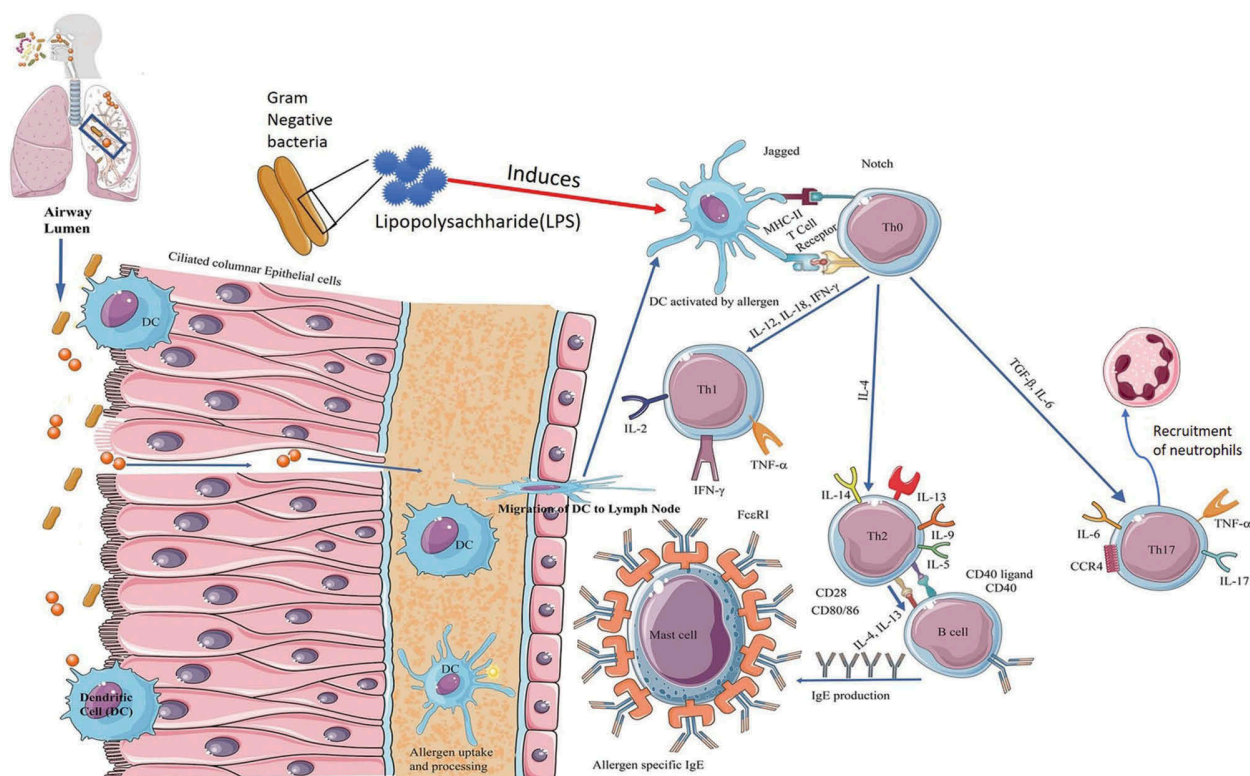
186

Figure 1. Sensitization of dendritic cells by allergens in the airway lumen. Different bacteria enter through the nasal cavity into the lung. In the airway lumen, these bacteria are captured by the patrolling DCs. The DCs become activated by the cell wall component LPS of Gram-negative bacteria. The mature DCs then migrate to the regional lymph node such as the mediastinal lymph node for lungs. At the LN, they present the processed allergen by MHCII to naïve T cells. The naïve T cells acquire the characteristics of Th2 cells by the interaction of MHCII and jagged receptor on activated DC to TCR and notch receptor respectively on naïve T cells. Two important Th2 pro-inflammatory cytokines IL-4 and IL-13 lead to ligation of costimulatory molecules CD40 and CD80/86 on Th2 cells with CD40 L and CD28 on B cells. The activation leads the B cells to produce allergen-specific IgE which binds to the high-affinity receptor FcεRI on tissue-resident mast cells. The process sensitizes them to respond when the host is later exposed to the same bacteria and/or LPS. Modified and reproduced with permission from Ref. [142], copyright 2017 The American Chemical Society.

the airway and vasodilation (Figure 2). As a result, there is increased mucous formation and stimulation of the nociceptors on the airway. The production of several cytokines by Th2 cells results in the activation of B cells (Figure 1) which is responsible for the synthesis of allergen-specific antibodies. The antibodies in the systemic circulation move from the lymph node and bind the FcεRI receptor (Figure 1) on the mast cell. When a second invasion of the allergen is encountered, the host is already sensitized, and the response is very rapid.

In addition, mast cells rapidly release TNF-α, IL-8, TGF-β, IL-10 for the activation of other immune cells like T cells, B cells, and DCs [30]. The hypersensitivity reaction develops in 2–6 h after exposure and reaches the climax after 6–9 h [23]. Although there is a clear distinction between acute and chronic inflammation phases, it is yet unclear how local inflammation in the airway converts to chronic inflammation. Cytokines such as IL-33 have been found to induce chronic inflammation in the airway epithelium along with the enhanced production of IL-6 and IL-8 in COPD pathogenesis [24]. Several layers of the airway mucosa are affected by chronic asthma with increased numbers of goblet and mast cells along with the presence of common respiratory viruses (Figure 2) [31].

Another aspect of airway inflammation is the recruitment of neutrophils. Cells secreting IL-17 (i.e. Th17 cells) recruit neutrophils at the mucosal surface [32] (Figure 2). Because of neutrophil recruitment, there is constriction of the smooth muscle in the airway wall causing shortening of breath, in patients with COPD [33]. Along with lumen constriction, airway remodeling is also observed in both COPD and asthma. Airway remodeling is driven by the epithelial-mesenchymal trophic unit (EMTU), the interaction between structural and immune cells. Due to the increased number of neutrophils in COPD patients, there is activation of the EMTU. A successful response to an allergen is associated with its elimination, resolution, and repair phase. The inducer of inflammation can be categorized into exogenous and endogenous inducers [34]. Exogenous inducers include microbial and nonmicrobial inducers like irritants, foreign bodies, and toxins. Endogenous inducers are released from stressed or damaged cells such as heat shock proteins, uric acid, and endogenous molecules like alarmins [35], etc. reviewed in detail by Creagh and colleagues [36]. In the coming section, we will focus on bacterial endotoxin-mediated inflammation in the airway.

2.1.1. Bacterial endotoxin-mediated airway inflammation
A range of bacteria such as *Staphylococcus aureus, Pseudomonas aeruginosa, Streptococcus pneumoniae, Klebsiella pneumoniae*, and *Mycobacterium tuberculosis* cause pathological lung infections. In response to infection and tissue injury, innate immune cells of the body such as DCs, Mφs, and mast cells recognize pathogens and damaged cells
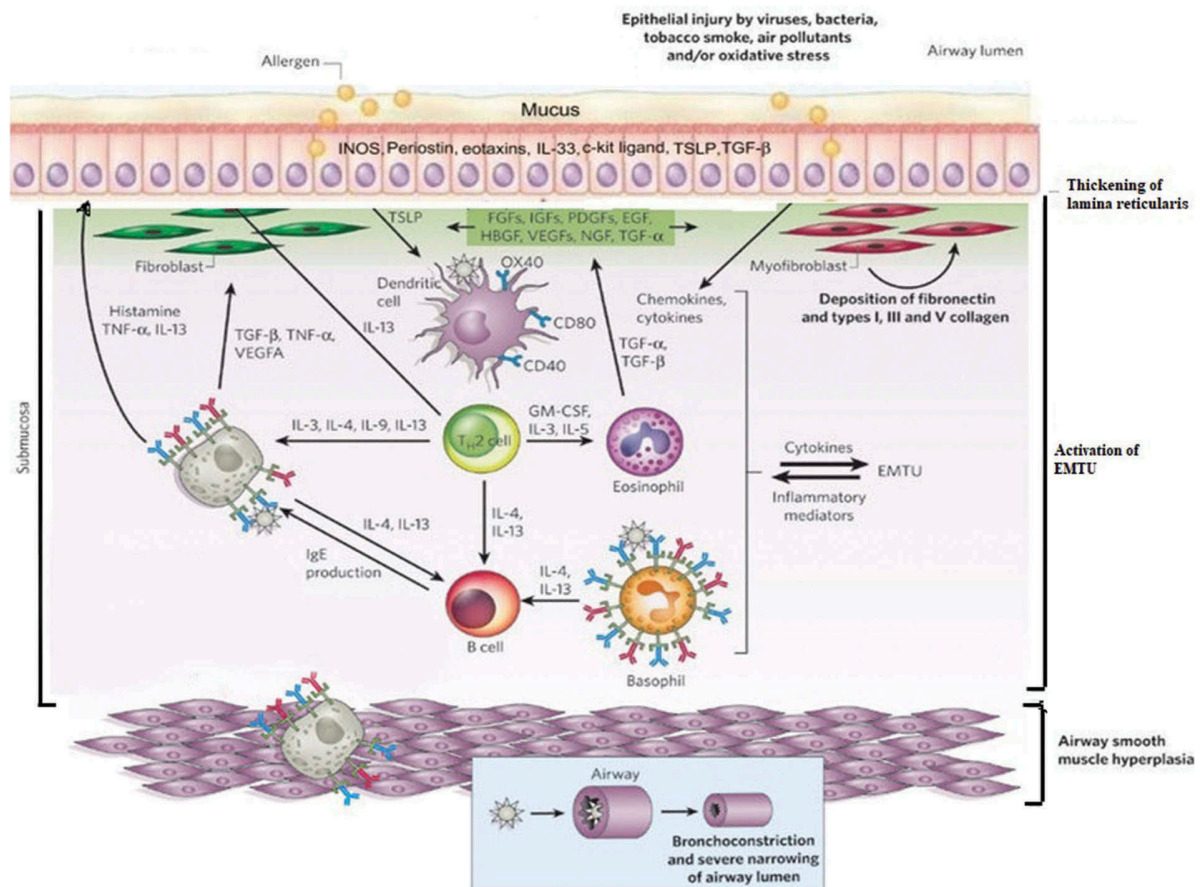
Figure 2. The chronic aspect of allergen-induced airway inflammation. Repeated and persistent exposure of allergens such as bacteria leads to chronic inflammation which has several effects. In the tissues, cells of the innate immune system including eosinophils, basophils, neutrophils, and monocyte–macrophage lineage cells are found. Other cells including Th2 cells, other types of T cells, and B cells of adaptive immune response are also present in the tissues. Mast cells develop in the tissue, and these cells display large amounts of IgE bound to FcεRI. Last, complex interactions are initiated between recruited and tissue-resident innate and adaptive immune cells, epithelial cells, and structural cells. These cells include fibroblasts, myofibroblasts, and airway smooth muscle cells along with blood vessels and lymphatic vessels. Repetitive epithelial injury due to chronic allergic inflammation can be exacerbated by exposure to pathogens or environmental factors, and the consequent repair response results in the epithelial–mesenchymal trophic unit (EMTU) being activated. This unit is thought to sustain Th2-cell-associated inflammation, to promote sensitization to additional allergens or allergen epitopes (e.g. epithelial-cell-derived TSLP can upregulate the expression of costimulatory molecules such as CD40 and CD80 by DCs). These processes result in many functionally important changes in the structure of the affected tissue such as hyperplasia of goblet cells, which is associated with increased mucous production. These changes include substantial thickening of the airway walls. In individuals who have such thickened airway walls, bronchoconstriction can result in more severe narrowing of the airway lumen than occurs in airways with normal wall thickness. In some individuals, especially those with severe asthma, Th17 cells (which secrete IL-17) may also contribute to the recruitment of neutrophils to sites of inflammation (shown in Figure 1). Modified and reproduced with permission from Ref. [22], copyright 2008 Nature.

by pattern recognition receptors (PRRs) which are germline-encoded intracellular or surface expressed. These PRRs detect PAMPs such as bacterial and viral nucleic acids and cell-wall components. The TLR family is one of the major PRRs that can detect pathogens as well as tissue damage. It induces both innate (immediate) and adaptive immune responses. Whilst the adaptive immune response results in B cells and cytotoxic T cells, it is the innate cells which offer the first line of recognition of pathogens by the TLRs. The TLRs have leucine-rich repeats and can recognize bacterial and viral PAMPs extracellularly or through endo-lysosomes. TLR1, TLR2, TLR4, TLR5, TLR6, TLR11 are extracellular whereas TLR3, TLR7, TLR8, TLR9, and TLR10 are endo-lysosomal.

LPS is the main agonist of TLR4. LPS binds to LPS binding protein, MD-2, CD14, and TLR4. Therefore, stimulation using LPS needs the participation of several molecules not just TLR4. The signaling downstream upon LPS binding has been divided into MyD88-dependent and -independent pathways. The MyD88-dependent pathway results in pro-inflammatory cytokines production whereas the MyD88-independent pathway mediates the induction of Type I interferons. MyD88 recruits and activates IRAK4 which after subsequent downstream activation induces the transcription factors NF-κβ and AP1. This results in the production of pro-inflammatory cytokines such as TNF-α, IL-1β, IL-6, IL-12, IL-23 and activation markers such as CD40, CD80, CD86, and MHCII. The LPS–TLR4 pathway has been reviewed elsewhere [37].

TLR2 responds to the cell wall of Gram-positive bacteria which is composed of peptidoglycan [38]. The TLR2 response activates cytotoxic CD8$^+$ T cells and produces IFN-γ. In AMs, the expression of TLR2 and TLR4 is reduced in patients with COPD and in smokers [39] in comparison to autologous monocytes. Continuous exposure to LPS present in cigarette smoke (cell-wall from colonized bacteria, surviving combustion during smoking) may down-modulate the pulmonary immune response [39]. The reason could be due to the natural

selection of a heterogeneous subpopulation of Mφs or a general AM phenotype under environmental stress. The reduced expression of these TLRs means that COPD patients are much more prone to lower respiratory tract infection. Bacterial infection is not only associated with the bacterial cell wall other components such as flagella are also important (recognized by TLR5 [40]). Therefore, the TLRs have a significant role in recognition of a pathogen and responding via downstream signaling. Interaction of APCs with LPS is essential in understanding the adaptive immune response.

When monocytes and DCs come in contact with a PRR, they express costimulatory molecules for T lymphocyte activation and are said to induce an adaptive immune response [41]. In an analogous way, Mφs undergo cell activation in response to LPS or IFN-γ [43]. When immature Mφs circulating in the blood come across bacterial or viral infections or bacterial components such as LPS, they undergo activation. Studies of these cells of the innate immune system by Thompson et al. and others have revealed that the subsets have specialized in secreting cytokines that have different targets and functions. For example, Mφs secrete pro-inflammatory cytokines which include IL-1, IL-6, IL-12, TNF-α, and IFN-γ [41,42]. Other than these cytokines, IL-8 secretion leads to infiltration by neutrophils and TNF-α leads to increased production of cell adhesion molecules in the lung capillary endothelial cells for neutrophil attachment. Neutrophils are self-recruiting, secreting IL-8 themselves to promote chemotactic invasion of more neutrophils [43].

As the mechanism is so complex, studying only a single factor would mean getting an incomplete picture of airway inflammation. Therefore, there is a need to study airway inflammation using different models. However, the existing models used to study the disease have some limitations as discussed in the following section.

2.1.2. Role of LPS in acute pulmonary inflammation

Acute pulmonary inflammation has a high mortality rate with the absence of specific treatment. Acute lung injury (ALI) is defined as an acute lung disease characterized by rapid onset respiratory failure, severe hypoxemia, and decrease in static respiratory system compliance which accounts for morbidity of around 40% [44]. Pulmonary inflammation in the acute phase (1–6 days) is characterized by damaged endothelium and surface epithelium along with edema, with neutrophil and Mφ accumulation. The clinical condition of pulmonary inflammation is known as Acute Respiratory Distress syndrome (ARDS) which is characterized by sepsis, pneumonia, and major trauma. The injury to the lung epithelium and endothelium is caused primarily by neutrophils and platelets. However, there is lack of successful pharmacologic therapy. The pathophysiology and resolution of ARDS have been reviewed previously [44]. Therefore, the role of neutrophils in initiating the inflammation and the damage it causes needs to be understood.

Neutrophils are the first immune cells to reach the site of inflammation in the lung post an insult with LPS. Transmigrated neutrophils then secrete proteolytic enzymes and reactive oxygen species (ROS) which damages the lung endothelium and epithelium. The harm does not end in edema. The ROS leads to

promutagenic alterations in DNA and causes a carcinogenic response post-chronic inflammation. Transcriptome analysis by Güngör and colleagues showed 218 genes which are differentially expressed with LPS induction in the presence of neutrophils [45]. Many pathways were found altered. Importantly complement pathways, CCR3 signaling, IL-10 signaling, and antigen presentation by MHCI were altered between LPS with and without neutrophils. CCR3 is responsible for eosinophil activation pointing toward a chronic inflammatory state. Whereas, IL-10 a pleiotropic anti-inflammatory cytokine represses the pro-inflammatory cytokines TNF-α, IL-6, and IL-1β secreted by Mφs. Pharmacotherapeutic studies using proteins such as B7H3 and bufexamac have showed potential in attenuating LPS-induced injury [46,47]. This opens the possibility of utilizing these molecules in ameliorating the clinical condition of pulmonary inflammation. Vascular compartments, pulmonary tissue, and the underlying endothelial cells are also affected by LPS. Since LPS affects vascular compartments and pulmonary tissue, therefore, the factors which alter them need to be studied.

It has been observed that higher concentrations of endotoxin similar to that present in sepsis exhibit several pro-inflammatory responses. These responses include the increased expression of cell adhesion molecules, ROS production, loss of endothelial monolayer integrity, and barrier function [48]. ROS generated in the vasculature from endothelial cells are produced from a family of oxidases. These oxidases, specifically NADPH oxidases (Nox), are involved in lung inflammation, ischemia, and sepsis. Two Nox enzymes, Nox2 and Nox4, are responsible for endothelial cell migration and production of ROS [49]. Redox active endosomes in endothelial and other pulmonary cells generate superoxides in the endosome lumen in response to pro-inflammatory cytokines TNF-α and IL-1β. Redox active endosomes are reviewed elsewhere [50]. The loss of monolayer integrity of endothelial cells leads to leaking of the lung capillaries and as a result, the fluid fills up the alveolar airspace causing pulmonary edema. The protein thrombomodulin (TM) and activated protein C (APC) are involved in maintaining homeostasis and vascular integrity [51]. LPS induces the expression of tissue factor on vascular endothelial cells causing hypercoagulability. The TM/APC axis is also affected with LPS. A lectin-like domain in TM is essential for survival of mice exposed to LPS. Absence of the domain leads to neutrophil infiltration. In the naïve lung, the polymorphonuclear leukocytes appear to be marginated to the vascular wall. During inflammation, immune cells and pre-marginated cells undergo transendothelial and transepithelial migration into alveolar space and the interstitium in the lung.

2.2. ALI model to study endotoxin mediated inflammation

ALI is characterized by alveolar epithelial and endothelial damage. This leads to secretion of pro-inflammatory mediators in the host along with severe hypoxemia, pulmonary edema. To study the pathophysiological mechanism of ALI, treatment of laboratory animals with bacterial LPS is the most accepted model. LPS can be administered directly or indirectly

to give injury to the lung. Direct administration of LPS into the lung involves intratracheal or intranasal administration, otherwise it is administered intraperitoneally. Direct injury to the lung affects the lung epithelium, whereas an indirect injury leads to disruption of the vascular endothelium. Not limited to this, there are several differences between direct and indirect challenge, such as less edema is observed in indirect injury which have been reviewed by others [52]. Administration of LPS directly in the lung leads to neutrophil recruitment within 4 h and induces the production of pro-inflammatory cytokines, chemokines, activation markers, and adhesion molecules leading to damage to the lung tissue. The acute lung injury model is reviewed elsewhere [53,54].

The ALI model is useful for studying lung inflammation but needs addition of specific end points to replicate the physical aspects of the disease. For example, introducing plethysmography as a readout for resistance and dynamic compliance is useful when demonstrating the severity of the disease. Other non-invasive techniques such as nebulization are effective in administering LPS. The method is of clinical relevance in studying and designing trials. With fluorescent molecules which can be conjugated to antibodies, it is possible to visually study emphysema and airway constriction. Therefore, live imaging of the tissue coupled with plethysmography would be an ideal solution to understand lung injury in detail and for the development of minimally invasive ways to study drug responses.

2.3. Agents targeting inflammatory pathways

Th2 inflammation involves the activation of effector responses evolved against multicellular parasites such as helminths. Th2 cells provide help to B cells for antibody production especially for IgE class switching. Two main cytokines (IL-4 and IL-13) characterize Th2 inflammation. IL-4 differentiates naïve CD4$^+$ T cells to Th2 phenotype and participates in the chemotaxis of eosinophils and class switching of IgE. IL-13 not only influences eosinophil chemotaxis and class switching of IgE but also mediates goblet cell metaplasia and smooth muscle contractility [55]. Therefore, these two cytokines are prime targets in inflammatory pathways. Several humanized monoclonal antibodies have been made to target these cytokines but are discontinued either because the primary goals are not met or due to failure to inhibit the cytokines toward activation of the inflammatory pathways. Summary of the antibodies directed toward the blocking of IL-4 and IL-13 is reviewed elsewhere [55]. Out of all the trialed antibodies, dupilumab and lebrikizumab were able to decrease the chemokine CCL17 thereby preventing the induction and chemotaxis of T cells [56,57]. These biologics also lowered the total amount of IgE. A single cytokine blocker, tralokinumab, inhibits IL-13. Tralokinumab proved to be successful at two high doses after 12 weeks of treatment [58]. However, blocking one cytokine was not beneficial in comparison to dupilumab which targeted both IL-4 and IL-13. Other anti-IL-13 antibodies such as anrukinzumab and anti-IL-4 antibodies such as pascolizumab, pitakinra have been trialed, yet dupilumab is efficient in reducing the symptoms of Th2 inflammation in asthma [59]. Since inflammation

is not only Th2 based, therefore, we focus on to another type of inflammation which involves neutrophils.

Another type of inflammation, Th17-mediated, is responsible for the recruitment of neutrophils at the site of infection. Th17-mediated inflammation aims at extracellular pathogens for an adaptive immune response. Th17 cells are responsible for the production of IL-17 family of cytokines but do not express IL-4. Pro-inflammatory effects of IL-17 include accumulation of neutrophils and proteolytic enzymes such as neutrophil elastase and MMP9 [60]. Type 3 ILCs are important for airway neutrophilia as they express IL-17A during ALI induced by LPS [61]. Earlier studies by Roos and colleagues showed that the *il17a* gene was observed only in AMs of smoke-exposed mice [61]. Furthermore, an increased expression of submucosal IL17A in lung tissue of COPD patients was observed. In asthma, IL-17A not only recruits neutrophils and releases their proteases but is also involved in negative feedback on the release of IL-23 from Mφs, therefore, constituting a Th17 regulator. This prevents excess signaling and maintains an efficient antibacterial host defense without tissue damage [60]. These observations suggest that the cytokine has a key role in the pathobiology of COPD, making it an important target for treatment. To date, many anti-IL-17 inhibitors have been developed and successfully used in other inflammatory diseases such as brodalumab (AMG827) for psoriasis. One such anti-IL-17 inhibitor, CNTO6785, was used to treat COPD as part of a phase 2 trial. Unfortunately, there was no difference in the efficacy end point in comparison to the placebo, inferring that CNTO6785 is not a successful therapeutic target for COPD [62]. Very recently, a new target for reducing airway inflammation has been found. G-CSF has been found to attenuate airway inflammation and systemic inflammation along with reduction in lung tissue destruction in a COPD model [63]. Therefore, new humanized antibodies targeting these cytokines and biomarker may be beneficial as a therapeutic target against asthma and COPD.

3. The myeloid system

Myeloid lineage cells are usually the first to respond to the invasion of a pathogen and communicate the presence of an insult to cells of the lymphoid lineage. Their origin lies with the multipotent hematopoietic stem cells. Myeloid cells can recognize damage and PAMPs through the help of germline-encoded surface receptors. When the cells lose their ability to self-renewal, they are committed to one single type of development. The myeloid lineage comprises of neutrophils, basophils, eosinophils, monocytes, mast cells, and DCs. The commitment associated with progenitor cells depends on the growth factors and cytokines. As discussed above, when induced, they express costimulatory molecules for T lymphocyte activation. A network of cells is present in the bone marrow which is responsible for providing the microenvironment for hematopoiesis; these are known as stromal cells [64]. The primary and most significant function of the myeloid system is in providing innate immunity to the body [65]. The receptors of the cells participating in innate immunity recognize broad structural motifs that are highly conserved within microbial species but are generally absent from the host.

190

These receptors are the pattern recognition receptors (described previously). The cells of the innate immune system have been found to secrete cytokines that have different targets and functions. For example, the cytokines secreted by the Mφs in Section 3.1 include pro-inflammatory cytokines such as IL-1, IL-6, IL-12, TNF-α, and IFN-α [65].

The formation of all lymphoid cell types including monocytes, Mφ, and DCs has originated from human multi-lymphoid progenitors identified as a distinct population of Thy-1^{neg-lo} CD45RA$^+$ cells in the CD34$^+$CD38$^-$ stem cell confinement[66]. Therefore, in humans, these myeloid lineages arise specifically in early lymphoid lineage. Lymph node-resident DCs (LN-DCs) are subdivided into conventional DC (cDC) subsets in mice. The subsets are CD11b and CD8a in mice whereas in humans, they are BDCA1 and BDCA3. Robbins and colleagues hence showed through clustering analysis that a distinct branch is formed in the leukocyte family with a conserved transcriptional signature in all LN-DC subsets [67]. The myeloid progenitor cells giving rise to monocytes have Mφs and DCs as their subtypes. Several surface markers like CD14, CD40, CD11b, CD64, CD68, and F4/80 (murine) or EMR1 (human), Lysozyme M, MAC-1/MAC-3 are found on Mφ which help researchers to distinguish them from monocytes [68]. DCs and Mφs share a common origin (the myeloid progenitor) but Mφ remains fixed in the tissue and DCs migrate toward the site of infection. Also, Mφ can be identified by the expression of CD64 in humans [69]. Studying the expression profile of human DCs, it has been determined that MHC II is highly expressed, whereas lineage markers like CD3 (for T cells), CD19/20 (for B cells), and CD56 (for NK cells) are absent and therefore DCs have been further classified according to these markers [70].

3.1. Mφ differentiation and subtypes

During the early stages of inflammation CCR2^{hi}Ly6C$^+$ inflammatory and CCR^{low}Ly6C$^-$ resident, monocytes differentiate into M1 and M2 Mφs, respectively [71] (see Table 1). It is possible that monocytes, Mφs, and DC are highly plastic and can cross-differentiate into different subsets in response to environmental changes by activating diverse pathways. For example, (1) Ly6C downregulation is associated with M2 Mφ function [72], (2) Ly6C$^+$ monocytes preferentially differentiate to CXC3CR1^{hi} Mφ [73], (3) CCR7 and CCR8 Ly6C^{middle} Mφ differentiate into DCs [74], and (4) anti-inflammatory M2 Mφ induction can be promoted from inflammatory monocytes by basophil-derived IL-4 at sites of inflammation [75].

When immature Mφs encounter an infection or LPS, they undergo activation. A classically activated Mφ refers to an M1 Mφ that has been activated in response to LPS or IFN-γ [76]. Cell activation of Mφ by Th1 cytokines IFN-γ and TNF-α is type I activation where the cytokines produced by M1 Mφs are IL-1β, IL-12, IL-6, and TNF-α. Alternatively, activated Mφs are also called M2 Mφ which refers to Mφs having undergone cell activation in response to IL-4 or glucocorticoids producing cytokines IL-10, IL-1ra, and TGF-β [77] (Table 1). It has been found that M1 Mφ has more expression of IL-12 and IL-23 but low IL-10 with immunostimulatory properties for Th1 cell activation. Similarly, M2 Mφ has a higher IL-10 and CD206 expression but lower levels of IL-12

and IL-23 but express scavenger receptors which M1 Mφ do not[78]. M2 Mφs are bestowed with pro-antigen presenting capacity, promote angiogenesis, tissue remodeling, and repair, suppressing immunity involving Th1 cells. They support the Th2 cell response which is deemed necessary for encapsulating and killing parasites where the M2 Mφs are activated by IL-4 and IL-13 [79]. Receptor expression in M2 Mφs is specific and higher expression of mannose receptor (MR1), Dectin-1, and arginase has been found [80].

Another category of Mφ known as M4 Mφ (Table 1) is induced by the chemokine CXCL4 from platelets [81]. A separate subset of Mφs, CD4$^+$, and CD8$^+$ Mφ kill tumor cells by a mechanism involving NKG 2D receptors, granzymes, and perforin [82]. In the tumor micro-environment, different cells provide support to the tumor cells during the transition to malignancy. The Mφs present in the tumor micro-environment play a pro-tumoral role and are called as Tumor-associated Mφs. The TAMs originate from the circulating Ly6C$^+$ CCR2$^+$ monocytes, which are derived from bone marrow hematopoietic stem cells [83]. TAMs in the resting stage express immune-suppressive cytokines IL-10, phagocyte-related receptor Msr2 and C1g, inflammatory cytokines CCL2 and CCL5, and chemokines CXCL9, CXCL10, and CXCL16 where the expression is inducible by interferons. During the activation of TAMs by LPS, several pro-inflammatory cytokines such as IL-1β, IL-6, TNF-α, and chemokine CCL3 were aberrantly expressed but upregulated the expression of immune-suppressive cytokines IL-10, TGF-β as well IFN inducible chemokines CCL5, CXCL9, CXCL10, and CXCL16 [84].

3.1.1. AMs

Alveolar Mφ defends the body against any pathogens or allergic particles, infectious agents, and toxins by preventing their entry through the nasal route (see Table 1). They remain in the lung and do not migrate to the lymph nodes, unlike DCs. Alveolar Mφ secretes a range of cytokines e.g. IL-1β, IL-6, TNF-α, and chemokines including IL-8 along with arachidonic metabolites [85]. AMs take up inhaled antigens. Polymorphonuclear neutrophils undergo apoptosis during resolution of inflammation and hence several surface markers like phosphatidylserine, loss of sialic acid residues on antigens, and lowered expression of surface CD16 moieties take place [86]. When these neutrophils undergo phagocytosis, production of anti-inflammatory cytokines such as TGF-β and IL-10 takes place along with a reduction in the levels of production of pro-inflammatory cytokines by Mφ [85].

In one study by Knapp and colleagues, it was observed that in Mφ-depleted mice, there were higher levels of TNF-α, IL-1β, and mouse chemokine KC along with activated neutrophils in the blood. AMs are the major phagocytic effector cells in the lung capable of clearing an infection. Depletion of these cells leads to high numbers of apoptotic and necrotic cells which explains the necessity of the alveolar Mφs and the lack of efficient pathogen removal without their presence. An insult to lung with LPS induces pulmonary inflammation by inducing necrosis in AMs leading to pro-IL-1α and neutrophil recruitment in the lung [87]. These CD11c$^+$ alveolar Mφs are the source of IL-23 during LPS-induced ALI which is Th17 regulator.

Table 1. A summary of the different macrophage subsets induced by LPS along with their function, markers and mediators.

Subset	Cell development	Function	Surface Markers	Cytokines produced	Chemokines induced	References
M1	They are formed from Monocytes when induced with LPS or TNF-α, IFN-α in the presence of GM-CSF	These cells promote the development of Th1 lymphocytes. They also promote metabolism of arginine into nitric oxide and citrulline. Therefore, they play a key role in the killing of pathogens and tumour cells.	They express prototypic M1 polarization markers, such as the indoleamine-pyrrole 2,3 dioxygenase; the lysosomal-associatedmembrane protein 3; IL-7R; CD86; MHCII; CD16/32; Ly6c; CD38, Gpr18; Fpr2; CD80; IL-1R I; TLR2; TLR4.	They produce pro-inflammatory cytokines: TNF-α, IL-1β, IL-6, IL-12, and IL-23. Other secretions include ROS, RNS, and iNOS	They secrete chemokines such as CCL2, CCL3, CCL4, CCL5, CCL8, CCL9, CCL10, and CCL11	[76],[80], [79], [78], [90], [91], [92], [93], [94]
M2	M2a subtype are induced by IL-4, IL-13	M2a secretes chemokines which leads to the build-up of Th2 cells, eosinophils, and basophils	They express Arg1, CD206, Egr2, c-Myc, CD163, MHCII, SR, MR, TGM2, DecoyR, IL-1R II Mice(only): Ym1, Fizz1, and Arg1	They produce IL-10, TGF-β, and IL-1Ra	They produce CCL17, CCL22, and CCL24	[95],[92], [90], [94], [93]
	M2b subtype are induced by LPS, ICs, ApC, and IL-1Ra	M2b macrophages promotes recruitment of Tregs and eosinophils that support aTh2 response	They express Arg1, CD206, Egr2, c-Myc, CD86, and MHCII	They produce TNF-α, IL-1β, IL-6, and IL-10	They only produce CCL1	[96],[90], [93], [94]
	M2c subtype are induced by IL-10, TGF-β, Gluc	They promote the development of Th2 lymphocytes and Tregs They also promote tissue regeneration and angiogenesis	They express Arg1, CD206, Egr2, c-Myc, CD163, TLR1, and TLR8	They produce IL-10, TGF-β	The only produce CCR2	[97],[90], [94][93]
	M2d induced by IL-6, LIF, and MCF	Their function is similar to ovarian TAMs but different from the other subsets	They express VEGF	They produce IL-10, IL-12, TNF-α,TGF-β	They produce CCL5, CXCL10, and CXCL16	[93,94]
M4	They are induced by CXCL4	Suppressed phagocytosis Expression of Proatherogenic and anti-atherogenic genes along with a higher expression of MMP7 and MMP12. Promote cholesterol efflux	They express SR-A, CD86, MHCII, CCR7, TLR2, and TLR4	They produce IL-6, IL-12, IL-10, TNF-α, TNFSF10(TRAIL), iNOS, Arg1	They produce CCL1, CCL2, CCL5, CCL18, and CCL22	[81]
Regulatory	They are induced by LPS, ICs	Parasite persistence (5) IL-10 produced leads the macrophage to an activating effect of IFN-γ and hence prefers the release of IL-4 and IL-10 by T cells. Modulate inflammatory immune responses and thereby limits tissue damage	They express CD206 but no other reliable, stable markers have been identified to date	They produce elevated level of IL-4, IL-10 and low levels of IL-12, IL-23	They produce CCL18, HB-EGF	[98],[99], [100], [101]
CD4⁺/CD8⁺	They are induced by GM-CSF in a dose-dependent manner	Able to kill tumor cells in a dose-dependent manner without MHC restriction	They express FasL, perforin, Granzyme b, NKR-P2 (rat homolog of human NKG2D)	They produce IL-18, IFN-γ, RANTES	Nonsignificant MDC	[82]
TAM	They are induced by LPS; pro-inflammatory cytokines: IL-1β, IL-6, TNF-α, and chemokine CCL3	Found in the stroma of tumors, these cells can regulate either positively or negatively the growth of various malignant cells	Resting TAM express phagocytosis mediated receptors – Msr2, C1q	Resting TAM produces immunosuppressive cytokines: IL-10, TGF-β	IFN-γ induced chemokines: CCL5, CXCL9, CXCL10, and CXCL16	[84],[102], [103]
Small	They are induced by LPS	Found in sputum of patients with CF and COPD. Also, an increased level is seen in pediatric CF bronchoalveolar lavage	They express CD14⁺, CD45⁺, HLA-DR⁺, CD68⁺ but lack CD66b	They produce TNF-α		[104,[105]
Alveolar	They are induced by LPS and IFN-γ (α) IL-4(β)	Their function is to clear pathogens and particulates without inducing an inflammatory response that may affect gaseous exchange Associated with diseases like COPD, asthma, idiopathic pulmonary fibrosis. They have a dual role in lung cancer by promoting and/or inhibiting tumor growth. They play a key role in determining viral lung infections	They express CD200⁺, scavenger receptors, CD64⁺ and MER (by monocyte-derived alveolar macrophages only)	They produce TNF-α, IL-6, NOS (a. when induced by LPS and IFN-γ) IL-13, TGF-β, Arg-1 (b. when induced by IL4)		[106], [107], [108], [109], [110]
Interstitial lung	They are induced by LPS and IFN-γ	They are involved in daily homeostasis and protection against continuous pathogen exposure from the environment Unavailability or depletion of these cells correlates with AIDS progression and pulmonary tissue damage	They express HLA-DRhi, CD11bhi, CD163⁺	They produce TNF-α		[111]

MDC: Monocyte Derived chemokine; TAM: tumor-associated macrophages; COPD: chronic obstructive pulmonary disease; MR: mannose receptor.

The alveolar Mφ expresses a high level of complement receptor, MR, and immunoglobulin receptor (F$_c$R) along with a range of scavenger receptors [88] (see Table 1). These Mφs have an active plasma membrane capable of phagocytosis of both opsonized and non-opsonized particles and have the capacity of recycling the entire plasma membrane every 30 min, therefore, ensuring that they internalize particles, pathogens, and surfactants by a range of receptor-independent plasma membrane ruffling and folding [89–111].

3.2. DC differentiation and subtypes

DCs have long membranous extensions resembling dendrites of nerve cells. These extend and retract dynamically. LN-DCs are subdivided into cDC subsets in mice as CD11b and CD8a whereas in humans as BDCA1 and BDCA3 along with plasmacytoid DCs (see supplementary Table 2). Robbins and colleagues showed through clustering analysis that a distinct branch is formed in the leukocyte family with a conserved transcriptional signature in all LN-DC subsets [67]. However, whether the same LN-DC subsets are present in lung needs to be validated. Different subsets of DCs migrate to the lungs during infection. DCs capture antigen at one place and present in another place. For example, DCs capture antigen in the lungs and then migrate to the lung draining lymph node and present the antigen [112]. But DCs from local draining lymph nodes after systemic challenge are immature in mice absent of TNF-α versus in wild-type mice. For the maturation of DCs, several signals like TNF-α and LPS are necessary. Outside the lymph nodes, immature DCs monitor for antigens and capture antigens. Then they migrate to lymph nodes where they present the antigen to naïve T cells. This process is known as an innate adaptive immune response. DCs require an increased level of CCR7, α6-cadherins, CD40, MMP-2, and/or MMP-9 and decreased level of E-cadherin for migration [113]. However, it is unclear as to how α6-cadherins assist migration. The patrolling behavior of immature DCs is slowed down during their locomotion. This is a result of myosin IIA disrupting the motor protein gradient [114]. However, this is beneficial as it enhances the antigen capture ability of the DCs.

In both mice and humans, DCs express different subsets [67] each having their own specific function (see supplementary Table 2). cDC refers to mice CD8a$^+$ cells expressing high levels of CD11c that enters lymph nodes by migrating from peripheral tissue via a lymphatic route [115] (see supplementary Table 2). The human thymus is the niche of cDC and plasmacytoid DCs among which a cDCs subset called BDCA3^{hi} DCs, expressing CD13 and low-intermediate levels of CD11c, CLEC9A, and high levels XCR1, IRF8 and TLR3 and HLA-DR exhibiting to TLR3 a strong stimulatory response which releases high levels of IFN-λ1 and CXCL10 [116]. Another subset of DCs, called double negative T cells with CD4$^-$ and CD8$^-$ expresses memory markers CD44, CD11a, CD103, and FasL with intermediate levels of TCR/CD3 and has subsets of γδ T cells, CD1a inactive iNKT cells, NK1.1$^+$ NKT-like cells, and NK1.1$^-$ DN T cells [117].

As Mφs play a significant role in maintaining inflammation by extending the extravasion of immature monocytes and neutrophils, allergen-specific CTLs also play a key role in airway inflammation. Allergen-specific CTLs strongly reduce airway inflammation. These CTLS produce IL-4 and IL-13 by the lung Th2 cells. These CTLSs are specific for increased caspase$^+$ DC production in mediastinal lymph node along with fewer CD103$^+$ and CD11b$^+$ DCs in the lung [118]. Th2 immunity is triggered by the phosphorylation of DNA-dependent protein kinase which is important in adaptive immunity mediated by DCs in allergic asthma. Traditional treatments for asthma decrease the number of DCs in the airway. Since the airway lacks DCs, Mφs may be the key cells involved in regulation and clearance of allergens from the airway during the treatments. However, this aspect needs investigation. House dust mite induce phosphorylation, thereby triggering Th2 immunity by a mechanism involving impaired presentation of mite antigens and generation of intracellular reactive ROS [119]. Another example is syndecan-4 (SDC4) expressed in DCs (see supplementary Table 2) activating Th2 mediated asthma [120].

4. New treatment strategies

Current treatments for ARDS and COPD include the use of bronchodilators and corticosteroids. In adults, corticosteroids are supplemented with a low dose of beta-2-agonist. However, the use of corticosteroids has resulted in resistance and hence there is a need to develop new anti-inflammatories. Despite no single asthma gene for target, proteases have been identified to play a key role [121]. Proteases such as serine proteases and metalloproteases can induce IL-32 and convert IL-1 and IL-18 zymogens to their active form to promote pro-inflammatory response [122]. Other proteases such as cathepsins stimulate IFN-γ production. Therefore, one of the strategies in combating inflammation in respiratory disease is by the use of protease inhibitors [123]. The serine protease inhibitors act by downregulating Th2 cytokines and Th17 cell function and inhibiting NF-κβ activation in the lung. Upon encountering LPS, DCs upregulate the production of protease inhibitors such as serine protease inhibitor 6 (Spi6) [124]. The protease inhibitors are necessary to protect the DCs from contact-mediated cytotoxicity of the CD8 T lymphocytes [125]. Furthermore, thymic stromal lymphopoietin (TSLP) is a protein of the cytokine family involved in maturation of T lymphocytes through activation of APCs [126–128]. TSLP is secreted by epithelial cells and enhances the maturation of CD11c$^+$ DCs [128]. In the thymus, TSLP activates both CD123$^+$ plasmacytoid and CD11c$^+$ myeloid DCs leading to regulatory T-cell production [129]. Overexpression of TSLP in the lung leads to severe airway inflammation and AHR [130]. TSLP is targeted by the antibody Tezepelumab [131]. It reduced exacerbations in patients with asthma. For a detailed account of TSLP and its role in asthma, see Ref. [132]. One of the treatment strategies involves the use of LPS inhibitors and statins. But they are not sufficient to downregulate inflammation.

4.1. LPS inhibitors

However, there is no single therapeutic approach capable of culminating LPS-induced inflammation completely. E5564 has shown great potential *in vivo* by blocking LPS-induced cytokines and blocks LPS itself. The molecule has been trialed in patients with endotoxemia and has showed successful results

in inhibiting all the effects of LPS. However, the immunological tolerance side is not investigated and therefore risks remain in the clinical use of the molecule. Another compound which has been found successful in blocking LPS is TAK-242 *in vitro*. The molecule would need further investigation before clinical use. Furthermore, treatments targeted at TNF-α, such as rhynchophilline, are available. However, rhynchophilline increases morbidity in mice due to cecal ligation. Other examples include berberine with yohimbine which can modulate the host immune response during endotoxemia in humans. For details on LPS inhibitors, see Ref. [133].

4.2. Statins as anti-inflammatories

Use of statins is another therapeutic approach. Simvastatin has been successfully used in a mouse model of allergic airways disease [134]. Statins can reduce expression of activation markers on DCs upon LPS-induced maturation [135], therefore, behaving as a potential well-characterized anti-inflammatory agent. Other key treatments which have come to the limelight include the use of anti-IgE (omalizumab) and anti-IL-5 (mepolizumab) for treatment of lung inflammation especially asthma [136]. Omalizumab acts by reducing FcεRI expression on basophils and mast cells as well preventing the binding of IgE to FcεRI receptors. The effect of lowered FcεRI was observed on DCs which affected their ability to prime naïve T cells toward a Th2 pathway and secretion of Th2 cytokines [137] thus preventing inflammation [138]. Treatments with omalizumab results in reduced sputum along with decreased epithelial and subepithelial cells. Other cells such as sub-mucosal B cells and CD4$^+$, CD8$^+$ T lymphocytes are also reduced [139]. Treatment with humanized antibodies is not limited to anti-IgE but several other targets such as anti-IL-4, TNF-α, and IL-13. Another approach is to directly deliver anti-inflammatory mediators (IL-10, IL-12, IFN-γ) or enhance their rate of production. Unconventional treatments include the use of antioxidants shown to have novel anti-inflammatory effects [140].

But none of the currently available treatments gives a greatly improved management of the disease, nor are they capable of a long-term sustainable treatment with fewer side effects. Very recently, cytokine-induced killer cells have been used to treat allergic airway inflammation (conventionally used in cancer treatment [141]). These cells could be used for personalized treatments against airways inflammation but need further investigation of the mechanisms involved. The future relies on the development of new anti-inflammatories to be delivered in the lung. However, combinations of multiple preclinical therapies can be used to bridge the gap in development of newer anti-inflammatories against LPS-induced airway inflammation. The new anti-inflammatories should be capable of providing both an immediate and a sustaining anti-inflammatory effect. One of the possible ways of treatment is by pulmonary nanomedicine.

5. Pulmonary nanomedicine: approaches to delivery and therapeutics

Recent development of surface functionalized nanoparticles has been exploited to conjugate drugs, anti-inflammatories, proteins, and other biologically relevant therapeutic molecules.

There are several ways by which the essential anti-inflammatories can be attached or conjugated to the nanoparticles [142]. It is known that inert 50 nm polystyrene nanoparticles conjugated with a neutral amino acid can inhibit allergic airway inflammation. These particles are immunosuppressive and are taken up by the APCs while the cell viability is unaffected [143]. Nanoparticles can be used to conjugate biologically useful molecules such as therapeutic antibodies, proteins, and amino acids. Very recently, amino acid-conjugated nanoparticles have gained interest due to their biocompatibility and ease of conjugation. Conjugated nanoparticle carrying a novel molecule of interest can provide a long-lasting response in the lung. This dimension of therapeutics points us to the use of anti-inflammatories providing a sustaining effect in the treatment of inflammation in the lung. Nanoparticles intended for use in vascular delivery have different properties which enables them to be used as anti-inflammatories.

Anti-inflammatories for vascular delivery utilize different types of nano-carriers to carry the drug inside the blood vessels. Nano-carriers include liposomes, dendrimers, antibody-and-polymer drug conjugates, solid lipid, and polymeric nanoparticles [144]. Nanoparticles need to be neutral and under the size of 300 nm for delivery to the vasculature. Recent studies have showed that the hydrodynamic size of the particles is crucial for vascular delivery. Nonspherical carriers have more retention time than spherical counterparts in blood flow. The targets of these nano-carriers include submicron particles in blood and endothelial cells for anti-inflammatory delivery. Nanoencapsulation of antioxidant enzymes followed by vascular deliver is also possible. Endothelial cells have many uptake mechanisms for anti-inflammatories such as clathrin mediated, caveolae-mediated and non-canonical endocytosis, and pinocytosis. Nano-carriers are generally taken up by the endocytic pathway where the nano-carriers target cell adhesion molecules such as E-selectin and VCAM-1. Antibodies binding to such cell adhesion molecules boost antioxidant binding, uptake, and protective effects in animal models of LPS-induced inflammation. Nano-carriers on one side are novel agents capable of delivering anti-inflammatories intracellularly and on the other hand, they accumulate in the microvasculature, kidneys, and reticuloendothelial system. For a detailed understanding of nano-carriers and their role in vascular delivery, see Ref. [144]. Therefore, cell adhesion molecules are important to study the behavior of nano-carriers for drug-delivery.

5.1 Significance of cell adhesion molecules for nano-carriers

Since cell adhesion molecules are important for nano-carriers to be endocytosed by the cells, numerous studies have demonstrated the accumulation of biotherapeutics in the pulmonary vasculature. In one such example, antioxidant molecules such as catalase and superoxide dismutase were conjugated to anti-PECAM-1 (a cell adhesion molecule) antibody for targeting ROS to alleviate vascular oxidative stress and endothelial inflammation [145,146]. In another study, dexamethasone-loaded lysozyme dextran nanogels having affinity for the cell adhesion molecule ICAM-1 were used to ameliorate acute pulmonary inflammation caused by LPS induced ALI

[147]. Therefore, target-specific delivery is possible using nano-carriers carrying drugs for delivery.

In the treatment of respiratory diseases, the lung provides a large surface area along with a low-enzyme-controlled environment so that drugs can be delivered for systemic therapies. However, multiple barriers such as humidity, mucociliary clearance, and AMs affect the efficacy of drugs [148]. Pulmonary delivery prevents the degradation of the active pharmacophore in the gastrointestinal tract and the first-pass metabolism in the liver. Targeted delivery of drugs into the blood circulating through the lung is complicated due to several anatomical and physiological challenges such as a thin semipermeable epithelium and an extremely thin alveolar–capillary barrier. The size/lumen diameter of the airways can be a challenge as well. Therefore, many molecules tend to deposit into the trachea or the large airways and are unable to reach deep into the alveoli. To overcome such challenges, nanomedicines are the ideal solution for delivery. Exosomes are an excellent example for encapsulation and delivery of anti-inflammatory agents. Exosome encapsulating curcumin has been found to be effective in protecting against LPS induced septic shock [149]. In one study, nano-carriers were able to distinguish between inflamed versus healthy tissue. The nano-carriers targeted the cell adhesion molecule PECAM present in the healthy lung but absent from the inflamed lung due to hypoxic vasoconstriction. This leads to the conclusion that intra-organ region-specific delivery of drugs is possible, overcoming local abnormalities of perfusion and permeability.

6. Five-year view

A deeper insight into how APCs work in response to endotoxin and other inflammatory signals would mean newer drug targets and therefore a better way to look at airways inflammation. With the focus shifting toward the immune side of the airway inflammation, new immunomodulatories need to be developed.

Currently, natural compounds capable of attenuating inflammation are the subject of intense study. In the coming years, many more will be found which can reduce inflammation. However, an anti-inflammatory compound is not successful until it is translated to clinical use. It has also been suggested to include anti-inflammatory foods in our diet. In this aspect, there are several *anti-inflammatory* foods such as olive oil, salmon, berries, and tomatoes containing high amounts of functional amino acids. Interestingly, these amino acids are attachable to nano-carriers specifically spherical polystyrene nanoparticles, which are nonbiodegradable. Furthermore, it has been found that these amino acid-conjugated nanoparticles can inhibit allergic airway inflammation [143]. If we combine these amino acids with biodegradable nanoparticles such as with iron oxide for delivery into the lung, it could be used as a sustainable therapeutic and low-cost medication. Therefore, these amino acids could be the key to future anti-inflammatories [150].

APCs can serve as excellent therapeutic targets. Drugs such as anti-inflammatories should be able to attenuate inflammation by downregulating activation of the APCs. In doing so, the release of pro-inflammatory mediators will be reduced as a result there will be less injury to the lung. As we develop new ways and treatments to attenuate airway inflammation, the understanding of the role of APCs as therapeutic targets will be vital. Every individual is unique and therefore needs different methods of treatment and management of disease. Therefore, personalized medicine and care for individual patients focused at the extent and severity of the disease need to be developed with the APCs in mind.

Considering the developing field of nanotechnology, it is highly likely that cost-effective nanoparticles could be used as therapeutics against airway inflammation. The changing lifestyle of people would also impact the way we look at this disease and therefore a more personalized treatment or care for the affected individuals would be necessary.

Currently, the models used to study acute and chronic inflammation are capable of mimicking many but not all aspects of human lung inflammation. Therefore, focusing on development of advanced disease models to study asthma and COPD would be necessary to investigate the disease from new perspectives. COPD can lead to nonreversible alveolar degradation. Therefore, new strategies to promote tissue remodeling and alveolar reconstruction could open a new field for COPD treatment.

Key issues

- The most important problem associated with airway inflammation is reducing the symptoms for relief of patients. Therefore, a better management of diseases is necessary.
- The increasing level of pollution giving rise to accumulation of ultra-fine particulate in the airway leading to inflammation.
- LPS is present everywhere to give inflammation to the airway as the lung is a non-sterile environment in direct contact with the atmosphere.
- Although there are abundant compounds, proteins, pharmacophores made which ameliorates the effect of LPS, none of the therapies provides prevention to LPS-induced inflammation.
- Brodalumab (AMG827) which was found successful against psoriasis has not been trialed for the treatment of COPD.
- Drugs to enlarge the narrowed airway due to COPD need to be developed.
- Very recently, GCSF has been found to be a successful target in the treatment of COPD. Therefore, anti-GCSF therapy should be trialed for COPD treatment.
- Transcriptomic data are required in finding new drug targets for asthma and identifying new pathways which may play a role in reducing inflammation.
- Current treatments with bronchodilators have several side effects. Therefore, there is a need to develop new anti-inflammatories. The anti-inflammatories should be able to provide both an immediate and lasting effect.

Notes on contributor

Declaration of interest

Reviewer disclosures

ORCID

Amlan Chakraborty http://orcid.org/0000-0002-2917-6486

References

1. Ferkol T, Schraufnagel D. The global burden of respiratory disease. Ann Am Thorac Soc. 2014;11(3):404–406.
2. Allen IC. Bacteria-mediated acute lung inflammation. In: Allen IC, editor. Mouse models of innate immunity: methods and protocols. Totowa, NJ: Humana Press; 2013. p. 163–175.
3. Knapp S. LPS and bacterial lung inflammation models. Drug Discovery Today: Disease Models. 2009;6(4):113–118.
4. Wang JP, Kurt-Jones EA, Finberg RW. Innate immunity to respiratory viruses. Cell Microbiol. 2007;9(7):1641–1646.
5. Woodland DL. Cell-mediated immunity to respiratory virus infections. Curr Opin Immunol. 2003;15(4):430–435.
6. Starkhammar M, Larsson O, Kumlien Georén S, et al. Toll-like receptor ligands lps and poly (I:C) exacerbate airway hyperresponsiveness in a model of airway allergy in mice, independently of inflammation. PLOS ONE. 2014;9(8):e104114.
7. Manni ML, Mandalapu S, McHugh KJ, et al. Molecular mechanisms of airway hyperresponsiveness in a murine model of steroid-resistant airway inflammation. J Immunol. 2016;196(3):963–977.
8. Barnes PJ, Burney PGJ, Silverman EK, et al. Chronic obstructive pulmonary disease. Nat Rev Dis Primers. 2015;1:15076.
9. McDonough JE, Yuan R, Suzuki M, et al. Small-airway obstruction and emphysema in chronic obstructive pulmonary disease. N Engl J Med. 2011;365(17):1567–1575.
10. Hamid Q. Pathogenesis of small airways in asthma. Respiration. 2012;84(1):4–11.
11. Murdoch JR, Lloyd CM. Chronic inflammation and asthma. Mutat Res. 2010;690(1–2):24–39.
12. Li N, Harkema JR, Lewandowski RP, et al. Ambient ultrafine particles provide a strong adjuvant effect in the secondary immune response: implication for traffic-related asthma flares. Am J Physiol Lung Cell Mol Physiol. 2010;299(3):L374–L383.
13. May S, Romberger DJ, Poole JA. Respiratory health effects of large animal farming environments. J Toxicol Environ Health B Crit Rev. 2012;15(8):524–541.
14. Snelgrove RJ, Jackson PL, Hardison MT, et al. A critical role for lta$_4$h in limiting chronic pulmonary neutrophilic inflammation. Science. 2010;330(6000):90–94.
15. De Alba J, Raemdonck K, Dekkak A, et al. House dust mite induces direct airway inflammation in vivo: implications for future disease therapy? Eur Respir J. 2010;35(6):1377–1387.
16. Beasley R, Semprini A, Mitchell EA. Risk factors for asthma: is prevention possible? The Lancet. 2015;386(9998):1075–1085.
17. Huang Z, Kraus VB. Does lipopolysaccharide-mediated inflammation have a role in OA? Nat Rev Rheumatol. 2016;12(2):123–129.
18. Zeuke S, Ulmer AJ, Kusumoto S, et al. TLR4-mediated inflammatory activation of human coronary artery endothelial cells by LPS. Cardiovasc Res. 2002;56(1):126–134.
19. Dahl R. Systemic side effects of inhaled corticosteroids in patients with asthma. Respir Med. 2006;100(8):1307–1317.
20. Barnes PJ. Corticosteroid resistance in patients with asthma and chronic obstructive pulmonary disease. J Allergy Clin Immunol. 2013;131(3):636–645.
21. Ashley NT, Weil ZM, Nelson RJ. Inflammation: mechanisms, costs, and natural variation. Annu Rev Ecol Evol Syst. 2012;43(1):385–406.
22. Galli SJ, Tsai M, Piliponsky AM. The development of allergic inflammation. Nature. 2008;454(7203):445–454.
23. Kay AB. Allergy and allergic diseases. New England J Med. 2001;344(1):30–37.
24. Shang J, Zhao J, Wu X, et al. Interleukin-33 promotes inflammatory cytokine production in chronic airway inflammation. Biochemistry Biol. 2015;93(4):359–366.
25. Sjöberg LC, Nilsson AZ, Lei Y, et al. Interleukin 33 exacerbates antigen driven airway hyperresponsiveness, inflammation and remodeling in a mouse model of asthma. Sci Rep. 2017;7(1):4219.
26. Buist AS. Similarities and differences between asthma and chronic obstructive pulmonary disease: treatment and early outcomes. Eur Respir J. 2003;21(39suppl):30s–35s.
27. Greenfeder S, Umland SP, Cuss FM, et al. Th2 cytokines and asthma — the role of interleukin-5 in allergic eosinophilic disease. Respir Res. 2001;2(2):71–79.
28. Aoshiba K, Nagai A. Differences in airway remodeling between asthma and chronic obstructive pulmonary disease. Clin Rev Allergy Immunol. 2004;27(1):35–43.
29. Moldoveanu B, Otmishi P, Jani P, et al. Inflammatory mechanisms in the lung. J Inflamm Res. 2009;2:1–11.
30. Bradding P, Walls AF, Holgate ST. The role of the mast cell in the pathophysiology of asthma. J Allergy Clin Immunol. 2006;117(6):1277–1284.
31. Folkerts G, Ww BUSSE, Fp NIJKAMP, et al. Virus-induced airway hyperresponsiveness and asthma. Am J Respir Crit Care Med. 1998;157(6):1708–1720.
32. Pelletier M, Maggi L, Micheletti A, et al. Evidence for a cross-talk between human neutrophils and Th17 cells. Blood. 2010;115(2):335–343.
33. Baraldo S, Turato G, Badin C, et al. Neutrophilic infiltration within the airway smooth muscle in patients with COPD. Thorax. 2004;59(4):308–312.
34. Medzhitov R. Origin and physiological roles of inflammation. Nature. 2008;454(7203):428–435.
35. Chan JK, Roth J, Oppenheim JJ, et al. Alarmins: awaiting a clinical response. J Clin Invest. 2012;122(8):2711–2719.
36. Creagh EM, O'Neill LAJ. TLRs, NLRs and RLRs: a trinity of pathogen sensors that co-operate in innate immunity. Trends Immunol. 2006;27(8):352–357.
37. Lu Y-C, Yeh W-C, Ohashi PS. LPS/TLR4 signal transduction pathway. Cytokine. 2008;42(2):145–151.
38. Yoshimura A, Lien E, Ingalls RR, et al. Recognition of gram-positive bacterial cell wall components by the innate immune system occurs via toll-like receptor 2. J Immunol. 1999;163(1):1–5.
39. Droemann D, Goldmann T, Tiedje T, et al. Toll-like receptor 2 expression is decreased on alveolar macrophages in cigarette smokers and COPD patients. Respir Res. 2005;6(1):68.
40. Zhang Z, Louboutin J-P, Weiner DJ, et al. Human airway epithelial cells sense pseudomonas aeruginosa infection via recognition of flagellin by toll-like receptor 5. Infect Immun. 2005;73(11):7151–7160.
41. Thompson MR, Kaminski JJ, Kurt-Jones EA, Fitzgerald KA. Pattern recognition Receptors and the Innate Immune Response to Viral Infection. Viruses. 2011;3(6):920.
42. Dobrovolskaia MA, Medvedev AE, Thomas KE, et al. Induction of in vitro reprogramming by toll-like receptor (TLR)2 and TLR4 agonists

in murine macrophages: effects of TLR "homotolerance" versus "heterotolerance" on NF-kappa B signaling pathway components. J Immunol. 2003;170(1):508–519.

43. Takahashi G, Andrews D, Lilly M, et al. Effect of granulocyte-macrophage colony-stimulating factor and interleukin-3 on interleukin-8 production by human neutrophils and monocytes. Blood. 1993;81 (2):357–364.

44. Matthay MA, Zemans RL. The acute respiratory distress syndrome: pathogenesis and treatment. Annu Rev Pathol. 2011;6:147–163.

45. Güngör N, Pennings JL, Knaapen AM, et al. Transcriptional profiling of the acute pulmonary inflammatory response induced by LPS: role of neutrophils. Respir Res. 2010;11(1):24.

46. Li Y, Huang J, Foley NM, et al. B7H3 ameliorates LPS-induced acute lung injury via attenuation of neutrophil migration and infiltration. Sci Rep. 2016;6:31284.

47. Xiao Q, Dong N, Yao X, et al. Bufexamac ameliorates LPS-induced acute lung injury in mice by targeting LTA4H. Sci Rep. 2016;6:25298.

48. Stoll LL, Denning GM, Weintraub NL. Potential role of endotoxin as a proinflammatory mediator of atherosclerosis. Arterioscler Thromb Vasc Biol. 2004;24(12):2227–2236.

49. Pendyala S, Usatyuk PV, Gorshkova IA, et al. Regulation of NADPH oxidase in vascular endothelium: the role of phospholipases, protein kinases, and cytoskeletal proteins. Antioxid Redox Signal. 2009;11(4):841–860.

50. Oakley FD, Abbott D, Li Q, et al. Signaling components of redox active endosomes: the redoxosomes. Antioxid Redox Signal. 2009;11(6):1313–1333.

51. Ikezoe T. Thrombomodulin/activated protein C system in septic disseminated intravascular coagulation. Journal of Intensive Care. 2015;3(1):1.

52. Shaver CM, Bastarache JA. Clinical and biological heterogeneity in ards: direct versus indirect lung injury. Clin Chest Med. 2014;35 (4):639–653.

53. Johnson ER, Matthay MA. Acute lung injury: epidemiology, pathogenesis, and treatment. J Aerosol Med Pulm Drug Deliv. 2010;23 (4):243–252.

54. Matute-Bello G, Frevert CW, Martin TR. Animal models of acute lung injury. Am J Physiol Lung Cell Mol Physiol. 2008;295(3):L379–L399.

55. Gandhi NA, Pirozzi G, Graham NMH. Commonality of the IL-4/IL-13 pathway in atopic diseases. Expert Rev Clin Immunol. 2017;13 (5):425–437.

56. Wenzel S, Ford L, Pearlman D, et al. Dupilumab in persistent asthma with elevated eosinophil levels. New England J Med. 2013;368(26):2455–2466.

57. Corren J, Lemanske RF, Hanania NA, et al. Lebrikizumab treatment in adults with asthma. New England J Med. 2011;365(12):1088–1098.

58. Popovic B, Breed J, Rees DG, et al. Structural characterisation reveals mechanism of il-13-neutralising monoclonal antibody tralokinumab as inhibition of binding to il-13Rα1 and IL-13Rα2. J Mol Biol. 2017;429(2):208–219.

59. Bagnasco D, Ferrando M, Varricchi G, Passalacqua G, Canonica GW. A Critical Evaluation of anti-il-13 and anti-il-4 strategies in severe asthma. Int Arch Allergy Immunol. 2016;170(2):122–131.

60. Lindén A, Dahlén B. Interleukin-17 cytokine signalling in patients with asthma. Eur Respir J. 2014;44(5):1319–1331.

61. Roos AB, Stampfli MR. Targeting Interleukin-17 signalling in cigarette smoke-induced lung disease: mechanistic concepts and therapeutic opportunities. Pharmacol Ther. 2017;178:123–131.

62. Eich A, Urban V, Jutel M, et al. A randomized, placebo-controlled phase 2 trial of cnto 6785 in chronic obstructive pulmonary disease. COPD: J Chronic Obstructive Pulm Dis. 2017;14(5):476–483.

63. Tsantikos E, Lau M, Castelino CMN, et al. Granulocyte-CSF links destructive inflammation and comorbidities in obstructive lung disease. J Clin Invest. 2018;128(6):2406–2418.

64. Kindt TJ, Goldsby RA, Osborne BA, et al. Kuby immunology. New York, NY: W.H. Freeman, c2007; 2007.

65. Janeway CA, Paul Travers J, Walport M, et al. Immunobiology. New York, NY: Garland Science; 2001.

66. Doulatov S, Notta F, Eppert K, et al. Revised map of the human progenitor hierarchy shows the origin of macrophages and dendritic cells in early lymphoid development. Nat Immunol. 2010;11(7):585–593.

67. Robbins SH, Walzer T, Dembele D, et al. Novel insights into the relationships between dendritic cell subsets in human and mouse revealed by genome-wide expression profiling. Genome Biol. 2008;9(1):R17.

68. Khazen W, J-P M, Tomkiewicz C, et al. Expression of macrophage-selective markers in human and rodent adipocytes. FEBS Letters. 2005;579(25):5631–5634.

69. Zaba LC, Fuentes-Duculan J, Steinman RM, et al. Normal human dermis contains distinct populations of CD11c+BDCA-1+ dendritic cells and CD163+FXIIIA+ macrophages. J Clin Invest. 2007;117(9):2517–2525.

70. Ziegler-Heitbrock L, Ancuta P, Crowe S, et al. Nomenclature of monocytes and dendritic cells in blood. Blood. 2010;116(16):e74–e80.

71. Auffray C, Fogg D, Garfa M, et al. Monitoring of blood vessels and tissues by a population of monocytes with patrolling behavior. Science. 2007;317(5838):666–670.

72. Arnold L, Henry A, Poron F, et al. Inflammatory monocytes recruited after skeletal muscle injury switch into antiinflammatory macrophages to support myogenesis. J Exp Med. 2007;204(5):1057–1069.

73. Rivollier A, He J, Kole A, et al. Inflammation switches the differentiation program of Ly6C^hi monocytes from antiinflammatory macrophages to inflammatory dendritic cells in the colon. J Exp Med. 2012;209(1):139–155.

74. Qu C, Edwards EW, Tacke F, et al. Role of CCR8 and other chemokine pathways in the migration of monocyte-derived dendritic cells to lymph nodes. J Exp Med. 2004;200(10):1231–1241.

75. Egawa M, Mukai K, Yoshikawa S, et al. Inflammatory monocytes recruited to allergic skin acquire an anti-inflammatory m2 phenotype via basophil-derived interleukin-4. Immunity. 2013;38(3):570–580

76. Gordon S. Alternative activation of macrophages. Nat Rev Immunol. 2003;3(1):23–35.

77. Ma X, Yuan Y, Zhang Z, et al. An analog of Ac-SDKP improves heart functions after myocardial infarction by suppressing alternative activation (M2) of macrophages. Int J Cardiol. 2014;175(2):376–378.

78. Martinez FO, Gordon S, Locati M, et al. Transcriptional profiling of the human monocyte-to-macrophage differentiation and polarization: new molecules and patterns of gene expression. J Immunol. 2006;177(10):7303–7311.

79. Martinez FO, Sica A, Mantovani A, et al. Macrophage activation and polarization. Front Biosci. 2008;13:453–461.

80. Gordon S, Taylor PR. Monocyte and macrophage heterogeneity. Nat Rev Immunol. 2005;5(12):953–964.

81. Gleissner CA, Shaked I, Little KM, et al. CXC chemokine ligand 4 induces a unique transcriptome in monocyte-derived macrophages. J Immunol. 2010;184(9):4810–4818.

82. Baba T, Ishizu A, Iwasaki S, et al. CD4(+)/CD8(+) macrophages infiltrating at inflammatory sites: a population of monocytes/macrophages with a cytotoxic phenotype. Blood. 2006;107(5):2004–2012.

83. Liu Y, Cao X. The origin and function of tumor-associated macrophages. Cell And Mol Immunol. 2014;12:1.

84. Biswas SK, Gangi L, Paul S, et al. A distinct and unique transcriptional program expressed by tumor-associated macrophages (defective NF-kappaB and enhanced IRF-3/STAT1 activation). Blood. 2006;107(5):2112–2122.

85. Haslett C. Granulocyte apoptosis and its role in the resolution and control of lung inflammation. Am J Respir Crit Care Med. 1999;160 (supplement_1):S5–S11.

86. Schagat TL, Wofford JA, Wright JR. Surfactant protein a enhances alveolar macrophage phagocytosis of apoptotic neutrophils. J Immunol. 2001;166(4):2727–2733.

87. Dagvadorj J, Shimada K, Chen S, et al. Lipopolysaccharide induces alveolar macrophage necrosis via CD14 and the P2x7 receptor leading to Interleukin-1α release. Immunity. 2015;42(4):640–653.

88. Mosser DM, Edelson PJ. Activation of the alternative complement pathway by Leishmania promastigotes: parasite lysis and attachment to macrophages. J Immunol. 1984;132(3):1501–1505.

89. Gordon SB, Read RC. Macrophage defences against respiratory tract infections: the immunology of childhood respiratory infections. Br Med Bull. 2002;61(1):45–61.

197

90. Kigerl KA, Gensel JC, Ankeny DP, et al. Identification of two distinct macrophage subsets with divergent effects causing either neurotoxicity or regeneration in the injured mouse spinal cord. J Neurosci. 2009;29(43):13435–13444.

91. Hissong BD, Byrne GI, Padilla ML, et al. Upregulation of interferon-induced indoleamine 2,3-dioxygenase in human macrophage cultures by lipopolysaccharide, muramyl tripeptide, and interleukin-1. Cell Immunol. 1995;160(2):264–269.

92. Jablonski KA, Amici SA, Webb LM, et al. novel markers to delineate murine m1 and m2 macrophages. PLoS One. 2015;10(12):e0145342.

93. Duluc D, Delneste Y, Tan F, et al. Tumor-associated leukemia inhibitory factor and IL-6 skew monocyte differentiation into tumor-associated macrophage-like cells. Blood. 2007;110(13):4319–4330.

94. Hao N-B, M-H L, Fan Y-H, et al. Macrophages in tumor microenvironments and the progression of tumors. Clin Dev Immunol. 2012;11:2012.

95. Gundra UM, Girgis NM, Ruckerl D, et al. Alternatively activated macrophages derived from monocytes and tissue macrophages are phenotypically and functionally distinct. Blood. 2014;123(20):e110–e122.

96. Zhang W, Xu W, Xiong S. Blockade of notch1 signaling alleviates murine lupus via blunting macrophage activation and M2b polarization. J Immunol. 2010;184(11):6465–6478.

97. Lu J, Cao Q, Zheng D, et al. Discrete functions of M2a and M2c macrophage subsets determine their relative efficacy in treating chronic kidney disease. Kidney Int. 2013;84(4):745–755.

98. Miles SA, Conrad SM, Alves RG, et al. A role for IgG immune complexes during infection with the intracellular pathogen Leishmania. J Exp Med. 2005;201(5):747–754.

99. Edwards JP, Zhang X, Frauwirth KA, et al. Biochemical and functional characterization of three activated macrophage populations. J Leukoc Biol. 2006;80(6):1298–1307.

100. Edwards JP, Zhang X, Mosser DM. The expression of heparin-binding epidermal growth factor-like growth factor by regulatory macrophages. J Immunol. 2009;182(4):1929–1939.

101. Fleming BD, Mosser DM. Regulatory macrophages: setting the Threshold for Therapy. Eur J Immunol. 2011;41(9):2498–2502.

102. Mantovani A, Sozzani S, Locati M, et al. Macrophage polarization: tumor-associated macrophages as a paradigm for polarized M2 mononuclear phagocytes. Trends Immunol. 2002;23(11):549–555.

103. Ohno S, Suzuki N, Ohno Y, et al. Tumor-associated macrophages: foe or accomplice of tumors? Anticancer Res. 2003;23(6a):4395–4409.

104. Garratt LW, Wright AKA, Ranganathan SC, et al. Small macrophages are present in early childhood respiratory disease. Journal of Cystic Fibrosis. 2012;11(3):201–208.

105. Frankenberger M, Menzel M, Betz R, et al. Characterization of a population of small macrophages in induced sputum of patients with chronic obstructive pulmonary disease and healthy volunteers. Clin Exp Immunol. 2004;138(3):507–516.

106. Morales-Nebreda L, Misharin AV, Perlman H, et al. The heterogeneity of lung macrophages in the susceptibility to disease. Eur Respir Rev. 2015;24(137):505–509.

107. Leema George SU, Ganguly K, Tobias S. Macrophage polarization in lung biology and diseases, lung inflammation. InTech; 2014. DOI: 10.5772/57567. Available from: https://www.intechopen.com/books/lung-inflammation/macrophage-polarization-in-lung-biology-and-diseases

108. Almatroodi SA, McDonald CF, Pouniotis DS. Alveolar macrophage polarisation in lung cancer. Lung Cancer International. 2014;9:2014.

109. Pribul PK, Harker J, Wang B, et al. Alveolar macrophages are a major determinant of early responses to viral lung infection but do not influence subsequent disease development. J Virol. 2008;82(9):4441–4448.

110. Guilliams M, De Kleer I, Henri S, et al. Alveolar macrophages develop from fetal monocytes that differentiate into long-lived cells in the first week of life via GM-CSF. J Exp Med. 2013;210(10):1977–1992.

111. Cai Y, Sugimoto C, Arainga M, et al. In vivo characterization of alveolar and interstitial lung macrophages in rhesus macaques: implications for understanding lung disease in humans. J Immunol. 2014;192(6):2821–2829.

112. Desch AN, Gibbings SL, Clambey ET, et al. Dendritic cell subsets require cis-activation for cytotoxic CD8 T-cell induction. Nat Commun. 2014;5:4674.

113. Lutz MB, Schuler G. Immature, semi-mature and fully mature dendritic cells: which signals induce tolerance or immunity? Trends Immunol. 2002;23(9):445–449.

114. Chabaud M, Heuze ML, Bretou M, et al. Cell migration and antigen capture are antagonistic processes coupled by myosin II in dendritic cells. Nat Commun. 2015;6:7526.

115. Shortman K, Liu YJ. Mouse and human dendritic cell subtypes. Nat Rev Immunol. 2002;2(3):151–161.

116. Martinez VG, Canseco NM, Hidalgo L, et al. A discrete population of IFN lambda-expressing BDCA3hi dendritic cells is present in human thymus. Immunol Cell Biol. 2015;93(7):673–678.

117. Neyt K, GeurtsvanKessel CH, Lambrecht BN. Double-negative T resident memory cells of the lung react to influenza virus infection via CD11c dendritic cells. In: Mucosal Immunol. 2016 Jul;9(4):999-1014.

118. Daniels NJ, Hyde E, Ghosh S, et al. Antigen-specific cytotoxic T lymphocytes target airway CD103(+) and CD11b(+) dendritic cells to suppress allergic inflammation. Mucosal Immunol. 2016;9(1):229–239.

119. Mishra A, Brown AL, Yao X, et al. Dendritic cells induce Th2-mediated airway inflammatory responses to house dust mite via DNA-dependent protein kinase. Nat Commun. 2015;6:6224.

120. Polte T, Petzold S, Bertrand J, et al. Critical role for syndecan-4 in dendritic cell migration during development of allergic airway inflammation. Nat Commun. 2015;6:7554.

121. Reed CE, Kita H. The role of protease activation of inflammation in allergic respiratory diseases. J Allergy Clin Immunol. 2004;114(5):997–1008.

122. Safavi F, Rostami A. Role of serine proteases in inflammation: bowman–birk protease inhibitor (BBI) as a potential therapy for autoimmune diseases. Exp Mol Pathol. 2012;93(3):428–433.

123. Lin -C-C, Lin L-J, S-D W, et al. The effect of serine protease inhibitors on airway inflammation in a chronic allergen-induced asthma mouse model. Mediators Inflamm. 2014;10:2014.

124. Andrew KA, Simkins HMA, Witzel S, et al. Dendritic cells treated with lipopolysaccharide up-regulate serine protease inhibitor 6 and remain sensitive to killing by cytotoxic t lymphocytes in vivo. J Immunol. 2008;181(12):8356–8362.

125. Lovo E, Zhang M, Wang L, et al. 6 is required to protect dendritic cells from the kiss of death. J Immunol. 2012;188(3):1057–1063.

126. He R, Geha RS. Thymic stromal lymphopoietin. Ann N Y Acad Sci. 2010;1183(1):13–24.

127. Noh JY, Shin JU, Park CO, et al. Thymic stromal lymphopoietin regulates eosinophil migration via phosphorylation of l-plastin in atopic dermatitis. Exp Dermatol. 2016;25(11):880–886.

128. Reche PA, Soumelis V, Gorman DM, et al. Human thymic stromal lymphopoietin preferentially stimulates myeloid cells. J Immunol. 2001;167(1):336–343.

129. Hanabuchi S, Ito T, W-R P, et al. Thymic stromal lymphopoietin-activated plasmacytoid dendritic cells induce the generation of foxp3$^+$ regulatory t cells in \human thymus. J Immunol. 2010;184(6):2999–3007.

130. Zhou B, Comeau MR, Smedt TD, et al. Thymic stromal lymphopoietin as a key initiator of allergic airway inflammation in mice. Nat Immunol. 2005;6:1047.

131. Corren J, Parnes JR, Wang L, et al. Tezepelumab in adults with uncontrolled asthma. New England J Med. 2017;377(10):936–946.

132. West EE, Kashyap M, Leonard WJ, et al. Regulator of asthma pathogenesis. Drug Discov Today Dis Mech. 2012;9(3–4).

133. Wang H-D, Lu D-X, Qi R-B. Therapeutic strategies targeting the LPS signaling and cytokines. Pathophysiology. 2009;16(4):291–296.

134. Liu J-N, Suh D-H, Yang E-M, et al. Attenuation of airway inflammation by simvastatin and the implications for asthma treatment: is the jury still out? Exp Mol Med. 2014;46:e113.

135. Yilmaz A, Reiss C, Weng A, *et al*. Differential effects of statins on relevant functions of human monocyte-derived dendritic cells. J Leukoc Biol. 2006;79(3):529–538.

136. Sy CB, Siracusa MC. The therapeutic potential of targeting cytokine alarmins to treat allergic airway inflammation. Front Physiol. 2016;7:214.

137. Prussin C, Griffith DT, Boesel KM, et al. Omalizumab treatment downregulates dendritic cell FceRI expression. J Allergy Clin Immunol. 2003;112(6):1147–1154.

138. Schroeder JT, Bieneman AP, Chichester KL, *et al*. Decreases in human dendritic cell dependent T_H2-like responses after acute *in vivo* IgE neutralization. J Allergy Clin Immunol. 2010;125(4):896–901.e896

139. Samitas K, Delimpoura V, Zervas E, et al. Anti-IgE treatment, airway inflammation and remodelling in severe allergic asthma: current knowledge and future perspectives. Eur Respir Rev. 2015;24(138):594–601.

140. Braskett M, Riedl MA. Novel antioxidant approaches to the treatment of upper airway inflammation. Curr Opin Allergy Clin Immunol. 2010;10(1):34–41.

141. Pluangnooch P, Timalsena S, Wongkajornsilp A, et al. Cytokine-induced killer cells: a novel treatment for allergic airway inflammation. PLOS ONE. 2017;12(10):e0186971.

142. Chakraborty A, Boer JC, Selomulya C, et al. Amino acid functionalized inorganic nanoparticles as cutting-edge therapeutic and diagnostic agents. In: Bioconjugate Chemistry. 2018;29(3):657–671.

143. Hardy CL, LeMasurier JS, Belz GT, *et al*. Inert 50-nm polystyrene nanoparticles that modify pulmonary dendritic cell function and inhibit allergic airway inflammation. J Immunol. 2012;188(3):1431–1441.

144. Howard MD, Hood ED, Zern B, et al. Nanocarriers for vascular delivery of anti-inflammatory agents. Annu Rev Pharmacol Toxicol. 2014;54:205–226.

145. Han J, Shuvaev VV, Muzykantov VR. Catalase and superoxide dismutase conjugated with platelet-endothelial cell adhesion molecule antibody distinctly alleviate abnormal endothelial permeability caused by exogenous reactive oxygen species and vascular endothelial growth factor. J Pharmacol Exp Ther. 2011;338(1):82–91.

146. Shuvaev VV, Han J, Yu KJ, *et al*. PECAM-targeted delivery of SOD inhibits endothelial inflammatory response. FASEB J. 2011;25(1):348–357.

147. Coll Ferrer MC, Shuvaev VV, Zern BJ, et al. Targeted nanogels loaded with dexamethasone alleviate pulmonary inflammation. PLOS ONE. 2014;9(7):e102329.

148. Labiris NR, Dolovich MB. Pulmonary drug delivery. Part I: physiological factors affecting therapeutic effectiveness of aerosolized medications. Br J Clin Pharmacol. 2003;56(6):588–599.

149. Sun D, Zhuang X, Xiang X, *et al*. A novel nanoparticle drug delivery system: the anti-inflammatory activity of curcumin is enhanced when encapsulated in exosomes. Mol Ther. 2010;18(9):1606–1614.

150. De Simone R, Vissicchio F, Mingarelli C, *et al*. Branched-chain amino acids influence the immune properties of microglial cells and their responsiveness to pro-inflammatory signals chimica Et Biophysica Acta (BBA). Bio Molecular Basis of Disease. 2013;1832(5):650–659.

199

References

Abdelhalim, M. A. K. (2011), 'Exposure to gold nanoparticles produces cardiac tissue damage that depends on the size and duration of exposure', *Lipids in Health and Disease* **10**, 205–205.

Akagi, T., Wang, X., Uto, T., Baba, M. and Akashi, M. (2007), 'Protein direct delivery to dendritic cells using nanoparticles based on amphiphilic poly(amino acid) derivatives', *Biomaterials* **28**(23), 3427–3436.

Aksoy, E., Vanden Berghe, W., Detienne, S., Amraoui, Z., Fitzgerald, K., Haegeman, G., Goldman, M. and Willems, F. (2005), 'Inhibition of phosphoinositide 3-kinase enhances trif-dependent nf-kb activation and ifn-β synthesis downstream of toll-like receptor 3 and 4', *European Journal of Immunology* **35**(7), 2200–2209.

al Mahbub, A. and Haque, A. (2016), 'X-ray computed tomography imaging of the microstructure of sand particles subjected to high pressure one-dimensional compression', *Materials* **9**(11), 890.

Alarcon-Aguilar, F. J., Almanza-Perez, J., Blancas, G., Angeles, S., Garcia-Macedo, R., Roman, R. and Cruz, M. (2008), 'Glycine regulates the production of pro-inflammatory cytokines in lean and monosodium glutamate-obese mice', *European Journal of Pharmacology* **599**(1), 152–158.

Alessandrini, F., Schulz, H., Takenaka, S., Lentner, B., Karg, E., Behrendt, H. and Jakob, T. (2006), 'Effects of ultrafine carbon particle inhalation on allergic inflammation of the lung', *Journal of Allergy and Clinical Immunology* **117**(4), 824–830.

Alessandro, R. (2013), 'Interleukin-6 and lung inflammation: Evidence for a causative role in inducing respiratory system resistance increments', *Inflammation and Allergy - Drug Targets (Discontinued)* **12**(5), 315–321.

Allen, I. C. (2013), *Bacteria-Mediated Acute Lung Inflammation*, Humana Press, Totowa, NJ, pp. 163–175.

Almatroodi, S. A., McDonald, C. F. and Pouniotis, D. S. (2014), 'Alveolar macrophage polarisation in lung cancer', *Lung Cancer International* **2014**, 9.

Almeida, J. P. M., Chen, A. L., Foster, A. and Drezek, R. (2011), 'In vivo biodistribution of nanoparticles', *Nanomedicine* **6**(5), 815–835.

Altes, T. A., Eichinger, M. and Puderbach, M. (2007), 'Magnetic resonance imaging of the lung in cystic fibrosis', *Proceedings of the American Thoracic Society* **4**(4), 321–327.

Alvarado-Vásquez, N., Zamudio, P., Cerón, E., Vanda, B., Zenteno, E. and Carvajal-Sandoval, G. (2003), 'Effect of glycine in streptozotocin-induced diabetic rats', *Comparative Biochemistry and Physiology Part C: Toxicology and Pharmacology* **134**(4), 521–527.

Ananieva, E. A., Powell, J. D. and Hutson, S. M. (2016), 'Leucine Metabolism in T Cell Activation: mTOR Signaling and Beyond', *Advances in Nutrition* **7**(4), 798S–805S.

Andrew, K. A., Simkins, H. M. A., Witzel, S., Perret, R., Hudson, J., Hermans, I. F., Ritchie, D. S., Yang, J. and Ronchese, F. (2008), 'Dendritic cells treated with lipopolysaccharide up-regulate serine protease inhibitor 6 and remain sensitive to killing by cytotoxic t lymphocytes in vivo', *The Journal of Immunology* **181**(12), 8356–8362.

Anozie, U. C. and Dalhaimer, P. (2017), 'Molecular links among non-biodegradable nanoparticles, reactive oxygen species, and autophagy', *Advanced Drug Delivery Reviews* **122**, 65–73.

Antignano, F., Ibaraki, M., Kim, C., Ruschmann, J., Zhang, A., Helgason, C. D. and Krystal, G. (2010a), 'Ship is required for dendritic cell maturation', *The Journal of Immunology* **184**(6), 2805–2813.

Antignano, F., Ibaraki, M., Ruschmann, J., Jagdeo, J. and Krystal, G. (2010b), 'Ship negatively regulates flt3l-derived dendritic cell generation and positively regulates myd88-independent tlr-induced maturation', *Journal of Leukocyte Biology* **88**(5), 925–935.

Aoshiba, K. and Nagai, A. (2004), 'Differences in airway remodeling between asthma and chronic obstructive pulmonary disease', *Clinical Reviews in Allergy and Immunology* **27**(1), 35–43.

Aragao-Santiago, L., Hillaireau, H., Grabowski, N., Mura, S., Nascimento, T. L., Dufort, S., Coll, J.-L., Tsapis, N. and Fattal, E. (2016), 'Compared in vivo toxicity in mice of lung delivered biodegradable and non-biodegradable nanoparticles', *Nanotoxicology* **10**(3), 292–302.

Ariano, P., Zamburlin, P., Gilardino, A., Mortera, R., Onida, B., Tomatis, M., Ghiazza, M., Fubini, B. and Lovisolo, D. (2011), 'Interaction of spherical silica nanoparticles with neuronal cells: Size-dependent toxicity and perturbation of calcium homeostasis', *Small* **7**(6), 766–774.

Arnold, L., Henry, A., Poron, F., Baba-Amer, Y., van Rooijen, N., Plonquet, A., Gherardi, R. K. and Chazaud, B. (2007), 'Inflammatory monocytes recruited after skeletal muscle injury switch into antiinflammatory macrophages to support myogenesis', *The Journal of Experimental Medicine* **204**(5), 1057–1069.

Arslan, O., Singh, A. P., Belkoura, L. and Mathur, S. (2013), 'Cysteine-functionalized zwitterionic zno quantum dots', *Journal of Materials Research* **28**(14), 1947–1954.

Arvizo, R. R., Miranda, O. R., Moyano, D. F., Walden, C. A., Giri, K., Bhattacharya, R., Robertson, J. D., Rotello, V. M., Reid, J. M. and Mukherjee, P. (2011), 'Modulating pharmacokinetics, tumor uptake and biodistribution by engineered nanoparticles', *PLOS ONE* **6**(9), e24374.

Ashley, N. T., Weil, Z. M. and Nelson, R. J. (2012), 'Inflammation: Mechanisms, costs, and natural variation', *Annual Review of Ecology, Evolution, and Systematics* **43**(1), 385–406.

Auffray, C., Fogg, D., Garfa, M., Elain, G., Join-Lambert, O., Kayal, S., Sarnacki, S., Cumano, A., Lauvau, G. and Geissmann, F. (2007), 'Monitoring of blood vessels and tissues by a population of monocytes with patrolling behavior', *Science* **317**(5838), 666–670.

Baba, T., Ishizu, A., Iwasaki, S., Suzuki, A., Tomaru, U., Ikeda, H., Yoshiki, T. and Kasahara, M. (2006), 'Cd4(+)/cd8(+) macrophages infiltrating at inflammatory sites: a population of monocytes/macrophages with a cytotoxic phenotype', *Blood* **107**(5), 2004–2012.

Bachem, A., Güttler, S., Hartung, E., Ebstein, F., Schaefer, M., Tannert, A., Salama, A., Movassaghi, K., Opitz, C., Mages, H. W., Henn, V., Kloetzel, P.-M., Gurka, S. and Kroczek, R. A. (2010), 'Superior antigen cross-presentation and xcr1 expression define human cd11c+cd141+ cells as homologues of mouse cd8+ dendritic cells', *The Journal of Experimental Medicine* **207**(6), 1273–1281.

Bagnasco, D., Ferrando, M., Varricchi, G., Passalacqua, G. and Canonica, G. W. (2016), 'A critical evaluation of anti-il-13 and anti-il-4 strategies in severe asthma', *International Archives of Allergy and Immunology* **170**(2), 122–131.

Ballester, M., Jeanbart, L., de Titta, A., Nembrini, C., Marsland, B. J., Hubbell, J. A. and Swartz, M. A. (2015), 'Nanoparticle conjugation enhances the immunomodulatory effects of intranasally delivered cpg in house dust mite-allergic mice', **5**, 14274.

Banchereau, J., Thompson-Snipes, L., Zurawski, S., Blanck, J.-P., Cao, Y., Clayton, S., Gorvel, J.-P., Zurawski, G. and Klechevsky, E. (2012), 'The differential production of cytokines by human langerhans cells and dermal cd14+ dcs controls ctl priming', *Blood* **119**(24), 5742–5749.

Baraldo, S., Turato, G., Badin, C., Bazzan, E., Beghé, B., Zuin, R., Calabrese, F., Casoni, G., Maestrelli, P., Papi, A., Fabbri, L. M. and Saetta, M. (2004), 'Neutrophilic infiltration within the airway smooth muscle in patients with copd', *Thorax* **59**(4), 308–312.

Barick, K. C. and Hassan, P. A. (2012), 'Glycine passivated fe3o4 nanoparticles for thermal therapy', *Journal of Colloid and Interface Science* **369**(1), 96–102.

Barnes, P. J. (2013), 'Corticosteroid resistance in patients with asthma and chronic obstructive pulmonary disease', *Journal of Allergy and Clinical Immunology* **131**(3), 636–645.

Barton, L. E., Auffan, M., Bertrand, M., Barakat, M., Santaella, C., Masion, A., Borschneck, D., Olivi, L., Roche, N., Wiesner, M. R. and Bottero, J.-Y. (2014), 'Transformation of pristine and citrate-functionalized ceo2 nanoparticles in a laboratory-scale activated sludge reactor', *Environmental Science and Technology* **48**(13), 7289–7296.

Baudish, K., de Paula Vieira, R., Cicko, S., Ayata, K., Hossfeld, M., Ehrat, N., Gomez-Munoz, A., Eltzschig, H. K. and Idzko, M. (2016), 'C1p attenuates lipopolysaccharide-induced acute lung injury by preventing nf-kb activation in neutrophils', *The Journal of Immunology* **196**(5), 2319–2326.

Berghian-Grosan, C., Olenic, L., Katona, G., Perde-Schrepler, M. and Vulcu, A. (2014), 'l-leucine for gold nanoparticles synthesis and their cytotoxic effects evaluation', *Amino Acids* **46**(11), 2545–2552.

Biswas, S. K., Gangi, L., Paul, S., Schioppa, T., Saccani, A., Sironi, M., Bottazzi, B., Doni, A., Vincenzo, B., Pasqualini, F., Vago, L., Nebuloni, M., Mantovani, A. and Sica, A. (2006), 'A distinct and unique transcriptional program expressed by tumor-associated macrophages (defective nf-kappab and enhanced irf-3/stat1 activation)', *Blood* **107**(5), 2112–22.

Blanco, E., Shen, H. and Ferrari, M. (2015), 'Principles of nanoparticle design for overcoming biological barriers to drug delivery', *Nat Biotech* **33**(9), 941–951.

Bloem, J. L., Reijnierse, M., Huizinga, T. W. J. and van der Helm-van Mil, A. H. M. (2018), 'Mr signal intensity: staying on the bright side in mr image interpretation', *RMD Open* **4**(1), e000728.

Bozinovski, S., Seow, H. J., Crack, P. J., Anderson, G. P. and Vlahos, R. (2012), 'Glutathione peroxidase-1 primes pro-inflammatory cytokine production after lps challenge in vivo', *PLOS ONE* **7**(3), e33172.

Bradding, P., Walls, A. F. and Holgate, S. T. (2006), 'The role of the mast cell in the pathophysiology of asthma', *Journal of Allergy and Clinical Immunology* **117**(6), 1277–1284.

Braet, F., Wisse, E., Bomans, P., Frederik, P., Geerts, W., Koster, A., Soon, L. and Ringer, S. (2007), 'Contribution of high-resolution correlative imaging techniques in the study of the liver sieve in three-dimensions', *Microscopy Research and Technique* **70**(3), 230–242.

Braskett, M. and Riedl, M. A. (2010), 'Novel antioxidant approaches to the treatment of upper airway inflammation', *Current Opinion in Allergy and Clinical Immunology* **10**(1), 34–41.

Buist, A. (2003), 'Similarities and differences between asthma and chronic obstructive pulmonary disease: treatment and early outcomes', *European Respiratory Journal* **21**(39 suppl), 30s–35s.

Cai, H. and Yao, P. (2014), 'Gold nanoparticles with different amino acid surfaces: Serum albumin adsorption, intracellular uptake and cytotoxicity', *Colloids and Surfaces B: Biointerfaces* **123**, 900–906.

Cai, K., Hou, Y., Hu, Y., Zhao, L., Luo, Z., Shi, Y., Lai, M., Yang, W. and Liu, P. (2011), 'Correlation of the cytotoxicity of tio2 nanoparticles with different particle sizes on a sub-200-nm scale', *Small* **7**(21), 3026–3031.

Cai, Y., Sugimoto, C., Arainga, M., Alvarez, X., Didier, E. S. and Kuroda, M. J. (2014), 'In vivo characterization of alveolar and interstitial lung macrophages in rhesus macaques: Implications for understanding lung disease in humans', *The Journal of Immunology* **192**(6), 2821–2829.

Carruthers, M., Trinick, T., Jankowska, E. and Traish, A. (2008), 'Prevention and treatment of systemic glucocorticoid side effects', *Cardiovascular diabetology* **7**, 30.

Carvalho, T. C., Peters, J. I. and Williams, R. O. (2011), 'Influence of particle size on regional lung deposition – what evidence is there?', *International Journal of Pharmaceutics* **406**(1), 1–10.

Casals, C., Barrachina, M., Serra, M., Lloberas, J. and Celada, A. (2007), 'Lipopolysaccharide up-regulates mhc class ii expression on dendritic cells through an ap-1 enhancer without affecting the levels of ciita', *The Journal of Immunology* **178**(10), 6307–6315.

Catapano, A. L., Corsini, A., Nordestgaard, B. G., Newman, C. B., Bruckert, E., Stroes, E., Stein, E., Mach, F., Raal, F. J., Kees Hovingh, G., Vladutiu, G. D., de Backer, G., Ginsberg, H. N., Ginsberg, H. N., Ray, K. K., Tokgozoglu, L., Leiter, L., John Chapman, M., John Chapman, M., Roden, M., Wiklund, O., Thompson, P. D., Santos, R. D., Hegele, R. A., Krauss, R. M., Jacobson, T. A., Laufs, U., Marz, W., Panel, E. A. S. C., Panel, E. A. S. C., Stroes, E. S., Tokgozoglu, L., Nordestgaard, B. G., Bruckert, E., De Backer, G., Krauss, R. M., Laufs, U., Santos, R. D., Hegele, R. A., Hovingh, G. K., Leiter, L. A., Thompson, P. D., Mach, F., Marz, W., Newman, C. B., Wiklund, O., Jacobson, T. A., Chapman, M. J., Ginsberg, H. N., Catapano, A. L., Corsini, A., Vladutiu, G. D., Raal, F. J., Ray, K. K., Roden, M. and Stein, E. (2015), 'Statin-associated muscle symptoms: impact on statin therapy—european atherosclerosis society consensus panel statement on assessment, aetiology and management', *European Heart Journal* **36**(17), 1012–1022.

Cervellino, A., Frison, R., Cernuto, G., Guagliardi, A. and Masciocchi, N. (2014), 'Lattice parameters and site occupancy factors of magnetite-maghemite core-shell nanoparticles. a critical study', *Journal of Applied Crystallography* **47**(5), 1755–1761.

Chabaud, M., Heuze, M. L., Bretou, M., Vargas, P., Maiuri, P., Solanes, P., Maurin, M., Terriac, E., Le Berre, M., Lankar, D., Piolot, T., Adelstein, R. S., Zhang, Y., Sixt, M., Jacobelli, J., Benichou, O., Voituriez, R., Piel, M. and Lennon-Dumenil, A. M. (2015), 'Cell migration and antigen capture are antagonistic processes coupled by myosin ii in dendritic cells', *Nat Commun* **6**, 7526.

Chakraborty, A., Boer, J. C., Selomulya, C. and Plebanski, M. (2017), 'Amino acid functionalized inorganic nanoparticles as cutting-edge therapeutic and diagnostic agents', *Bioconjugate Chemistry* **29**(3), 657–671.

Chakraborty, A., Boer, J. C., Selomulya, C., Plebanski, M. and Royce, S. G. (2018), 'Insights into endotoxin-mediated lung inflammation and future treatment strategies.', *Expert Review of Respiratory Medicine* **12**(11), 941–955.

Chakraborty, A., Patni, P., Suhag, D., Saini, G., Singh, A., Chakrabarti, S. and Mukherjee, M. (2015), 'N-doped carbon nanosheets with antibacterial activity: mechanistic insight', *RSC Advances* **5**(30), 23591–23598.

Chan, J. K., Roth, J., Oppenheim, J. J., Tracey, K. J., Vogl, T., Feldmann, M., Horwood, N. and Nanchahal, J. (2012), 'Alarmins: awaiting a clinical response', *The Journal of Clinical Investigation* **122**(8), 2711–2719.

Chang, Y.-W., Tseng, C.-P., Lee, C.-H., Hwang, T.-L., Chen, Y.-L., Su, M.-T., Chong, K.-Y., Lan, Y.-W., Wu, C.-C., Chen, K.-J., Lu, F.-H., Liao, H.-R., Hsueh, C. and Hsieh, P.-W. (2018), 'B-nitrostyrene derivatives attenuate lps-mediated acute lung injury via the inhibition of neutrophil-platelet interactions and net release', *American Journal of Physiology-Lung Cellular and Molecular Physiology* **314**(4), L654–L669.

Chithrani, B. D., Ghazani, A. A. and Chan, W. C. W. (2006), 'Determining the size and shape dependence of gold nanoparticle uptake into mammalian cells', *Nano Letters* **6**(4), 662–668.

Chongprasert, S., Knopp, S. A. and Nail, S. L. (2001), 'Characterization of frozen solutions of glycine', *Journal of Pharmaceutical Sciences* **90**(11), 1720 – 1728.

Coll Ferrer, M. C., Shuvaev, V. V., Zern, B. J., Composto, R. J., Muzykantov, V. R. and Eckmann, D. M. (2014), 'Icam-1 targeted nanogels loaded with dexamethasone alleviate pulmonary inflammation', *PLOS ONE* **9**(7), e102329.

Collin, M., McGovern, N. and Haniffa, M. (2013), 'Human dendritic cell subsets', *Immunology* **140**(1), 22–30.

Colonna, M., Trinchieri, G. and Liu, Y. J. (2004), 'Plasmacytoid dendritic cells in immunity', *Nat Immunol* **5**(12), 1219–26.

Corren, J., Lemanske, R. F., Hanania, N. A., Korenblat, P. E., Parsey, M. V., Arron, J. R., Harris, J. M., Scheerens, H., Wu, L. C., Su, Z., Mosesova, S., Eisner, M. D., Bohen, S. P. and Matthews, J. G. (2011), 'Lebrikizumab treatment in adults with asthma', *New England Journal of Medicine* **365**(12), 1088–1098.

Corren, J., Parnes, J. R., Wang, L., Mo, M., Roseti, S. L., Griffiths, J. M. and van der Merwe, R. (2017), 'Tezepelumab in adults with uncontrolled asthma', *New England Journal of Medicine* **377**(10), 936–946.

Coutinho, A. E. and Chapman, K. E. (2011), 'The anti-inflammatory and immunosuppressive effects of glucocorticoids, recent developments and mechanistic insights', *Molecular and Cellular Endocrinology* **335**(1), 2 – 13.

Cova, E., Piloni, D., Codullo, V., Inghilleri, S., Breda, S., Prosperi, D., Colombo, M., Montecucco, C., Distler, J. H. and Meloni, F. (2017), 'Imatinib-loaded gold nanoparticles ameliorate experimental lung fibrosis induced by bleomycin', *European Respiratory Journal* **50**(suppl 61).

Creagh, E. M. and O'Neill, L. A. J. (2006), 'Tlrs, nlrs and rlrs: a trinity of pathogen sensors that co-operate in innate immunity', *Trends in Immunology* **27**(8), 352–357.

Cruz, M., Maldonado-Bernal, C., Mondragón-Gonzalez, R., Sanchez-Barrera, R., Wacher, N. H., Carvajal-Sandoval, G. and Kumate, J. (2008), 'Glycine treatment decreases proinflammatory cytokines and increases interferon-γ in patients with type 2 diabetes', *Journal of Endocrinological Investigation* **31**(8), 694–699.

Dagvadorj, J., Shimada, K., Chen, S., Jones, H. D., Tumurkhuu, G., Zhang, W., Wawrowsky, K. A., Crother, T. R. and Arditi, M. (2015), 'Lipopolysaccharide induces alveolar macrophage necrosis via cd14 and the p2x7 receptor leading to interleukin-1α release', *Immunity* **42**(4), 640–653.

Dahl, R. (2006), 'Systemic side effects of inhaled corticosteroids in patients with asthma', *Respiratory Medicine* **100**(8), 1307–1317.

Dailey, L. A., Schmehl, T., Gessler, T., Wittmar, M., Grimminger, F., Seeger, W. and Kissel, T. (2003), 'Nebulization of biodegradable nanoparticles: impact of nebulizer technology and nanoparticle characteristics on aerosol features', *Journal of Controlled Release* **86**(1), 131 – 144.

Daniels, N. J., Hyde, E., Ghosh, S., Seo, K., Price, K. M., Hoshino, K., Kaisho, T., Okada, T. and Ronchese, F. (2016), 'Antigen-specific cytotoxic t lymphocytes target airway cd103(+) and cd11b(+) dendritic cells to suppress allergic inflammation', *Mucosal Immunol* **9**(1), 229–39.

Davide, P., Norberto, M., Antonietta, G., José Manuel, D.-V. and Natividad, G. (2013), 'Poly(amino acid) functionalized maghemite and gold nanoparticles', *Nanotechnology* **24**(7), 075102.

Davies, L. C., Jenkins, S. J., Allen, J. E. and Taylor, P. R. (2013), 'Tissue-resident macrophages', *Nat Immunol* **14**(10), 986–95.

De Haar, C., Hassing, I., Bol, M., Bleumink, R. and Pieters, R. (2006), 'Ultrafine but not fine particulate matter causes airway inflammation and allergic airway sensitization to co-administered antigen in mice', *Clinical and Experimental Allergy* **36**(11), 1469–1479.

de Jong, A., Pena-Cruz, V., Cheng, T.-Y., Clark, R. A., Van Rhijn, I. and Moody, D. B. (2010), 'Cd1a-autoreactive t cells are a normal component of the human [alpha][beta] t cell repertoire', *Nat Immunol* **11**(12), 1102–1109.

De Simone, R., Vissicchio, F., Mingarelli, C., De Nuccio, C., Visentin, S., Ajmone-Cat, M. A. and Minghetti, L. (2013), 'Branched-chain amino acids influence the immune properties of microglial cells and their responsiveness to pro-inflammatory signals', *Biochimica et Biophysica Acta (BBA) - Molecular Basis of Disease* **1832**(5), 650–659.

De Souza, K. C. B., Petrovick, P. R., Bassani, V. L. and Ortega, G. G. (2000), 'The adjuvants aerosil 200 and gelita-sol-p influence on the technological characteristics of spray-dried powders from passiflora edulis var. flavicarpa', *Drug Development and Industrial Pharmacy* **26**(3), 331–336.

de Souza Xavier Costa, N., Ribeiro Júnior, G., dos Santos Alemany, A. A., Belotti, L., Zati, D. H., Frota Cavalcante, M., Matera Veras, M., Ribeiro, S., Kallás, E. G., Nascimento Saldiva, P. H., Dolhnikoff, M. and Ferraz da Silva, L. F. (2017), 'Early and late pulmonary effects of nebulized lps in mice: An acute lung injury model', *PLOS ONE* **12**(9), e0185474.

Decuzzi, P., Pasqualini, R., Arap, W. and Ferrari, M. (2008), 'Intravascular delivery of particulate systems: Does geometry really matter?', *Pharmaceutical Research* **26**(1), 235.

Delgado, A. V., González-Caballero, F., Hunter, R. J., Koopal, L. K. and Lyklema, J. (2007), 'Measurement and interpretation of electrokinetic phenomena', *Journal of Colloid and Interface Science* **309**(2), 194–224.

Desai, R. J., Bateman, B. T., Huybrechts, K. F., Patorno, E., Hernandez-Diaz, S., Park, Y., Dejene, S. Z., Cohen, J., Mogun, H. and Kim, S. C. (2017), 'Risk of serious infections associated with use of immunosuppressive agents in pregnant women with autoimmune inflammatory conditions: cohort study', *BMJ* **356**, j895.

Desch, A. N., Gibbings, S. L., Clambey, E. T., Janssen, W. J., Slansky, J. E., Kedl, R. M., Henson, P. M. and Jakubzick, C. (2014), 'Dendritic cell subsets require cis-activation for cytotoxic cd8 t-cell induction', *Nature Communication* **5**.

Dobrovolskaia, M. A., Medvedev, A. E., Thomas, K. E., Cuesta, N., Toshchakov, V., Ren, T., Cody, M. J., Michalek, S. M., Rice, N. R. and Vogel, S. N. (2003), 'Induction of in vitro reprogramming by toll-like receptor (tlr)2 and tlr4 agonists in murine macrophages: Effects of tlr "homotolerance" versus "heterotolerance" on nf-b signaling pathway components', *The Journal of Immunology* **170**(1), 508–519.

Donovan, C., Royce, S. G., Vlahos, R. and Bourke, J. E. (2015), 'Lipopolysaccharide does not alter small airway reactivity in mouse lung slices', *PLOS ONE* **10**(3), e0122069.

Doulatov, S., Notta, F., Eppert, K., Nguyen, L. T., Ohashi, P. S. and Dick, J. E. (2010), 'Revised map of the human progenitor hierarchy shows the origin of macrophages and dendritic cells in early lymphoid development', *Nat Immunol* **11**(7), 585–93.

Droemann, D., Goldmann, T., Tiedje, T., Zabel, P., Dalhoff, K. and Schaaf, B. (2005), 'Toll-like receptor 2 expression is decreased on alveolar macrophages in cigarette smokers and copd patients', *Respiratory Research* **6**(1), 68.

Duluc, D., Delneste, Y., Tan, F., Moles, M.-P., Grimaud, L., Lenoir, J., Preisser, L., Anegon, I., Catala, L., Ifrah, N., Descamps, P., Gamelin, E., Gascan, H., Hebbar, M. and Jeannin, P. (2007), 'Tumor-associated leukemia inhibitory factor and il-6 skew monocyte differentiation into tumor-associated macrophage-like cells', *Blood* **110**(13), 4319–4330.

Ebner, S., Ratzinger, G., Krösbacher, B., Schmuth, M., Weiss, A., Reider, D., Kroczek, R. A., Herold, M., Heufler, C., Fritsch, P. and Romani, N. (2001), 'Production of il-12 by human monocyte-derived dendritic cells is optimal when the stimulus is given at the onset of maturation, and is further enhanced by il-4', *The Journal of Immunology* **166**(1), 633–641.

Edwards, J. P., Zhang, X., Frauwirth, K. A. and Mosser, D. M. (2006), 'Biochemical and functional characterization of three activated macrophage populations', *J Leukoc Biol* **80**(6), 1298–307.

Edwards, J. P., Zhang, X. and Mosser, D. M. (2009), 'The expression of heparin-binding epidermal growth factor-like growth factor by regulatory macrophages', *J Immunol* **182**(4), 1929–39.

Egawa, M., Mukai, K., Yoshikawa, S., Iki, M., Mukaida, N., Kawano, Y., Minegishi, Y. and Karasuyama, H. (2013), 'Inflammatory monocytes recruited to allergic skin acquire an anti-inflammatory m2 phenotype via basophil-derived interleukin-4', *Immunity* **38**(3), 570–580.

Eich, A., Urban, V., Jutel, M., Vlcek, J., Shim, J. J., Trofimov, V. I., Liam, C.-K., Kuo, P.-H., Hou, Y., Xiao, J., Branigan, P. and O'Brien, C. D. (2017), 'A randomized, placebo-controlled phase 2 trial of cnto 6785 in chronic obstructive pulmonary disease', *COPD: Journal of Chronic Obstructive Pulmonary Disease* **14**(5), 476–483.

Fardet, L., Petersen, I. and Nazareth, I. (2016), 'Common infections in patients prescribed systemic glucocorticoids in primary care: A population-based cohort study', *PLOS Medicine* **13**(5), 1–20.

Feng, Q., Liu, Y., Huang, J., Chen, K., Huang, J. and Xiao, K. (2018), 'Uptake, distribution, clearance, and toxicity of iron oxide nanoparticles with different sizes and coatings', *Scientific Reports* **8**(1), 2082.

Feng, Y., Su, J., Zhao, Z., Zheng, W., Wu, H., Zhang, Y. and Chen, T. (2014), 'Differential effects of amino acid surface decoration on the anticancer efficacy of selenium nanoparticles', *Dalton Transactions* **43**(4), 1854–1861.

Ferkol, T. and Schraufnagel, D. (2014), 'The global burden of respiratory disease', *Annals of the American Thoracic Society* **11**(3), 404–406.

Fifis, T., Gamvrellis, A., Crimeen-Irwin, B., Pietersz, G. A., Li, J., Mottram, P. L., McKenzie, I. F. and Plebanski, M. (2004), 'Size-dependent immunogenicity: therapeutic and protective properties of nano-vaccines against tumors', *J Immunol* **173**(5), 3148–54.

Fischer, H. and Widdicombe, J. H. (2006), 'Mechanisms of acid and base secretion by the airway epithelium', *The Journal of membrane biology* **211**(3), 139–150.

Fischer, M. J. E. (2010), *Amine Coupling Through EDC/NHS: A Practical Approach*, Humana Press, Totowa, NJ, pp. 55–73.

Fleming, B. D. and Mosser, D. M. (2011), 'Regulatory macrophages: Setting the threshold for therapy', *European Journal of Immunology* **41**(9), 2498–2502.

Fogarty, A., Broadfield, E., Lewis, S., Lawson, N. and Britton, J. (2004), 'Amino acids and asthma: a case-control study', *European Respiratory Journal* **23**(4), 565–568.

Folkerts, G., Busse, W., Nijkamp, F., Sorkness, R. and Gern, J. (1998), 'Virus-induced airway hyperresponsiveness and asthma', *American Journal of Respiratory and Critical Care Medicine* **157**(6), 1708–1720.

Froh, M., Thurman, R. G. and Wheeler, M. D. (2002), 'Molecular evidence for a glycine-gated chloride channel in macrophages and leukocytes', *American Journal of Physiology - Gastrointestinal and Liver Physiology* **283**(4), G856–G863.

Frohlich, E. (2012), 'The role of surface charge in cellular uptake and cytotoxicity of medical nanoparticles', *International Journal of Nanomedicine* **7**, 5577–5591.

Galli, S. J., Tsai, M. and Piliponsky, A. M. (2008), 'The development of allergic inflammation', *Nature* **454**(7203), 445–454.

Gandhi, N. A., Pirozzi, G. and Graham, N. M. H. (2017), 'Commonality of the il-4/il-13 pathway in atopic diseases', *Expert Review of Clinical Immunology* **13**(5), 425–437.

Garratt, L. W., Wright, A. K. A., Ranganathan, S. C., Grigg, J. and Sly, P. D. (2012), 'Small macrophages are present in early childhood respiratory disease', *Journal of Cystic Fibrosis* **11**(3), 201–208.

George, B.-B. G., Wei, Q. L., Shen, L., Wei, K. W., Tony, K. H. L., Chee, K. T. and Pik, E. C. (2019), 'Quantification of hepatic steatosis in chronic liver disease using novel automated method of second harmonic generation and two-photon excited fluorescence', *Nature Scientific Reports* **9**, 2975.

Ghasempour, S., Shokrgozar, M. A., Ghasempour, R. and Alipour, M. (2015), 'Investigating the cytotoxicity of iron oxide nanoparticles in in vivo and in vitro studies', *Experimental and Toxicologic Pathology* **67**(10), 509–515.

Gholami, A., Rasoul-amini, S., Ebrahiminezhad, A., Seyed Hassan, S. and Ghasemi, Y. (2015), 'Lipoamino acid coated superparamagnetic iron oxide nanoparticles concentration and time dependently enhanced growth of human hepatocarcinoma cell line (hep-g2)', *Journal of Nanomaterials* .

Gielen, M., Thomas, P. and Smart, T. G. (2015), 'The desensitization gate of inhibitory cys-loop receptors', **6**, 6829.

Gilliet, M., Cao, W. and Liu, Y.-J. (2008), 'Plasmacytoid dendritic cells: sensing nucleic acids in viral infection and autoimmune diseases', *Nat Rev Immunol* **8**(8), 594–606.

Gleissner, C. A., Shaked, I., Little, K. M. and Ley, K. (2010), 'Cxc chemokine ligand 4 induces a unique transcriptome in monocyte-derived macrophages', *J Immunol* **184**(9), 4810–8.

Güngör, N., Pennings, J. L., Knaapen, A. M., Chiu, R. K., Peluso, M., Godschalk, R. W. and Van Schooten, F. J. (2010), 'Transcriptional profiling of the acute pulmonary inflammatory response induced by lps: role of neutrophils', *Respiratory Research* **11**(1), 24.

Gordon, S. (2003), 'Alternative activation of macrophages', *Nat Rev Immunol* **3**(1), 23–35.

Gordon, S. B. and Read, R. C. (2002), 'Macrophage defences against respiratory tract infections: The immunology of childhood respiratory infections', *British Medical Bulletin* **61**(1), 45–61.

Gordon, S. and Taylor, P. R. (2005*a*), 'Monocyte and macrophage heterogeneity', *Nature Reviews Immunology* **12**(5), 953–964.

Gordon, S. and Taylor, P. R. (2005*b*), 'Monocyte and macrophage heterogeneity', *Nat Rev Immunol* **5**(12), 953–64.

Gossuin, Y., Gillis, P., Hocq, A., Vuong, Q. L. and Roch, A. (2009), 'Magnetic resonance relaxation properties of superparamagnetic particles', *Wiley Interdisciplinary Reviews: Nanomedicine and Nanobiotechnology* **1**(3), 299–310.

Greenfeder, S., Umland, S. P., Cuss, F. M., Chapman, R. W. and Egan, R. W. (2001), 'Th2 cytokines and asthma — the role of interleukin-5 in allergic eosinophilic disease', *Respiratory Research* **2**(2), 71–79.

Griffiths, K. L., Tan, J. K. and O'Neill, H. C. (2014), 'Characterization of the effect of lps on dendritic cell subset discrimination in spleen', *Journal of Cellular and Molecular Medicine* **18**(9), 1908–1912.

Grommes, J., Mörgelin, M. and Soehnlein, O. (2012), 'Pioglitazone attenuates endotoxin-induced acute lung injury by reducing neutrophil recruitment', *European Respiratory Journal* **40**(2), 416–423.

Gross, N. J. and Barnes, P. J. (2017), 'New therapies for asthma and chronic obstructive pulmonary disease', *American Journal of Respiratory and Critical Care Medicine* **195**(2), 159–166.

Gschwandtner, M., Schäkel, K., Werfel, T. and Gutzmer, R. (2011), 'Histamine h4 receptor activation on human slan-dendritic cells down-regulates their pro-inflammatory capacity', *Immunology* **132**(1), 49–56.

Guha, M. and Mackman, N. (2002), 'The phosphatidylinositol 3-kinase-akt pathway limits lipopolysaccharide activation of signaling pathways and expression of inflammatory mediators in human monocytic cells', *Journal of Biological Chemistry* **277**(35), 32124–32132.

Gundra, U. M., Girgis, N. M., Ruckerl, D., Jenkins, S., Ward, L. N., Kurtz, Z. D., Wiens, K. E., Tang, M. S., Basu-Roy, U., Mansukhani, A., Allen, J. E. and Loke, P. (2014), 'Alternatively activated macrophages derived from monocytes and tissue macrophages are phenotypically and functionally distinct', *Blood* **123**(20), e110–e122.

Guo, C., Xia, Y., Niu, P., Jiang, L., Duan, J., Yu, Y., Zhou, X., Li, Y. and Sun, Z. (2015), 'Silica nanoparticles induce oxidative stress, inflammation, and endothelial dysfunction in vitro via activation of the mapk/nrf2 pathway and nuclear factor-kb signaling', *International Journal of Nanomedicine* **10**, 1463–1477.

Han, G.-M., Jiang, H.-X., Huo, Y.-F. and Kong, D.-M. (2016), 'Simple synthesis of amino acid-functionalized hydrophilic upconversion nanoparticles capped with both carboxyl and amino groups for bimodal imaging', *Journal of Materials Chemistry B* **4**(19), 3351–3357.

Han, J., Shuvaev, V. V. and Muzykantov, V. R. (2011), 'Catalase and superoxide dismutase conjugated with platelet-endothelial cell adhesion molecule antibody distinctly alleviate abnormal endothelial permeability caused by exogenous reactive oxygen species and vascular endothelial growth factor', *Journal of Pharmacology and Experimental Therapeutics* **338**(1), 82–91.

Hanabuchi, S., Ito, T., Park, W.-R., Watanabe, N., Shaw, J. L., Roman, E., Arima, K., Wang, Y.-H., Voo, K. S., Cao, W. and Liu, Y.-J. (2010), 'Thymic stromal lymphopoietin-activated plasmacytoid dendritic cells induce the generation of foxp3+ regulatory t cells in human thymus', *The Journal of Immunology* **184**(6), 2999–3007.

Haniffa, M., Shin, A., Bigley, V., McGovern, N., Teo, P., See, P., Wasan, P. S., Wang, X.-N., Malinarich, F., Malleret, B., Larbi, A., Tan, P., Zhao, H., Poidinger, M., Pagan, S., Cookson, S., Dickinson, R., Dimmick, I., Jarrett, R. F., Renia, L., Tam, J., Song, C., Connolly, J., Chan, J. K. Y., Gehring, A., Bertoletti, A., Collin, M. and Ginhoux, F. (2012), 'Human tissues contain cd141hi cross-presenting dendritic cells with functional homology to mouse cd103+ nonlymphoid dendritic cells', *Immunity* **37**(1), 60–73.

Hao, N.-B., Lü, M.-H., Fan, Y.-H., Cao, Y.-L., Zhang, Z.-R. and Yang, S.-M. (2012), 'Macrophages in tumor microenvironments and the progression of tumors', *Clinical and Developmental Immunology* **2012**, 11.

Hardy, C. L., LeMasurier, J. S., Belz, G. T., Scalzo-Inguanti, K., Yao, J., Xiang, S. D., Kanellakis, P., Bobik, A., Strickland, D. H., Rolland, J. M., O'Hehir, R. E. and Plebanski, M. (2012), 'Inert 50-nm polystyrene nanoparticles that modify pulmonary dendritic cell function and inhibit allergic airway inflammation', *The Journal of Immunology* **188**(3), 1431–1441.

Hardy, C. L., LeMasurier, J. S., Mohamud, R., Yao, J., Xiang, S. D., Rolland, J. M., O'Hehir, R. E. and Plebanski, M. (2013), 'Differential uptake of nanoparticles and microparticles by pulmonary apc subsets induces discrete immunological imprints', *The Journal of Immunology* **191**(10), 5278–5290.

Harris, J. F., Aden, J., Lyons, C. R. and Tesfaigzi, Y. (2007), 'Resolution of lps-induced airway inflammation and goblet cell hyperplasia is independent of il-18', *Respiratory research* **8**(1), 24–24.

Haslett, C. (1999), 'Granulocyte apoptosis and its role in the resolution and control of lung inflammation', *American Journal of Respiratory and Critical Care Medicine* **160**(supplement1), S5–S11.

Hattori, Y., Hattori, S. and Kasai, K. (2003), 'Lipopolysaccharide activates akt in vascular smooth muscle cells resulting in induction of inducible nitric oxide synthase through nuclear factor-kappa b activation', *European Journal of Pharmacology* **481**(2), 153 – 158.

Hazeki, K., Kinoshita, S., Matsumura, T., Nigorikawa, K., Kubo, H. and Hazeki, O. (2006), 'Opposite effects of wortmannin and 2-(4-morpholinyl)-8-phenyl-1(4h)-benzopyran-4-one hydrochloride on toll-like receptor-mediated nitric oxide production: Negative regulation of nuclear factor-kb by phosphoinositide 3-kinase', *Molecular Pharmacology* **69**(5), 1717–1724.

He, C., Hu, Y., Yin, L., Tang, C. and Yin, C. (2010), 'Effects of particle size and surface charge on cellular uptake and biodistribution of polymeric nanoparticles', *Biomaterials* **31**(13), 3657–3666.

He, R. and Geha, R. S. (2010), 'Thymic stromal lymphopoietin', *Annals of the New York Academy of Sciences* **1183**(1), 13–24.

Hennies, C. M., Lehn, M. A. and Janssen, E. M. (2015), 'Quantitating mhc class ii trafficking in primary dendritic cells using imaging flow cytometry', *Journal of Immunological Methods* **423**, 18 – 28.

Herz, U., Renz, H. and Wiederman, U. (2004), 'Animal models of type i allergy using recombinant allergens', *Methods* **32**(3), 271 – 280.

Hissong, B. D., Byrne, G. I., Padilla, M. L. and Carlin, J. M. (1995), 'Upregulation of interferon-induced indoleamine 2,3-dioxygenase in human macrophage cultures by lipopolysaccharide, muramyl tripeptide, and interleukin-1', *Cell Immunol* **160**(2), 264–9.

Hänsel, A., Günther, C., Ingwersen, J., Starke, J., Schmitz, M., Bachmann, M., Meurer, M., Rieber, E. P. and Schäkel, K. (2011), 'Human slan (6-sulfo lacnac) dendritic cells are inflammatory dermal dendritic cells in psoriasis and drive strong th17/th1 t-cell responses', *Journal of Allergy and Clinical Immunology* **127**(3), 787–794.e9.

Howard, M. D., Hood, E. D., Zern, B., Shuvaev, V. V., Grosser, T. and Muzykantov, V. R. (2014), 'Nanocarriers for vascular delivery of anti-inflammatory agents', *Annual review of pharmacology and toxicology* **54**, 205–226.

Hua-dong, W., Xiu-xiu, L., Da-xiang, L., Ren-bin, Q., Yan-ping, W., Yong-mei, F. and Li-wei, W. (2009), 'Glycine inhibits the lps-induced increase in cytosolic ca2+ concentration and tnfa production in cardiomyocytes by activating a glycine receptor', *Acta Pharmacologica Sinica* **30**, 1107 – 1114.

Huang, K., Ma, H., Liu, J., Huo, S., Kumar, A., Wei, T., Zhang, X., Jin, S., Gan, Y., Wang, P. C., He, S., Zhang, X. and Liang, X.-J. (2012), 'Size-dependent localization and penetration of ultrasmall gold nanoparticles in cancer cells, multicellular spheroids, and tumors in vivo', *ACS Nano* **6**(5), 4483–4493.

Iijima, N. and Iwasaki, A. (2014), 'A local macrophage chemokine network sustains protective tissue-resident memory cd4 t cells', *Science* **346**(6205), 93–98.

Ikejima, K., Iimuro, Y., Forman, D. T. and Thurman, R. G. (1996), 'A diet containing glycine improves survival in endotoxin shock in the rat', *American Journal of Physiology-Gastrointestinal and Liver Physiology* **271**(1), G97–G103.

Ikezoe, T. (2015), 'Thrombomodulin/activated protein c system in septic disseminated intravascular coagulation', *Journal of Intensive Care* **3**(1), 1.

Inbaraj, B. S., Kao, T. H., Tsai, T. Y., Chiu, C. P., Kumar, R. and Chen, B. H. (2011), 'The synthesis and characterization of poly(γ-glutamic acid)-coated magnetite nanoparticles and their effects on antibacterial activity and cytotoxicity', *Nanotechnology* **22**(7), 075101.

Inoue, K.-i., Koike, E., Yanagisawa, R., Hirano, S., Nishikawa, M. and Takano, H. (2009), 'Effects of multi-walled carbon nanotubes on a murine allergic airway inflammation model', *Toxicology and Applied Pharmacology* **237**(3), 306–316.

Inoue, K.-i., Yanagisawa, R., Koike, E., Nishikawa, M. and Takano, H. (2010), 'Repeated pulmonary exposure to single-walled carbon nanotubes exacerbates allergic inflammation of the airway: Possible role of oxidative stress', *Free Radical Biology and Medicine* **48**(7), 924–934.

Islam, M. I. U. and Langrish, T. A. G. (2010), 'An investigation into lactose crystallization under high temperature conditions during spray drying', *Food Research International* **43**(1), 46–56.

Ito, T., Inaba, M., Inaba, K., Toki, J., Sogo, S., Iguchi, T., Adachi, Y., Yamaguchi, K., Amakawa, R., Valladeau, J., Saeland, S., Fukuhara, S. and Ikehara, S. (1999), 'A cd1a+/cd11c+ subset of human blood dendritic cells is a direct precursor of langerhans cells', *The Journal of Immunology* **163**(3), 1409–1419.

Jablonski, K. A., Amici, S. A., Webb, L. M., Ruiz-Rosado Jde, D., Popovich, P. G., Partida-Sanchez, S. and Guerau-de Arellano, M. (2015), 'Novel markers to delineate murine m1 and m2 macrophages', *PLoS One* **10**(12), e0145342.

Janeway, C. A., Jr, P. T., Walport, M. and Shlomchik, M. J. (2001), *Immunobiology*, 5th edition edn, New York: Garland Science.

Javitt, D. C., Silipo, G., Cienfuegos, A., Shelley, A. M., Bark, N., Park, M., Lindenmayer, J. P., Suckow, R. and Zukin, S. R. (2001), 'Adjunctive high-dose glycine in the treatment of schizophrenia', *Int J Neuropsychopharmacol* **4**(4), 385–91.

Jin-Wook, Y., Elizabeth, C. and Samir, M. (2010), 'Factors that control the circulation time of nanoparticles in blood: Challenges, solutions and future prospects', *Current Pharmaceutical Design* **16**(21), 2298–2307.

Johnson, E. R. and Matthay, M. A. (2010), 'Acute lung injury: Epidemiology, pathogenesis, and treatment', *Journal of Aerosol Medicine and Pulmonary Drug Delivery* **23**(4), 243–252.

Johnson, K. M., Fain, S. B., Schiebler, M. L. and Nagle, S. (2013), 'Optimized 3d ultrashort echo time pulmonary mri', *Magnetic Resonance in Medicine* **70**(5), 1241–1250.

Jones, L. A., Kreem, S., Shweash, M., Paul, A., Alexander, J. and Roberts, C. W. (2010), 'Differential modulation of tlr3- and tlr4-mediated dendritic cell maturation and function by progesterone', *The Journal of Immunology* **185**(8), 4525–4534.

Jones, M. R., Simms, B. T., Lupa, M. M., Kogan, M. S. and Mizgerd, J. P. (2005), 'Lung nf-kb activation and neutrophil recruitment require il-1 and tnf receptor signaling during pneumococcal pneumonia', *The Journal of Immunology* **175**(11), 7530–7535.

Katholnig, K., Linke, M., Pham, H., Hengstschläger, M. and Weichhart, T. (2013), 'Immune responses of macrophages and dendritic cells regulated by mtor signalling', *Biochemical Society Transactions* **41**(4), 927–933.

Katsnelson, B. A., Privalova, L. I., Sutunkova, M. P., Tulakina, L. G., Pichugova, S. V., Beykin, J. B. and Khodos, M. J. (2012), 'Interaction of iron oxide fe_3o_4 nanoparticles and alveolar macrophages in vivo', *Bull Exp Biol Med* **152**(5), 627–629.

Kay, A. (2001), 'Allergy and allergic diseases', *New England Journal of Medicine* **344**(1), 30–37.

Kejian, Z., Qianyun, S., Ulrich, M. and Min, Z. (2000), 'Human monocyte-derived dendritic cells expressing both chemotactic cytokines il-8, mcp-1, rantes and their receptors, and their selective migration to these chemokines', *Chin Med J* **113**(12), 1124–1128.

Kettler, K., Krystek, P., Giannakou, C., Hendriks, A. J. and de Jong, W. H. (n.d.), 'Exploring the effect of silver nanoparticle size and medium composition on uptake into pulmonary epithelial 16hbe14o-cells', *Journal of Nanoparticle Research* **18**, 182.

Khazen, W., M'Bika, J.-P., Tomkiewicz, C., Benelli, C., Chany, C., Achour, A. and Forest, C. (2005), 'Expression of macrophage-selective markers in human and rodent adipocytes', *FEBS Letters* **579**(25), 5631–5634.

Kigerl, K. A., Gensel, J. C., Ankeny, D. P., Alexander, J. K., Donnelly, D. J. and Popovich, P. G. (2009), 'Identification of two distinct macrophage subsets with divergent effects causing either neurotoxicity or regeneration in the injured mouse spinal cord', *J Neurosci* **29**(43), 13435–44.

Kim, H., Uto, T., Akagi, T., Baba, M. and Akashi, M. (2010*a*), 'Amphiphilic poly(amino acid) nanoparticles induce size-dependent dendritic cell maturation', *Advanced Functional Materials* **20**(22), 3925–3931.

Kim, H., Uto, T., Akagi, T., Baba, M. and Akashi, M. (2010*b*), 'Amphiphilic poly(amino acid) nanoparticles induce size-dependent dendritic cell maturation', *Advanced Functional Materials* **20**(22), 3925–3931.

Kim, J.-S., Yoon, T.-J., Yu, K.-N., Noh, M. S., Woo, M., Kim, B.-G., Lee, K.-H., Sohn, B.-H., Park, S.-B., Lee, J.-K. and Cho, M.-H. (2006), 'Cellular uptake of magnetic nanoparticle is mediated through energy-dependent endocytosis in a549 cells', *J Vet Sci* **7**(4), 321–326.

Kim, T.-H., Kim, M., Park, H.-S., Shin, U. S., Gong, M.-S. and Kim, H.-W. (2012), 'Size-dependent cellular toxicity of silver nanoparticles', *Journal of Biomedical Materials Research Part A* **100A**(4), 1033–1043.

Kin, N. W. and Sanders, V. M. (2006), 'Cd86 stimulation on a b cell activates the phosphatidylinositol 3-kinase/akt and phospholipase cy2/protein kinase cab signaling pathways', *The Journal of Immunology* **176**(11), 6727–6735.

Kindt, T. J., Goldsby, R. A., Osborne, B. A. and Kuby, J. (2007), *Kuby immunology*, 6th ed. / thomas j. kindt, richard a. goldsby, barbara a. osborne edn, New York : W.H. Freeman, c2007.

Klug, G., Kampf, T., Bloemer, S., Bremicker, J., Ziener, C. H., Heymer, A., Gbureck, U., Rommel, E., Nöth, U., Schenk, W. A., Jakob, P. M. and Bauer, W. R. (2010), 'Intracellular and extracellular t1 and t2 relaxivities of magneto-optical nanoparticles at experimental high fields', *Magnetic Resonance in Medicine* **64**(6), 1607–1615.

Knapp, S. (2009), 'Lps and bacterial lung inflammation models', *Drug Discovery Today: Disease Models* **6**(4), 113–118.

Krebs, D. L., Chehal, M. K., Sio, A., Huntington, N. D., Da, M. L., Ziltener, P., Inglese, M., Kountouri, N., Priatel, J. J., Jones, J., Tarlinton, D. M., Anderson, G. P., Hibbs, M. L. and Harder, K. W. (2012), 'Lyn-dependent signaling regulates the innate immune response by controlling dendritic cell activation of nk cells', *The Journal of Immunology* **188**(10), 5094–5105.

Kurosaka, K., Watanabe, N. and Kobayashi, Y. (2001), 'Production of proinflammatory cytokines by resident tissue macrophages after phagocytosis of apoptotic cells', *Cellular Immunology* **211**(1), 1–7.

Kusaka, T., Nakayama, M., Nakamura, K., Ishimiya, M., Furusawa, E. and Ogasawara, K. (2014), 'Effect of silica particle size on macrophage inflammatory responses', *PLoS One* **9**(3), e92634.

Labiris, N. R. and Dolovich, M. B. (2003), 'Pulmonary drug delivery. part i: Physiological factors affecting therapeutic effectiveness of aerosolized medications', *British Journal of Clinical Pharmacology* **56**(6), 588–599.

Lai, S. K., Wang, Y.-Y. and Hanes, J. (2009), 'Mucus-penetrating nanoparticles for drug and gene delivery to mucosal tissues', *Advanced Drug Delivery Reviews* **61**(2), 158 – 171.

Lappalainen, U., Whitsett, J. A., Wert, S. E., Tichelaar, J. W. and Bry, K. (2005), 'Interleukin-1b causes pulmonary inflammation, emphysema, and airway remodeling in the adult murine lung', *American Journal of Respiratory Cell and Molecular Biology* **32**(4), 311–318.

Larson, T. A., Joshi, P. P. and Sokolov, K. (2012), 'Preventing protein adsorption and macrophage uptake of gold nanoparticles via a hydrophobic shield', *ACS Nano* **6**(10), 9182–9190.

Lauterbach, H., Bathke, B., Gilles, S., Traidl-Hoffmann, C., Luber, C. A., Fejer, G., Freudenberg, M. A., Davey, G. M., Vremec, D., Kallies, A., Wu, L., Shortman, K., Chaplin, P., Suter, M., O'Keeffe, M. and Hochrein, H. (2010), 'Mouse cd8α+ dcs and human bdca3+ dcs are major producers of ifn-λ in response to poly ic', *The Journal of Experimental Medicine* **207**(12), 2703–2717.

Lawrence, T. (2009), 'The nuclear factor nf-kb pathway in inflammation', *CSH Perspectives in Biology* **1**(6), a001651.

LeBrasseur, N. (2008), *Shuffling of neuronal receptors*, Vol. 181.

Lee, H. J., Jang, K.-S., Jang, S., Kim, J. W., Yang, H.-M., Jeong, Y. Y. and Kim, J.-D. (2010*a*), 'Poly(amino acid)s micelle-mediated assembly of magnetite nanoparticles for ultra-sensitive long-term mr imaging of tumors', *Chemical Communications* **46**(20), 3559–3561.

Lee, H. J., Jang, K.-S., Jang, S., Kim, J. W., Yang, H.-M., Jeong, Y. Y. and Kim, J.-D. (2010*b*), 'Poly(amino acid)s micelle-mediated assembly of magnetite nanoparticles for ultra-sensitive long-term mr imaging of tumors', *Chemical Communications* **46**(20), 3559–3561.

Leema George, Swapna Upadhyay, K. G., Tobias and Stoeger (2014), *Macrophage Polarization in Lung Biology and Diseases, Lung Inflammation*, InTech.

Li, X., Bradford, B. U., Wheeler, M. D., Stimpson, S. A., Pink, H. M., Brodie, T. A., Schwab, J. H. and Thurman, R. G. (2001), 'Dietary glycine prevents peptidoglycan polysaccharide-induced reactive arthritis in the rat: Role for glycine-gated chloride channel', *Infection and Immunity* **69**(9), 5883–5891.

Li, X., Tupper, J. C., Bannerman, D. D., Winn, R. K., Rhodes, C. J. and Harlan, J. M. (2003), 'Phosphoinositide 3 kinase mediates toll-like receptor 4-induced activation of nf-kb in endothelial cells', *Infection and Immunity* **71**(8), 4414–4420.

Li, Y., Huang, J., Foley, N. M., Xu, Y., Li, Y. P., Pan, J., Redmond, H. P., Wang, J. H. and Wang, J. (2016), 'B7h3 ameliorates lps-induced acute lung injury via attenuation of neutrophil migration and infiltration', *Scientific Reports* **6**, 31284.

Lichtenstein, L., Mattijssen, F., de Wit, N. J., Georgiadi, A., Hooiveld, G. J., van der Meer, R., He, Y., Qi, L., Köster, A., Tamsma, J. T., Tan, N. S., Müller, M. and Kersten, S. (2010), 'Angptl4 protects against severe proinflammatory effects of saturated fat by inhibiting fatty acid uptake into mesenteric lymph node macrophages', *Cell Metabolism* **12**(6), 580–592.

Lin, C.-C., Lin, L.-J., Wang, S.-D., Chiang, C.-J., Chao, Y.-P., Lin, J. and Kao, S.-T. (2014), 'The effect of serine protease inhibitors on airway inflammation in a chronic allergen-induced asthma mouse model', *Mediators of Inflammation* **2014**, 10.

Lin, R., Liu, W., Woo, M. W., Chen, X. D. and Selomulya, C. (2015), 'On the formation of "coral-like" spherical α-glycine crystalline particles', *Powder Technology* **279**, 310–316.

Lin, R., Woo, M. W., Wu, Z., Liu, W., Ma, J., Chen, X. D. and Selomulya, C. (2017), 'Spray drying of mixed amino acids: The effect of crystallization inhibition and humidity treatment on the particle formation', *Chemical Engineering Science* **167**, 161–171.

Linden, A. and Dahlen, B. (2014), 'Interleukin-17 cytokine signalling in patients with asthma', *European Respiratory Journal* **44**(5), 1319–1331.

Liu, C., Li, B. and Xu, C. (2014), 'Colorimetric chiral discrimination and determination of enantiometric excess of d/l-tryptophan using silver nanoparticles', *Microchimica Acta* **181**(11), 1407–1413.

Liu, J.-N., Suh, D.-H., Yang, E.-M., Lee, S.-I., Park, H.-S. and Shin, Y. S. (2014*a*), 'Attenuation of airway inflammation by simvastatin and the implications for asthma treatment: is the jury still out?', *Experimental and Molecular Medicine* **46**, e113.

Liu, J.-N., Suh, D.-H., Yang, E.-M., Lee, S.-I., Park, H.-S. and Shin, Y. S. (2014*b*), 'Attenuation of airway inflammation by simvastatin and the implications for asthma treatment: is the jury still out?', *Experimental and Molecular Medicine* **46**, e113.

Liu, L., Sha, R., Yang, L., Zhao, X., Zhu, Y., Gao, J., Zhang, Y. and Wen, L.-P. (2018), 'Impact of morphology on iron oxide nanoparticles-induced inflammasome activation in macrophages', *ACS Applied Materials and Interfaces* **10**(48), 41197–41206.

Liu, P.-S., Wang, H., Li, X., Chao, T., Teav, T., Christen, S., Di Conza, G., Cheng, W.-C., Chou, C.-H., Vavakova, M., Muret, C., Debackere, K., Mazzone, M., Huang, H.-D., Fendt, S.-M., Ivanisevic, J. and Ho, P.-C. (2017), 'a-ketoglutarate orchestrates macrophage activation through metabolic and epigenetic reprogramming', *Nature Immunology* **18**, 985.

Liu, W., Wu, W., Selomulya, C. and Chen, X. D. (2011*a*), 'A single step assembly of uniform microparticles for controlled release applications', *Soft Matter* **7**(7), 3323–3330.

Liu, W., Wu, W., Selomulya, C. and Chen, X. D. (2011*b*), 'A single step assembly of uniform microparticles for controlled release applications', *Soft Matter* **7**(7), 3323–3330.

Liu, Y.-J. (2005), 'Ipc: Professional type 1 interferon-producing cells and plasmacytoid dendritic cell precursors', *Annual Review of Immunology* **23**(1), 275–306.

Liu, Y., Wang, X. and Hu, C. A. (2017), 'Therapeutic potential of amino acids in inflammatory bowel disease', *Nutrients* **9**(9).

Lora, J. M., Zhang, D. M., Liao, S. M., Burwell, T., King, A. M., Barker, P. A., Singh, L., Keaveney, M., Morgenstern, J., Gutiérrez-Ramos, J. C., Coyle, A. J. and Fraser, C. C. (2005), 'Tumor necrosis factor-α triggers mucus production in airway epithelium through an ikb kinase b-dependent mechanism', *Journal of Biological Chemistry* **280**(43), 36510–36517.

Lovo, E., Zhang, M., Wang, L. and Ashton-Rickardt, P. G. (2012), 'Serine protease inhibitor 6 is required to protect dendritic cells from the kiss of death', *The Journal of Immunology* **188**(3), 1057–1063.

Lu, Y.-C., Yeh, W.-C. and Ohashi, P. S. (2008), 'Lps/tlr4 signal transduction pathway', *Cytokine* **42**(2), 145–151.

Lunov, O., Syrovets, T., Loos, C., Beil, J., Delacher, M., Tron, K., Nienhaus, G. U., Musyanovych, A., Mailänder, V., Landfester, K. and Simmet, T. (2011), 'Differential uptake of functionalized polystyrene nanoparticles by human macrophages and a monocytic cell line', *ACS Nano* **5**(3), 1657–1669.

Lutz, M. B. and Schuler, G. (2002), 'Immature, semi-mature and fully mature dendritic cells: which signals induce tolerance or immunity?', *Trends in Immunology* **23**(9), 445–449.

Lynch, J. W. (2004), 'Molecular structure and function of the glycine receptor chloride channel', *Physiological Reviews* **84**(4), 1051–1095.

Ma, D. and Clark, E. (2009), 'The role of cd40 and cd154/cd40l in dendritic cells', *Seminars in Immunology* **21**(5), 265 – 272.

Ma, X., Yuan, Y., Zhang, Z., Zhang, Y. and Li, M. (2014), 'An analog of ac-sdkp improves heart functions after myocardial infarction by suppressing alternative activation (m2) of macrophages', *Int J Cardiol* **175**(2), 376–8.

Manni, M. L., Mandalapu, S., McHugh, K. J., Elloso, M. M., Dudas, P. L. and Alcorn, J. F. (2016), 'Molecular mechanisms of airway hyperresponsiveness in a murine model of steroid-resistant airway inflammation', *The Journal of Immunology* **196**(3), 963–977.

Mantovani, A., Sozzani, S., Locati, M., Allavena, P. and Sica, A. (2002), 'Macrophage polarization: tumor-associated macrophages as a paradigm for polarized m2 mononuclear phagocytes', *Trends in Immunology* **23**(11), 549–555.

Marasini, N., Giddam, A., Batzloff, M., Good, M., Skwarczynski, M. and Toth, I. (2017), 'Poly-l-lysine-coated nanoparticles are ineffective in inducing mucosal immunity against group a streptococcus', *Biochemical compounds* **5**(1), 1.

Martin, A. R., Thompson, R. B. and Finlay, W. H. (2008), 'Mri measurement of regional lung deposition in mice exposed nose-only to nebulized superparamagnetic iron oxide nanoparticles', *Journal of Aerosol Medicine and Pulmonary Drug Delivery* **21**(4), 335–342.

Martinez, F. O., Gordon, S., Locati, M. and Mantovani, A. (2006), 'Transcriptional profiling of the human monocyte-to-macrophage differentiation and polarization: new molecules and patterns of gene expression', *J Immunol* **177**(10), 7303–11.

Martinez, F. O., Sica, A., Mantovani, A. and Locati, M. (2008), 'Macrophage activation and polarization', *Front Biosci* **13**, 453–61.

Martinez, V. G., Canseco, N. M., Hidalgo, L., Valencia, J., Entrena, A., Fernandez-Sevilla, L. M., Hernandez-Lopez, C., Sacedon, R., Vicente, A. and Varas, A. (2015), 'A discrete population of ifn lambda-expressing bdca3hi dendritic cells is present in human thymus', *Immunol Cell Biol* **93**(7), 673–8.

Matthay, M. A. and Zemans, R. L. (2011), 'The acute respiratory distress syndrome: Pathogenesis and treatment', *Annual review of pathology* **6**, 147–163.

Matute-Bello, G., Frevert, C. W. and Martin, T. R. (2008), 'Animal models of acute lung injury', *American Journal of Physiology - Lung Cellular and Molecular Physiology* **295**(3), L379–L399.

Maxwell, M. J., Duan, M., Armes, J. E., Anderson, G. P., Tarlinton, D. M. and Hibbs, M. L. (2011), 'Genetic segregation of inflammatory lung disease and autoimmune disease severity in ship-1-/- mice', *The Journal of Immunology* **186**(12), 7164–7175.

Mazuel, F., Espinosa, A., Luciani, N., Reffay, M., Le Borgne, R., Motte, L., Desboeufs, K., Michel, A., Pellegrino, T., Lalatonne, Y. and Wilhelm, C. (2016), 'Massive intracellular biodegradation of iron oxide nanoparticles evidenced magnetically at single-endosome and tissue levels', *ACS Nano* **10**(8), 7627–7638.

McGuire, V. A., Gray, A., Monk, C. E., Santos, S. G., Lee, K., Aubareda, A., Crowe, J., Ronkina, N., Schwermann, J., Batty, I. H., Leslie, N. R., Dean, J. L. E., O'Keefe, S. J., Boothby, M., Gaestel, M. and Arthur, J. S. C. (2013), 'Cross talk between the akt and p38α pathways in macrophages downstream of toll-like receptor signaling', *Molecular and Cellular Biology* **33**(21), 4152–4165.

McVey, M., Tabuchi, A. and Kuebler, W. M. (2012), 'Microparticles and acute lung injury', *American Journal of Physiology - Lung Cellular and Molecular Physiology* **303**(5), L364–L381.

Medina, C., Santos-Martinez, M. J., Radomski, A., Corrigan, O. I. and Radomski, M. W. (2007), 'Nanoparticles: pharmacological and toxicological significance', *British journal of pharmacology* **150**(5), 552–558.

Medzhitov, R. (2008), 'Origin and physiological roles of inflammation', *Nature* **454**(7203), 428–435. 10.1038/nature07201.

Mikhaylova, M., Kim, D. K., Bobrysheva, N., Osmolowsky, M., Semenov, V., Tsakalakos, T. and Muhammed, M. (2004), 'Superparamagnetism of magnetite nanoparticles: dependence on surface modification', *Langmuir* **20**(6), 2472–7.

Miles, S. A., Conrad, S. M., Alves, R. G., Jeronimo, S. M. and Mosser, D. M. (2005), 'A role for igg immune complexes during infection with the intracellular pathogen leishmania', *J Exp Med* **201**(5), 747–54.

Minye, Q., Xiang, T. and Ma, J. (2017), 'Yi-qi-ping-chuan-fang reduces tslp elevation caused by lps + poly(i:c) via inhibiting tlr4/myd88/nf-kb signaling pathway', *Evidence-Based Complementary and Alternative Medicine* p. 12.

Misawa, M. and Takahashi, J. (2011), 'Generation of reactive oxygen species induced by gold nanoparticles under x-ray and uv irradiations', *Nanomedicine: Nanotechnology, Biology and Medicine* **7**(5), 604–614.

Mishra, A., Brown, A. L., Yao, X., Yang, S., Park, S. J., Liu, C., Dagur, P. K., McCoy, J. P., Keeran, K. J., Nugent, G. Z., Jeffries, K. R., Qu, X., Yu, Z. X., Levine, S. J. and Chung, J. H. (2015), 'Dendritic cells induce th2-mediated airway inflammatory responses to house dust mite via dna-dependent protein kinase', *Nat Commun* **6**, 6224.

Mittag, D., Proietto, A. I., Loudovaris, T., Mannering, S. I., Vremec, D., Shortman, K., Wu, L. and Harrison, L. C. (2011), 'Human dendritic cell subsets from spleen and blood are similar in phenotype and function but modified by donor health status', *The Journal of Immunology* **186**(11), 6207–6217.

Moghadam-Kia, S. and Werth, V. P. (2010), 'Prevention and treatment of systemic glucocorticoid side effects', *International Journal of Dermatology* **49**(3), 239–248.

Mohr, K., Sommer, M., Baier, G., Schöttler, S., Okwieka, P., Tenzer, S., Katharina Landfester, V. M., Schmidt, M. and Meyer, R. G. (2014), 'Aggregation behavior of polystyrene-nanoparticles in human blood serum and its impact on the in vivo distribution in mice', *Journal of Nanomedicine and Nanotechnology* **5**, 193.

Moldoveanu, B., Otmishi, P., Jani, P., Walker, J., Sarmiento, X., Guardiola, J., Saad, M. and Yu, J. (2009), 'Inflammatory mechanisms in the lung', *Journal of inflammation research* **2**, 1–11.

Moller, W., Felten, K., Sommerer, K., Scheuch, G., Meyer, G., Meyer, P., Haussinger, K. and Kreyling, W. G. (2008), 'Deposition, retention, and translocation of ultrafine particles from the central airways and lung periphery', *American Journal of Respiratory and Critical Care Medicine* **177**(4), 426–432.

Moore, T. L., Rodriguez-Lorenzo, L., Hirsch, V., Balog, S., Urban, D., Jud, C., Rothen-Rutishauser, B., Lattuada, M. and Petri-Fink, A. (2015), 'Nanoparticle colloidal stability in cell culture media and impact on cellular interactions', *Chemical Society Reviews* **44**(17), 6287–6305.

Morales-Nebreda, L., Misharin, A. V., Perlman, H. and Budinger, G. S. (2015), 'The heterogeneity of lung macrophages in the susceptibility to disease', *European Respiratory Review* **24**(137), 505–509.

Morelli, A. E., Rubin, J. P., Erdos, G., Tkacheva, O. A., Mathers, A. R., Zahorchak, A. F., Thomson, A. W., Falo, L. D. and Larregina, A. T. (2005), 'Cd4+ t cell responses elicited by different subsets of human skin migratory dendritic cells', *The Journal of Immunology* **175**(12), 7905–7915.

Moret, F. M., Hack, C. E., van der Wurff-Jacobs, K. M., de Jager, W., Radstake, T. R., Lafeber, F. P. and van Roon, J. A. (2013), 'Intra-articular cd1c-expressing myeloid dendritic cells from rheumatoid arthritis patients express a unique set of t cell-attracting chemokines and spontaneously induce th1, th17 and th2 cell activity', *Arthritis Res Ther* **15**(5), R155.

Mosser, D. M. and Edelson, P. J. (1984), 'Activation of the alternative complement pathway by leishmania promastigotes: parasite lysis and attachment to macrophages', *J Immunol* **132**(3), 1501–5.

Muhlfeld, C. and Ochs, M. (2013), 'Quantitative microscopy of the lung: a problem-based approach. part 2: stereological parameters and study designs in various diseases of the respiratory tract', *American Journal of Physiology-Lung Cellular and Molecular Physiology* **305**(3), L205–L221.

Nakayama, M. (2018), 'Macrophage recognition of crystals and nanoparticles', *Frontiers in Immunology* **9**, 103.

Nandiyanto, A. B. D. and Okuyama, K. (2011), 'Progress in developing spray-drying methods for the production of controlled morphology particles: From the nanometer to submicrometer size ranges', *Advanced Powder Technology* **22**(1), 1–19.

Neveu, W. A., Allard, J. B., Dienz, O., Wargo, M. J., Ciliberto, G., Whittaker, L. A. and Rincon, M. (2009), 'Il-6 is required for airway mucus production induced by inhaled fungal allergens', *The Journal of Immunology* **183**(3), 1732–1738.

Neyt, K., GeurtsvanKessel, C. H. and Lambrecht, B. N. (2015), 'Double-negative t resident memory cells of the lung react to influenza virus infection via cd11c dendritic cells', *Mucosal Immunology* .

Noh, J. Y., Shin, J. U., Park, C. O., Lee, N., Jin, S., Kim, S. H., Kim, J. H., Min, A., Shin, M. H. and Lee, K. H. (2016), 'Thymic stromal lymphopoietin regulates eosinophil migration via phosphorylation of l-plastin in atopic dermatitis', *Experimental Dermatology* **25**(11), 880–886.

Nuttall, F. Q., Nuttall, J. A. and Gannon, M. C. (2002), 'The metabolic response to ingested glycine', *The American Journal of Clinical Nutrition* **76**(6), 1302–1307.

Ogata, M., Ito, T., Shimamoto, K., Nakanishi, T., Satsutani, N., Miyamoto, R. and Nomura, S. (2013), 'Plasmacytoid dendritic cells have a cytokine-producing capacity to enhance icos ligand-mediated il-10 production during t-cell priming', *International Immunology* **25**(3), 171–182.

Oh, E., Delehanty, J. B., Sapsford, K. E., Susumu, K., Goswami, R., Blanco-Canosa, J. B., Dawson, P. E., Granek, J., Shoff, M., Zhang, Q., Goering, P. L., Huston, A. and Medintz, I. L. (2011), 'Cellular uptake and fate of pegylated gold nanoparticles is dependent on both cell-penetration peptides and particle size', *ACS Nano* **5**(8), 6434–6448.

Ohno, S., Suzuki, N., Ohno, Y., Inagawa, H., Soma, G. and Inoue, M. (2003), 'Tumor-associated macrophages: foe or accomplice of tumors?', *Anticancer Res* **23**(6a), 4395–409.

Ohshima, H. (1995), 'Electrophoresis of soft particles', *Advances in Colloid and Interface Science* **62**(2), 189–235.

Pal, S., Mitra, K., Azmi, S., Ghosh, J. K. and Chakraborty, T. K. (2011), 'Towards the synthesis of sugar amino acid containing antimicrobial noncytotoxic cap conjugates with gold nanoparticles and a mechanistic study of cell disruption', *Organic and Biomolecular Chemistry* **9**(13), 4806–4810.

Palasz, A. and Czekaj, P. (2000), 'Toxicological and cytophysiological aspects of lanthanides action', *Acta Biochim Pol* **47**(4), 1107–14.

Pan, Y., Neuss, S., Leifert, A., Fischler, M., Wen, F., Simon, U., Schmid, G., Brandau, W. and Jahnen-Dechent, W. (2007), 'Size-dependent cytotoxicity of gold nanoparticles', *Small* **3**(11), 1941–1949.

Parameswaran, N. and Patial, S. (2010), 'Tumor necrosis factor-α signaling in macrophages', *Critical reviews in eukaryotic gene expression* **20**(2), 87–103.

Paranjpe, M. and Müller-Goymann, C. C. (2014), 'Nanoparticle-mediated pulmonary drug delivery: a review', *International journal of molecular sciences* **15**(4), 5852–5873.

Pascual, M., Fernandez-Lizarbe, S. and Guerri, C. (2011), 'Role of tlr4 in ethanol effects on innate and adaptive immune responses in peritoneal macrophages', *Immunol Cell Biol* **89**(6), 716–27.

Patricia, G., Maria H, G., Shih Wei, W., Jennifer Y, K., Urs P, S. and Gomez-Munoz, A. (2008), 'Ceramide 1-phosphate stimulates macrophage proliferation through activation of the pi3-kinase/pkb, jnk and erk1/2 pathways', *Cellular Signalling* **20**(4), 726–736.

Paul, D. R. and Robeson, L. M. (2008), 'Polymer nanotechnology: Nanocomposites', *Polymer* **49**(15), 3187–3204.

Pauls, S. D. and Marshall, A. J. (2017), 'Regulation of immune cell signaling by ship1: A phosphatase, scaffold protein, and potential therapeutic target', *European Journal of Immunology* **47**(6), 932–945.

Pelletier, M., Maggi, L., Micheletti, A., Lazzeri, E., Tamassia, N., Costantini, C., Cosmi, L., Lunardi, C., Annunziato, F., Romagnani, S. and Cassatella, M. A. (2010), 'Evidence for a cross-talk between human neutrophils and th17 cells', *Blood* **115**(2), 335–343.

Pendyala, S., Usatyuk, P. V., Gorshkova, I. A., Garcia, J. G. N. and Natarajan, V. (2009), 'Regulation of nadph oxidase in vascular endothelium: The role of phospholipases, protein kinases, and cytoskeletal proteins', *Antioxidants and Redox Signaling* **11**(4), 841–860.

Penna, G., Vulcano, M., Sozzani, S. and Adorini, L. (2002), 'Differential migration behavior and chemokine production by myeloid and plasmacytoid dendritic cells', *Human Immunology* **63**(12), 1164–1171.

Pluangnooch, P., Timalsena, S., Wongkajornsilp, A. and Soontrapa, K. (2017), 'Cytokine-induced killer cells: A novel treatment for allergic airway inflammation', *PLOS ONE* **12**(10), e0186971.

Podojil, J. R. and Miller, S. D. (2009), 'Cross-linking of cd80 on cd4+ t cells activates a calcium-dependent signaling pathway', *The Journal of Immunology* **182**(2), 766–773.

Polte, T., Petzold, S., Bertrand, J., Schutze, N., Hinz, D., Simon, J. C., Lehmann, I., Echtermeyer, F., Pap, T. and Averbeck, M. (2015), 'Critical role for syndecan-4 in dendritic cell migration during development of allergic airway inflammation', *Nat Commun* **6**, 7554.

Ponzoni, M., Pastorino, F., Di Paolo, D., Perri, P. and Brignole, C. (2018), 'Targeting macrophages as a potential therapeutic intervention: Impact on inflammatory diseases and cancer', *International Journal of Molecular Sciences* **19**(7).

Popovic, B., Breed, J., Rees, D. G., Gardener, M. J., Vinall, L. M. K., Kemp, B., Spooner, J., Keen, J., Minter, R., Uddin, F., Colice, G., Wilkinson, T., Vaughan, T. and May, R. D. (2017), 'Structural characterisation reveals mechanism of il-13-neutralising monoclonal antibody tralokinumab as inhibition of binding to il-13rα1 and il-13rα2', *Journal of Molecular Biology* **429**(2), 208–219.

Pérez-Juste, J., Pastoriza-Santos, I., Liz-Marzán, L. M. and Mulvaney, P. (2005), 'Gold nanorods: Synthesis, characterization and applications', *Coordination Chemistry Reviews* **249**(17–18), 1870–1901.

Pribul, P. K., Harker, J., Wang, B., Wang, H., Tregoning, J. S., Schwarze, J. and Openshaw, P. J. M. (2008), 'Alveolar macrophages are a major determinant of early responses to viral lung infection but do not influence subsequent disease development', *Journal of Virology* **82**(9), 4441–4448.

Prussin, C., Griffith, D. T., Boesel, K. M., Lin, H., Foster, B. and Casale, T. B. (2003), 'Omalizumab treatment downregulates dendritic cell fceri expression', *Journal of Allergy and Clinical Immunology* **112**(6), 1147–1154.

Pujalte, I., Passagne, I., Brouillaud, B., Treguer, M., Durand, E., Ohayon-Courtes, C. and L'Azou, B. (2011), 'Cytotoxicity and oxidative stress induced by different metallic nanoparticles on human kidney cells', *Particle and Fibre Toxicology* **8**(1), 10.

Pusnik, K., Peterlin, M., Cigic, I. K., Marolt, G., Kogej, K., Mertelj, A., Gyergyek, S. and Makovec, D. (2016), 'Adsorption of amino acids, aspartic acid, and lysine onto iron-oxide nanoparticles', *The Journal of Physical Chemistry C* **120**(26), 14372–14381.

Qu, C., Edwards, E. W., Tacke, F., Angeli, V., Llodrá, J., Sanchez-Schmitz, G., Garin, A., Haque, N. S., Peters, W., van Rooijen, N., Sanchez-Torres, C., Bromberg, J., Charo, I. F., Jung, S., Lira, S. A. and Randolph, G. J. (2004), 'Role of ccr8 and other chemokine pathways in the migration of monocyte-derived dendritic cells to lymph nodes', *The Journal of Experimental Medicine* **200**(10), 1231–1241.

Rad, A. M., Janic, B., Iskander, A. S. M., Soltanian-Zadeh, H. and Arbab, A. S. (2007), 'Measurement of quantity of iron in magnetically labeled cells: comparison among different uv/vis spectrometric methods', *BioTechniques* **43**(5), 627–636.

Rahul, R., Somnath, B., Hong, Z., Corban, S., Muneeb, A. S., Scott, H. V., Yogendra, K., Sajani, D., David, J. P. and Goonewardena, S. N. (2017), 'Nanoparticle-macrophage interactions: A balance between clearance and cell-specific targeting', *Bioorganic and Medicinal Chemistry* **25**(16), 4487–4496.

Rauh, M., Sly, L., Kalesnikoff, J., Hughes, M., Cao, L.-P., Lam, V. and Krystal, G. (2004), 'The role of ship1 in macrophage programming and activation', *Biochemical Society Transactions* **32**(5), 785–788.

Reche, P. A., Soumelis, V., Gorman, D. M., Clifford, T., Liu, M.-r., Travis, M., Zurawski, S. M., Johnston, J., Liu, Y.-J., Spits, H., de Waal Malefyt, R., Kastelein, R. A. and Bazan, J. F. (2001), 'Human thymic stromal lymphopoietin preferentially stimulates myeloid cells', *The Journal of Immunology* **167**(1), 336–343.

Reed, C. E. and Kita, H. (2004), 'The role of protease activation of inflammation in allergic respiratory diseases', *Journal of Allergy and Clinical Immunology* **114**(5), 997–1008.

River, J. and Tessarollo, L. (2008), 'Genetic background and the dilemma of translating mouse studies to humans', *Immunity* **28**(1), 1–4.

Rivollier, A., He, J., Kole, A., Valatas, V. and Kelsall, B. L. (2012), 'Inflammation switches the differentiation program of ly6chi monocytes from antiinflammatory macrophages to inflammatory dendritic cells in the colon', *The Journal of Experimental Medicine* **209**(1), 139–155.

Robbins, S. H., Walzer, T., Dembele, D., Thibault, C., Defays, A., Bessou, G., Xu, H., Vivier, E., Sellars, M., Pierre, P., Sharp, F. R., Chan, S., Kastner, P. and Dalod, M. (2008), 'Novel insights into the relationships between dendritic cell subsets in human and mouse revealed by genome-wide expression profiling', *Genome Biol* **9**(1), R17.

Rodriguez, P., Plana, D., Fermin, D. J. and Koper, M. T. M. (2014), 'New insights into the catalytic activity of gold nanoparticles for co oxidation in electrochemical media', *Journal of Catalysis* **311**, 182–189.

Rogueda, P. G. and Traini, D. (2007), 'The nanoscale in pulmonary delivery. part 1: deposition, fate, toxicology and effects', *Expert Opin Drug Deliv* **4**(6), 595–606.

Romani, N., Gruner, S., Brang, D., Kämpgen, E., Lenz, A., Trockenbacher, B., Konwalinka, G., Fritsch, P. O., Steinman, R. M. and Schuler, G. (1994), 'Proliferating dendritic cell progenitors in human blood', *The Journal of Experimental Medicine* **180**(1), 83–93.

Roos, A. B. and Stampfli, M. R. (2017), 'Targeting interleukin-17 signalling in cigarette smoke-induced lung disease: Mechanistic concepts and therapeutic opportunities', *Pharmacology and Therapeutics* **178**, 123–131.

Ross, R., Ross, X.-L., Ghadially, H., Lahr, T., Schwing, J., Knop, J. and Reske-Kunz, A. B. (1999), 'Mouse langerhans cells differentially express an activated t cell-attracting cc chemokine', *Journal of Investigative Dermatology* **113**(6), 991–998.

Rowe, R. C., Sheskey, P. J., Cook, W. G. and Quinn, M. E. (2013), 'Handbook of pharmaceutical excipients – 7th edition', *Pharmaceutical Development and Technology* **18**(2), 544–544.

Rutkowski, R., Moniuszko, T., Stasiak-Barmuta, Aand Kosztyła-Hojna, B., Alifier, M., Rutkowski, K. and Tatarczuk-Krawiel, A. (2003), 'Cd80 and cd86 expression on lps-stimulated monocytes and the effect of cd80 and cd86 blockade on il-4 and ifn-gamma production in nonatopic bronchial asthma', *Archivum Immunologiae et Therapiae Experimentalis* **51**(6), 421 – 428.

S, W.-G., AM, R., S, A., JD, L., TE, M., AM, N. and J, S. (2017), 'Impact of morphology on iron oxide nanoparticles-induced inflammasome activation in macrophages', *International Journal of Nanomedicine* **12**, 3927–3940.

Sadeghiani, N., Barbosa, L. S., Silva, L. P., Azevedo, R. B., Morais, P. C. and Lacava, Z. G. M. (2005), 'Genotoxicity and inflammatory investigation in mice treated with magnetite nanoparticles surface coated with polyaspartic acid', *Journal of Magnetism and Magnetic Materials* **289**, 466–468.

Sadikot R, T., Kolanjiyil A, V., C, K. and I, R. (2017), 'Nanomedicine for treatment of acute lung injury and acute respiratory distress syndrome', *Biomedicine Hub* **2**(2), 5–5.

Safavi, A. and Farjami, E. (2011), 'Construction of a carbon nanocomposite electrode based on amino acids functionalized gold nanoparticles for trace electrochemical detection of mercury', *Analytica Chimica Acta* **688**(1), 43–48.

Samitas, K., Delimpoura, V., Zervas, E. and Gaga, M. (2015), 'Anti-ige treatment, airway inflammation and remodelling in severe allergic asthma: current knowledge and future perspectives', *European Respiratory Review* **24**(138), 594–601.

Saponaro, C., Cianciulli, A., Calvello, R., Dragone, T., Iacobazzi, F. and Panaro, M. A. (2012), 'The pi3k/akt pathway is required for lps activation of microglial cells', *Immunopharmacology and Immunotoxicology* **34**(5), 858–865.

Saptarshi, S. R., Duschl, A. and Lopata, A. L. (2013), 'Interaction of nanoparticles with proteins: relation to bio-reactivity of the nanoparticle', *Journal of Nanobiotechnology* **11**(1), 26.

Sarkar, S., Das, K., Ghosh, M. and Das, P. K. (2015), 'Amino acid functionalized blue and phosphorous-doped green fluorescent carbon dots as bioimaging probe', *RSC Advances* **5**(81), 65913–65921.

Saturnino, C., Bortoluzzi, M., Napoli, M., Popolo, A., Pinto, A., Longo, P. and Paolucci, G. (2013), 'New insights on cytotoxic activity of group 3 and lanthanide compounds: complexes with [n,n,n]-scorpionate ligands', *Journal of Pharmacy and Pharmacology* **65**(9), 1354–1359.

Schagat, T. L., Wofford, J. A. and Wright, J. R. (2001), 'Surfactant protein a enhances alveolar macrophage phagocytosis of apoptotic neutrophils', *The Journal of Immunology* **166**(4), 2727–2733.

Schmidt, K., Ziu, M., Schmidt, N., Vaghasia, P., Cargioli, T, G., Doshi, S., Albert, M., Black, P., Carroll, R. and Sun, Y. (2004), 'Volume reconstruction techniques improve the correlation between histological and in vivo tumor volume measurements in mouse models of human gliomas', *Journal of Neuroncology* **68**(3), 207–215.

Schroeder, J. T., Bieneman, A. P., Chichester, K. L., Hamilton, R. G., Xiao, H., Saini, S. S. and Liu, M. C. (2009), 'Decreases in human dendritic cell dependent th2-like responses after acute in vivo ige neutralization', *Journal of Allergy and Clinical Immunology* **125**(4), 896–901.e6.

Schwartz, D. A., Christ, W. J., Kleeberger, S. R. and Wohlford-Lenane, C. L. (2001), 'Inhibition of lps-induced airway hyperresponsiveness and airway inflammation by lps antagonists', *American Journal of Physiology-Lung Cellular and Molecular Physiology* **280**(4), L771–L778.

Selim ME, H. A. (2012), 'Gold nanoparticles induce apoptosis in mcf-7 human breast cancer cells', *Asian Pacific Journal of Cancer Prevention* **13**(4), 1617–1620.

Seville, P. C., ying Li, H. and Learoyd, T. P. (2007), 'Spray-dried powders for pulmonary drug delivery', *Critical Reviews and trade in Therapeutic Drug Carrier Systems* **24**(4), 307–360.

Shahabi, S., Treccani, L. and Rezwan, K. (2015), 'Amino acid-catalyzed seed regrowth synthesis of photostable high fluorescent silica nanoparticles with tunable sizes for intracellular studies', *Journal of Nanoparticle Research* **17**(6), 1–15.

Shang, J., Zhao, J., Wu, X., Xu, Y., Xie, J. and Zhao, J. (2015), 'Interleukin-33 promotes inflammatory cytokine production in chronic airway inflammation', *Biochemistry and Cell Biology* **93**(4), 359–366.

Shaver, C. M. and Bastarache, J. A. (2014), 'Clinical and biological heterogeneity in ards: Direct versus indirect lung injury', *Clinics in chest medicine* **35**(4), 639–653.

Sheller, J. R., Polosukhin, V. V., Mitchell, D., Cheng, D.-S., Jr., R. S. P. and Blackwell, T. S. (2009), 'Nuclear factor kappa b induction in airway epithelium increases lung inflammation in allergen-challenged mice', *Experimental Lung Research* **35**(10), 883–895.

Shi, J., Sun, X., Zou, X. and Zhang, H. (2014), 'Amino acid-dependent transformations of citrate-coated silver nanoparticles: Impact on morphology, stability and toxicity', *Toxicology Letters* **229**(1), 17–24.

Shortman, K. and Liu, Y. J. (2002), 'Mouse and human dendritic cell subtypes', *Nat Rev Immunol* **2**(3), 151–61.

Shuvaev, V. V., Han, J., Yu, K. J., Huang, S., Hawkins, B. J., Madesh, M., Nakada, M. and Muzykantov, V. R. (2011), 'Pecam-targeted delivery of sod inhibits endothelial inflammatory response', *The FASEB Journal* **25**(1), 348–357.

Sjöberg, L. C., Nilsson, A. Z., Lei, Y., Gregory, J. A., Adner, M. and Nilsson, G. P. (2017), 'Interleukin 33 exacerbates antigen driven airway hyperresponsiveness, inflammation and remodeling in a mouse model of asthma', *Scientific Reports* **7**(1), 4219.

Soo Choi, H., Lui, W., Misra, P., Tanaka, E., Zimmer, J. P., IttyIpe, B., Bawendi, M. G. and Frangioni, J. V. (2007), 'Renal clearence of quantum dots', *Nat Biotechnol* **25**.

Sou, T., Forbes, R. T., Gray, J., Prankerd, R. J., Kaminskas, L. M., McIntosh, M. P. and Morton, D. A. (2016), 'Designing a multi-component spray-dried formulation platform for pulmonary delivery of biopharmaceuticals: The use of polyol, disaccharide, polysaccharide and synthetic polymer to modify solid-state properties for glassy stabilisation', *Powder Technology* **287**, 248 – 255.

Spittler, A., Reissner, C. M., Oehler, R., Gornikiewicz, A., Gruenberger, T., Manhart, N., Brodowicz, T., Mittleboeck, M., Boltz-Nitulescu, G. and Roth, E. (1999), 'Immunomodulatory effects of glycine on lps-treated monocytes: reduced tnf-α production and accelerated il-10 expression', *The FASEB Journal* **13**(3), 563–571.

Starkhammar, M., Larsson, O., Kumlien Georén, S., Leino, M., Dahlén, S.-E., Adner, M. and Cardell, L.-O. (2014), 'Toll-like receptor ligands lps and poly (i:c) exacerbate airway hyperresponsiveness in a model of airway allergy in mice, independently of inflammation', *PLOS ONE* **9**(8), e104114.

Stoll, L. L., Denning, G. M. and Weintraub, N. L. (2004), 'Potential role of endotoxin as a proinflammatory mediator of atherosclerosis', *Arteriosclerosis, Thrombosis, and Vascular Biology* **24**(12), 2227–2236.

Strassheim, D., Kim, J.-Y., Park, J.-S., Mitra, S. and Abraham, E. (2005), 'Involvement of ship in tlr2-induced neutrophil activation and acute lung injury', *The Journal of Immunology* **174**(12), 8064–8071.

Sun, D., Zhuang, X., Xiang, X., Liu, Y., Zhang, S., Liu, C., Barnes, S., Grizzle, W., Miller, D. and Zhang, H.-G. (2010), 'A novel nanoparticle drug delivery system: The anti-inflammatory activity of curcumin is enhanced when encapsulated in exosomes', *Molecular Therapy* **18**(9), 1606–1614.

Sy, C. B. and Siracusa, M. C. (2016), 'The therapeutic potential of targeting cytokine alarmins to treat allergic airway inflammation', *Frontiers in Physiology* **7**, 214.

Takahashi, G., Andrews, D. d., Lilly, M., Singer, J. and Alderson, M. (1993), 'Effect of granulocyte-macrophage colony-stimulating factor and interleukin-3 on interleukin-8 production by human neutrophils and monocytes', *Blood* **81**(2), 357–364.

Takahashi, M., Togao, O., Obara, M., van Cauteren, M., Ohno, Y., Doi, S., Kuro-O, M., Malloy, C., Hsia, C. C. and Dimitrov, I. (2010), 'Ultra-short echo time (ute) mr imaging of the lung: Comparison between normal and emphysematous lungs in mutant mice', *Journal of Magnetic Resonance Imaging* **32**(2), 326–333.

Takahashi, T. and Kubo, H. (2014), 'The role of microparticles in chronic obstructive pulmonary disease', *International Journal of Chronic Obstructive Pulmonary Disease* **9**, 303–314.

Takeda, K., Kaisho, T. and Akira, S. (2003), 'Toll-like receptors', *Annual Review of Immunology* **21**(1), 335–376.

Thiel, M., Wolfs, M.-J., Bauer, S., Wenning, A. S., Burckhart, T., Schwarz, E. C., Scott, A. M., Renner, C. and Hoth, M. (2010), 'Efficiency of t-cell costimulation by cd80 and cd86 cross-linking correlates with calcium entry', *Immunology* **129**(1), 28–40.

Thomas, C., Gupta, V. and Ahsan, F. (2009), 'Influence of surface charge of plga particles of recombinant hepatitis b surface antigen in enhancing systemic and mucosal immune responses', *International Journal of Pharmaceutics* **379**(1), 41–50.

Thompson, M. R., Kaminski, J. J., Kurt-Jones, E. A. and Fitzgerald, K. A. (2011), 'Pattern recognition receptors and the innate immune response to viral infection', *Viruses* **3**(6), 920.

Tiwari, P., Vig, K., Dennis, V. and Singh, S. (2011), 'Functionalized gold nanoparticles and their biomedical applications', *Nanomaterials* **1**(1), 31.

Tsantikos, E., Lau, M., Castelino, C. M. N., Maxwell, M. J., Passey, S. L., Hansen, M. J., McGregor, N. E., Sims, N. A., Steinfort, D. P., Irving, L. B., Anderson, G. P. and Hibbs, M. L. (2018), 'Granulocyte-csf links destructive inflammation and comorbidities in obstructive lung disease', *The Journal of Clinical Investigation* **128**(6), 2406–2418.

Tsune, I., Ikejima, K., Hirose, M., Yoshikawa, M., Enomoto, N., Takei, Y. and Sato, N. (2003), 'Dietary glycine prevents chemical-induced experimental colitis in the rat', *Gastroenterology* **125**(3), 775–85.

Tu, G.-w., Shi, Y., Zheng, Y.-j., Ju, M.-j., He, H.-y., Ma, G.-g., Hao, G.-w. and Luo, Z. (2017), 'Glucocorticoid attenuates acute lung injury through induction of type 2 macrophage', *Journal of Translational Medicine* **15**(1), 181.

Vaine, C. A., Patel, M. K., Zhu, J., Lee, E., Finberg, R. W., Hayward, R. C. and Kurt-Jones, E. A. (2013), 'Tuning innate immune activation by surface texturing of polymer microparticles: The role of shape in inflammasome activation', *The Journal of Immunology* **190**(7), 3525–3532.

Van Den Eynden, J., SahebAli, Sheen et al. Brône, B., Hellings, N., Steels, P., Harvey, R. J. and Rigo, J.-M. (2009), 'Glycine and glycine receptor signalling in non-neuronal cells', *Frontiers in Molecular Neuroscience* **2**.

van der Aar, A. M., Sylva-Steenland, R. M. R., Bos, J. D., Kapsenberg, M. L., de Jong, E. C. and Teunissen, M. B. M. (2007), 'Cutting edge: Loss of TLR2, TLR4, and TLR5 on langerhans cells abolishes bacterial recognition', *The Journal of Immunology* **178**(4), 1986–1990.

van Rijt, S. H., Bein, T. and Meiners, S. (2014), 'Medical nanoparticles for next generation drug delivery to the lungs', *Eur Respir J* **44**(3), 765–74.

Vargas, M. H., Del-Razo-Rodríguez, R., López-García, A., Lezana-Fernández, J. L., Chávez, J., Furuya, M. E. Y. and Marín-Santana, J. C. (2017), 'Effect of oral glycine on the clinical, spirometric and inflammatory status in subjects with cystic fibrosis: a pilot randomized trial', *BMC Pulmonary Medicine* **17**(1), 206.

Vedantam, P., Huang, G. and Tzeng, T. R. J. (2013), 'Size-dependent cellular toxicity and uptake of commercial colloidal gold nanoparticles in du-145 cells', *Cancer Nanotechnology* **4**(1), 13–20.

Vela Ramirez, J. E., Roychoudhury, R., Habte, H. H., Cho, M. W., Pohl, N. L. and Narasimhan, B. (2014), 'Carbohydrate-functionalized nanovaccines preserve hiv-1 antigen stability and activate antigen presenting cells', *Journal of biomaterials science* **25**(13), 1387–406.

Verma, A. and Stellacci, F. (2010), 'Effect of surface properties on nanoparticle–cell interactions', *Small* **6**(1), 12–21.

Voynow, J. A. and Rubin, B. K. (2009), 'Mucins, mucus, and sputum', *CHEST* **135**(2), 505–512.

Walkey, A. J., Summer, R., Ho, V. and Alkana, P. (2012), 'Acute respiratory distress syndrome: epidemiology and management approaches', *Clinical epidemiology* **4**, 159–169.

Walkin, L., Herrick, S. E., Summers, A., Brenchley, P. E., Hoff, C. M., Korstanje, R. and Margetts, P. J. (2013), 'The role of mouse strain differences in the susceptibility to fibrosis: a systematic review', *Fibrogenesis and Tissue Repair* **6**(1), 18.

Wang, H.-D., Lu, D.-X. and Qi, R.-B. (2009), 'Therapeutic strategies targeting the lps signaling and cytokines', *Pathophysiology* **16**(4), 291–296.

Wang, L., Bao, J., Wang, L., Zhang, F. and Li, Y. (2006), 'One-pot synthesis and bioapplication of amine-functionalized magnetite nanoparticles and hollow nanospheres', *Chemistry* **12**(24), 6341–7.

Wang, L., Wang, X., Bhirde, A., Cao, J., Zeng, Y., Huang, X., Sun, Y., Liu, G. and Chen, X. (2014), 'Carbon-dot-based two-photon visible nanocarriers for safe and highly efficient delivery of sirna and dna', *Adv Healthcare Mater* **3**.

Wang, W. (2000), 'Lyophilization and development of solid protein pharmaceuticals', *International Journal of Pharmaceutics* **203**(1), 1–60.

Wang, Y., Anilkumar, P., Cao, L., Liu, J.-H., Luo, P. G., Tackett, K. N., Sahu, S., Wang, P., Wang, X. and Sun, Y.-P. (2011), 'Carbon dots of different composition and surface functionalization: cytotoxicity issues relevant to fluorescence cell imaging', *Experimental Biology and Medicine* **236**(11), 1231–1238.

Wangoo, N., Bhasin, K. K., Mehta, S. K. and Suri, C. R. (2008), 'Synthesis and capping of water-dispersed gold nanoparticles by an amino acid: Bioconjugation and binding studies', *Journal of Colloid and Interface Science* **323**(2), 247–254.

Wei, L., Wang, D. and Nail, S. (2005), 'Freeze-drying of proteins from a sucrose-glycine excipient system: Effect of formulation composition on the initial recovery of protein activity', *American Association of Pharmaceutical Science and Technology* **6**(2), E150–E157.

Weifeng, Y., Li, L., Yujie, H., Weifeng, L., Zhenhui, G. and Wenjie, H. (2016), 'Inhibition of acute lung injury by tnfr-fc through regulation of an inflammation-oxidative stress pathway', *PLOS ONE* **11**(3), e0151672.

Weinstein, S. L., Finn, A. J., Davé, S. H., Meng, F., Lowell, C. A., Sanghera, J. S. and DeFranco, A. L. (2000), 'Phosphatidylinositol 3-kinase and mtor mediate lipopolysaccharide-stimulated nitric oxide production in macrophages via interferon-β', *Journal of Leukocyte Biology* **67**(3), 405–414.

Wenzel, S., Ford, L., Pearlman, D., Spector, S., Sher, L., Skobieranda, F., Wang, L., Kirkesseli, S., Rocklin, R., Bock, B., Hamilton, J., Ming, J. E., Radin, A., Stahl, N., Yancopoulos, G. D., Graham, N. and Pirozzi, G. (2013), 'Dupilumab in persistent asthma with elevated eosinophil levels', *New England Journal of Medicine* **368**(26), 2455–2466.

West, E. E., Kashyap, M. and Leonard, W. J. (2012), 'Tslp: A key regulator of asthma pathogenesis', *Drug discovery today. Disease mechanisms* **9**(3-4), 10.1016/j.ddmec.2012.09.003.

Wheeler, M., Stachlewitz, R. F., Yamashina, S., Ikejma, K., Morrow, A. L. and Thurman, R. G. (2000), 'Glycine-gated chloride channels in neutrophils attenuate calcium influx and superoxide production', *The FASEB Journal* **14**(3), 476–484.

Wilson, K. L., Xiang, S. D. and Plebanski, M. (2015), 'Montanide, poly i:c and nanoparticle based vaccines promote differential suppressor and effector cell expansion: a study of induction of cd8 t cells to a minimal plasmodium berghei epitope', *Front Microbiol* **6**, 29.

Wilson, M. S., Madala, S. K., Ramalingam, T. R., Gochuico, B. R., Rosas, I. O., Cheever, A. W. and Wynn, T. A. (2010), 'Bleomycin and il-1β mediated pulmonary fibrosis is il-17a dependent', *Journal of Experimental Medicine* **207**(3), 535–552.

Wilson, M. and Wynn, T. (2009), 'Pulmonary fibrosis: pathogenesis, etiology and regulation', *Mucosal Immunology* **2**, 103–121.

Wu, W. D., Amelia, R., Hao, N., Selomulya, C., Zhao, D., Chiu, Y.-L. and Chen, X. D. (2011), 'Assembly of uniform photoluminescent microcomposites using a novel micro-fluidic-jet-spray-dryer', *AIChE Journal* **57**(10), 2726–2737.

Xia, Z., Wang, Z. and Xiaotong, H. (2018), 'Different concentrations of lipopolysaccharide regulate barrier function through the pi3k/akt signalling pathway in human pulmonary microvascular endothelial cells', *Nature Scientific Reports* **8**, 9963.

Xiang, S. D., Fuchsberger, M., Karlson, T. D. L., Hardy, C. L., Selomulya, C. and Plebanski, M. (2012), *Nanoparticles, Immunomodulation and Vaccine Delivery*, WORLD SCIENTIFIC, pp. 449–475.

Xiang, S. D., Scholzen, A., Minigo, G., David, C., Apostolopoulos, V., Mottram, P. L. and Plebanski, M. (2006), 'Pathogen recognition and development of particulate vaccines: Does size matter?', *Methods* **40**(1), 1–9.

Xiao, Q., Dong, N., Yao, X., Wu, D., Lu, Y., Mao, F., Zhu, J., Li, J., Huang, J., Chen, A., Huang, L., Wang, X., Yang, G., He, G., Xu, Y. and Lu, W. (2016), 'Bufexamac ameliorates lps-induced acute lung injury in mice by targeting lta4h', *Scientific Reports* **6**, 25298.

Xing, R., Zhang, F., Xie, J., Aronova, M., Zhang, G., Guo, N., Huang, X., Sun, X., Liu, G., Bryant, L. H., Bhirde, A., Liang, A., Hou, Y., Leapman, R. D., Sun, S. and Chen, X. (2011), 'Polyaspartic acid coated manganese oxide nanoparticles for efficient liver mri', *Nanoscale* **3**(12), 4943–4945.

Xu, F. L., You, H. B., Li, X. H., Chen, X. F., Liu, Z. J. and Gong, J. P. (2008), 'Glycine attenuates endotoxin-induced liver injury by downregulating tlr4 signaling in kupffer cells', *The American Journal of Surgery* **196**(1), 139–148.

Yan-Ru Zhang, S. . L. S. and Sheng-Qing, W. (2014), 'A dual function magnetic nanomaterial modified with lysine for removal of organic dyes from water solution', *Chem Eng J* **239**.

Yan-Ru Zhang, S. . Q. W. and Shi-Li, S. (2013), 'A novel water treatment magnetic nanomaterial for removal of anionic and cationic dyes under severe condition', *Chem Eng J* **233**.

Yang, H.-M., Park, C. W., Woo, M.-A., Kim, M. I., Jo, Y. M., Park, H. G. and Kim, J.-D. (2010*a*), 'Her2/neu antibody conjugated poly(amino acid)-coated iron oxide nanoparticles for breast cancer mr imaging', *Biomacromolecules* **11**(11), 2866–2872.

Yang, H.-M., Park, C. W., Woo, M.-A., Kim, M. I., Jo, Y. M., Park, H. G. and Kim, J.-D. (2010*b*), 'Her2/neu antibody conjugated poly(amino acid)-coated iron oxide nanoparticles for breast cancer mr imaging', *Biomacromolecules* **11**(11), 2866–2872.

Yang, W., Peters, J. I. and Williams, R. O. (2008), 'Inhaled nanoparticles a current review', *International Journal of Pharmaceutics* **356**(1), 239 – 247.

Yang, X.-F., Xu, Y., Qu, D.-S. and Li, H.-Y. (2015), 'The influence of amino acids on aztreonam spray-dried powders for inhalation', *Asian Journal of Pharmaceutical Sciences* **10**(6), 541 – 548.

Yang, X., Han, D., Xing Wang, X., Kun Liu, L. and Zhou, X. (2017), 'Glycine protects against non-alcoholic hepatitis by downregulation of the tlr4 signaling pathway', *Int J Clin Exp Pathol* **10**, 10261–10268.

Yen, H.-J., Hsu, S.-h. and Tsai, C.-L. (2009), 'Cytotoxicity and immunological response of gold and silver nanoparticles of different sizes', *Small* **5**(13), 1553–1561.

Yilmaz, A., Reiss, C., Weng, A., Cicha, I., Stumpf, C., Steinkasserer, A., Daniel, W. G. and Garlichs, C. D. (2006), 'Differential effects of statins on relevant functions of human monocyte-derived dendritic cells', *Journal of Leukocyte Biology* **79**(3), 529–538.

Yoshimura, A., Lien, E., Ingalls, R. R., Tuomanen, E., Dziarski, R. and Golenbock, D. (1999), 'Cutting edge: Recognition of gram-positive bacterial cell wall components by the innate immune system occurs via toll-like receptor 2', *The Journal of Immunology* **163**(1), 1–5.

Yu, Z.-Z., Wu, Q.-H., Zhang, S.-L., Miao, J.-Y., Zhao, B.-X. and Su, L. (2016), 'Two novel amino acid-coated super paramagnetic nanoparticles at low concentrations label and promote the proliferation of mesenchymal stem cells', *RSC Advances* **6**(12), 10159–10161.

Zaba, L. C., Fuentes-Duculan, J., Steinman, R. M., Krueger, J. G. and Lowes, M. A. (2007), 'Normal human dermis contains distinct populations of cd11c+bdca-1+ dendritic cells and cd163+fxiiia+ macrophages', *The Journal of Clinical Investigation* **117**(9), 2517–2525.

Zabot, G. P., Carvalhal, G. F., Marroni, N. P., Hartmann, R. M., da Silva, V. D. and Fillmann, H. S. (2014), 'Glutamine prevents oxidative stress in a model of mesenteric ischemia and reperfusion', *World Journal of Gastroenterology* **20**(32), 11406–11414.

Zhang, Y., Zhou, X. and Zhou, B. (2012), 'Dc-derived tslp promotes th2 polarization in lps-primed allergic airway inflammation', *European Journal of Immunology* **42**(7), 1735–1743.

Zhang, Z., Louboutin, J.-P., Weiner, D. J., Goldberg, J. B. and Wilson, J. M. (2005), 'Human airway epithelial cells sense pseudomonas aeruginosa infection via recognition of flagellin by toll-like receptor 5', *Infection and Immunity* **73**(11), 7151–7160.

Zhao, M., Kircher, M. F., Josephson, L. and Weissleder, R. (2002), 'Differential conjugation of tat peptide to superparamagnetic nanoparticles and its effect on cellular uptake', *Bioconjugate Chemistry* **13**(4), 840–844.

Zhongshi, L., Xingui, L., Yegui, X. and Shunying, L. (2014), "smart' gold nanoshells for combined cancer chemotherapy and hyperthermia', *Biomedical Materials* **9**(2), 025012.

Zhou, B., Comeau, M. R., Smedt, T. D., Liggitt, H. D., Dahl, M. E., Lewis, D. B., Gyarmati, D., Aye, T., Campbell, D. J. and Ziegler, S. F. (2005), 'Thymic stromal lymphopoietin as a key initiator of allergic airway inflammation in mice', *Nature Immunology* **6**, 1047.

Zhou, F., Ciric, B., Li, H., Yan, Y., Li, K., Cullimore, M., Lauretti, E., Gonnella, P., Zhang, G.-X. and Rostami, A. (2012), 'Il-10 deficiency blocks the ability of lps to regulate expression of tolerance-related molecules on dendritic cells', *European Journal of Immunology* **42**(6), 1449–1458.

Ziegler-Heitbrock, L., Ancuta, P., Crowe, S., Dalod, M., Grau, V., Hart, D. N., Leenen, P. J. M., Liu, Y.-J., MacPherson, G., Randolph, G. J., Scherberich, J., Schmitz, J., Shortman, K., Sozzani, S., Strobl, H., Zembala, M., Austyn, J. M. and Lutz, M. B. (2010), 'Nomenclature of monocytes and dendritic cells in blood', *Blood* **116**(16), e74–e80.

Index